# 2. PRINCIPAL DESIGN CRITERIA

The FuelSolutions™ Storage System components, including the storage cask and the transfer cask, are designed based on the bounding FuelSolutions™ canister dimensions and weights, and the thermal and radiological source terms, as documented in the FuelSolutions™ Canister Storage FSARs. This chapter defines the design criteria that are specific to the FuelSolutions™ W21 canister design and demonstrates that the FuelSolutions™ W21 canister and its contents are within the design basis parameters used for the FuelSolutions™ W150 Storage Cask and W100 Transfer Cask. The FuelSolutions™ W21 canister design criteria are summarized in Table 2.0-1 and described in the sections that follow.

## Table 2.0-1 - W21 Canister Design Criteria Summary (7 Pages)

| Type | Criteria | Basis | FSAR Reference |
|---|---|---|---|
| **Design Life:** | | | |
| Design | 100 yrs. | - | Section 2.1.2 |
| Regulatory | 20 yrs. | 10CFR72.42(a) & 10CFR72.236(g) | - |
| **Structural:** | | | |
| Design & Fabrication Codes: | | | |
| Shell Assembly | ASME Code, Section III, Subsections NB and NF | 10CFR72.24(c)(4) | Sections 1.2.1.3 & 2.1.2 |
| Basket Assembly | ASME Code, Section III, Subsection NG | 10CFR72.24(c)(4) | Sections 1.2.1.3 & 2.1.2 |
| Outer Closure Plate Vertical Lifting Points | ANSI N14.6/NUREG-0612 | 10CFR72.24(c)(4) | Section 2.1.2 |
| Design Dead Weights: | | | |
| Max. Loaded Canister (dry) | 80,888 lb. | ANSI/ANS 57.9 | Table 3.2-1 |
| Max. Empty Canister (dry) | 45,608 lb. | ANSI/ANS 57.9 | Table 3.2-1 |
| Design Cavity Pressures: | | | |
| Normal: | | | |
| Dry Storage | 10 psig | ANSI/ANS 57.9 | Section 2.3.1.2 |
| Blowdown | 30 psig | ANSI/ANS 57.9 | Section 2.3.1.2 |
| Off-normal: | | | |
| Dry Storage | 16 psig | ANSI/ANS 57.9 | Section 2.3.2.2 |
| Reflood | 100 psig | ANSI/ANS 57.9 | Section 2.3.2.4 |
| Postulated Accident | 69 psig | ANSI/ANS 57.9 | Section 2.3.3.4 |
| Response and Degradation Limits | SNF assemblies confined in dry, inert environment | 10CFR72.122(h)(1) | Section 1.2.1.3 |

## Table 2.0-1 - W21 Canister Design Criteria Summary (7 Pages)

| Type | Criteria | Basis | FSAR Reference |
|---|---|---|---|
| **Criticality:** | | 10CFR72.124 & 10CFR.236(c) | |
| Method of Control | Fixed Borated Neutron Absorber | - | Sections 1.2.1.3 & 2.1.2 |
| Min. Boron Loading | 20 mg/cm$^2$ $B_{10}$ | - | Section 6.3.1 |
| Max. $k_{eff}$ | 0.95 | - | Section 6.1 |
| Min. Burnup | 0.0 GWd/MTU (fresh fuel) | - | Sections 2.1.2 & 6.3.1 |
| **Radiation Protection/Shielding:** | | 10CFR72.126, & 10CFR72.128(a)(2) | |
| Confinement Cask: (normal/off-normal/accident) | | | |
| Canister Closure | ALARA | 10CFR20 | Sections 10.1, 10.2, & 10.3 |
| Canister Transfer | ALARA | 10CFR20 | Sections 10.1, 10.2, & 10.3 |
| Exterior of Shielding: (normal/off-normal/accident) | | | |
| Transfer Mode Position | ALARA | 10CFR20 | Section 5.4.2 of WSNF 200 |
| Storage Mode Position | See FuelSolutions™ Storage System FSAR | 10CFR20 | Section 5.4.1 of WSNF 200 |
| ISFSI Controlled Area Boundary | See FuelSolutions™ Storage System FSAR | 10CFR72.104 & 10CFR72.106 | Section 10.4 |
| **Design Bases:** | | 10CFR72.236(a) | |
| Spent Fuel Specification: | | | |
| Assemblies/Canister | Up to 21 | - | Section 2.2 & Section 12.3 |
| Type of Cladding | Zircaloy* | - | Section 2.2 & Section 12.3 |
| Fuel Condition | Intact* | - | Section 2.2 & Section 12.3 |
| * Also designed to accommodate failed fuel, stainless clad fuel, MOX fuel, and consolidated fuel (Sections 1.2.3 & 2.2) by future amendment. | | | |
| Class/Type/Configuration | See Table 2.2-1 | - | Section 2.2 &Table 2.2-1 |
| Max. Burnup | 60,000 MWd/MTU | - | Section 12.3 |

## Table 2.0-1 - W21 Canister Design Criteria Summary (7 Pages)

| Type | Criteria | Basis | FSAR Reference |
|---|---|---|---|
| Max. Enrichment | 4.6 to 5.0 w/o $^{235}U$ (varies by fuel design) | - | Sections 6.1 & 12.3 |
| Max. Decay Heat/Canister: | | | |
| > 0 ≤ 60 GWd/MTU | 25.1 kW (0.184 kW/in) | - | Section 4.1.5 & Table 4.1-4 |
| Max. Fuel Assembly Weights: | | | |
| w/o Control Components | 1,515 lb. | - | Table 1.2-3 |
| w/ Control Components | 1,680 lb. | - | Table 1.2-3 |
| Max. Fuel Assembly Irradiated Lengths: | | | |
| w/o Control Components | 180.0 in. | - | Table 1.2-3 |
| w/ Control Components | 173.5 in. | - | Table 1.2-3 |
| Max. Fuel Assembly Irradiated Width | 8.54 in. | - | Table 1.2-3 |
| Fuel Rod Fill Gas: | | | |
| Pressure (max.) | 500 psig | - | Section 4.4.1.6 & Table 4.4-6 |
| Volume (max.) | 505 cu. in. | - | Section 4.4.1.6 & Table 4.4-6 |
| **Normal Design Event Conditions:** | | 10CFR72.122(b)(1) | |
| Ambient Outside Temperatures | See FuelSolutions™ Storage System FSAR | ANSI/ANS 57.9 | Section 2.3.1.1 |
| Handling Loads: | | | |
| Vertical | 15% of dead wt. | CMAA #70 | Section 2.3.1.4 |
| Horizontal | 45,000 lb. push or pull, either end | - | Section 2.3.1.4 |
| Wet/Dry Loading | Wet | - | Section 1.2.2 |
| Transfer Orientation | Vertical or Horizontal | - | Section 1.2.2 |
| Storage Orientation | Vertical | - | Section 1.2.2 |

## Table 2.0-1 - W21 Canister Design Criteria Summary (7 Pages)

| Type | Criteria | Basis | FSAR Reference |
|---|---|---|---|
| Fuel Rod Rupture Releases: | | | |
| Fuel Rod Failures | 1% | - | Sections 2.3.1.2 & 4.4.1.5 |
| Fill Gases | 100% | - | Sections 2.3.1.2 & 4.4.1.5 |
| Fission Gases | 30% | - | Sections 2.3.1.2 & 4.4.1.5 |
| Confinement Boundary Leakage | $2 \times 10^{-5}$ atm-cm$^3$/sec | - | Sections 2.3.1.5 & 7.2 |
| **Off-Normal Design Event Conditions:** | | 10CFR72.122(b)(1) | |
| Ambient Temperature | See FuelSolutions™ Storage System FSAR | ANSI/ANS 57.9 | Section 2.3.2.1 |
| Misaligned Cask Horizontal Canister Transfer Load | 70,000 lb. push/50,000 lb. pull, either end | - | Section 2.3.2.3 |
| Fuel Rod Rupture Releases: | | | |
| Fuel Rod Failures | 10% | - | Sections 2.3.2.2 & 4.4.1.5 |
| Fill Gases | 100% | - | Sections 2.3.2.2 & 4.4.1.5 |
| Fission Gases | 30% | - | Sections 2.3.2.2 & 4.4.1.5 |
| Confinement Boundary Leakage | $2 \times 10^{-5}$ atm-cm$^3$/sec | - | Sections 2.3.2.6 & 7.2 |
| **Design-Basis (Postulated) Accident Design Events and Conditions:** | | 10CFR72.24(d)(2) & 10CFR72.94 | |
| Drop/Tip-Over Cases | See FuelSolutions™ Storage System FSAR | - | Section 2.3.3.2 |
| Fire | See FuelSolutions™ Storage System FSAR | 10CFR72.122(c) | Section 2.3.3.3 |
| Fuel Rod Rupture Releases: | | | |
| Fuel Rod Failures | 100% | - | Sections 2.3.3.4 & 4.4.1.5 |
| Fill Gases | 100% | - | Sections 2.3.3.4 & 4.4.1.5 |
| Fission Gases | 30% | - | Sections 2.3.3.4 & 4.4.1.5 |
| Particulates & Volatiles | See Table 7.4-1 of FuelSolutions™ Storage System FSAR | - | Sections 2.3.3.5 & 7.3.1 |
| Confinement Boundary Leakage | $2 \times 10^{-5}$ atm-cm$^3$/sec | - | Sections 2.3.3.5 & 7.3 |

## Table 2.0-1 - W21 Canister Design Criteria Summary (7 Pages)

| Type | Criteria | Basis | FSAR Reference |
|---|---|---|---|
| Explosive Overpressure | See FuelSolutions™ Storage System FSAR | 10CFR72.122(c) | Section 2.3.3.6 |
| Air Flow Blockage: | | | |
| Vent Blockage | See FuelSolutions™ Storage System FSAR | 10CFR72.128(a)(4) | Section 2.3.3.1.1 |
| Ambient Temperature | See FuelSolutions™ Storage System FSAR | 10CFR72.128(a)(4) | Section 2.3.3.1.1 |
| **Design-Basis Natural Phenomenon Design Events and Conditions:** | | 10CFR72.92 & 10CFR72.122(b)(2) | |
| Flood Water Depth | 50 ft. | ANSI/ANS 57.9 | Section 2.3.4.1 |
| Seismic | See FuelSolutions™ Storage System FSAR | 10CFR72.102(f) & RG 1.60 | Section 2.3.4.3 |
| Wind | Protected by Casks | ASCE 7 | Section 2.3.4.4 |
| Tornado & Missiles | Protected by Casks | RG 1.76 & NUREG-0800 | Section 2.3.4.2 |
| Burial Under Debris | Bounded by Air Flow Blockage Criteria | - | Section 2.3.4.5 |
| Lightning | See FuelSolutions™ Storage System FSAR | NFPA 78 | Section 2.3.4.6 |
| Snow and Ice | Protected by Casks | ASCE 7 | Section 2.3.4.7 |

## 2.1 Structures, Systems, and Components Important to Safety

### 2.1.1 Identification of Items Important to Safety

As identified in Chapter 1 of this FSAR, the FuelSolutions™ W21 canister is a structure, system, and component (SSC) that is classified as important to safety in accordance with 10CFR72. Table 2.1-1 of the FuelSolutions™ Storage System FSAR[1] provides a summary of the FuelSolutions™ Storage System components and support equipment (including the FuelSolutions™ canisters and related equipment) and defines their safety classification.

### 2.1.2 Design Bases and Criteria

*General*

Consistent with the findings of the NRC's Waste Confidence Decision Review,[2] the FuelSolutions™ W21 canister is designed for 100 years of service, while satisfying the requirements of 10CFR72. The design considerations that assure canister performance throughout the service life include addressing the following:

- Corrosion
- Structural fatigue effects
- Maintenance of helium atmosphere
- Allowable fuel cladding temperatures
- Neutron absorber boron depletion.

The adequacy of the canister design for the intended service life is discussed in Section 3.4.4 of this FSAR.

*Structural*

The FuelSolutions™ W21 canister structural components include the internal basket assembly and the shell assembly. The internal basket assembly is designed and fabricated as a core support structure in accordance with the applicable requirements of Section III, Subsection NG[3] of the ASME Code, to the maximum extent practicable, as discussed in Section 2.5.1. The shell assembly is designed and fabricated as a Class 1 component pressure vessel in accordance with Section III, Subsection NB[4] and NF[5] of the ASME Code, to the maximum extent practicable, as

---

[1] WSNF-220, *FuelSolutions™ Storage System Final Safety Analysis Report*, NRC Docket No. 72-1026, BNFL Fuel Solutions.

[2] *Nuclear Regulatory Commission 10 CFR Part 51 Waste Confidence Decision Review*, U.S. Nuclear Regulatory Commission, September 11, 1990.

[3] American Society of Mechanical Engineers (ASME) Boiler and Pressure Vessel Code, Section III, Division 1, Subsection NG, *Core Support Structures*, 1995 Edition.

[4] American Society of Mechanical Engineers (ASME) Boiler and Pressure Vessel Code, Section III, Division 1, Subsection NB, *Class 1 Components*, 1995 Edition.

discussed in Section 2.5.1. The principal exception is the top end inner and outer closure plate welds to the canister shell, as discussed in Section 2.5.2. The top end closure design complies with guidance provided in NRC Interim Staff Guidance #4 (ISG-4).[6] In addition, the top end outer closure plate is designed in accordance with the requirements of ANSI N14.6[7] for critical lifts to facilitate vertical canister transfer.

The canister top end closure plate welds are partial penetration welds that are structurally qualified by analysis, as presented in Chapter 3 of this FSAR. The inner closure plate welds are inspected by performing a liquid penetrant examination of the root pass and final weld surface. The integrity of the top end inner closure plate welds is verified by performing a pneumatic pressure test, and a helium leak test in accordance with the *technical specification* requirements contained in Section 12.3 of the FuelSolutions™ Storage System FSAR. The outer closure plate weld is inspected by performing a liquid penetrant examination of the root pass, intermediate pass, and final weld surface. This weld NDE is in compliance with ISG-4. The associated critical flaw size evaluation to support the NDE acceptance basis is provided in Section 3.9.5 of this FSAR. This critical flaw size evaluation also supports the optional use of UT inspection of the outer closure plate to shell weld.

The structural analysis of the FuelSolutions™ W21 canister, in conjunction with the redundant closures and nondestructive examination, pneumatic pressure testing, and helium leak testing performed during canister fabrication and canister closure, provides assurance of canister closure integrity in lieu of the specific weld joint requirements of Section III, Subsection NB.

Further discussion and justification for the FuelSolutions™ canister closure design and fabrication requirements are provided in Section 2.5.2. Compliance with the ASME Code as it is applied to the design and fabrication of the FuelSolutions™ W21 canister and the associated justification are discussed in Section 2.5.1.

The FuelSolutions™ W21 canister is designed for all normal, off-normal, and postulated accident condition loadings, as defined in Section 2.3. These design loadings include the postulated drop accidents while in the cavity of the FuelSolutions™ W150 Storage Cask or the FuelSolutions™ W100 Transfer Cask, as defined in the FuelSolutions™ Storage System FSAR. The load combinations for which the canister is designed are defined in Section 2.3.5 of this FSAR.

*Thermal*

As discussed in Section 4.3.2 of this FSAR, the FuelSolutions™ W21 canister allowable fuel cladding temperatures imposed to prevent cladding degradation during long-term dry storage conditions are based on a cladding creep methodology, with strains due to creep not exceeding

---

[5] American Society of Mechanical Engineers (ASME) Boiler and Pressure Vessel Code, Section III, Division I, Subsection NF, *Supports*, 1995 Edition.

[6] ISG-4, *Cask Closure Weld Inspections*, Spent Fuel Project Office Interim Staff Guidance-4, United States Nuclear Regulatory Commission, Revision 1, May 21, 1999.

[7] ANSI N14.6, *Special Lifting Devices for Shipping Containers Weighing 10,000 Pounds (4,500 kg) or More*, American National Standards Institute, 1993.

1% and remaining below the tertiary creep regime. In addition, allowable fuel cladding temperatures are developed using the Diffusion Controlled Cavity Growth (DCCG) methodology provided in UCID-21181.[8] The DCCG methodology is not limited by fuel assembly burnup levels and is, therefore, applicable to the full range of burnups for which SNF assemblies are qualified for dry storage by this FSAR. The allowable cladding temperatures, which correspond to moderate and high burnups for the SNF assembly classes to be stored in the FuelSolutions™ W21 canister, are provided in Section 4.3.2 of this FSAR.

The short-term cladding temperature that is applicable to normal and off-normal conditions, as well as the fuel loading, canister closure, and canister transfer operations in the storage cask and transfer cask, is limited to 400°C to avoid accelerated cladding creep and/or cladding annealing effects. For accident conditions, the allowable cladding temperature is 570°C based on PNL-4835.[9] Further, the FuelSolutions™ W21 canister is backfilled with helium during canister sealing operations to promote heat transfer and prevent cladding degradation in accordance with the *technical specification* contained in Section 12.3 of this FSAR.

The allowable temperatures for the structural steel components of the FuelSolutions™ W21 canister are based on the temperature limits provided in ASME Section II, Part D [10] tables referenced in ASME Section III, Subsections NB, NF, and NG, for those load conditions under which material properties are relied on for a structural load combination. For off-normal and accident conditions in which there are no concurrent significant structural loads (e.g., a postulated accidental cask drop), a short-term allowable temperature is established based on ASME Code Case N-47-33.[11] The specific allowable temperatures for the components of the canister are provided in Section 4.3.1 of this FSAR.

The FuelSolutions™ W21 canister is designed for a bounding thermal source term, as described in Section 4.1.5 of this FSAR. The maximum allowable storage cask temperatures are limited when containing the FuelSolutions™ W21 canister, in accordance with the *technical specification* contained in Section 12.3 of this FSAR.

*Shielding*

The allowable doses for an ISFSI or CISF using the FuelSolutions™ Storage System with the FuelSolutions™ W21 canister are delineated in 10CFR72.104 and 72.106.[12] Compliance with this criteria is necessarily site-specific and is to be demonstrated by the licensee, as discussed in Section 2.1.2 of the FuelSolutions™ Storage System FSAR.

---

[8] UCID-21181, *Spent Fuel Cladding Integrity During Dry Storage*, M.W. Schwartz and M.C. Witte, Lawrence Livermore National Laboratory, September 1987.

[9] PNL-4835, *Technical Basis for Storage of Zircaloy-Clad Spent Fuel in Inert Gases*, Johnson, A.B. and Gilbert, E.R., Pacific Northwest Laboratories, September 1983.

[10] American Society of Mechanical Engineers (ASME), Boiler and Pressure Vessel Code, Section II, *Materials*, Part D, *Properties*, 1995 Edition.

[11] Case N-47-33, *Class 1 Components in Elevated Temperature Service*, American Society of Mechanical Engineers (ASME), Boiler and Pressure Vessel Code, 1995 Code Cases, Nuclear Components, 1995 Edition.

[12] Title 10, U.S. Code of Federal Regulations, Part 72 (10CFR72), *Licensing Requirements for the Independent Storage of Spent Nuclear Fuel and High-Level Radioactive Waste*, 1995.

The FuelSolutions™ W21 canister provides axial shielding at the top and bottom ends to maintain occupational exposures ALARA during canister closure and canister transfer operations. The maximum allowable axial dose rates for the FuelSolutions™ W21 canister are controlled in accordance with plant-specific procedures and ALARA requirements (discussed in Section 10.1.3 of the FuelSolutions™ Storage System FSAR).

The FuelSolutions™ W21 canister is designed for the radiological source term specification, as described in Section 5.2 of this FSAR. The radiological source term for the FuelSolutions™ W21 canister is limited based on the Functional and Operating Limits contained in the *technical specification* in Section 12.3 of this FSAR. Representative calculated dose rates for the FuelSolutions™ W21 canister are provided in Section 5.4.2 of the FuelSolutions™ Storage System FSAR. These dose rates are used to perform an occupational exposure evaluation in accordance with 10CFR20,[13] as discussed in Sections 10.1 and 10.3 of the FuelSolutions™ Storage System FSAR.

*Criticality*

The FuelSolutions™ W21 canister provides criticality control for all design basis normal, off-normal, and postulated accident conditions, as discussed in Section 6.3.1 of this FSAR. The effective neutron multiplication factor for storage and transportation is limited to $k_{eff} < 0.95$ for fresh unirradiated intact fuel with optimum fresh water moderation and close reflection, including all biases and uncertainties. In addition, $k_{eff}$ is shown to be less than the upper subcritical limit (USL) established using the methodology presented in NUREG/CR-5661.[14]

Criticality control is maintained by the geometric spacing of the fuel assemblies and fixed borated neutron absorbing materials incorporated into the canister basket assembly. The minimum specified boron concentration verified during material manufacture is further reduced by 25 % for criticality analysis. No credit is taken for soluble boron or burnup. Permanent deformations of the canister basket assembly for postulated accident conditions are considered in the criticality analysis. The maximum allowable initial enrichment for fuel assemblies to be stored in the FuelSolutions™ W21 canister are limited in accordance with the *technical specification* contained in Section 12.3 of this FSAR.

*Confinement*

The FuelSolutions™ W21 canister provides for confinement of all radioactive materials for all design basis normal, off-normal, and postulated accident conditions, as discussed in Sections 1.2.1.3 and 7.1 of this FSAR. An evaluation of the release of available fission products in accordance with specified release fractions based on the canister design leak rate is considered, as discussed in Section 7.3. The confinement function of the FuelSolutions™ W21 canister is verified through pneumatic pressure testing and helium leak testing performed in accordance

[13] Title 10, U.S. Code of Federal Regulations, Part 20 (10CFR20), *Standards for Protection Against Radiation*, 1995.

[14] Dyer, H. R., and Parks, C. V., *Recommendations for Preparing the Criticality Safety Evaluation of Transportation Packages*, NUREG/CR-5661, Oak Ridge National Laboratories, April 1997.

with the *technical specifications* contained in Section 12.3 of the FuelSolutions™ Storage System FSAR.

*Operations*

There are no radioactive effluents that result from storage or transfer operations. Effluents generated during canister loading are handled by the plant's radwaste system and procedures.

Generic operating procedures for the FuelSolutions™ Storage System using the FuelSolutions™ W21 canister are provided in Chapter 8 of the FuelSolutions™ Storage System FSAR. Canister-specific parameters are provided in Chapter 8 of this FSAR. The licensee will develop site-specific detailed operating procedures based on requirements that comply with the 10CFR50[15] *technical specifications* for the plant and the 10CFR72 *technical specifications* contained in Section 12.3 of this FSAR and the FuelSolutions™ Storage System FSAR.

*Acceptance Tests and Maintenance*

The fabrication acceptance basis and maintenance program to be applied to the FuelSolutions™ W21 canister are described in Chapter 9 of this FSAR. The operational controls and limits to be applied to the FuelSolutions™ W21 canister are contained in Chapter 12 of this FSAR and the FuelSolutions™ Storage System FSAR. Application of these requirements will assure that the FuelSolutions™ W21 canister is fabricated, operated, and maintained in a manner that satisfies the design criteria defined in this chapter.

*Decommissioning*

The FuelSolutions™ W21 canister is designed to be transportable and is not required to be unloaded prior to shipment off-site. Decommissioning of the FuelSolutions™ Storage System using the FuelSolutions™ W21 canister is addressed in Chapter 14 of the FuelSolutions™ Storage System FSAR.

[15] Title 10, U.S. Code of Federal Regulations, Part 50 (10CFR50), *Domestic Licensing of Production and Utilization Facilities*, 1995.

This page intentionally left blank.

## 2.2 Spent Fuel to be Stored

The FuelSolutions™ W21 canister is designed to accommodate up to 21 SNF assemblies. The FuelSolutions™ W21 canister accommodates all domestic commercial PWR SNF assembly classes, with the following exceptions:

- South Texas
- Indian Point 1
- Haddam Neck
- San Onofre 1
- CE 16x16 (with control components)
- CE 16x16 System 80 (with control components)

The PWR fuel assemblies may be stored either with or without control components. Most PWR fuel assembly classes are accommodated within the FuelSolutions™ W21 canister without the need for fuel assembly spacers, as described in Section 1.2.1.3. The fuel assembly classes accommodated by the FuelSolutions™ W21 canister, and the corresponding FuelSolutions™ W21 canister class and type designated for use with each fuel assembly class, are provided in Table 1.2-3. Those fuel assembly classes that require the use of either a Type I or Type II fuel assembly spacer are also identified. Table 2.2-1 lists the specific fuel assembly types and associated characteristics acceptable for storage in the FuelSolutions™ W21 canister.

In addition to dimensional acceptance (specified in Table 1.2-3), the SNF assemblies to be stored in the FuelSolutions™ W21 canister must be intact zircaloy-clad fuel with no known or suspected cladding defects greater than pinhole leaks or hairline cracks. For SNF assemblies with burnup exceeding 45 GWd/MTU (up to 60 GWd/MTU), the cladding oxide thickness is limited to 70 μm. It is the responsibility of the licensee to assure that the fuel assemblies to be placed in the FuelSolutions™ W21 canister meet these criteria. Fuel assemblies that do not meet these criteria are considered damaged fuel, and are not acceptable for storage in the FuelSolutions™ W21 canister at this time. Missing or damaged fuel rods may be replaced with dummy rods that displace an equal amount of water as the original rods to permit storage in the FuelSolutions™ W21 canister.

The structural analysis of the FuelSolutions™ W21 canister for the bounding fuel assembly classes (maximum total weight and maximum weight per unit length) and demonstration of compliance with the applicable acceptance criteria, as documented in Chapter 3 of this FSAR, qualifies all the fuel assembly classes listed in Table 1.2-3 for storage in the designated FuelSolutions™ W21 canister class and type (see Tables 1.2-1 and 1.2-2). In addition, the maximum total loaded weight of the FuelSolutions™ W21 canister is shown to be bounded by or equivalent to the design basis canister weight used in the structural analysis of the FuelSolutions™ W150 Storage Cask and W100 Transfer Cask, as documented in Section 2.2 of the FuelSolutions™ Storage System FSAR.

Thermal qualification of the SNF assembly classes listed in Table 1.2-3 for storage in the FuelSolutions™ W21 canister is dependent on the characteristics of the unburned fuel assembly, the characteristics of the fuel assembly at the time of reactor discharge, and the time since

discharge (cooling time). A range of combinations of initial enrichment and burnup are included in the development of thermal and radiological source terms, as documented in Section 5.2 of this FSAR. The required minimum cooling time as a function of initial enrichment and burnup for each fuel assembly class accommodated by the FuelSolutions™ W21 canister is determined such that all thermal acceptance criteria for the FuelSolutions™ Storage System are satisfied as the basis for thermal fuel qualification, as described in Section 5.2 of this FSAR and the FuelSolutions™ Storage System FSAR.

For the purpose of evaluating the thermal performance of the FuelSolutions™ W21 canister, bounding design basis thermal source terms (decay heat power axial peaking profile) are used in the thermal analysis of the canister, as documented in Section 4.1.3 of this FSAR. In addition, the maximum total heat load and the axial heat load distribution for the FuelSolutions™ W21 canister are shown to be bounded by or equivalent to those used in the design basis thermal analysis of the FuelSolutions™ W150 Storage Cask and W100 Transfer Cask, as documented in Section 4.1.3 of the FuelSolutions™ Storage System FSAR.

Radiological qualification of the SNF assembly classes listed in Table 1.2-3 to be stored in the FuelSolutions™ W21 canister is also dependent on the characteristics of the unburned fuel assembly, the characteristics of the fuel assembly at the time of reactor discharge, and the time since discharge (cooling time). A range of combinations of initial enrichment and burnup are included in the development of thermal and radiological source terms, as documented in Section 5.2 of this FSAR. The required minimum cooling time as a function of initial enrichment and burnup for each fuel assembly class accommodated by the FuelSolutions™ W21 canister is determined such that the design basis allowable dose rates for the FuelSolutions™ Storage System are satisfied as the basis for radiological fuel qualification, as described in Section 5.2 of this FSAR and the FuelSolutions™ Storage System FSAR. For the purpose of evaluating the radiological performance of the FuelSolutions™ W21 canister, representative radiological source terms (neutron and gamma) are used in the shielding analysis of the canister, as documented in Section 5.2.2 of this FSAR and the FuelSolutions™ Storage System FSAR. In addition, representative dose rates for the FuelSolutions™ W150 Storage Cask and W100 Transfer Cask are provided in Section 5.4 of the FuelSolutions™ Storage System FSAR.

As documented in Section 6.3 of this FSAR, the criticality analysis for the most reactive fuel assembly classes and the demonstration of compliance with the applicable acceptance criteria, qualifies the fuel assembly classes listed in Table 1.2-3 and the specific fuel assembly types listed in Table 2.2-1 for storage in the designated FuelSolutions™ W21 canister class and type (see Tables 1.2-1 and 1.2-2). The maximum acceptable initial enrichments, regardless of burnup or cooling time for the fuel assembly classes accommodated by the FuelSolutions™ W21 canister, are provided in Section 6.1 of this FSAR and summarized in Table 2.2-1.

The *technical specification* requirements that must be satisfied to qualify SNF assemblies for storage in the FuelSolutions™ W21 canister are included in Section 12.3 of this FSAR.

The FuelSolutions™ W21 canister, as designed, will also accommodate damaged fuel, stainless clad fuel, MOX fuel, and consolidated fuel. The corresponding payload specifications and qualification basis for storage of these contents will be included in a future revision of this FuelSolutions™ Canister Storage FSAR.

## Table 2.2-1 - Fuel Assemblies Acceptable for Storage in the FuelSolutions™ W21 Canister (5 pages)

| Assembly Class(1), (2) | Assembly Type | Maximum Uranium Loading (kg) | Linear Uranium Loading (kg/in) | W21-1(3) Initial Enrichment (w/o $^{235}U$) | W21-2(3) Initial Enrichment (w/o $^{235}U$) | Applicable Cooling Table(4) | | Criticality Class(7) |
|---|---|---|---|---|---|---|---|---|
| | | | | | | Standard(5) | Limiting(6) | |
| **Single Reactor Assembly Classes (continued)** | | | | | | | | |
| Yankee Rowe | CE 15x16 Yankee Rowe | 450 | 3.27 | [5.0 | [5.0 | W21-1-A | W21-1-A | 15x16 |
| | ANF 15x16 Yankee Rowe | | | | | | | |
| | Other(9) | | | | | | | |
| | UNC 15x16 Yankee Rowe | 450 | 3.27 | [5.0 | [5.0 | W21-1-B | W21-1-B | 15x16A |
| | Other(9) | | | | | | | |

Notes: See page 2.2-8.

Table 2.2-1 Notes:

(1) Assembly Class is defined per EIA Spent Fuel Discharge Report.[16]

(2) Fuel cladding shall be zircaloy, including zirconium-niobium alloys (e.g., Zirlo). Maximum assembly burnup is limited to 60,000 MWd/MTU. Fuel assembly dimensions and weights for each fuel assembly class are provided in Table 1.2-3. Fuels with integral fuel burnable absorbers (IFBA) are not qualified for storage at this time.

(3) Fuel loading specifications W21-1 and W21-2 are defined in accordance with Section 2.1.1 of the *technical specifications* contained in Section 12.3.

(4) Cooling tables in Section 5.2 include information on heat load and provide the required cooling time as a function of burnup and initial enrichment, which meets the thermal and radiological acceptance criteria defined in Chapters 4 and 5, respectively.

(5) "Standard" includes fuel assemblies with no control components or with negligible core region cobalt activation. These include thimble plugs, control rod assemblies, and zircaloy clad burnable poison rod assemblies (BPRAs) and axial power shaping rod assemblies (APSRAs).

(6) "Limiting" includes fuel assemblies containing control components with potentially significant cobalt activation. These include neutron source assemblies, and stainless steel clad BPRAs and APSRAs.

(7) Criticality Class definitions are per Table 6.1-1, and include definitions of cladding type and other fuel assembly characteristics relevant to criticality safety.

(8) Gray APSRAs for B&W 15x15 fuel class are not qualified for storage at this time.

(9) Other fuel assemblies that meet the defined parameters are qualified for storage.

(10) CE 16x16 and CE 16x16 System 80 assembly classes are qualified for storage without control components.

[16] Energy Information Administration, *Spent Nuclear Fuel Discharges from U.S. Reactors 1993*, U.S. Department of Energy, 1995.

## 2.3 Design Loadings

The FuelSolutions™ W21 canister is designed to provide safe dry storage of SNF in an ISFSI or CISF for 100 years at any location in the contiguous United States. The storage cask and transfer cask serve to provide biological shielding, physical protection, and structural support for the canister during storage and transfer under all design basis normal, off-normal, and postulated accident conditions, as addressed in the FuelSolutions™ Storage System FSAR. The FuelSolutions™ W21 canister is also designed for off-site transportation.

In accordance with 10CFR72, a range of long- and short-term natural ambient conditions are considered in the thermal evaluation of the W21 canister in the storage cask and transfer cask. These ambient conditions are assumed to occur concurrently with the design basis normal, off-normal, postulated accident (e.g., blocked vents, loss of neutron shield, etc.) and natural phenomena events and form the basis for the design of the W21 canister within the storage cask and transfer cask.

The design basis off-normal, postulated accident, and natural phenomena conditions are defined in Sections 2.3.1.5, 2.3.2.6, and 2.3.4, respectively. Consistent with the definitions in ANSI/ANS-57.9,[17] off-normal events are anticipated to occur with moderate frequency or on the order of once per calendar year. Postulated accident events are defined as those that might occur only once during the use of the canister within the storage cask or transfer cask.

The design basis conditions considered for the FuelSolutions™ W21 canister are as follows:

Normal Conditions

- Normal Ambient Conditions
- Internal Pressure
- Dead Load
- Handling Load
- Leakage of the Confinement Boundary

Off-Normal Conditions

- Extreme Ambient Conditions
- Internal Pressure
- Misaligned Cask During Horizontal Transfer
- Reflood Pressure

[17] ANSI/ANS 57.9, *Design Criteria for an Independent Spent Fuel Storage Installation (Dry Storage Type)*, American National Standards Institute, 1984.

- Hydraulic Ram Failure During Horizontal Transfer
- Leakage of the Confinement Boundary

Accident Conditions

- Accident Thermal Conditions
  - Storage Cask Vent Blockage
  - Transfer Cask Loss of Neutron Shield
- Cask Drop
- Storage Cask Tip-over on J-skid
- Fire
- Internal Pressure
- Leakage of the Confinement Boundary
- Explosive Overpressure

Natural Phenomena

- Flooding
- Tornado
- Earthquake
- Wind
- Burial Under Debris
- Lightning
- Snow and Ice

The canister is designed for the most severe environmental conditions and natural phenomena postulated to occur during storage over the entire service life of the canister, including canister fuel loading, closure, and transfer using the FuelSolutions™ W100 Transfer Cask and canister dry storage in a FuelSolutions™ W150 Storage Cask. The normal environmental conditions include the annual variation of ambient temperature, solar radiation (insolation), wind, snow, and ice. The off-normal environmental conditions include extreme ambient temperatures and insolation. The accident environmental conditions and natural phenomena include wind resulting from a tornado, impact of a missile generated by tornado, flood, earthquake, fire, and explosion. Totally blocked inlet and/or outlet vents on the storage cask and loss of the neutron shield on the transfer cask are also included in the accident conditions.

The effects of the normal, off-normal, and accident condition loadings defined in this section on the FuelSolutions™ W150 Storage Cask and W100 Transfer Cask are evaluated in the FuelSolutions™ Storage System FSAR.

## 2.3.1 Normal Conditions

### 2.3.1.1 Normal Ambient Conditions

The ambient conditions used for the design basis analysis of the FuelSolutions™ W21 canister for normal conditions are provided in Section 2.3.1.1 of the FuelSolutions™ Storage System FSAR. The corresponding structural and thermal analyses of the FuelSolutions™ W21 canister for normal ambient conditions during canister fuel loading, closure, transfer, and dry storage are documented in Sections 3.5 and 4.4 of this FSAR.

### 2.3.1.2 Internal Pressure

The normal condition internal pressure for the FuelSolutions™ W21 canister during dry storage is based on the initial canister helium backfill pressure, the normal condition canister temperatures, and an assumed failure of 1% of the fuel rods with complete release of their associated fill gases and 30% of their fission gases to the canister cavity. The design basis internal pressure for this condition is 10 psig. The structural effects of normal condition internal pressure on the canister are evaluated in Section 3.5 of this FSAR.

Normal condition internal pressure during draining of the canister cavity after the inner closure plate is welded to the canister shell is also evaluated. This load is defined as a 30 psig internal pressure, which is monitored in accordance with the operating procedures contained in Section 8.1.8 of the FuelSolutions™ Storage System FSAR. The structural effects of this load are also evaluated in Section 3.5 of this FSAR.

### 2.3.1.3 Dead Load

This load includes the dead weight of the materials of construction and the contents for the FuelSolutions™ W21 canister, acting either horizontally or vertically.

### 2.3.1.4 Handling Load

For normal conditions, this load includes normal handling loads associated with vertical or horizontal transfer of the FuelSolutions™ W21 canister from or to a FuelSolutions™ W100 Transfer Cask, and to or from a FuelSolutions™ W150 Storage Cask or a transportation cask.

For vertical canister transfer, the handling load is defined as 15%[18] of the maximum loaded canister weight, which acts on the top end outer closure plate of the canister. For horizontal canister transfer between a storage cask, transfer cask, or transportation cask, the handling load is defined as a pushing or pulling axial force of 45,000 pounds acting on the outer closure plate of either end of the canister due to friction forces that developed between the canister shell and cask rails. The vibration loading normally incident to on-site transfer is conservatively defined in

[18] CMAA #70, *Specifications for Electric Overhead Traveling Cranes*, Crane Manufacturers Association of America (CMAA), 1988.

accordance with NUREG/CR-0128[19] as ±0.6 *g* acting in the vertical direction, ±0.3 *g* acting in the longitudinal direction, and ±0.2 *g* acting in the lateral direction, simultaneously.

The structural effects of normal condition handling loads on the canister are evaluated in Section 3.5 of this FSAR. The effects of these loads on the FuelSolutions™ W100 Transfer Cask and W150 Storage Cask are addressed in the FuelSolutions™ Storage System FSAR.

#### 2.3.1.5 Leakage of the Confinement Boundary Under Normal Conditions

The FuelSolutions™ W21 canister is evaluated for the release of internal gases and aerosol contents to the atmosphere based on the design leak rate of the canister as defined in the *technical specification* in Section 12.3 of the FuelSolutions™ Storage System FSAR. It is assumed for this evaluation that 1% of all fuel rods fail. The corresponding nuclide release fractions are used to determine the quantity of radioactive material available for release. The radiological evaluation for this postulated event, including the assumptions used in the analysis, is documented in Section 7.2 of this FSAR.

### 2.3.2 Off-Normal Conditions

#### 2.3.2.1 Extreme Ambient Conditions

The extreme ambient conditions used for the design basis analysis of the FuelSolutions™ W21 canister for off-normal conditions are provided in Section 2.3.2.1 of the FuelSolutions™ Storage System FSAR. The temperature distribution in the canister for off-normal conditions and comparisons to allowable values is provided in Section 4.5 of this FSAR. The structural effects of off-normal condition temperatures on the canister are evaluated in Section 3.6 of this FSAR.

#### 2.3.2.2 Internal Pressure

The off-normal condition internal pressure for the FuelSolutions™ W21 canister during dry storage is based on the initial canister helium backfill pressure, the off-normal condition canister temperatures, and an assumed failure of 10% of the fuel rods with complete release of their associated fill gases and 30% of their fission gases to the canister cavity. The design basis internal pressure for this condition is 16 psig. The structural effects of off-normal condition internal pressure on the canister are evaluated in Section 3.6 of this FSAR.

The off-normal condition internal pressure is conservatively used as the initial condition for the evaluation of the FuelSolutions™ W21 canister for the postulated blockage of the storage cask vents discussed in Section 2.3.3.1.

---

[19] NUREG/CR-0128, *Shock and Vibration Environment for a Large Shipping Container During Truck Transport*, U.S. Nuclear Regulatory Commission, May 1978.

- Off-Normal Loads – Extreme ambient conditions, off-normal internal pressure, misalignment during canister horizontal transfer, reflood.
- Postulated Accident and Natural Phenomena Loads – Complete blockage of storage cask air inlet and outlet vents, transfer cask loss of neutron shield, cask drop, cask tip-over, fire, accident internal pressure, flood, earthquake.

The FuelSolutions™ W21 canister internal basket and shell assembly components are designed for the load combinations shown in Table 2.3-1. These combinations are categorized based on the ASME service level criteria for evaluation against the associated allowable values. The allowable values are provided in Chapter 3 of this FSAR.

Load combination results and comparisons to allowable values for the FuelSolutions™ W21 canister for normal, off-normal, and accident conditions are provided in Sections 3.5, 3.6, and 3.7 of this FSAR, respectively.

## Table 2.3-1 - W21 Canister Load Combinations[1,2]

| Comb. No. | Dead-weight | Handling | Internal Pressure | Thermal | Earth-quake | Drop or Tip-over | Flood |
|---|---|---|---|---|---|---|---|
| **Normal Operating Conditions (Service Level A)** | | | | | | | |
| A1 | $D_{V1}$ | | $P_b$ | | | | |
| A2 | $D_v$ | | P | T | | | |
| A3 | $D_h$ | | P | T | | | |
| A4 | $D_v$ | $L_{hv}$ | P | T | | | |
| A5 | $D_h$ | $L_{hh1}$ or $L_{hh2}$ | P | T | | | |
| **Off-Normal Conditions (Service Level B)** | | | | | | | |
| B1 | $D_v$ | | $P_o$ | $T_o$ | | | |
| B2 | $D_v$ | $L_{hv}$ | $P_o$ | $T_o$ | | | |
| B3 | $D_h$ | $L_{hh1}$ or $L_{hh2}$ | $P_o$ | $T_o$ | | | |
| B4 | $D_h$ | $L_m$ | P | T | | | |
| **Off-Normal Conditions (Service Level C)** | | | | | | | |
| C1 | $D_v$ | | $P_r$ | $T_r$ | | | |
| **Postulated Accident Conditions (Service Level D)** | | | | | | | |
| D1 | $D_v$ | $L_{hv}$ | $P_a$ | $T_o$ | | | |
| D2 | $D_h$ | $L_{hh1}$ or $L_{hh2}$ | $P_a$ | $T_o$ | | | |
| D3 | | | $P_o$ | T | | $A_S$ | |
| D4 | | | $P_o$ | T | | $A_t$ | |
| D5 | | | $P_o$ | T | | $A_{S1}$ | |
| D6 | $D_v$ or $D_h$ | | $P_o$ | T | E | | |
| D7 | $D_v$ or $D_h$ | | $P_o$ | $T_a$ | | | |
| D8 | $D_v$ | | P | T | | | F |

Table 2.3-1 Notes:

(1) Allowable canister shell stresses are in accordance with ASME Section III, Subsections NB and NF. Allowable canister basket stresses are in accordance with ASME Section III, Subsection NG.

(2) Load definitions are as follows:

$D_v$ = Loading due to deadweight - vertical canister

$D_{V1}$ = Loading due to deadweight - vertical canister with weight of auxiliary shield plate and automated welder, excluding weight of outer closure plate

(continued on next page)

# 2.5 Supplemental Information

## 2.5.1 ASME Code Compliance

As discussed in Section 2.1.2, the FuelSolutions™ W21 canister is designed and fabricated with Section III of the ASME Code to the maximum extent practicable, consistent with other canister-based dry storage systems previously approved by the NRC. The clarifications made to the applicable portions of the ASME Code and the basis for these clarifications is provided in Table 2.5-1.

## Table 2.5-1 - ASME Code Requirements Compliance Summary (13 pages)

| Item | ASME Code Requirement | Issue | Alternative Compliance Basis |
|---|---|---|---|
| **Section III, Subsection NCA (applicable to both Canister and Basket):** | | | |
| 1 | **General for Subsection NCA** | 1. The terms "Certificate Holder" and "Owner" used throughout this subsection are not applicable for a 10CFR72 system.<br>2. The Division 2 (concrete) requirement provided throughout this subsection are not applicable for a 10CFR72 system. | 1. BNFL Fuel Solutions (BFS) bears the responsibilities associated with a "Certificate Holder" or "Owner" relative to the FuelSolutions™ SFMS.<br>2. This compliance summary table only addresses FuelSolutions™ canisters, which do not contain any concrete. |
| 2 | **NCA-1140, "Use of Code Editions, Addenda, and Cases:"**<br>"(a)(1) Under the rules of this Section, the Owner or his designees shall establish the Code Edition and Addenda to be included in the Design Specifications . . ." | The FuelSolutions™ SFMS documentation does not include an ASME Code Design Specification. | The requirements and criteria typically contained in an ASME Code Design Specification are contained in this FSAR. |

## Table 2.5-1 - ASME Code Requirements Compliance Summary (13 pages)

| Item | ASME Code Requirement | Issue | Alternative Compliance Basis |
|---|---|---|---|
| 3 | **NCA-1210, "Components:"**<br>"Each component of a nuclear power plant shall require a Design Specification (NCA-3250), Design Report (NCA-3350, NCA-3550), and other design documents specified in NCA-3800. Data Reports and stamping shall be as required in NCA-8000." | The FuelSolutions™ SFMS documentation does not contain the following ASME Code documents:<br>1. Design Specification<br>2. Design Report<br>3. Owner's Certificate of Authorization<br>4. Authorized Inspection Agency Written Agreement<br>5. Owner's Data Report<br>6. Overpressure Protection Report. | 1. See Item 2.<br>2. The information typically reported in an ASME Code Design Report is contained in this FSAR.<br>3. An Owner's Certificate of Authorization, a written agreement with an Authorized Inspection Agency, an Owner's Data Report, and an Overpressure Protection Report are not typically provided for components licensed under 10CFR72. |
| 4 | **NCA-1220, "Materials"** | Not all non-pressure retaining materials specified in this FuelSolutions™ Canister Storage FSAR are listed as ASME Section III materials. | FuelSolutions™ canisters are purchased, identified, controlled, and manufactured using a graded quality approach in accordance with the NRC-approved BFS QA Program based on NQA-1, NRC Regulatory Guide 7.10, and NUREG/CR-6407 criteria. |
| 5 | **NCA-1281, "Activities and Requirements:"**<br>"... Data Reports and stamping shall be as required in NCA-8000." | See Item 19. | See Item 19. |
| 6 | **NCA-2000, "Classification of Components"** | The classification of components is usually provided in a Design Specification. | See Item 2. |

## Table 2.5-1 - ASME Code Requirements Compliance Summary (13 pages)

| Item | ASME Code Requirement | Issue | Alternative Compliance Basis |
|---|---|---|---|
| 7 | **NCA-2142, "Establishment of Design, Service, and Test Loadings and Limits:"**<br>"In the Design Specification, the Owner or his designee shall identify the loadings and combinations of loadings and establish the appropriate Design, Service, and Test Limits for each component or support . . ." | See Item 2. | See Item 2. |
| 8 | **NCA-3100, "General"** | ASME Code accreditation does not apply. | See Item 1. |
| 9 | **NCA-3200, "Owner's Responsibilities"** | An Owner's responsibilities under the ASME Code do not apply. | An Owner's Certificate of Authorization, a Design Specification, a Design Report, an Overpressure Protection Report, and an Owner's Data Report are not typically provided for components licensed under 10CFR72. |
| 10 | **NCA-3300, "Responsibilities of a Designer - Division 2"** | See Item 1. | See Item 1. |
| 11 | **NCA-3400, "Responsibilities of an N Certificate Holder - Division 2"** | See Item 1. | See Item 1. |
| 12 | **NCA-3500, "Responsibilities of an N Certificate Holder - Division 1"** | See Item 1. | See Item 1. Design and fabrication requirements are provided in this FSAR and related procurement/fabrication drawings and specifications. |
| 13 | **NCA-3600, "Responsibilities of an NPT Certificate Holder"** | See Item 1. | See Item 12. |
| 14 | **NCA-3700, "Responsibilities of an NA Certificate Holder"** | See Item 1. | See Item 12. |

## Table 2.5-1 - ASME Code Requirements Compliance Summary (13 pages)

| Item | ASME Code Requirement | Issue | Alternative Compliance Basis |
|---|---|---|---|
| 15 | **NCA-3800, "Metallic Material Organization's Quality System Program"** | Materials for a FuelSolutions™ canister may be purchased from suppliers that are not certified per the requirements of NCA-3800. | Material suppliers are qualified per NCA-3800 or the NRC-approved BFS QA Program based on the requirements of NQA-1, NRC Regulatory Guide 7.10, and NUREG/CR-6407 criteria. |
| 16 | **NCA-3900, "Nonmetallic Material Manufacturer's and Constituent Suppliers Quality System Programs"** | See Item 1. | See Item 1. |
| 17 | **NCA-4000, "Quality Assurance"** | These QA requirements do not apply. | See Item 4. |
| 18 | **NCA-5000, "Authorized Inspection"** | The manufacturing or operation of the FuelSolutions™ SFMS does not use an Authorized Inspection Agency. | An Authorized Inspection Agency is not typically used in the manufacturing or operation of components licensed under 10CFR72. |
| 19 | **NCA-8000, "Certificates of Authorization, Nameplates, Code Symbol Stamping, and Data Reports"** | The FuelSolutions™ SFMS does not use an ASME Code Certificate of Authorization, a Code Symbol Stamp, or a Data Report. | An ASME Code Certificate of Authorization, a Code Symbol Stamp, or a Data Report are not typically required for components licensed under 10CFR72. Nameplate information is provided on each FuelSolutions™ canister. |
| **Section III, Subsection NB (applicable to Canister pressure-retaining components):** | | | |
| 20 | **NB-1130, "Boundary of Components:"**<br>"The Design Specification shall define the boundary of a component to which piping or another component is attached." | See Item 6. | See Item 6. |

## Table 2.5-1 - ASME Code Requirements Compliance Summary (13 pages)

| Item | ASME Code Requirement | Issue | Alternative Compliance Basis |
|---|---|---|---|
| 21 | **NB-1132.2, "Jurisdictional Boundary:"**<br>"The jurisdictional boundary between a pressure-retaining component and an attachment defined in the Design Specification shall not be any closer to the pressure-retaining portion of the component than as defined in (a) through (g) below . . ." | See Item 6. | See Item 6. |
| 22 | **NB-2160, "Deterioration of Material In Service:"**<br>"It is the responsibility of the Owner to select material suitable for the conditions stated in the Design Specifications (NCA-3250), with specific attention being given to the effects of service conditions upon the properties of the material. . . . Any special requirement shall be specified in the Design Specifications (NCA-3252 and NB-3124) . . ." | See Item 2. | See Item 2. |
| 23 | **NB-2610, "Documentation and Maintenance of Quality System Programs:"**<br>"(a) Except as provided in (b) below, Material Manufacturers and Material Suppliers shall have a Quality System Program or an Identification and Verification Program, as applicable, which meets the requirements of NCA-3800 . . ." | See Item 15. | See Item 15. |

## Table 2.5-1 - ASME Code Requirements Compliance Summary (13 pages)

| Item | ASME Code Requirement | Issue | Alternative Compliance Basis |
|---|---|---|---|
| 24 | **NB-3113, "Service Conditions:"**<br>"Each service condition to which the components may be subjected shall be classified in accordance with NCA-2142 and Service Limits (NCA-2142.4(b)) designated in the Design Specifications in such detail as will provide a complete basis for design, construction, and inspection in accordance with this Article . . ." | See Item 2. | See Item 2. |
| 25 | **NB-3134, "Leak Tightness:"**<br>"Where a system leak tightness greater than that required or demonstrated by a hydrostatic test is required, the leak tightness requirements for each component shall be set forth in the Design Specifications." | See Item 2. | See Item 2. |
| 26 | **NB-3220, "Stress Limits for Other Than Bolts"** | This section makes a number of references to an ASME Code Design Specification. See Item 2. | See Item 2. |
| 27 | **NB-4121, "Means of Certification:"**<br>"The Certificate Holder for an item shall certify, by application of the appropriate Code Symbol and completion of the appropriate Data Report in accordance with NCA-8000, that materials used comply with the requirements of NB-2000 and that the fabrication or installation complies with the requirements of this Article." | The FuelSolutions™ SFMS does not use an ASME Code Symbol Stamp or a Data Report. | An ASME Code Symbol Stamp or Data Report are not typically required for components licensed under 10CFR72. Also see Item 15. |

## Table 2.5-1 - ASME Code Requirements Compliance Summary (13 pages)

| Item | ASME Code Requirement | Issue | Alternative Compliance Basis |
|---|---|---|---|
| 28 | **NB-4243, "Category C Weld Joints in Vessels and Similar Weld Joints in Other Components:"**<br>"Category C weld joints in vessels and similar weld joints in other components shall be full penetration joints . . . Either a butt welded joint or a full penetration corner joint as shown in Fig. NB-4243-1 shall be used." | The FuelSolutions™ canister top end closure employs the following cover-to-shell weld types:<br>1. Top inner cover - a single-sided partial penetration weld.<br>2. Top outer cover - a single-sided partial penetration weld. | The FuelSolutions™ canister top end closure employs multi-pass, redundant welds subjected to multi-level liquid penetrant examinations and a combined pneumatic pressure and helium leak rate test at a hydrostatic test pressure to assure structural integrity and leak tightness.<br>The design of the inner closure weld incorporates a stress-reduction factor of 0.9 to account for use of multi-pass PT examination and helium leak testing. The design of the outer closure weld complies with ISG-4.<br>The examination of the inner and outer closure plate welds complies with guidance provided in ISG-4. |
| 29 | **NB-5231, "General Requirements:"**<br>"(a) Category C full penetration butt welded joints in vessels and similar welded joints in other components shall be examined by the radiographic and either liquid penetrant or magnetic particle method." | The FuelSolutions™ canister top end closures are not radiographically examined. | See Item 28. |

## Table 2.5-1 - ASME Code Requirements Compliance Summary (13 pages)

| Item | ASME Code Requirement | Issue | Alternative Compliance Basis |
|---|---|---|---|
| 30 | **NB-6112, "Pneumatic Testing:"**<br>"A pneumatic test in accordance with NB-6300 may be substituted for the hydrostatic test when permitted by NB-6112.1(a)."<br>**NB-6112.1, "Pneumatic Test Limitations:"**<br>"(a) A pneumatic test may be used in lieu of a hydrostatic test only when any of the following conditions exists:<br>(1) when components, appurtenances, or systems are so designed or supported that they cannot safely be filled with liquid;<br>(2) when components, appurtenances, or systems which are not readily dried are to be used in services where traces of the testing medium cannot be tolerate.<br>(b) A pneumatic test at a pressure not to exceed 25% of the Design Pressure may be applied, prior to either a hydrostatic or a pneumatic test, as a means of locating leaks." | The FuelSolutions™ canisters employ a combined pneumatic pressure and helium leak rate test at a hydrostatic test pressure to assure structural integrity and leak tightness. | Because a dry SNF assembly storage canister is a 10CFR72 licensed component requiring a helium leak rate test, the combination of this leak rate test with a pneumatic pressure test at a hydrostatic test pressure is operationally efficient and consistent with ALARA principles, while still being very conservative due to the molecular size of the testing medium and the use of helium leak rate vs. visual examination acceptance criteria. |
| 31 | **NB-6200, "Hydrostatic Tests"** | See Item 30. | See Item 30. |
| 32 | **NB-7000, "Overpressure Protection"** | A FuelSolutions™ canister is not designed to include an overpressure protection device. | By their very nature, canisters and casks designed to dry store SNF assemblies are licensed without any type of overpressure protection device or vent path of any kind. |

## Table 2.5-1 - ASME Code Requirements Compliance Summary (13 pages)

| Item | ASME Code Requirement | Issue | Alternative Compliance Basis |
|---|---|---|---|
| 33 | **NB-8000, "Nameplates, Stamping, and Reports"** | The FuelSolutions™ SFMS does not use an ASME Code Symbol Stamp or a Data Report. | An ASME Code Symbol Stamp or a Data Report are not typically required for components licensed under 10CFR72. Nameplate information is provided on each FuelSolutions™ canister. |
| **Section III, Subsection NG (applicable to Basket):** | | | |
| 34 | **NG-2160, "Deterioration of Material In Service:"**<br>"It is the responsibility of the Owner to select material suitable for the conditions stated in the Design Specifications (NCA-3250), with specific attention being given to the effects of service conditions upon the properties of the material." | See Item 2. | See Item 2. |
| 35 | **NG-2330, "Test Requirements and Acceptance Standards"** | FuelSolutions™ canister basket material is not impact tested to the requirements of NG-2330. | Canister basket is licensed for storage and transportation, and therefore materials are impact tested in accordance with NRC criteria provided in Regulatory Guide 7.11 and NUREG/CR-6407 for Category II materials. |
| 36 | **NG-2610, "Documentation and Maintenance of Quality System Programs:"**<br>"(a)Except as provided in (b) below, Material Manufacturers and Material Suppliers shall have a Quality System Program or an Identification and Verification Program, as applicable, which meets the requirements of NCA-3800 . . ." | See Item 15. | See Item 15. |

## Table 2.5-1 - ASME Code Requirements Compliance Summary (13 pages)

| Item | ASME Code Requirement | Issue | Alternative Compliance Basis |
|---|---|---|---|
| 37 | **NG-3113, "Service Loadings:"**<br>"Each loading to which the structure may be subjected shall be classified in accordance with NCA-2142 and Service Limits (NCA-2142.4(b)) designated in the Design Specifications in such detail as will provide a complete basis for design, construction, and inspection in accordance with this Article . . ." | See Item 2. | See Item 2. |
| 38 | **NG-3220, "Stress Limits for Other Than Threaded Structural Fasteners"** | This section makes a number of references to an ASME Code Design Specification. See Item 2. | See Item 2. |
| 39 | **NG-4121, "Means of Certification:"**<br>"The Certificate Holder for an item shall certify, by application of the appropriate Code Symbol and completion of the appropriate Data Report in accordance with NCA-8000, that materials used comply with the requirements of NG-2000 and that the fabrication or installation complies with the requirements of this Article." | The FuelSolutions™ SFMS does not use an ASME Code Symbol Stamp or a Data Report. | An ASME Code Symbol Stamp or Data Report are not typically required for components licensed under 10CFR72. Also see Item 15. |
| 40 | **NG-8000, "Nameplates, Stamping, and Reports"** | The FuelSolutions™ SFMS does not use an ASME Code Symbol Stamp or a Data Report. | An ASME Code Symbol Stamp or a Data Report are not typically required for components licensed under 10CFR72. Nameplate information is provided on each FuelSolutions™ canister. |

## Table 2.5-1 - ASME Code Requirements Compliance Summary (13 pages)

| Item | ASME Code Requirement | Issue | Alternative Compliance Basis |
|---|---|---|---|
| **Section III, Subsection NF (applicable to Canister non-pressure retaining components):** | | | |
| 41 | **NF-1111.1, "Design Requirements:"**<br>**"In addition to the requirements of NCA-3240, the Owner shall be responsible that loads . . . are adequately transferred without loss of the pressure boundary integrity for the Design or Service Loadings specified in the Design Specification governing the component or piping."** | See Item 2. | See Item 2. |
| 42 | **NF-1130, "Boundaries of Jurisdiction"** | See Item 6. | See Item 6. |
| 43 | **NF-2130, "Certification of Material:"**<br>**"(a) Material used in construction of component supports shall be certified. Certified Material Test Reports in accordance with NCA-3867.4 shall be provided."** | See Item 15. | See Item 15. When CMTRs are required by the BFS Quality Assurance Program, they will be provided per the requirements of NCA-3862. |
| 44 | **NF-2160, "Deterioration of Material In Service:"**<br>**"It is the responsibility of the Owner to select material suitable for the conditions stated in the Design Specifications (NCA-3250), with specific attention being given to the effects of Service Conditions upon the properties of the material."** | See Item 2. | See Item 2. |
| 45 | **NF-2310, "Material to be Impact Tested"** | See Item 6. | See Item 6. |

## Table 2.5-1 - ASME Code Requirements Compliance Summary (13 pages)

| Item | ASME Code Requirement | Issue | Alternative Compliance Basis |
|---|---|---|---|
| 46 | **NF-2610, "Documentation and Maintenance of Quality System Programs:"**<br>**"(a) Except as provided in (b) below. Material Manufacturers and Material Suppliers shall have a Quality System Program or an Identification and Verification Program, as applicable, which meets the requirements of NCA-3800 . . . ."** | See Item 15. | See Item 15. |
| 47 | **NF-3113, "Service Conditions:"**<br>**"Each service condition to which the piping or component may be subjected shall be categorized in accordance with NCA-2142.2 and Service Limits [NCA-2142.4(b)] designated in the Design Specifications in such detail as will provide a complete basis for design in accordance with this Article."** | See Item 2. | See Item 2. |
| 48 | **NF-3132, "Stress Analysis:"**<br>**"A detailed stress analysis or Design Report, as required by NCA-3550 for all piping or component supports, shall be prepared in sufficient detail to show that each of the stress limits of NF-3200 or NF-3300 is satisfied when the piping component support is subjected to the loadings of NF-3110."** | See Item 3. | See Item 3. |
| 49 | **NF-3220, "Design by Analysis for Class 1"** | See Item 3. | See Item 3. |

## Table 2.5-1 - ASME Code Requirements Compliance Summary (13 pages)

| Item | ASME Code Requirement | Issue | Alternative Compliance Basis |
|---|---|---|---|
| 50 | **NF-4121, "Means of Certification:"**<br>**"The Certificate Holder for an item shall certify, by application of the appropriate Code Symbol and completion of the appropriate Data Report in accordance with NCA-8000, that materials used comply with the requirements of NB-2000 and that the fabrication or installation complies with the requirements of NF-4000."** | The FuelSolutions™ SFMS will not use an ASME Code Symbol Stamp or a Data Report. | ASME Code Symbol Stamping or a Data Report is not typically required for components licensed under 10CFR72. Also see Item 15. |
| 51 | **NF-4213, "Qualification of Forming Processes for Impact Property Requirements"** | See Item 2. | See Item 2. |
| 52 | **NF-8000, "Nameplates, Stamping, and Reports"** | The FuelSolutions™ SFMS will not use ASME Code Symbol Stamping or a Data Report. | ASME Code Symbol Stamping or a Data Report is not typically required for components licensed under 10CFR72. Nameplate information will be provided on the FuelSolutions™ W21 Canister. |

## 2.5.2 FuelSolutions™ Canister Top End Closure Weld Design Basis and Nondestructive Examination Justification

This FSAR section discusses the FuelSolutions™ canister top end closure design basis, including the justification for performing PT examination of the canister closure welds. The canister top end closure design and examination are in compliance with the guidance provided in NRC Interim Staff Guidance #4 (ISG-4).

### 2.5.2.1 Introduction

The NRC has recently raised concerns relative to top closure weld details and nondestructive examination (NDE) practices used in canisters for the storage of dry SNF assemblies. As required by 10CFR72 for independent SNF assembly and high-level radioactive waste storage systems, a "cask" must be designed to provide redundant sealing of confinement systems (10CFR72.236(c)) and be inspected to ascertain that there are no "cracks, pinholes, uncontrolled voids, or other defects" that could significantly reduce confinement effectiveness (10CFR72.236(j)). The current NRC concerns are based on recurring defects in Ventilated Storage Cask (VSC)-24 canister closure welds since 1995, as discussed in a recent NRC inspection report.[20]

The following presents a justification for the closure weld details and the associated NDE for the FuelSolutions™ canisters to be used to dry store SNF assemblies. The weld details and examination and testing practices described herein meet or exceed those for existing NRC-certified systems. They are based on related operating experience gained since the late 1980s and the resulting steady evolution in canister weld geometry and welding processes. This supplement also addresses technical issues raised by the VSC-24 closure weld details as they relate to a FuelSolutions™ canister.

### 2.5.2.2 NUREG-1536 Criteria

NUREG-1536[21] provides guidelines for use by the NRC staff in the preparation of safety reviews for dry cask storage systems. NUREG-1536 provides the following statements concerning canister closure details and inspection practices:

Section 3.0, "Structural Evaluation," paragraph V.1.b.ii, "Structural Design Features:"

> *"Review confinement boundary weld designs for compliance with the design code used for the confinement boundary. Acceptable requirements appear in ASME* (American Society of Mechanical Engineers) *Code* (Boiler and Pressure Vessel Code - BPVC) *Section III, Subsections NB-3352 and NC-3352, "Permissible*

[20] Inspection Report 72-1007/97-212, U.S. Nuclear Regulatory Commission, August 29, 1997.

[21] NUREG-1536, *Standard Review Plan for Dry Cask Storage Systems*, U.S. Nuclear Regulatory Commission, January 1997.

*Types of Welded Joints," and NB-4240 and NC-4240, "Requirements for Weld Joints in Components."*

*The NRC has previously accepted alternative confinement boundary weld designs (such as NB-5200 or NC-5200, typically for Category C welded joints). These acceptable alternatives achieve equivalent structural integrity, but do not meet all the provisions of NB-3352 or NC-3352 for full penetration welds, or do not meet the NDE requirements for full volumetric nondestructive examination. The NRC has also accepted alternative designs for the welds of the head or flat end plate to the cylindrical portion of the confinement vessel. However, the NRC has required the alternative designs to include redundant welds to provide redundant sealing of the confinement systems."*

Section 7.0, "Confinement Evaluation," paragraph III.3, "Redundant Sealing:"

*"The cask design must provide redundant sealing of the confinement boundary. (10 CFR 72.236(e))."*

Section 7.0, paragraph V.2, "Confinement Monitoring Capabilities:"

*"For redundant seal welded closures, ensure that the applicant has provided adequate justification that the seal welds have been sufficiently tested and inspected to ensure that the weld will behave similarly to the adjacent parent material of the cask. Any inert gas should not leak or diffuse through the weld and cask material in excess of the design leak rate."*

Section 8.0, "Operating Procedures," paragraph V.1, "Welding and Sealing:"

*"For seal-welded confinement cask closures, and to ensure ALARA, verify that the SAR specifies the use of a remotely operated welder to make seal welds of the confinement closures. Also verify that the procedures provide for acceptable non-destructive examination of these welds. In addition to leak testing discussed above, the NRC accepts dye penetrant tests on both the root and cover pass of the seal welds on the confinement cask closures (including inner closure; any closure over vent accesses for draining, evacuating, purging, and backfilling the cask interior; and the outer closure).*

*Verify that the SAR includes acceptable provisions for correction of weld defects and any additional drying and purging that may be necessary. Weld tests should be specified, and be in compliance with descriptions for those tests in the American Society of Mechanical Engineers (ASME) Boiler and Pressure Vessel Code (B&PV)."*

Section 9.0, "Acceptance Tests and Maintenance Program," paragraph IV, "Acceptance Criteria:"

*"In general, the acceptance tests and maintenance programs outlined in the SAR should cite appropriate authoritative codes and standards. The staff has previously accepted the following as the regulatory basis for the design, fabrication, inspection, and testing of DCSS components: . . ."*

| *SYSTEM/COMPONENT* | *ACCEPTABLE REGULATORY BASIS** |
|---|---|
| *Confinement System* | *American Society of Mechanical Engineers (ASME), "Boiler and Pressure Vessel (B&PV) Code," Section III, Subsection NB or NC.*<br><br>*"American National Standard for Radioactive Materials— Leakage Tests on Packages for Shipment" (ANSI N14.5-1987).* |
| --- | --- |
| * *The SAR should clearly identify any exceptions to the listed codes and standards.* | |

Section 9.0, paragraph V.1.a, "Visual and Nondestructive Inspections:"

*"Confinement boundary welds and welds for components associated with redundant sealing, must meet the requirements of ASME Code, Section III, Article NB/NC-5200, "Required Examination of Welds." This section generally requires RT for volumetric examination and either PT or MT for surface examination. The ASME-approved specifications for RT, PT, and MT are detailed in ASME Code, Section V, Articles 2, 6, and 7, respectively.*

*For confinement welds that cannot be volumetrically examined using RT, the licensee may use 100-percent UT. The ASME-approved UT specifications are detailed in ASME Code, Section V, Article 5. Acceptance criteria should be defined in accordance with NB/NC-5330, "Ultrasonic Acceptance Standards." Cracks, lack of fusion, or incomplete penetration are unacceptable, regardless of length.*

*The NRC has accepted multiple surface examinations of welds, combined with helium leak tests for inspecting the final redundant seal welded closures."*

Section 9.0, paragraph V.1.b, "Structural/Pressure Tests:"

*"The confinement boundary (including that of the redundant seal) should be hydrostatically tested to 125 percent of the design pressure, in accordance with ASME Code, Section III, Article NB-6000. (Article NCA-2142.1, defines the design pressure as it applies to Level A Service Limits. As such, in determining the design pressure, the licensee should consider fission gas release from 1 percent of the fuel rods.) The test pressure should be maintained for a minimum of 10 minutes, after which a visual inspection should be performed to detect any leakage. All accessible welds should be inspected using PT. Any evidence of cracking or permanent deformation should constitute cause for rejection. SAR Section 9 should clearly specify the hydrostatic test pressure."*

Section 9.0, paragraph V.1.c, "Leak Tests:"

> *"The licensee should perform leak tests on all boundaries relevant to confinement. These include the primary confinement boundary, the boundary of the redundant seal, and (if applicable) any additional boundaries used in the pressure monitoring system. For all-welded cask confinements, the NRC staff has, with adequate justification, considered it acceptable for licensees to omit leak testing of the second cask closure weld and the seal welds for the closure plates of the purge and vent valves. For such cases, leak testing must show that the inner closure weld meets the leakage limits."*

In addition to these requirements, NRC has issued ISG-4 regarding cask closure weld inspections. This guidance states that the "closure weld for the outer cover plate for austenitic stainless steel designs may be inspected using either volumetric or multiple pass dye penetrant techniques", subject to certain conditions.

As demonstrated in this section, the FuelSolutions™ canister closure weld design, NDE, and leak testing requirements are in complete compliance with NUREG-1536 and ISG-4. Any exceptions to the ASME Code requirements that are taken are consistent with NUREG-1536 and ISG-4.

### 2.5.2.3 Background

The FuelSolutions™ canister closure weld design, NDE, and leak testing requirements are based on operating experience gained since the late 1980s and the resulting steady evolution in canister weld geometry and welding process improvements. An Electric Power Research Institute (EPRI) report, NP-6941,[22] documents closure welding issues observed and solutions implemented during the Carolina Power & Light (CP&L)/DOE Cooperative Dry Storage Demonstration Project in the late 1980s. The purpose of this project was to performance test the handling/loading practices and heat transfer and shielding characteristics of the NUHOMS®-07P[23] SNF dry storage system. The system used an IF-300 transportation cask to transfer loaded Dry Shielded Canisters (DSCs) from the plant's fuel building to Horizontal Storage Modules (HSMs) within an ISFSI at the H. B. Robinson Nuclear Power Plant.

Figure 2.5-1 presents the general configuration of the original NUHOMS® DSC closure details. This original DSC design has an overall length to accommodate PWR fuel and a relatively thin cylindrical shell with thick lead shield plugs at its ends. The closure plate and canister shell are made from stainless steel, as are the top shield plug plates that encase a lead core. The absence of shielding along the cylindrical shell requires the canister to be placed inside a transfer or transportation cask during all fuel loading and handling outside the spent fuel pool.

---

[22] NP-6941, *NUHOMS® Modular Spent-Fuel Storage System: Performance Testing*, Electric Power Research Institute, September 1990.

[23] NUH-001, *Topical Report for the NUTECH Horizontal Modular Storage System for Irradiated Nuclear Fuel*, NUTECH Engineers, Inc., Revision 2A.

Consequently, with the canister inside a cask, the location that can best accommodate a closure plate-to-shell weld and still permit the placement of the top shield plug following SNF assembly loading is a corner joint in-board of the canister shell flush with the end of the canister. This location poses inherent difficulties in using weld details that can be volumetrically examined reliably. Repositioning of the closure weld along the canister shell side-wall would result in substantially higher radiation exposure to the operators of this system and is not considered to be a desirable alternative. Thus, the original canister weld closure design incorporates the following features and requirements dating back to 1986[24] to meet the intent of an ASME Code, Class 1 pressure vessel:

- Volumetric examination of all full penetration canister shell seam welds.
- A "double closure" to assure confinement through the ends of the canister by requiring the welding of both the top shield plug and closure plates to the canister shell.
- Multi-level liquid penetrant (PT) examinations. These examinations include the final surface of the top shield plug-to-canister shell weld and the root pass and final surface of the closure plate-to-canister shell weld.
- Helium leak testing of the top shield plug-to-canister shell weld.
- No penetrations in the canister's outer confinement boundary that could lead to a leak path.

Until recently, this approach was judged to provide a "closure system" with safety margins equivalent to a single full penetration, volumetrically examined weld as discussed NUREG-1536 for SNF storage systems and the NRC SER[25] for the NUHOMS® system. The NRC NUHOMS® system SER states the following:

> *"The double seal welds at the top and bottom of the DSC do not comply with all the requirements for the ASME B&PV Code, Section III, Subsection NB. The inspection procedures outlined in the SAR do not comply with the Code; however, the NRC staff has determined that an exception to Code requirements for volumetric weld inspection is permissible due to the following:*
>
> 1. *The closure to the confinement boundary is a double-weld design, i.e., two weld joints provide confinement.*
> 2. *The gauge pressure (for normal operation) inside the DSC is on the order of 1 psig. Therefore, pressure stresses are very low.*
> 3. *The test method of ensuring a gas tight seal for the inner top seal weld is helium leak detection which is very sensitive. Also dye penetrant testing will be performed at two levels including the weld root pass and cover pass on the outer seal weld to ensure no weld surface imperfections. The test method of ensuring a*

[24] *Safety Analysis Report for NUTECH Horizontal Modular System for Irradiated Fuel Topical Report*, U.S. Nuclear Regulatory Commission, March 28, 1986.

[25] *Safety Evaluation Report of VECTRA Technologies, Inc. (a.k.a. Pacific Nuclear Fuel Services, Inc.) Safety Analysis Report for the Standardized NUHOMS® Horizontal Modular Storage System for Irradiated Nuclear Fuel*, U.S. Nuclear Regulatory Commission, December 1994.

*gas tight seal for the bottom welds consists of a helium leak test by the fabricator for the inner seal weld in accordance with ASTM E499, in addition to two levels of dye penetrant testing for this weld. For the outer seal weld, a multi-level dye penetrant test is specified."*

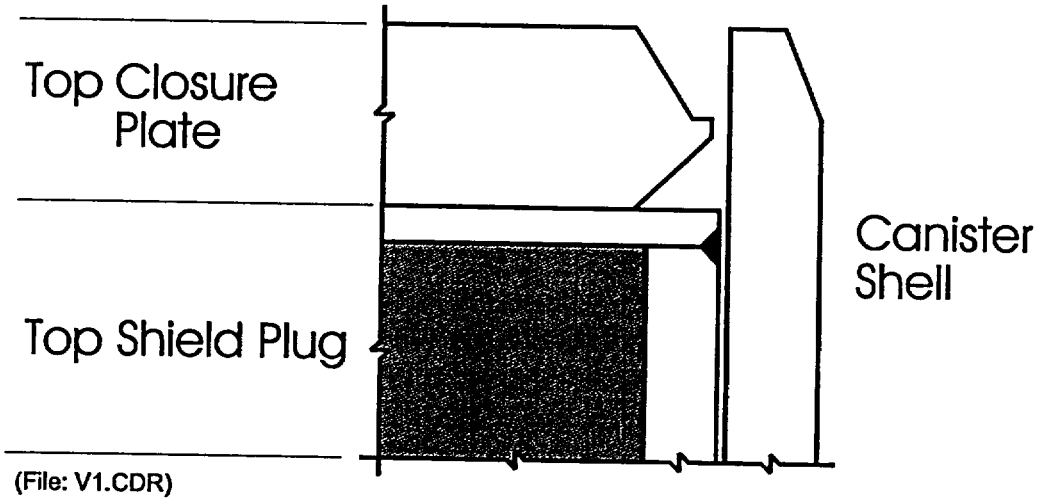


**Figure 2.5-1 - Original Closure Configuration**

*(prior to closure welding)*

After SNF assembly loading, placement of the top shield plug, and transfer of the canister within the cask from the spent fuel pool to the decontamination area, the shield plug-to-canister shell weld is placed (see Figure 2.5-2). The final surface of this weld is inspected using the PT examination technique and ASME Code, Class 1 pressure vessel original construction acceptance criteria. The DSC is then drained of water, vacuum dried, and inerted with helium gas. The shield plug-to-shell weld is then helium leak rate tested using techniques in accordance with American Society for Testing and Materials (ASTM) Standard E 499.[26] The closure plate is then installed and the root pass of the closure plate-to-canister shell weld is placed. Before the balance of this weld is completed, the root pass is inspected using the PT examination technique and ASME Code acceptance criteria. This same examination technique and acceptance criteria is then used to inspect the final surface of this weld.

[26] ASTM E 499, *Standard Test Methods for Leaks Using the Mass Spectrometer Leak Detector in the Detector Probe Mode,* American Society of Testing and Materials.

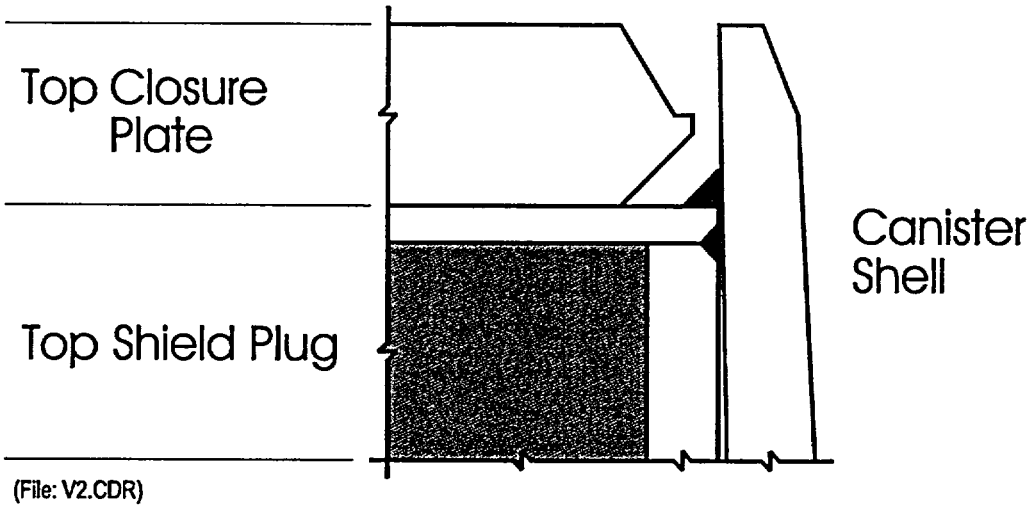


**Figure 2.5-2 - Original Shield Plug-to-Canister Shell Weld Configuration**

The canister closure weld described above was first implemented on a prototypical canister weld mock-up at the H. B. Robinson Nuclear Power Plant. EPRI Report No. NP-6941 provides the following discussion of welding issues observed during the CP&L/DOE demonstration project:

*"Weld Mockups and Weld Improvement Program*

*Another license requirement was the performance of a weld mockup test on a "dummy" canister as well as the removal of the cover plate and lead plug to demonstrate the ability to retrieve fuel assemblies. The original design called for the lead plug to be fillet welded to the DSC and for a full penetration weld to be performed in welding the top cover plate to the DSC shell* (see Figure 2.5-1). *Welding of the dummy canister began by welding the lead plug to the DSC shell. Although the welding process was successful, the DSC shell was drawn in during the welding, resulting in a tight fit for the cover plate to seat itself past the drawn-in portion of the DSC. Once past that point, the drawn-in shell* (actually the top cover weld preparation modified to clear the drawn-in shell inside diameter corner) *resulted in a larger-than-anticipated gap on the land area where the top cover plate would be welded to the DSC* (see Figure 2.5-2). *The welding procedure called for first tacking the cover plate in place before beginning the full penetration weld. The first tack was manually welded. When the second tack was made, the weld cracked. Two additional manual welds were attempted and both of them cracked as well. An automatic welder was brought in to try to control the heat during the tacking process, but these welds also cracked. At that point, the test was discontinued and the weld design and parameters were re-evaluated.*

*Root causes of the cracked weld were thought to be:*

1. *Too much shrinkage occurred during the welding of the lead plug; the top of the DSC had drawn in during welding. Consequently, when the top cover plate was being welded, the weakest place was the weld itself. When residual stresses in the weld needed relief, the tack weld was the location at which the stress was relieved.*
2. *The heat input was too high, resulting in excessive shrinkage.*
3. *The gap between the top cover plate and the DSC shell was too great.*

*To resolve these concerns, a welding development program was begun that instituted welding of six additional mockup DSCs. Principal improvements made during this program were as follows:*

1. *A change was made from a fillet weld to a bevel weld, which required chamfering of the lead plug, but resulted in much less weld metal being added to the DSC; thus, less shrinkage occurred* (see Figure 2.5-3).
2. *Using a high ferrite content weld metal, again resulted in less shrinkage.*
3. *Sequencing the welding pattern allowed more control over the heat input into the weld.*
4. *Reducing the gap between the cover plate and DSC shell resulted in reducing the amount of weld metal."*

The changing of the shield plug-to-shell weld from a fillet to a partial penetration detail permitted a reduction in the weld volume (i.e., shrinkage) a minimum of 30% (fillet vs. partial penetration weld throat widths), while maintaining the same weld strength.

The lessons learned during the CP&L/DOE demonstration project were incorporated into the NUHOMS®-24P[27] DSC design for the Oconee Nuclear Station, while maintaining the same inspection and testing requirements. This design continued to evolve with the incorporation of a chamfer at the inside diameter top corner of the shell (see Figure 2.5-4). This chamfer eliminated the need for any field reworking of the closure plate weld preparation to clear any draw-in of the canister shell caused by the top shield plug-to-canister shell weld.

[27] NUH-002, *Topical Report Amendment 2 for the NUTECH Horizontal Modular Storage System for Irradiated Nuclear Fuel - NUHOMS®-24P*, NUTECH Engineers, Inc., Revision 2A.

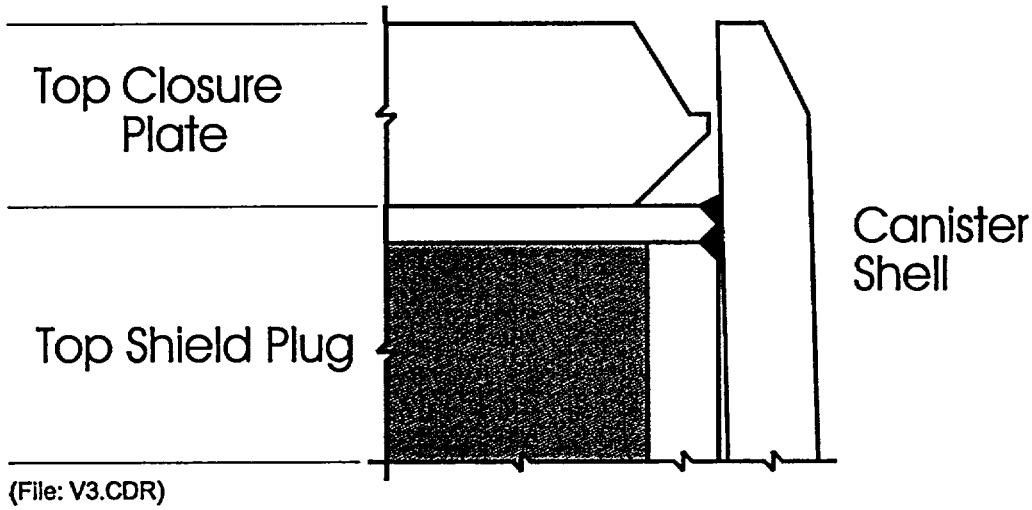


**Figure 2.5-3 - Modified Canister Closure and Weld Configuration**

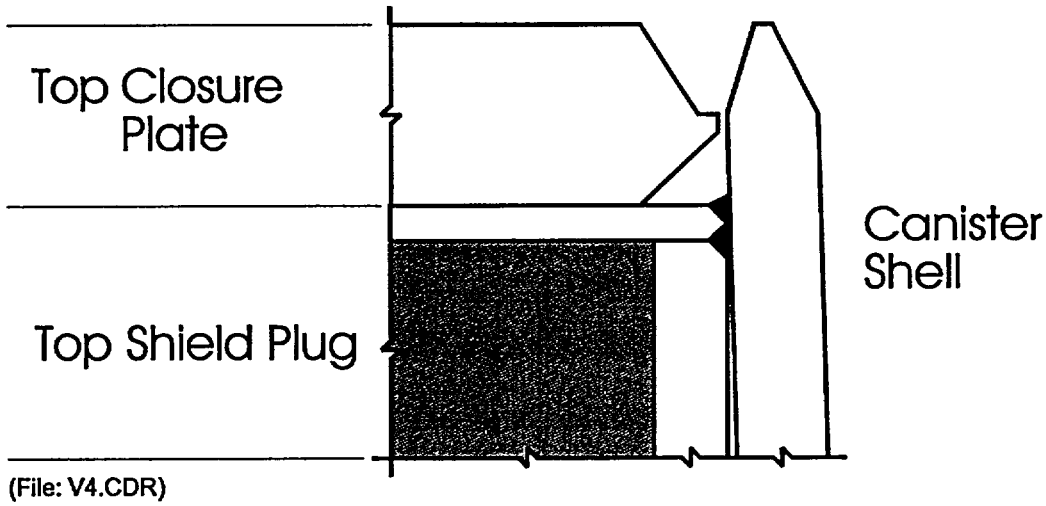


**Figure 2.5-4 - Modified Canister Shell Chamfer**

However, as the outside diameter of the top shield plugs were locally reduced to provide the required shield plug-to-canister shell gap during shop fabrication activities, the partial penetration weld joining the top and cylinder plates of the shield plug was also reduced (see Figure 2.5-5). In a few instances, this reduction in weld root size was large enough that trace amounts of the lead contained inside the shield plug appear to have remelted and caused

"wicking" of the lead into the shield plug-to-canister shell weld during canister closure welding operations. This lead contamination resulted in weld cracks that were discovered during PT examinations or helium leak rate testing and subsequently repaired. To prevent recurrence of this problem, the shield plug top plate-to-cylinder plate weld was relocated, as shown in Figure 2.5-6, for subsequent canisters successfully loaded at the Oconee and Calvert Cliffs plants over the past three to four years.

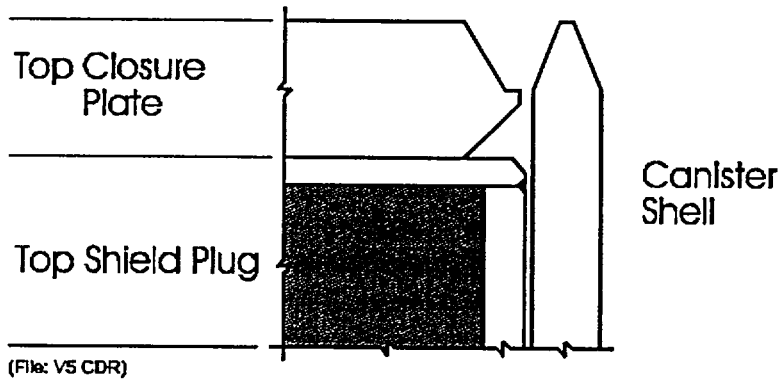


**Figure 2.5-5 - Localized Reduction of Top Shield Plug Outside Diameter**

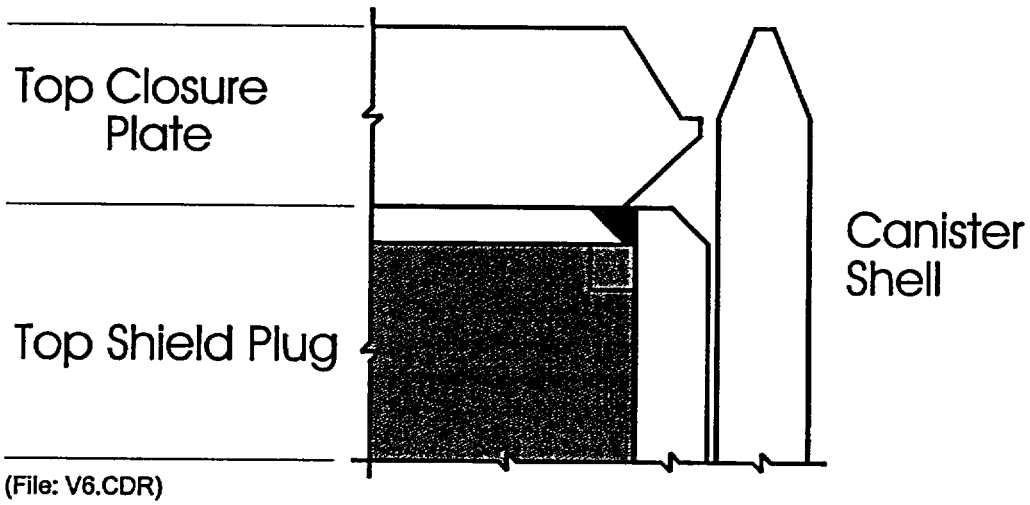


**Figure 2.5-6 - Modified Top Shield Plug Design**

Figure 2.5-7 presents the final enhancement in the current NUHOMS® DSC closure design,[28] while maintaining the same inspection and testing requirements as the original design. This design simplifies the fabrication process for the DSC closure by introducing an inner closure plate that is separate from the shield plug. This design permits the introduction of a shield plug-to-canister shell gap that is controlled by shielding and operating considerations and is independent of any weld gap requirements. Consequently, the new inner closure plate is fabricated to provide an optimum inner closure plate-to-canister shell weld gap that reduces welding shrinkage stresses and any draw-in of the canister shell (see Figure 2.5-8). This design was used to successfully load canisters at the Davis-Besse plant in late 1995/early 1996 and more recently at the Oconee Nuclear Station.

The closure design for these canisters has undergone a substantial evolution based on lessons learned and continuous improvement, with the goal of achieving optimum weld joint integrity and reliability. Unlike the VSC-24 design, no difficulties have been encountered in the placement or inspection of the current generation of canister closures. Consideration of any alternative or revised weld closure designs that have not undergone such an evolution, although they may be more amenable to volumetric examination, would not have the benefit of this operating experience and may be prone to unforeseen problems.

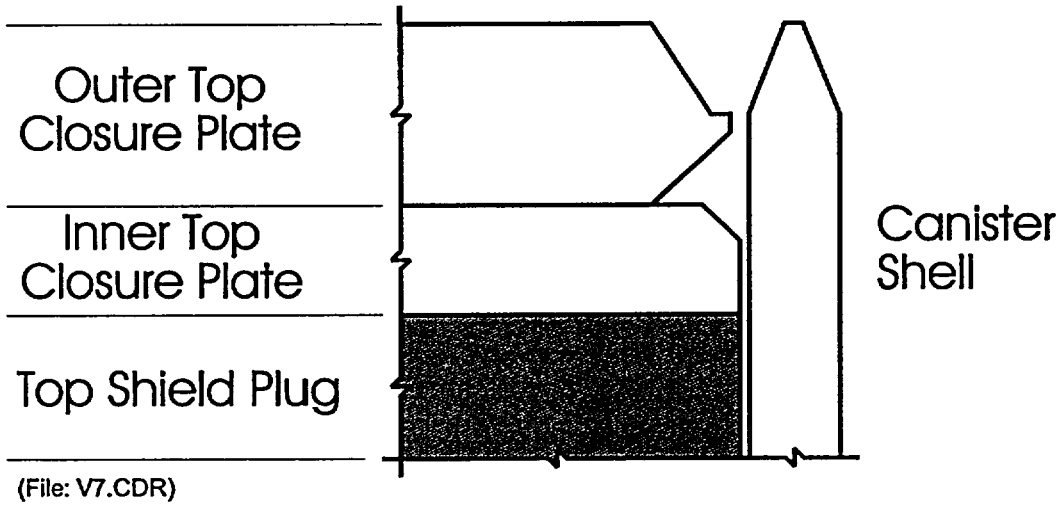


**Figure 2.5-7 - Enhanced Canister Closure Design Configuration**

[28] NUH-003, *Safety Analysis Report for the Standardized NUHOMS® Horizontal Modular Storage System for Irradiated Nuclear Fuel*, VECTRA Technologies, Inc.

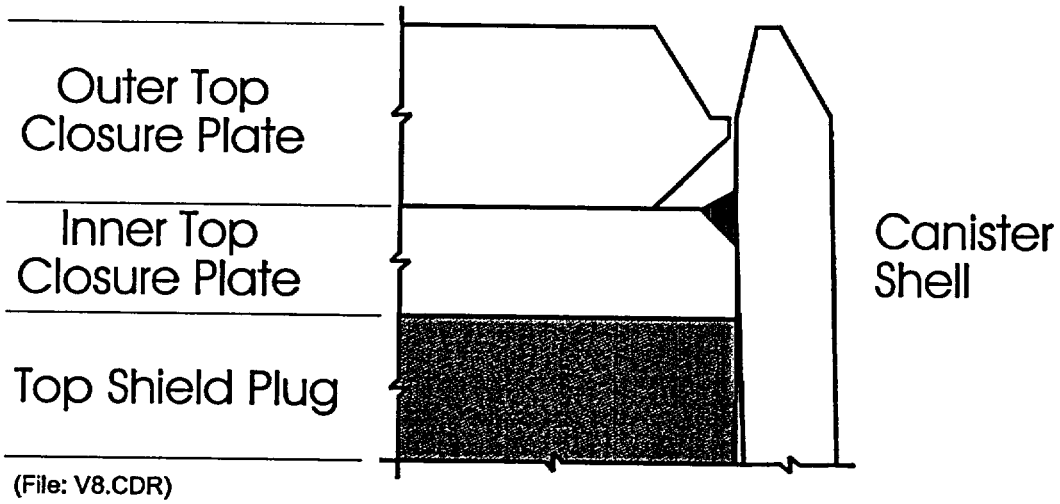


**Figure 2.5-8 - Reduction of Shell "Draw-in"**

### 2.5.2.4 FuelSolutions™ Closure Design Description

The closure design for the FuelSolutions™ canister builds on the experience gained on similar canister closure designs. As shown in Figure 2.5-9, the closure design for the FuelSolutions™ canister described in Section 1.2.1.3 of this FSAR is very similar to that shown in Figure 2.5-7. In addition, enhancements to the weld examination and leak testing requirements for this closure design have been incorporated, as discussed in Section 2.5.2.6.

The following design features have been incorporated into the FuelSolutions™ canister closure details based on the lessons learned and discussed above:

1. The shield plug is separate from the inner closure plate. This permits the fabrication of the shield plug to provide a gap based on operating and shielding considerations, as opposed to any weld gap requirements. This gap is larger than the inner top closure plate-to-shell weld gap, optimizing placement of the shield plug in the spent fuel pool after SNF assembly loading and assuring that the shield plug provides no inner top closure plate-to-shell welding shrinkage constraint.
2. Because the inner closure plate and shield plug are separate pieces, the fabrication of the inner closure plate provides an inner closure plate-to-shell weld gap that is optimized to provide the design partial penetration root depth and avoid welding shrinkage restraint, while minimizing the potential weld shrinkage volume.
3. The canister shell inside diameter top corner is chamfered to assure that the outer closure plate weld preparation will not need to be modified during canister SNF assembly loading operations. This assures that excessive outer closure plate-to-canister shell gaps are not

created to provide clearance past any shell draw-in caused by shrinkage in the inner closure plate-to-canister shell weld. By preventing these excessive gaps, tack and root pass welds will not crack due to excessive weld shrinkage. In addition, it facilitates welding torch access and orientation, and remote camera viewing by the AW/OS.

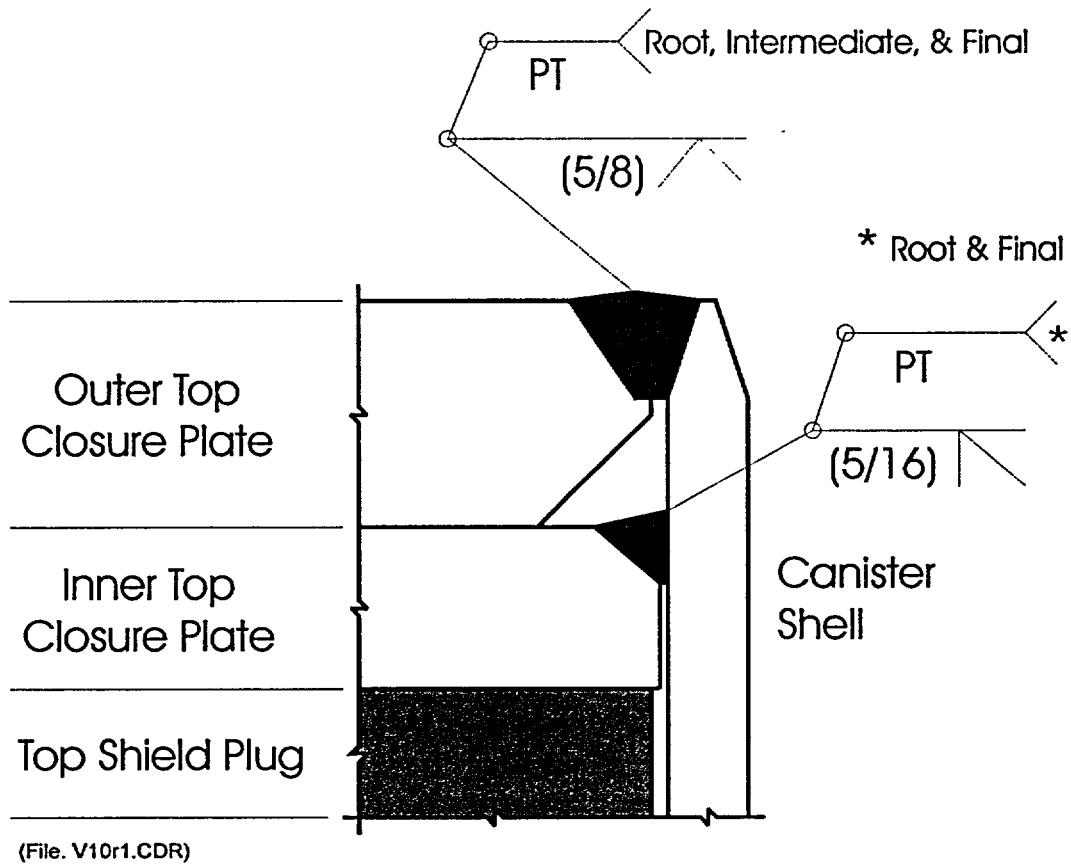


**Figure 2.5-9 - FuelSolutions™ Canister Closure Design**

In addition to these top closure configuration details, all plate materials used in the fabrication of the FuelSolutions™ canister shell and inner and outer top and bottom closure plates are austenitic stainless steel, procured in accordance with the vessel requirements of ASME Code, Section III, Subsection NB. Paragraph NB-2530 requires the ultrasonic examination of 100% of at least one major surface of all plates for vessels using the straight beam technique. This inherent requirement of Subsection NB assures that there are no significant subsurface defects in the inner and outer top closure plates and the canister shell that could lead to weld and base metal defects or base material delaminations in a material that is inherently free of these types of defects.

In addition to the closure configuration details designed to minimize welding shrinkage stresses, all filler materials used in field closure welding of the FuelSolutions™ canisters shall be stainless steel with a minimum ferrite content of 10 FN. As noted in the EPRI NP-6941 report, the use of "high" ferrite content weld metal results in less welding shrinkage and, therefore, shrinkage stress.

The long-term integrity of stainless steel materials in the design of a canister used for the dry storage of SNF assemblies is addressed in EPRI TR-102462.[29] This document addresses the following "specific aging phenomena:"

- Radiation effects
- Thermal aging
- Elevated temperature creep
- Low cycle fatigue.

EPRI TR-102462 concludes that there is little to no risk from the items listed above to the long-term integrity of SNF assembly dry-storage canisters fabricated from austenitic stainless steel.

The FuelSolutions™ canister design requires the following:

- PT examination of the final surface of the inner closure plate-to-shell weld and inner closure plate to vent and drain port body welds.
- PT examination of the root, intermediate, and final surface of the outer closure plate weld.
- Helium leak rate testing of the completed inner closure plate welds at an ASME Code pneumatic pressure test internal pressure using ASTM E 499 techniques.

Multi-level PT has historically been an acceptable substitute for volumetric examinations in difficult weld/component configurations and/or conditions and was successfully used to identify defects during the CP&L/DOE demonstration project and at Oconee and Calvert Cliffs. In addition, a helium leak rate test at a hydrostatic test pressure greatly exceeds the requirements of an ASME Code, Article NB-6000, pressure test based on the relative molecular size of the leakage medium. A similar combination of techniques and requirements satisfactorily verified that there were no significant defects in the top closure welds implemented during the loading of stainless steel canisters at the Robinson, Oconee, Calvert Cliffs, and Davis-Besse plants. The same methods can assure the long-term integrity of the FuelSolutions™ canisters in the future.

### 2.5.2.5 Comparison of FuelSolutions™ versus VSC-24 Canister Design Features

The FuelSolutions™ and VSC-24 canister closure design details differ in the following significant ways:

1. As shown in Figure 2.5-10, the VSC-24 permits a large gap between the top shield plug and the canister shell for ease in operations. This gap is so large that the insertion of shim plates is required prior to welding. These shims not only provide high welding shrinkage constraint,

[29] TR-102462, *Shipment of Spent Fuel in Storage Canisters*, Electric Power Research Institute, June 1993.

but significantly increase the weld volume. These two factors combine to set up a test of strengths between the top shield plug-to-canister shell weld and the canister shell through-wall tearing resistance potentially leading to defects in either or both materials.

This welding shrinkage constraint and magnitude of weld shrinkage volume do not exist in the FuelSolutions™ canister closure design. As discussed in Section 2.5.2.4, the separation of the shield plug and inner closure plate permits optimization of the gaps between these components and the canister shell to minimize/prevent any welding shrinkage constraint and minimize weld shrinkage volume. In addition, the FuelSolutions™ canister uses a 5/8-inch canister shell thickness as opposed to a 1-inch shell thickness used by the VSC-24 design. This difference in shell thicknesses/stiffnesses provides additional welding shrinkage stress in the VSC-24 design not present in the FuelSolutions™ canister. Further, the ductile stainless steel material used for the FuelSolutions™ canister containment boundary is not susceptible to the laminar tearing or hydrogen-induced cracking experienced in the carbon steel VSC-24 canister.

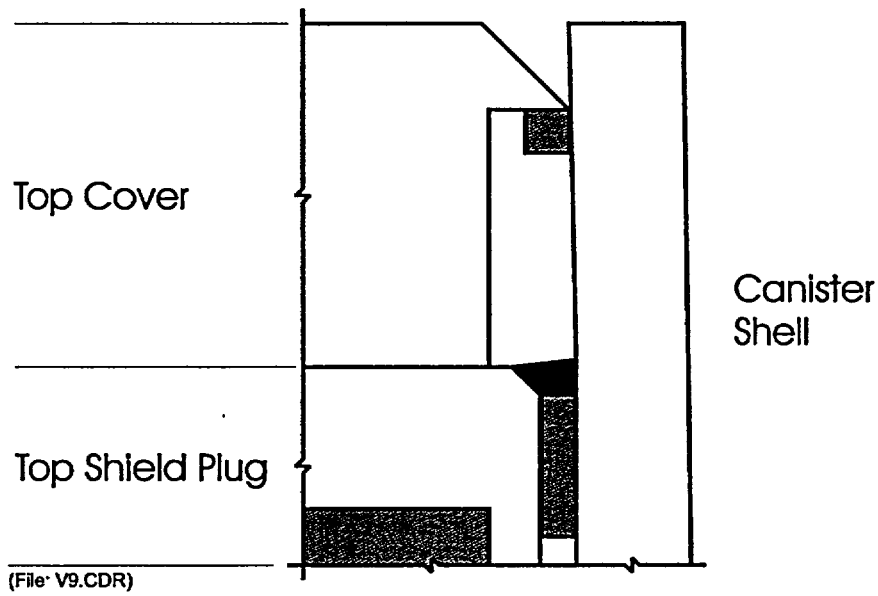


**Figure 2.5-10 - VSC-24 Top Closure Configuration[30]**

2. As discussed in the VSC FSAR,[30] the VSC-24 canister shell is made from SA-516,[31] Grade 70 carbon steel and is constructed in accordance with ASME Code, Section III,

[30] PSN-91-001, *Safety Analysis Report for the Ventilated Storage Cask System*, Pacific Sierra Nuclear Associates and Sierra Nuclear Corporation.

[31] ASME/ASTM SA-516/SA-516M, *Specification for Pressure Vessel Plates, Carbon Steel, for Moderate- and Lower-Temperature Service.*

Subsection NC.[32] Unlike Subsection NB, Paragraph NC-2530 only requires that the plate be examined in accordance with its material specification. In the case of SA-516 materials, ultrasonic examination is a "supplementary requirement" that must be specified in a purchase order for this material. This examination requirement was not specified for the VSC-24 shell materials that exhibited the defects noted in the NRC inspection report 72-1007/97-212.

The FuelSolutions™ canister top closure design greatly eliminates any concern about potential canister shell delaminations. Stainless steel plate materials are inherently more ductile than carbon steel materials because they have been shown historically to be much less susceptible to subsurface delaminations and other defects than carbon steel materials. Consequently, stainless steel plate materials are more resistant ("tougher") to the propagation of defects than carbon steel plate materials. In addition, stainless steel is predicted to have better long-term integrity than carbon steel due to the potential lowering of fracture toughness caused by thermally induced strain aging and general corrosion in carbon and low-alloy steels over the design life of a canister.

In addition to these welding detail and material differences, the PT examination of carbon versus stainless steel canisters has resulted in very different observed defects. The PT examinations noted in NRC inspection report 72-1007/97-212 revealed indications that sometimes grew significantly in length and depth as they were excavated for repair in their carbon steel materials. This was not the experience for the defects observed during the CP&L/DOE demonstration project or at Oconee or Calvert Cliffs. In these cases, the defects were highly localized, as evidenced by relatively small repair excavations in the stainless steel materials employed in these projects.

### 2.5.2.6 Additional NDE and Testing Requirements

As the result of recurring defects in the VSC-24 canister top closure welds, additional NDE and leak testing requirements have been proposed by the NRC for the closure welds of the TranStor™ canisters. These proposed additional NDE and leak testing requirements include the following:

1. PT examination of successive deposited weld layers, each having a maximum thickness of 1/8-inch,[33] and/or
2. Ultrasonic (UT) examination of the outer top closure weld volume and weld-to-cover fusion zone using an angle beam technique and the weld-to-shell fusion zone using a straight beam technique.[34]

---

[32] American Society of Mechanical Engineers (ASME) Boiler and Pressure Vessel Code, Section III, Division 1, Subsection NC, *Class 2 Components*, 1986 Edition with 1988 Addenda.

[33] Letter from the U.S. Nuclear Regulatory Commission to Sierra Nuclear, ACN 9705010064, Docket 7109268, Item 1-3, May 24, 1997.

[34] Letter from the U.S. Nuclear Regulatory Commission to Sierra Nuclear, ACN 9705010064, Docket 7109268, Item 7-1, May 24, 1997.

These proposed new NDE requirements have not been proven necessary for the closure design employed by the FuelSolutions™ canister discussed in Sections 2.5.2.3 and 2.5.2.4, especially in light of ALARA impacts associated with these requirements.

The PT examination specified for the FuelSolutions™ inner closure plate-to-canister shell root pass and final surface and combined pneumatic pressure/helium leak rate testing of the weld assures that there are no significant defects that could undermine the structural integrity of this weld or any through-wall defects that could undermine the confinement integrity of this weld. The PT examination of the FuelSolutions™ outer closure plate-to-canister shell weld root, intermediate, and final surface assures that there are no significant defects that could undermine the structural integrity of this redundant weld.

UT examination is specified as an alternate inspection method for the FuelSolutions™ canister top end outer closure plate-to-shell weld. Assuming various geometric detail and material transmissibility difficulties associated with UT examination of stainless steel in general and the outer closure weld in particular can be overcome, manual UT methods probably do not add sufficient assurance of structural integrity to offset added examination personnel radiation exposure. Remotely operated UT examination methods could provide added assurance of structural integrity for the outer closure plate weld, while reducing examination personnel radiation exposure compared to manual UT methods. However, the geometry of the outer closure plate-to-canister shell weld still presents the following challenges in obtaining an acceptable UT examination:

1. As shown in Figure 2.5-11, the geometry of any weld with a throat depth less than the thickness of the outer closure plate will introduce indications/reflectors that will be very difficult, if not impossible, to evaluate during UT examinations. The nose of the outer closure plate J-bevel weld prep will make it difficult to detect and interpret angle beam UT indications at the root of the weld and the chamfered outer top corner of the canister shell will do the same relative to the canister shell weld fusion zone.
2. As shown in Figure 2.5-12, adding to the outside top chamfer and J-bevel nose geometry challenges for angle beam UT examination are additional geometric reflectors associated with a permissible 1/8-inch maximum offset of the outer closure plate with the canister shell.
3. As shown in Figure 2.5-13, the crown (reinforcement) of the outer closure plate-to-canister shell weld may require its surface to be ground or machined flush to assure coupling between the UT transducer and the closure plate/weld surface during straight beam UT examinations. As shown in Figure 2.5-14, this coupling problem can be eliminated by "flat topping" the weld at an ALARA cost to operating personnel. In addition, the outer closure plate's chamfered lower corner (surface "a-b") and the nose of the weld's J-bevel will still confuse the detection and interpretation aspects of the UT examination process. These latter challenges will only be increased by the introduction of the permissible offset of the outer closure plate with the canister shell, as shown in Figure 2.5-15.
4. As shown in Figure 2.5-16 and Figure 2.5-17, it may be possible to insert angle and straight beam UT transducers between the outer surface of the canister and the inside surface of the cask top flange during "nominal" (1.25-inch gap) conditions (0.75- to 1.75-inch gap range).

However, the canister shell's outside chamfer, in combination with the weld prep J-bevel nose, will make UT detection and interpretation very difficult.

In addition to these geometry detail challenges, the ability to identify and size indications along the canister shell weld fusion zone from the top of the outer closure plate (see Figure 2.5-11 and Figure 2.5-12) or the outer closure plate weld fusion zone from the outside vertical face of the canister shell (see Figure 2.5-16 and Figure 2.5-17) will be difficult due to the inherent difficulty in the UT examination of stainless steel, which will be further complicated by differences in the base and weld metal grain structures. As demonstrated in various studies of the effectiveness of the UT examination technique on IGSCC in stainless steel reactor piping system weldments, it is very difficult to identify and size indications through weld metal.

Therefore, remotely operated UT examination methods might be shown to be able to examine a predetermined ("design") throat depth of the outer top closure weld while ignoring any indications/reflectors below this design depth. This approach has been used in the application of weld overlay repairs on IGSCC-susceptible reactor piping system weldments as part of an ASME Code, Section XI[35] inservice repair, but has not previously been acceptable for an ASME Code, Section III (new) construction.

These issues will need to be addressed in developing a UT weld examination approach and acceptance criteria in order to implement this alternative inspection technique. The acceptance criteria will need to be based upon and compatible with the critical flaw size as determined in Section 3.9.5 of this FSAR.

### 2.5.2.7 Summary

The FuelSolutions™ canister closure weld design, NDE, and leak testing requirements comply with current licensing requirements in the following ways:

1. The closure detail involves a flat end plate-to-cylindrical shell alternate confinement boundary weld design found acceptable by NUREG-1536, Section 3.0, and the NRC SER, when used as part of a redundant weld sealing system.
2. The redundant confinement boundary weld sealing system also complies with the requirements of 10CFR72.236(e).
3. Helium leak rate testing of the completed inner closure plate weld to assure that this inert gas does not leak or diffuse through the weld or "cask" material in excess of the design leak rate complies with NUREG-1536, Section 7.0, confinement monitoring capabilities criteria.
4. Dye penetrant testing of the root and cover passes of the confinement closure welds meeting the requirements of ASME Code, Subsection NB, complies with NUREG-1536, Section 8.0, welding and sealing criteria.

[35] American Society of Mechanical Engineers (ASME) Boiler and Pressure Vessel Code, Section XI, *Rules for Inservice Inspection of Nuclear Power Plant Components*, 1995 Edition.

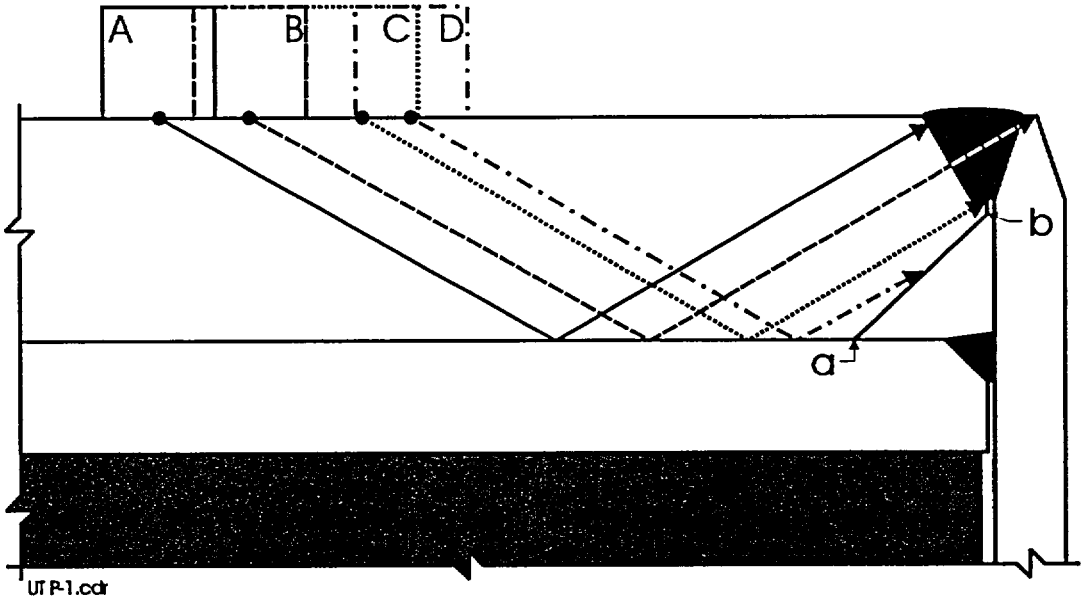


**Figure 2.5-11 - Outside Shell Chamfer and J-Bevel Weld Prep Nose Challenges to Angle Beam UT Examination**

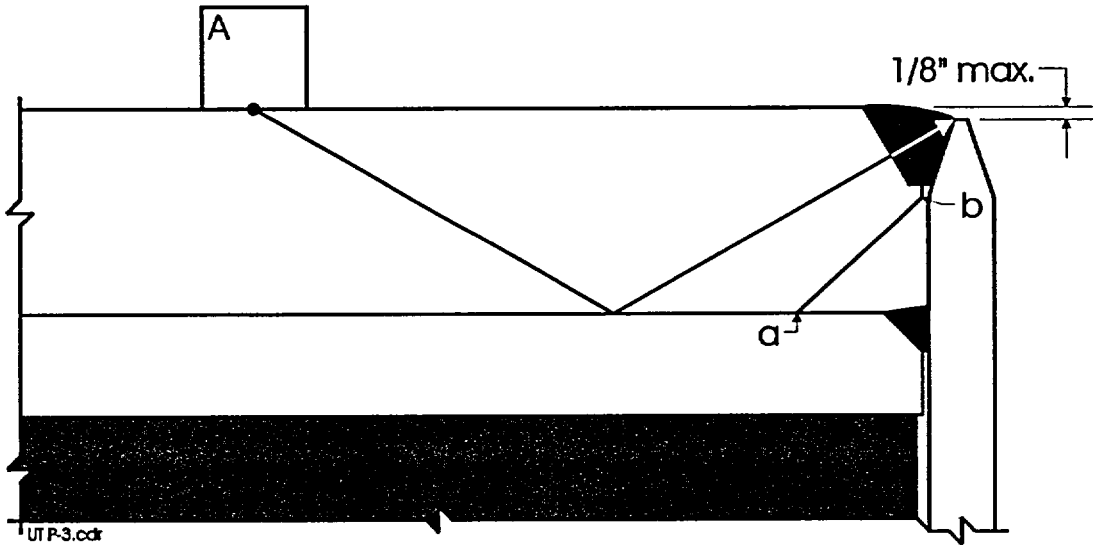


**Figure 2.5-12 - Outer Closure Plate-to-Canister Shell Offset Challenge to Angle Beam UT Examination**

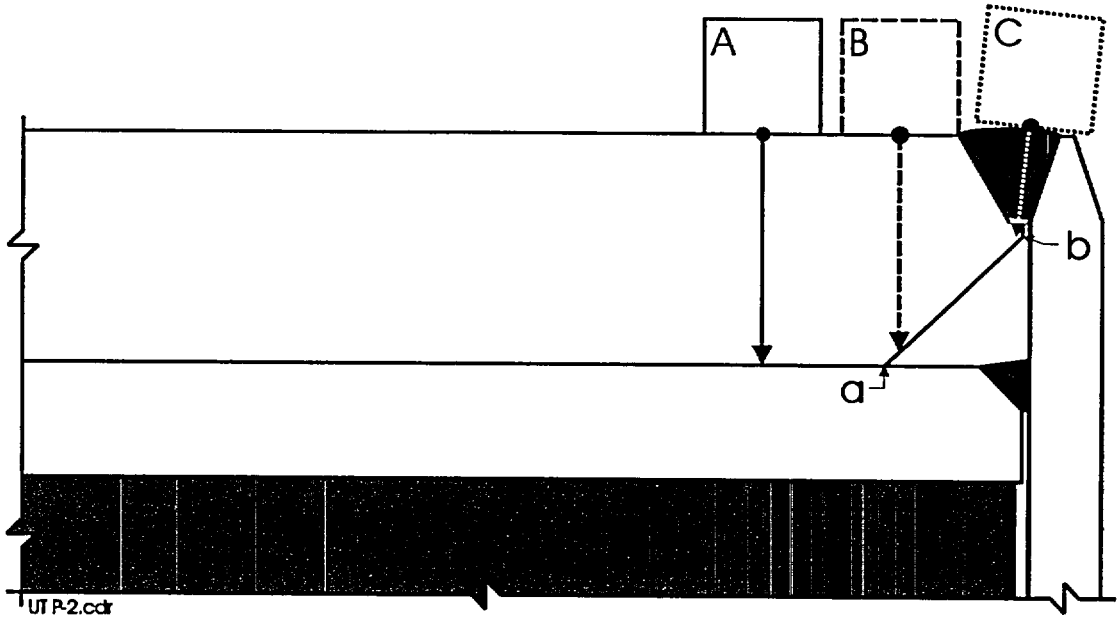


**Figure 2.5-13 - Weld Crown (Reinforcement) Challenge to Straight Beam UT Examination**

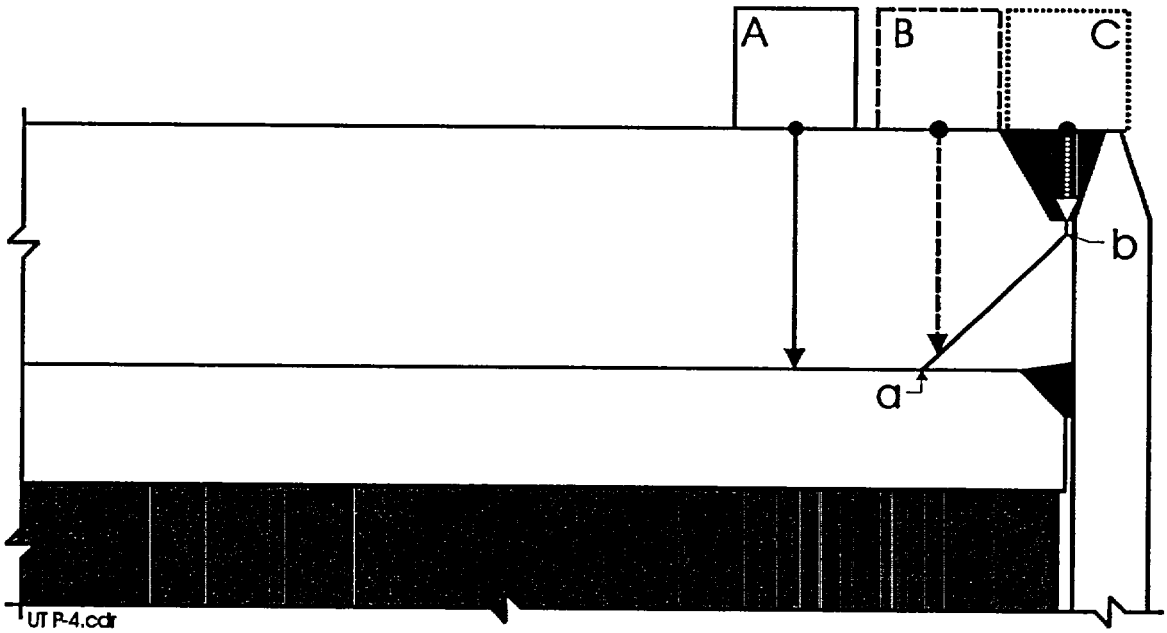


**Figure 2.5-14 - Outer Closure Plate Lower Chamfer and J-Bevel Weld Prep Nose Challenges to Straight Beam UT Examination**

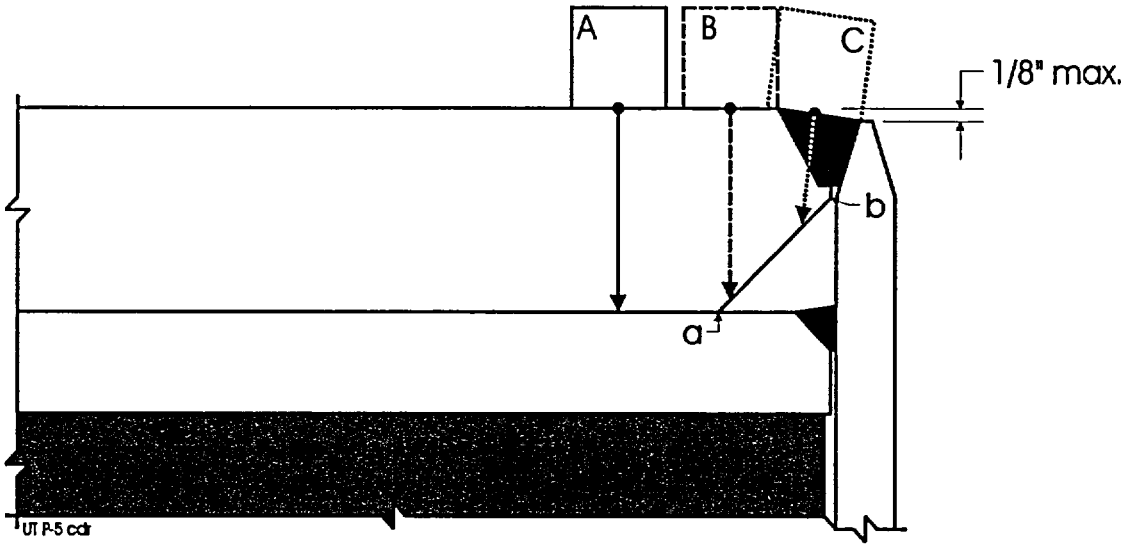


**Figure 2.5-15 - Outer Closure Plate-to-Canister Shell Offset Challenge to Straight Beam UT Examination**

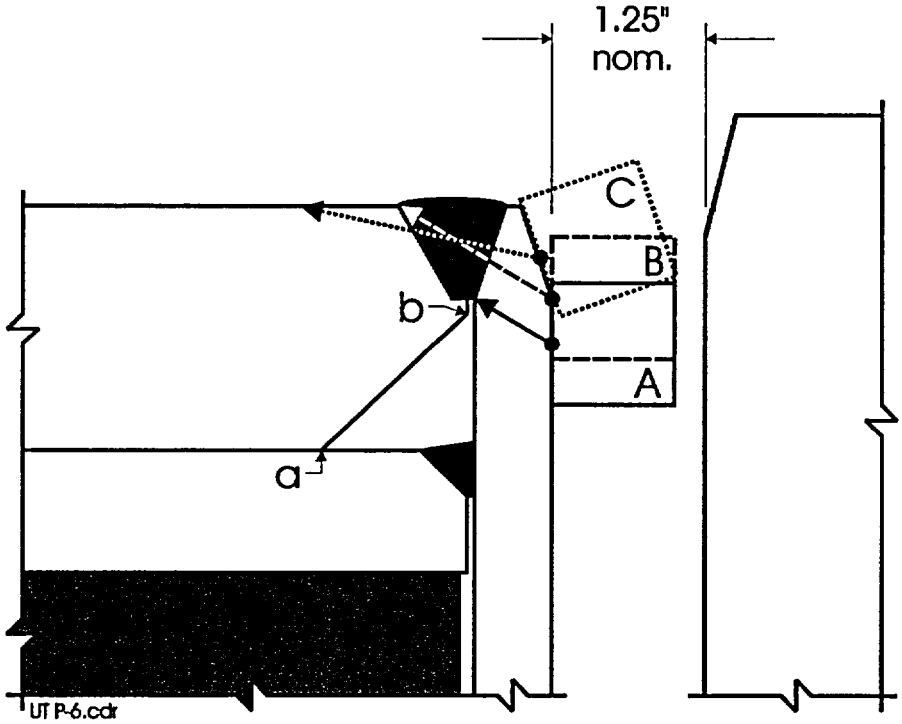


**Figure 2.5-16 - Canister Shell Chamfer and J-Bevel Weld Prep Nose Challenges to Angle Beam UT Examination**

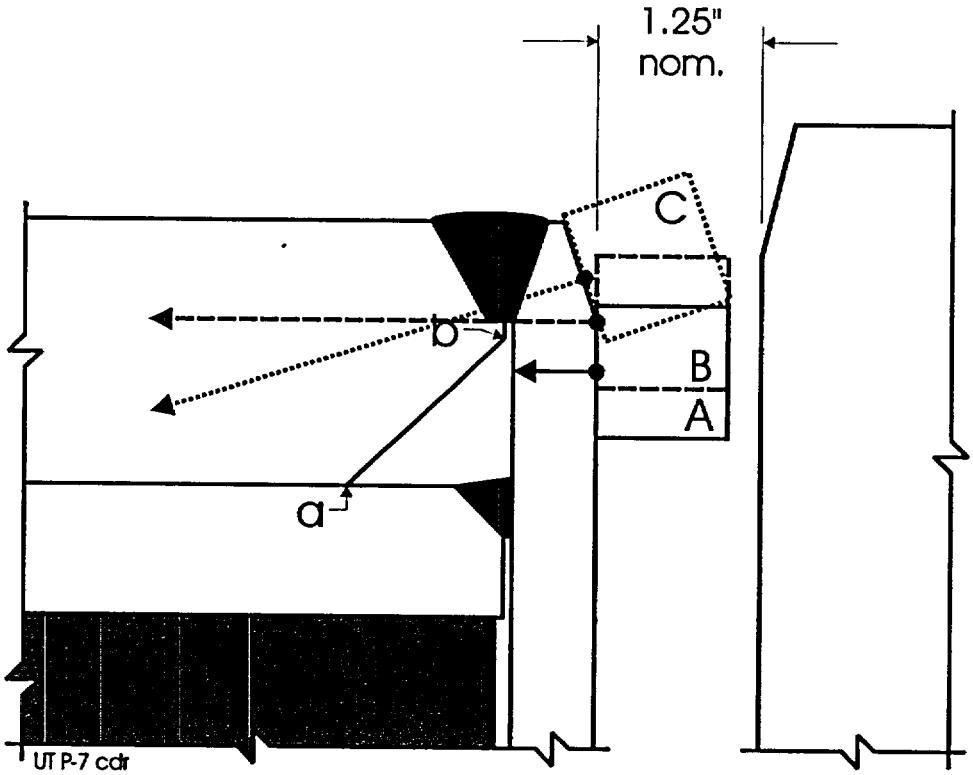


**Figure 2.5-17 - Canister Shell Chamfer and J-Bevel Weld Prep Nose Challenges to Straight Beam UT Examination**

5. The presentation of the FuelSolutions™ canister closure weld details and NDE requirements provided in this FSAR complies with the acceptance criteria reporting criteria of NUREG-1536, Section 9.0.
6. The use of multiple surface examinations of closure welds in combination with helium leak testing complies with NUREG-1536, Section 9.0, visual and NDE inspection criteria.
7. A combined helium leak rate test and ASME Code NB-6000 pressure test, using helium as the pressure test medium at a hydrostatic test pressure, meets the intent of the NUREG-1536, Section 9.0, structural/pressure test criteria.
8. The inability to leak test the outer top closure and vent/drain port cover welds is acknowledged as acceptable for an "all-welded cask" confinement in the NUREG-1536, Section 9.0, leak test criteria.
9. The use of multi-pass PT for examination of the outer closure of austenitic stainless steel canister designs has been found to be acceptable per NRC ISG-4.

Recent concerns raised during carbon steel canister top closure weld inspections do not offset the successful implementation of stainless steel top closure welds over the past ten years based on the following original NRC licensing commitments/requirements:

1. A "double closure" concept to assure confinement through the ends of the canister by requiring the welding of both the top shield plug and closure plate to the canister shell.
2. PT examinations including the final surface of the top shield plug-to-canister shell weld and the root pass and final surface of the closure plate-to-canister shell weld.
3. Helium leak testing of the top shield plug-to-canister shell weld.

The successful implementation of stainless steel closure welds has also been based on the following design details:

1. A separate inner closure plate and top shield plug that permits:
   a. The optimization of the top shield plug-to-canister shell gap relative to operating and shielding considerations, as opposed to weld fit-up gap considerations.
   b. The optimization of the inner closure plate-to-canister shell gap to provide the design partial penetration root depth, while avoiding excessive shrinkage restraint and minimizing weld shrinkage volume.
2. Chamfering of the canister shell inside diameter top corner to assure that the outer closure plate weld preparation will not need to be modified during canister SNF assembly loading operations. This will assure that excessive outer closure plate-to-canister shell gaps will not be created to avoid tack and root pass weld cracking due to excessive weld shrinkage.
3. The use of inherently tough stainless steel plate materials purchased to the requirements of ASME Code, Subsection NB vessel requirements.
4. The use of stainless steel filler materials with a minimum ferrite content of 10 FN in field closure welding of the FuelSolutions™ canisters to minimize welding shrinkage and, therefore, shrinkage stress.

All of the above licensing requirements and fundamental design details have resulted in a minimum of observed defects in stainless steel top closure welds and an ease in the repair of these defects due to their highly localized nature. The small quantity and size of these observed defects provides assurance that there are no significant defects in the top closure welds implemented during the loading of stainless steel canisters at the Robinson, Oconee, Calvert Cliffs, and Davis-Besse plants in the past, and assure the long-term integrity of these and new stainless steel canisters in the future.

This page intentionally left blank.

NUREG/CR-1815 prescribed maximum NDT temperatures. Drop weight testing of these materials in accordance with ASTM E-208 will be performed to demonstrate that the NDT temperature is at or below the $T_{NDT}$ test temperature. The $T_{NDT}$ test temperatures for the carbon steel spacer plate and support rod segment materials are established based upon the material thickness and the Lowest Service Temperature (LST) using Figure 7 of NUREG/CR-1815 as follows:

$T_{NDT}$ = LST - A

= -10°F (0.75-inch thick spacer plates: SA-517 or A514, Grades F or P)

= -70°F (3.00-inch diameter support rod segment: SA-564, Grade 630)

= -75°F (3.50-inch diameter support rod end caps: SA-564, Grade 630)

where:

LST = 0°F, LST for all on-site storage and transfer conditions for which the cask drop and tip-over accidents are postulated to occur.

A = Offset temperature per Figure 7 (curve $K_{ID}/\sigma_{yd}$) of NUREG/CR-1815

= 10°F (0.75-inch thick spacer plates: SA-517 or A514, Grades F or P)

= 70°F (3.00-inch diameter support rod segment: SA-564, Grade 630)

= 75°F (3.50-inch diameter support rod end caps: SA-564, Grade 630)

The effects of irradiation on material toughness properties is considered in accordance with the requirements of ASME NG-2332(d). The evaluation is based on an exposure of 100 years, conservatively assuming no decay of the neutron source. The total neutron fluence (8.81E+14 n/cm$^2$ for E>1.0 MeV and 3.97E+15 n/cm$^2$ for E>0.1 MeV) results in 1.88E-06 dpa iron atom displacements. According to Figure 3-1 of NUREG-1509,[7] the entire neutron energy spectrum of 1.88E-06 dpa will not change the fracture toughness properties of SA-517 or A514 carbon steels.

*Fatigue*

The principal mechanism for fatigue damage to the FuelSolutions™ W21 canister is low amplitude high cycle fatigue due to normal ambient temperature and internal pressure cycling over the 100-year service life.[8] As discussed in Sections 3.5.1.4.1 and 3.5.1.4.2, the analyses of the FuelSolutions™ W21 canister shell assembly and basket assembly demonstrate that normal operating cycles do not present a fatigue concern for the W21 canister components over the 100-year service life.

[7] NUREG-1509, *Radiation Effects on Reactor Vessel Supports*, Johnson, R. E., and Lipinski, R. E., U. S. Nuclear Regulatory Commission, May 1996.

[8] Title 10, Code of Federal Regulations, Part 51 (10CFR51), 7590-01, *Waste Confidence Decision Review*, U. S. Nuclear Regulatory Commission, September 11, 1990.

*Buckling*

The stability of the FuelSolutions™ W21 canister shell is evaluated in accordance with ASME Code Case N-284.[9] The evaluation includes factors to account for geometric and loading eccentricities in the shell. The buckling evaluation of the canister shell for the storage cask end drop is presented in Section 3.7.3.1. The buckling evaluation due to external pressure is presented in Section 3.7.7.

The buckling criteria of NUREG/CR-6322 and Article F-1341.4(a) of the ASME Code are used for the basket assembly structural components. For the basket assembly buckling evaluations performed in accordance with NUREG/CR-6322, the basket components are considered linear type members subjected to axial compression and bending. The basket assembly component stresses are evaluated using interactions 26, 27, and 28 of NUREG/CR-6322. The only exception to this is for the guide tube buckling evaluation for the storage cask end drop, in which the guide tube stress is limited to 2/3 of the theoretical buckling stress calculated based on classical plate buckling theory in accordance with Section 5.3 of NUREG/CR-6322. For the W21 basket assembly spacer plate plastic instability analyses performed in accordance with Article F-1341.4(a) of the ASME Code, the maximum applied load is limited to $0.7P_I$, where $P_I$ is the plastic instability load determined in accordance with Article NB-3213.24 of the ASME Code.

[9] Case N-284, *Metal Containment Shell Buckling Design Methods*, American Society of Mechanical Engineers (ASME) Boiler and Pressure Vessel Code, Code Cases, August 25, 1980.

hours. Therefore, short-term exposure to the temperatures of this magnitude does not have any significant effect on mechanical properties of the basket assembly materials.

### 3.3.2 Non-Structural Materials

The FuelSolutions™ W21M and W21T canister lead and DU shield plugs and aluminum/boron carbide neutron absorber panels are considered non-structural members. As such, no credit is taken for these components in the canister structural evaluation.

The W21M canister shell assembly top and bottom shield plugs for the Type LD and SD canister configurations include DU cores encased in stainless steel. Although the strength of DU is comparable to that of mild stainless steel at room temperature, as shown in Table 3.3-11, the fracture toughness of DU at extremely cold temperatures is not sufficient to preclude the possibility of brittle fracture. Consequently, it is conservatively assumed that DU has no tensile or bending strength, and is only capable of transferring compressive loads. The weight density and Poisson's ratio of DU are 0.686 $lb/in^3$ and 0.25, respectively.[13]

The W21T canister shell assembly top and bottom shield plugs for the Type LL and SL canister configurations include lead cores encased in stainless steel. The static and dynamic material properties of lead are summarized in Table 3.3-11. The weight density and Poisson's ratio of lead are 0.410 $lb/in^3$ and 0.43, respectively.[14]

The guide tube assembly uses aluminum/boron carbide (BORAL®) for the neutron absorber panels. The neutron absorber panels are assumed to have no load carrying capacity and are only designed to support bearing loads between the guide tube and supporting spacer plate ligaments. As such, the neutron absorber panels are captured between the guide tube and the outer wrapper, which are designed to maintain the geometry of the neutron absorber panels under all normal, off-normal, and postulated accident loading conditions. The mechanical properties of the neutron absorber panel material are summarized in Table 3.3-12. The neutron absorber material data is taken from the manufacturer's published data.

---

[13] Blasch, E. B., et al., *The Use of Uranium as a Shield Material*, Table 7, "Room Temperature Properties of Uranium Alloys," Nuclear Engineering and Design 13, North Holland Publishing Company, 1970.

[14] Hoffman, W., *Lead and Lead Alloys*, English Translation of 2nd German Ed., Springer-Verlag, NY-Heidelber, Berlin, 1970.

## Table 3.3-1 - Summary of FuelSolutions™ W21M Canister Materials

| Assy. | Component | Material[1] | Reference Table |
|---|---|---|---|
| Shell Assembly | Cylindrical Shell | SA-240, Type 316 | Table 3.3-3 |
| | Bottom Closure Plate | SA-240, Type 316 | Table 3.3-3 |
| | Bottom Shield Plug | A36 or DU | Table 3.3-8 & Table 3.3-11 |
| | Bottom End Plate | SA-240, Type 316 | Table 3.3-3 |
| | Top Inner and Outer Closure Plates | SA-240, Type 316 | Table 3.3-3 |
| | Top Shield Plug | A36 or DU | Table 3.3-8 & Table 3.3-11 |
| | Top Shield Plug Bottom Plate | SA-240, Type 316 | Table 3.3-3 |
| | Shield Plug Support Ring | SA-240, Type 316 | Table 3.3-3 |
| Basket Assembly | Type A Spacer Plate | SA-240, Type XM-19 | Table 3.3-5 |
| | Type B Spacer Plate | SA-517, Grade P or F<br>A514, Grade P or F | Table 3.3-9 |
| | Support Rod | SA-479, Type XM-19 | Table 3.3-5 |
| | Support Sleeve | SA-312, Type 304L | Table 3.3-6 |
| | Guide Tube | SA-240, Type 316 | Table 3.3-3 |
| | Guide Tube Attachment Bracket | SA-240, Type 316 | Table 3.3-3 |
| | Guide Tube Wrapper | SA-240, Type 316 | Table 3.3-3 |
| | Neutron Absorber Panels | BORAL® | Table 3.3-12 |

Notes:

(1) Permissible welding processes and filler metals are shown on the General Arrangement Drawings in Section 1.5.1.

## Table 3.3-2 - Summary of FuelSolutions™ W21T Canister Materials

| Assy. | Component | Material[1] | Reference Table |
|---|---|---|---|
| Shell Assembly | Cylindrical Shell | SA-240, Type 304 | Table 3.3-3 |
| | Bottom Closure Plate | SA-240, Type 304 | Table 3.3-3 |
| | Bottom Shield Plug | A36 or ASTM B29 Chemical Copper Lead | Table 3.3-8 & Table 3.3-11 |
| | Bottom End Plate | SA-240, Type 304, or SA-240, Type XM-19[4] | Table 3.3-3 and Table 3.3-5 |
| | Top Inner and Outer Closure Plates | SA-240, Type 304 | Table 3.3-3 |
| | Top Shield Plug | A36 or ASTM B29 Chemical Copper Lead | Table 3.3-8 & Table 3.3-11 |
| | Top Shield Plug Bottom Plate | SA-240, Type 304 | Table 3.3-3 |
| | Shield Plug Support Ring | SA-240, Type 304 | Table 3.3-3 |
| Basket Assembly | Type A Spacer Plate | SA-517, Grade P or F A514, Grade P or F | Table 3.3-9 |
| | Bottom End Type A Space Plate | SA-240, Type XM-19 | Table 3.3-5 |
| | Type B Spacer Plate | SA-517, Grade P or F A514, Grade P or F | Table 3.3-9 |
| | Support Rod | SA-564, Grade 630 | Table 3.3-7 |
| | Support Sleeve | SA-106, Class C | Table 3.3-10 |
| | Guide Tube | SA-240, Type 316 | Table 3.3-3 |
| | Guide Tube Attachment Bracket | SA-240, Type 316 | Table 3.3-3 |
| | Guide Tube Wrapper | SA-240, Type 316 | Table 3.3-3 |
| | Neutron Absorber panels | BORAL® | Table 3.3-12 |

Notes:

(1) Permissible welding processes and filler metals are shown on the General Arrangement Drawings in Section 1.5.1.

## Table 3.3-3 - Type 316 and Type 304 Stainless Steel Material Properties

| Material Spec. | Temp. (°F) | Yield Strength[1] $S_y$ (ksi) | Ultimate Strength[2] $S_u$ (ksi) | Design S.I.[3] $S_m$ (ksi) | Elastic Modulus[4] E (ksi ×10$^3$) | Mean Coefficient of Thermal Expansion,[5,6] (in/in/°F x 10$^{-6}$) |
|---|---|---|---|---|---|---|
| SA-240 Type 316 | -40 | 30.0 | 75.0 | 20.0 | 28.9 | 8.23 |
| | -20 | 30.0 | 75.0 | 20.0 | 28.7 | 8.28 |
| | 70 | 30.0 | 75.0 | 20.0 | 28.3 | -- |
| | 100 | 30.0 | 75.0 | 20.0 | 28.1 | 8.54 |
| | 200 | 25.8 | 75.0 | 20.0 | 27.6 | 8.76 |
| | 300 | 23.3 | 73.4 | 20.0 | 27.0 | 8.97 |
| | 400 | 21.4 | 71.8 | 19.3 | 26.5 | 9.21 |
| | 500 | 19.9 | 71.8 | 18.0 | 25.8 | 9.42 |
| | 600 | 18.8 | 71.8 | 17.0 | 25.3 | 9.60 |
| | 700 | 18.1 | 71.8 | 16.3 | 24.8 | 9.76 |
| SA-240 Type 304 | -40 | 30.0 | 75.0 | 20.0 | 28.9 | 8.21 |
| | -20 | 30.0 | 75.0 | 20.0 | 28.7 | 8.26 |
| | 70 | 30.0 | 75.0 | 20.0 | 28.3 | -- |
| | 100 | 30.0 | 75.0 | 20.0 | 28.1 | 8.55 |
| | 200 | 25.0 | 71.0 | 20.0 | 27.6 | 8.79 |
| | 300 | 22.5 | 66.0 | 20.0 | 27.0 | 9.00 |
| | 400 | 20.7 | 64.4 | 18.7 | 26.5 | 9.19 |
| | 500 | 19.4 | 63.5 | 17.5 | 25.8 | 9.37 |
| | 600 | 18.2 | 63.5 | 16.4 | 25.3 | 9.53 |
| | 700 | 17.7 | 63.5 | 16.0 | 24.8 | 9.69 |

Notes:

(1) ASME B&PV Code, Section II, Part D, Table Y-1.

(2) ASME B&PV Code, Section II, Part D, Table U.

(3) ASME B&PV Code, Section II, Part D, Table 2A.

(4) ASME B&PV Code, Section II, Part D, Table TM-1, Material Group G.

(5) ASME B&PV Code, Section II, Part D, Table TE-1, 16Cr-12Ni-2Mo, Coefficient B (mean from 70°F) for Type 316 stainless steel.

(6) ASME B&PV Code, Section II, Part D, Table TE-1, 18Cr-8Ni, Coefficient B (mean from 70°F) for Type 304 stainless steel.

$$P_m + P_b = \sqrt{\sigma^2 + 4\tau^2} = 17.9 \text{ ksi}$$

The Service Level A allowable primary membrane and primary membrane plus bending stress intensities for SA-240, Type 316 stainless steel at 500°F are 18.0 ksi and 27.0 ksi, respectively. Therefore, the W21 guide tube attachment brackets meet the Service Level A allowable stress design criteria for the vertical dead weight condition.

The W21 guide tube attachment brackets are welded to the guide tube with 0.5-inch long full depth ($t_w$ = 0.12-inch) fillet welds on both sides of each attachment bracket leg. The welds between the attachment bracket and guide tube are loaded in pure shear under vertical dead weight conditions. The shear stress in the guide tube to attachment bracket weld is calculated as follows:

$$f_v = \frac{V}{A_v} = 1.24 \text{ ksi}$$

where:

V = 105 lb., Maximum load per attachment bracket

$A_w$ = 0.085 in$^2$, Weld shear area
= $(0.707 \times t_w)(2d)$

d = 0.50 in., Weld length at sides of attachment bracket leg.

The welds between the long leg of the attachment bracket and bottom end spacer plate consists of 0.8-inch long by 0.12-inch fillet welds on both sides of the attachment bracket plus an all-around 0.12-inch fillet weld inside the 0.38-inch diameter hole. The welds between the attachment brackets and bottom end spacer plate support both a direct shear and bending moment under vertical dead weight conditions. The maximum shear stress in the attachment bracket to bottom end spacer plate welds due to vertical dead weight loading is calculated as follows:

$$f_v = \frac{V}{A_v} + \frac{Mc}{I_w} = \frac{V}{A_v} + \frac{(Ve)(l/2)}{I_w} = 3.40 \text{ ksi}$$

where:

V = 105 lb., Maximum load per attachment bracket

$A_w$ = 0.237 in$^2$, Weld shear area
= $(2l + \pi D)(0.707 \times t_w)$

e = 0.64 in., Moment arm to centroid of weld
= 1.1 - 0.12/2 - 0.4

$I_w$ = 0.0091 in$^3$, Weld moment of inertia
= $0.707 t_w \times [l^3/6 + \pi D^3/8]$

$l$ = 0.8 in., Weld length at sides of attachment bracket leg

D = 0.38 in., Hole diameter in bracket

The Service Level A allowable primary shear stress for SA-240, Type 316 stainless steel at 500°F is 10.8 ksi. For the attachment bracket welds, a 40% weld efficiency factor is applied in accordance with Table NG-3352-1 of the ASME Code for a single fillet with surface PT examination. Therefore, the allowable weld shear stress is 4.3 ksi. Therefore, the W21 guide tube attachment bracket welds meet the Service Level A allowable stress design criteria for the vertical dead weight condition.

#### 3.5.3.4.2 Horizontal Dead Weight

The W21 guide tube assembly is loaded by its own weight and the weight of the contained fuel assembly for the horizontal dead weight condition. The spacer plate ligaments provide vertical support along the bottom face of the guide tube assembly. The horizontal dead weight structural evaluation of the W21 guide tubes considers two bounding conditions for the fuel loading on the guide tube: (1) uniform fuel load assumption (i.e., SNF assembly load applied as a uniform pressure load over the supporting face of the guide tube), and (2) concentrated load at SNF assembly grid spacers.

*Uniform Fuel Loading*

For the uniform fuel loading condition, the stresses in the most highly loaded W21 guide tube span for horizontal dead weight loading, assuming the weight of the SNF assembly is applied to the bottom panel of the guide tube assembly, are determined by scaling the maximum guide tube stresses for a 60*g* side drop load by 1/60. These stresses are bounded by the W21 guide tube horizontal dead weight stresses calculated for the concentrated fuel load assumption.

The W21 guide tubes can be fabricated as a seamless tube or with full penetration longitudinal seam weld(s). The longitudinal seam weld in the guide tube can be positioned in either of the following ways: (1) when a surface liquid penetration examination (PT) only is performed, it is required that the weld be positioned at ¼ panel width, or (2) when both a Radiographic Examination (RT) and a PT are performed, the seam weld can be positioned anywhere in the guide tube.

When PT only is performed, the weld located at ¼ panel width is designed by applying a conservative weld quality factor of 0.60 (per Table NG-3352-1 of the ASME Code, the weld quality factor is 0.65). When both RT and PT are performed, a weld quality factor of 1.0 is appropriate (per Table NG-3352-1 of the ASME Code), and, therefore, the seam weld is automatically qualified by the qualification of the guide tube base metal. The longitudinal seam weld stresses in the remaining sections refer to the welds located at ¼ panel width.

The W21 guide tube longitudinal seam weld stress due to horizontal dead weight loading is again determined by scaling the maximum weld stresses calculated for a 60*g* side drop load by 1/60. The resulting primary membrane and primary membrane plus bending stresses in the seam weld are also found to be bounded by the stresses calculated for the concentrated fuel load assumption.

*Concentrated Loading at Fuel Grid Spacer Locations*

In addition to the uniform fuel loading assumption, the fuel assembly dead weight is assumed to be applied to the guide tube as concentrated loads at the location of the SNF grid spacers. As discussed in Section 3.5.3.3.2, the highest grid spacer tributary weight of 256.9 pounds occurs in the WE 15x15 fuel with control components, which is accommodated within the W21M-SD or W21T-SL basket assemblies. Although other basket assemblies have a slightly larger spacer plate spacing, the stresses in the W21M-SD or W21T-SL basket assembly guide tubes bound all others. Therefore, the analysis is based on the W21M-SD/W21T-SL guide tubes.

The horizontal dead weight stress analysis of the W21 guide tube is performed using the ½-symmetry multi-span finite element model. The SNF assembly dead weight load is applied as a uniform pressure over the area of the guide tube bottom panel which supports the SNF assembly grid spacer. The depth of the WE 15x15 in-core grid spacer varies from 1.50 inches for the standard design to 2.25 inches for the optimized fuel assembly. The smaller grid spacer depth will result in the highest guide tube stresses since the resulting pressure load is higher and the load is more concentrated at the guide tube mid-span. Therefore, a bounding horizontal dead weight stress evaluation is performed for the 1.50-inch deep grid spacer.

The maximum stress intensity at the middle fiber of the guide tube shell elements, which is conservatively classified as primary membrane, is 1.1 ksi. The maximum stress intensity at the extreme fibers of the guide tube shell elements (i.e., top and bottom fibers) is 16.8 ksi. This stress intensity is localized at the corner of the area supporting the fuel grid spacer. As such, it is classified as primary plus secondary since local yielding would relieve the stress without resulting in significant distortion. The primary membrane plus bending stress intensity is taken as the average stress along the outer edge of the area supporting the grid spacer, or 10.3 ksi. The Service Level A allowable primary membrane ($P_m$), primary membrane plus bending ($P_m$+$P_b$), and primary plus secondary ($P_m$+$P_b$+Q) stress intensities for SA-240, Type 316 stainless steel at 700°F are 16.3 ksi, 24.5 ksi, and 48.9 ksi, respectively. Therefore, the W21 guide tube stresses meets the Service Level A allowable stress design criteria for the horizontal dead weight condition assuming a concentrated fuel load at the grid spacer.

The stresses in the W21 guide tube longitudinal seam weld at ¼ panel width due to the horizontal dead weight load for the concentrated fuel load assumption are also evaluated using the finite element solution. The guide tube longitudinal seam welds are located at either the ¼ span of the panel width when only surface PT is performed or anywhere in the panel when both RT and PT are performed. The results show that the maximum primary membrane and primary membrane plus bending stress intensities in the W21 guide tube longitudinal seam weld due to horizontal dead weight loading (concentrated fuel load assumption) are 399 psi and 578 psi, respectively. The Service Level A allowable primary membrane ($P_m$) and primary membrane plus bending ($P_m$+$P_b$) stress intensities for SA-240, Type 316 stainless steel at 700°F are 16.3 ksi and 24.5 ksi, respectively. In accordance with Table NG-3352-1 of the ASME Code, the efficiency factor for a full-penetration weld with surface PT examination is 0.65. However, a conservative 60% weld efficiency factor is applied to the allowable stresses for a full penetration weld with surface PT examination, and thus, the W21 guide tube seam weld Service Level A allowable primary membrane and primary membrane plus bending stress intensities are 9.8 ksi and 14.7 ksi. Therefore, the W21 guide tube seam weld stresses meets the Service Level A allowable stress

design criteria for the horizontal dead weight condition assuming a concentrated fuel load at the grid spacer.

## 3.5.4 Normal Handling

This section provides the structural evaluation for normal handling of the loaded FuelSolutions™ W21 canister. The FuelSolutions™ Storage System is designed to transfer the canister both vertically and horizontally between the transfer cask, storage cask, and transportation cask, as described in Section 1.2.2 of the FuelSolutions™ Storage System FSAR. Three normal handling load conditions are evaluated for the FuelSolutions™ W21 canister as defined in Section 2.3.1.4: 1) vertical canister transfer handling, 2) horizontal canister transfer handling, and 3) on-site transport. Vertical canister transfer handling loads are equal to the dead weight of the canister plus an additional 15% increase to account for impulsive loading due to crane hoist motion in accordance with CMAA #70[23] recommendations. Horizontal canister transfer handling loads are equal to a hydraulic ram force of 45 kips applied to the top or bottom end of the canister and opposed by friction forces developed between the canister shell and the cask guide rails when the canister is transferred horizontally between casks, as defined in Section 2.3.1.4.

On-site transport shock and vibration loads are those encountered while towing the transfer trailer between the fuel building and ISFSI. The magnitude of shock and vibration loading experienced by the canister is insignificant due to the vibration isolation provided by the transfer trailer tires, described in Section 1.2.1.4.2 of the FuelSolutions™ Storage System FSAR, and the slow speed at which it is towed. Design basis on-site transport shock and vibration loads of $\pm 0.6g$ vertical, $\pm 0.3g$ longitudinal, and $\pm 0.2g$ lateral are conservatively used to provide a bounding structural evaluation, consistent with Section 2.3.1.4. The structural evaluation of the canister components for the normal vertical transfer and horizontal transfer handling loads is presented in the following sections.

### 3.5.4.1 Vertical Canister Transfer

#### 3.5.4.1.1 Shell Assembly

In normal or routine handling, the canister is transferred vertically between the transfer cask and storage cask using canister vertical lift fixture and/or an overhead crane, as described in Section 1.2.2.4 of the FuelSolutions™ Storage System FSAR. The loaded canister is supported by a pintle plate which is bolted to the top outer closure plate. The pintle plate distributes the lifting load to the perimeter of the outer closure plate and provides structural support for the outer closure plate. Of primary concern for this lift condition is the structural integrity of the canister shell assembly components in the top end region through which the lifting load is transferred.

[23] CMAA Specification #70, *Specification for Electric Overhead Traveling Cranes*, Crane Manufacturers Association of America, Inc., 1988.

As discussed in Section 3.1.1.1, three W21 canister assembly configurations are considered to be the most limiting for the structural analysis. These are the "bounding" canister shell assembly, which bounds all W21 canister shell assemblies with the exception of the W21T-LL, and W21T-LL canister shell assembly. The structural analysis of the W21 canister shell assembly designs for the handling loads is performed using the axisymmetric finite element models described in Section 3.9.3.1. The canister shell axisymmetric finite element models do not include the vertical lift plate which bolts to the top outer closure plate, conservatively ignoring the additional structural support it provides to the top outer closure plate.

The vertical lifting load is equal to dead weight of the dry loaded canister, plus an additional 15% to account for dynamic loads due to crane hoist motion. For each of the two bounding canister shell configurations, a bounding content weights (i.e., combined basket assembly and fuel deadweight) of 57 kips is conservatively assumed for the "bounding" canister shell model and 51 kips for the W21T-LL canister shell model. With the additional 15% factor for dynamic effects, these weights are increased to 65.6 kips and 58.7 kips, respectively. The load on the shell assembly due to the weight of the basket assembly and fuel is modeled as a uniform pressure over the inside of the bottom closure plate. A 1.15*g* vertical acceleration is applied to account for the self-weight of the canister shell assembly plus 15% for dynamic effects.

The bounding stresses in the W21 canister shell assemblies are summarized in Table 3.5-3. The results show that the maximum stresses in the W21 canister shell assembly due to the vertical canister transfer condition are less than the corresponding Service Level A allowable stresses.

The W21 canister shell top outer closure plate and its weld to the canister shell are evaluated in Section 3.4.3 and shown to provide factors of safety greater than 5 against yield and 10 against ultimate, in accordance with ANSI N14.6.

#### 3.5.4.1.2 Basket Assembly

For vertical canister transfer handling conditions, the canister basket assembly loading and boundary conditions are identical to those for the vertical dead weight condition. The stresses in the W21 canister basket assembly due to vertical canister transfer handling loads are equal to 15% of those calculated for vertical dead weight to account for dynamic loads due to crane hoist motion. The W21 basket assembly stresses for the 1.15*g* vertical dead weight plus handling load are equal to 1.15 times the maximum basket assembly stresses due to vertical dead weight. The canister basket assembly stresses due to vertical canister transfer handling loads are presented in Table 3.5-4. The results show that the canister basket assembly stresses due to these handling loads are less than the Service Level A allowable stresses.

### 3.5.4.2 Horizontal Canister Transfer

In normal or routine handling, the canister is transferred horizontally between the transfer cask and storage cask or transfer cask and transportation cask using a hydraulic ram and pintle system. The forces developed in the hydraulic ram result from friction forces between the canister shell and the transfer cask, storage cask, or transportation cask support rails. For normal transfer operations, the coefficient of friction between the canister shell and the rails is conservatively assumed to be 0.5. The magnitude of the pulling force in the hydraulic ram due to the sliding

friction force between the canister shell and the support rails is conservatively based on a bounding canister weight of 90,000 pounds. The resulting pulling force is 45,000 pounds.

The canister handling loads due to horizontal canister transfer affect only the canister shell assembly. For horizontal canister transfer conditions in which the canister assembly is pushed by the hydraulic ram, as described in the FuelSolutions™ Storage System FSAR, the canister top outer closure plate and bottom end plate are backed by the shield plugs and the top inner closure plate and the bottom closure plate. The support provided by the top inner closure plate and bottom closure plate, and shield plugs minimizes the stresses in the outer plates and welds. Even if no structural credit is taken for the backing support provided by the shield plugs, the stresses in the canister shell end plates due to horizontal push forces will be less than or equal to those due to horizontal pull forces since the pushing loads are opposed by internal pressure. When the canister assembly is pulled, the hydraulic ram forces are transferred to the canister shell assembly through a pintle plate which is bolted to the top outer closure plate or bottom end plate. The top outer closure plate or bottom end plate, and the plate to shell welds support the entire load. Therefore, the canister shell assembly stresses are highest for the horizontal canister transfer condition in which the canister is pulled. The canister basket assembly is not affected by the horizontal transfer ram load. Therefore, no structural evaluation of the canister basket assembly is performed for handling loads due to horizontal canister transfer.

As discussed in Section 3.1.1.1, two W21 canister assembly configurations are considered to be the most limiting for the structural analysis. These are the "bounding" canister shell assembly, which bounds all W21 canister shell assemblies except the W21T-LL, and W21T-LL canister shell assembly. The structural analysis of the W21 canister shell assembly designs for the horizontal canister transfer handling loads is performed using the axisymmetric finite element models described in Section 3.9.3.1. Two horizontal transfer stress analyses are performed with each model: a 45 kip pulling force applied to the top outer closure plate; and a 45 kip pulling force applied to the bottom end plate. The top end pull force is applied as an annular line load to the top outer closure plate at the pintle plate bolt circle radius (R=16 inches). Similarly, the bottom end pull force is applied as an annular line load to the bottom end plate at the pintle plate bolt circle radius (R=16 inches for the "bounding" canister shell and R=28 inches for W21T-LL canister shell). In all cases, the canister shell is restrained longitudinally at a single shell node opposite the end of the pull force. The shell assembly stresses due to horizontal dead weight are evaluated separately (Section 3.5.3.1.2) from the horizontal transfer pull force.

The bounding canister shell stresses due to horizontal canister transfer loading from the canister top and bottom ends are reported in Table 3.5-3. The analysis results show that the highest stresses in the top end of the canister shell assembly due to a horizontal canister transfer pulling force of 45 kips occur in the end plate weld region at the canister end to which the loads are applied. The maximum canister shell stress intensities due to the normal horizontal canister transfer loading are less than the Service Level A allowable stress intensities.

### 3.5.4.3 On-Site Transport

The W21 canister is transported between the plant's fuel building and the ISFSI inside the transfer cask which is mounted horizontally on the transfer skid and trailer, as described in the FuelSolutions™ Storage System FSAR. The loads associated with shock and vibration which occur during on-site transport operations are evaluated and shown to meet the structural design

criteria. As described in Section 2.3.1.4 of this FSAR, peak accelerations of 1.6*g* vertical (including dead weight), ±0.2*g* lateral, and ±0.3*g* longitudinal are conservatively used for on-site transport of the canister within the transfer cask.

#### 3.5.4.3.1 Canister Shell Assembly

The maximum stresses in the canister shell assembly due to the on-site transport shock and vibration loads are insignificant in comparison to the canister shell stresses resulting from the normal vertical and horizontal canister transfer loads. This is based on a comparison of the canister shell stresses due to normal horizontal transfer and scaled stresses from the horizontal and vertical dead weight conditions. For the on-site transport shock and vibration load condition, the canister shell stresses are approximately equal to 0.63 times the horizontal dead weight (i.e., SRSS of 0.6*g* vertical and 0.2*g* lateral) plus 0.3*g* times the vertical dead weight. As shown in Table 3.5-3, the canister shell stresses due to the normal vertical and horizontal transfer load conditions are substantial greater than those due to dead weight loads, even without applying the reduction factors described above. Therefore, the canister shell stresses due to on-site transport shock and vibration loads are clearly lower than the corresponding Service Level A allowable stresses.

#### 3.5.4.3.2 Spacer Plates

The W21 spacer plate stresses due to the on-site transport vibration loads are determined by scaling the maximum spacer plate stresses due to vertical and horizontal dead weight loads and adding the resulting stresses irrespective of sign and location. The vector sum of the +1.6*g* vertical and 0.2*g* lateral accelerations is 1.61*g* at an angle of 7° from vertical. In order to provide a bounding analysis for the on-site transport loads, a 2*g* vertical load is used to bound the vector sum of the in-plane vibration loads. Therefore, the W21 spacer plate stresses for the 2*g* vertical vibration load are equal to twice the maximum spacer plate stresses due to horizontal dead weight. The spacer plate stresses due to the 0.3*g* longitudinal vibration load are calculated by scaling the maximum spacer plate stresses due to vertical dead weight loading by 30%. The maximum stresses in the W21 spacer plates due to on-site transport handling loads are presented in Table 3.5-4. The results show that the W21 spacer plate stresses due to the on-site transport handling load are less than the Service Level A allowable stresses.

#### 3.5.4.3.3 Support Rod Assemblies

Bounding shock and vibration loads of 1.6*g* vertical (including deadweight), 0.3*g* longitudinal, and 0.2*g* lateral are conservatively used as the on-site transport design loads. The support rod stresses due to the axial load of 0.3*g* are calculated by scaling the 20*g* end drop stresses by 0.3*g*/20*g*. Similarly, the support sleeve stresses due to the axial load of 0.3g are calculated by scaling the 50*g* end drop stresses by 0.3*g*/50*g*. The support rod and support sleeve stresses due to the resultant lateral load of 1.61*g* (vertical and lateral handling loads) are calculated by scaling the 60*g* side drop stresses by 1.61*g*/60*g*. The maximum support rod and support sleeve stresses due to these loads are conservatively combined irrespective of sign and location. Table 3.5-4 summarizes the maximum on-site transport stresses in the most highly loaded W21 support rod and support sleeve. The results show that the maximum on-site transport stresses in the most

highly loaded W21 support rods and sleeves are less that the Service Level A allowable stresses for the weakest support rod and support sleeve materials.

#### 3.5.4.3.4 Guide Tubes

The W21 guide tubes are designed for bounding shock and vibration loads of +1.6*g* vertical (including dead weight), 0.3*g* longitudinal, and 0.2*g* lateral. The W21 guide tube stresses due to the on-site transport vibration loads are determined by scaling the maximum guide tube stresses due to vertical and horizontal dead weight loads and adding the resulting stresses irrespective of sign and location. The vector sum of the +1.6*g* vertical and 0.2*g* lateral accelerations is 1.61*g* at an angle of 7° from vertical. In order to provide a bounding analysis for the on-site transport loads, a 1.65*g* vertical load is used to bound the vector sum of the in-plane vibration loads. Therefore, the W21 guide tube stresses for the 1.65*g* vertical vibration load are equal to 1.65 times the maximum guide tube stresses due to horizontal dead weight. The guide tube stresses due to the 0.3*g* longitudinal vibration load are calculated by scaling the maximum guide tube stresses due to vertical dead weight loading by 30%. The maximum stresses in the W21 guide tubes due to on-site transport handling loads are presented in Table 3.5-4. The results show that the W21 guide tubes stresses due to the on-site transport handling load are less than the Service Level A allowable stresses.

### 3.5.5 Load Combinations and Comparison with Allowable Stresses

The bounding FuelSolutions™ W21 canister stresses resulting from the individual normal on-site transfer and storage load conditions are evaluated in the previous sections and summarized in Table 3.5-3 and Table 3.5-4 along with the corresponding Service Level A/B allowable stresses. The results show that the FuelSolutions™ W21 canister component stresses due to the normal on-site transfer and storage load conditions meet the Service Level A/B allowable stress criteria.

Load combinations for normal conditions are performed for the FuelSolutions™ W21 canister in accordance with Section 2.3. The normal load combinations are defined in Table 2.3-1. The structural evaluations of the W21 canister shell assembly and basket assembly for normal load combinations are presented in the following sections.

#### 3.5.5.1 Canister Shell Assembly

The W21 canister normal load combinations defined in Table 2.3-1 are simplified by identifying the bounding load combinations. Load combination A1 (vertical dead weight plus canister drainage internal pressure) is evaluated in Section 3.5.2.1. Load combination A3 is bounded by load combination A5 and need not be evaluated. Therefore, the canister shell normal load combination evaluation presented in this section considers only load combinations A2, A4, and A5.

The canister shell assembly stressed due to load combinations A2, A4, and A5 are evaluated using the axisymmetric and three-dimensional finite element models described in Sections 3.9.3.1 and 3.9.3.2, respectively. Load combination evaluations are performed for both the "bounding" canister shell model, which bounds all W21 canister shell assemblies with the exception of the W21T-LL, and the W21T-LL canister shell assembly. Separate evaluations are

performed for internal pressure acting on both the top inner and outer closures. Thermal loads are only included for the evaluation of secondary stress intensities.

For load combination A2, vertical dead weight, normal internal pressure, and normal thermal loads are applied simultaneously to the canister shell axisymmetric finite element models. For this condition, the canister shell is supported at the bottom end. The evaluation for load combination A4 is performed in a similar manner to load combination A2 with the addition of vertical canister transfer loads. For load combination A4, the canister shell is supported vertically at the location of the vertical transfer pintle plate bolt circle on top outer closure plate. The load combination A5 evaluation uses both the axisymmetric and three-dimensional finite element models. The axisymmetric model is used to determine the canister shell stresses due to normal horizontal canister transfer, normal internal pressure, and normal thermal loads. The canister shell stresses due to horizontal dead weight, which are calculated using the three-dimensional half-symmetry finite element model described in Section 3.9.3.2, are conservatively added absolutely to the maximum stresses calculated with the axisymmetric model.

The governing canister shell stresses for normal load combinations A1, A2, A4, and A5 are summarized in Table 3.5-5. The W21 canister shell normal load combination evaluation results show that the W21 canister shell stresses for all normal load combinations are less than the corresponding Service Level A allowable stresses.

### 3.5.5.2 Canister Basket Assembly

Since the W21 basket assembly is not a pressure retaining component, and therefore need not be evaluated for internal pressure loads, the governing normal load combinations for the W21 basket assembly are A4 ($D_v + L_{hv} + T$) and A5 ($D_h + L_{hhl} + T$). The W21 basket assembly stresses due to these normal load combinations are conservatively calculated by adding the maximum stresses due to the individual load conditions absolutely and irrespective of location. In addition to the normal load conditions evaluated in the previous sections, the effects of the support rod torque which is applied during fabrication of the basket assembly is also included in the load combinations. As shown in Section 3.9.4, the maximum shear stress in the support rod segment threads due to the torque preload is 1.8 ksi. The governing load combination stress results for each of the W21 basket assembly structural components are summarized in Table 3.5-6. The results show that the maximum stresses due to governing normal load combinations are less than the corresponding Service Level A allowable stresses.

As discussed in Section 3.5.1.3.3, the support sleeve axial compressive stresses due to normal thermal conditions are combined with the maximum support sleeves stressed due to dead weight and normal handling and evaluated for buckling in accordance with NUREG/CR-6322. The maximum combined axial compressive stress and bending stress in the W21 support sleeves result from load combination A4. The maximum interaction ratio for the W21T support sleeves bounds that of the W21M support sleeves since the W21T support sleeve axial compressive stress due to normal thermal loads is significantly larger than that of the W21M support sleeve. The maximum axial compressive stress and bending stress in the W21T support sleeves due to load combination A4 are 15.24 ksi and 0.05 ksi, respectively.

The allowable axial compressive, bending, and Euler buckling stresses for the W21T SA-106, Grade C support sleeve material at 600°F for normal conditions are calculated in accordance with

NUREG/CR-6322. The allowable stresses for carbon steel are function of the slenderness ratio and the parameter $C_c$ which is calculated as follows:

$$C_c = \sqrt{\frac{2\pi^2 E}{S_y}} = \sqrt{\frac{2\pi^2 (26.5x10^3)}{29.6}} = 132.9$$

$$F_a = \frac{\left[1 - \frac{1}{2}\left(\frac{KL}{rC_c}\right)^2\right] S_y}{\frac{5}{3} + \frac{3}{8}\left(\frac{KL}{rC_c}\right) - \frac{1}{8}\left(\frac{KL}{rC_c}\right)^3} = 17.6 \text{ ksi} \qquad \text{for carbon steels when } \frac{KL}{r} < C_c$$

$$F_b = 0.6\ S_y = 17.8 \text{ ksi}$$

$$F_e' = \frac{\pi^2 E}{1.92(KL/r)^2} = 6{,}063 \text{ ksi} \qquad \text{for carbon steel}$$

The total axial stress is the maximum of thermal compression and compression due to handling. Therefore, $f_a = 15.24$ ksi $> 0.15F_a$. Hence, equations 26 and 27 should be used.

Eq. 26: $$\frac{f_a}{F_a} + \frac{C_m \cdot f_b}{\left(1 - \frac{f_a}{F'_e}\right)F_b} = \frac{15.24}{17.6} + \frac{0.85 \cdot 0.05}{\left(1 - \frac{15.24}{6{,}063}\right)17.8} = 0.87 \quad < \quad 1.0$$

Eq. 27: $$\frac{f_a}{0.6F_y} + \frac{f_b}{F_b} = \frac{15.24}{0.6 \cdot 29.6} + \frac{0.05}{17.8} = 0.86 \quad < \quad 1.0$$

Therefore, the W21 support sleeves do not buckle due to controlling normal on-site storage and transfer load combinations.

### 3.5.6 Cold

The normal cold steady-state ambient temperature of 0°F with no fuel decay heat and no insolation results in a uniform temperature of 0°F throughout the canister. For this condition, the effects of differential thermal expansion between dissimilar materials within the canister assembly and the potential for brittle fracture and freezing of liquids are considered. The evaluation of the W21 canisters shows that no significant stresses result from differential thermal expansion.

Brittle fracture of the canister components for a lowest service temperature of 0°F is addressed in Section 3.1.2.3. Since the canister does not include any liquids, there is no potential damage due to freezing of liquids.

## Table 3.5-1 - W21 Canister Temperatures for Normal Thermal Conditions

| Canister Component | Maximum Temperatures (°F) | | Design Temperature[1] (°F) |
|---|---|---|---|
| | In Storage Cask | In Transfer Cask | |
| Guide Tube | 675 | 676 | 700 |
| Carbon Steel Spacer Plate | 662 | 668 | 700 |
| Stainless Steel Spacer Plate | 665 | 665 | 700 |
| Bottom End Spacer Plate | 350 | 450 | 500 |
| Support Rod & Support Sleeve | 472 | 599 | 600 |
| Canister Shell (center/ends)[2] | 409/288 | 559/268 | 300[3] |

Notes:

(1) Temperature on which allowable stresses are based.

(2) The maximum canister shell temperature in the central region of the canister cavity and at the end of the canister cavity are reported.

(3) The design temperature of 300°F is used for determining the canister shell allowable stresses since all of the controlling canister shell stresses occur in the top and bottom end regions.

## Table 3.5-2 - Comparison of W21 Canister Shell Assembly Temperatures for Normal Thermal Conditions

| Heat Load Profile | Gradient Location | Canister Shell Temperature Gradients (°F) | | | |
|---|---|---|---|---|---|
| | | Storage | | Transfer | |
| | | Normal Cold | Normal Hot | Normal Cold | Normal Hot |
| Maximum Thermal | Axial | 261 | 267 | 361 | 320 |
| | Radial | 35 | 32 | 49 | 41 |
| | Overall | 263 | 269 | 369 | 326 |
| Maximum Gradient | Axial | 301 | 306 | **404** | 357 |
| | Radial | 39 | 35 | **49** | 41 |
| | Overall | 301 | 306 | **406** | 358 |

## Table 3.5-3 - Bounding W21 Canister Shell Assembly Normal Condition Stress Summary

| Shell Component | Stress Type | Maximum Stresses[1] (ksi) | | | | | | | Allowable Stress[2] (ksi) |
|---|---|---|---|---|---|---|---|---|---|
| | | Dead Weight | | Handling | | Internal Pressure | | Normal | |
| | | Vertical | Horizontal | Vertical | Horizontal[3] | Normal[4] | Drainage[5] | Thermal | |
| Top Outer Closure Plate | $P_m$ | 0.0 | 0.4 | 0.4 | 0.6 | 0.2 | (10) | N/A | 20.0 |
| | $P_m+P_b$[6] | 0.2 | 0.7 | 2.8 | 11.1 | 3.2 | (10) | N/A | 30.0 |
| | $P_m+P_b+Q$ | 0.2 | 0.7 | 2.8 | 11.1 | 3.2 | (10) | 6.9 | 60.0 |
| Top Outer Closure Weld | $P_m$ | 0.1 | 0.8 | 1.8 | 2.6 | 1.1 | (10) | N/A | 16.0[7] |
| | Pure Shear[8] | 0.0 | 0.0 | 0.8 | 0.4 | 0.3 | (10) | N/A | 9.6[7] |
| | $P_m+P_b+Q$[6] | 0.6 | 3.9 | 5.2 | 13.7 | 5.9 | (10) | 2.5 | 48.0[7] |
| Top Inner Closure Plate | $P_m$ | 0.0 | 1.6 | 0.1 | 0.3 | 0.2 | 0.5 | N/A | 20.0 |
| | $P_m+P_b$ | 0.3 | 3.6 | 0.8 | 0.7 | 1.3 | 9.4 | N/A | 30.0 |
| | $P_m+P_b+Q$ | 0.3 | 3.6 | 0.8 | 0.7 | 1.3 | 9.4 | 6.7 | 60.0 |
| Top Inner Closure Weld | $P_m$ | 0.2 | 8.9 | 0.8 | 1.7 | 1.3 | 0.8 | N/A | 18.0[9] |
| | Pure Shear[8] | 0.1 | 4.5 | 0.4 | 0.9 | 0.6 | 0.4 | N/A | 10.8[9] |
| | $P_m+P_b+Q$ | 0.2 | 8.9 | 0.8 | 0.9 | 1.3 | 0.8 | 0.5 | 54.0[9] |
| Cylindrical Shell | $P_m$ | 0.2 | 3.3 | 3.7 | 5.3 | 2.3 | 1.6 | N/A | 20.0 |
| | $P_m+P_b$ | 0.5 | 7.7 | 14.7 | 12.0 | 7.2 | 2.1 | N/A | 30.0 |
| | $P_m+P_b+Q$ | 0.5 | 7.7 | 14.7 | 12.0 | 7.2 | 2.1 | 2.8 | 60.0 |
| Bottom Closure Plate | $P_m$ | 0.0 | 1.6 | 0.5 | 0.0 | 0.2 | 0.2 | N/A | 20.0 |
| | $P_m+P_b$ | 0.2 | 3.6 | 8.7 | 0.2 | 4.3 | 1.0 | N/A | 30.0 |
| | $P_m+P_b+Q$ | 0.2 | 3.6 | 8.7 | 0.2 | 4.3 | 1.0 | 6.9 | 60.0 |
| Bottom Shell Extension | $P_m$ | 0.2 | 3.3 | 2.1 | 10.9 | 0.9 | 0.2 | N/A | 20.0 |
| | $P_m+P_b$ | 0.6 | 7.7 | 2.8 | 12.1 | 1.2 | 0.5 | N/A | 30.0 |
| | $P_m+P_b+Q$ | 0.6 | 7.7 | 2.8 | 12.1 | 1.2 | 0.5 | 1.8 | 60.0 |
| Bottom End Plate (Except W21T-LL) | $P_m$ | 0.1 | 1.6 | 0.2 | 0.8 | 0.3 | 0.1 | N/A | 20.0 |
| | $P_m+P_b$ | 0.1 | 3.6 | 6.9 | 15.5 | 3.4 | 0.1 | N/A | 30.0 |
| | $P_m+P_b+Q$ | 0.1 | 3.6 | 6.9 | 15.5 | 3.4 | 0.1 | 6.5 | 60.0 |
| W21T-LL Bottom End Plate | $P_m$ | 0.0 | 1.6 | 0.2 | 0.9 | 0.7 | 0.1 | N/A | 31.4 |
| | $P_m+P_b$ | 0.2 | 3.6 | 8.3 | 30.1 | 5.0 | 0.2 | N/A | 47.1 |
| | $P_m+P_b+Q$ | 0.2 | 3.6 | 8.3 | 30.1 | 5.0 | 0.2 | 6.7 | 94.2 |
| Top Shield Plug Supt. Ring Weld | Pure Shear | 0.1 | 0.0 | 0.1 | 0.0 | 0.0 | 0.2 | 0.5 | 9.0 |
| Shell Extension Top Weld | Pure Shear | 0.3 | 0.3 | 0.8 | 1.1 | 0.3 | 0.2 | 0.1 | 9.0 |
| Shell Extension Bottom Weld | Pure Shear | 0.3 | 0.3 | 0.4 | 0.9 | 0.2 | 0.2 | 0.1 | 9.0 |

Notes on following page:

Notes for Table 3.5-3:

(1) Bounding stresses from "bounding" canister shell and W21T-LL canister shell structural evaluations.

(2) The allowable stresses are based on the properties of the canister shell materials (Type 304 stainless steel) at 300°F, except for the W21T-LL bottom end plate allowable stresses which are based on SA-240 Type XM-19 stainless steel at 300°F.

(3) Stresses due to horizontal ram load only, not including horizontal dead weight.

(4) Bounding stresses due to 10 psig normal internal design pressure, considered pressure acting on the top inner and outer closure plates, independently.

(5) Stresses due to 30 psig water drainage pressure plus vertical dead weight. For this condition, the canister shell top outer closure plate is not installed and the auxiliary shield plug and strongback are installed on top of the transfer cask and canister.

(6) The maximum bending stress in the top outer closure plate is determined using hand calculations assuming simply support edge conditions to demonstrate that the bending stress in the top outer closure weld may be classified as secondary.

(7) The allowable stresses for the top outer closure weld include a 0.8 weld efficiency factor in accordance with ISG-4.

(8) Pure shear stress in the welds are determined using hand calculations.

(9) The allowable stresses for the top inner closure weld include a 0.9 weld efficiency factor in accordance with Section 3.1.2.2 of this FSAR.

(10) The top outer closure plate and weld are not attached to the canister shell for this condition.

## Table 3.5-4 - W21 Canister Basket Assembly Normal Condition Stress Summary

| Basket Component | Stress Type | Maximum Stresses (ksi) | | | | | Allowable Stress (ksi) |
|---|---|---|---|---|---|---|---|
| | | Dead Weight | | Handling | | Normal Thermal[2] | |
| | | Vertical | Horizontal | Vertical[1] | On-Site Transport | | |
| 2.00" Thick Stainless Steel Spacer Plate | $P_m$ | 0.0 | 0.8 | 0.0 | 1.6 | N/A | 28.8 |
| | $P_m+P_b$ | 0.1 | 1.9 | 0.1 | 3.9 | N/A | 43.2 |
| | $P_m+P_b+Q$ | 0.2 | 2.8 | 0.3 | 5.6 | 70.3 | 86.4 |
| 0.75" Thick Carbon Steel Spacer Plate | $P_m$ | 0.0 | 1.8 | 0.0 | 3.6 | N/A | 35.9 |
| | $P_m+P_b$ | 0.3 | 4.3 | 0.3 | 8.7 | N/A | 53.9 |
| | $P_m+P_b+Q$ | 0.7 | 6.3 | 0 8 | 12.8 | 57.2 | 107.7 |
| 2.00" Thick Stainless Steel Bottom End Spacer Plate | $P_m$ | 0.0 | (5) | 0.0 | 1.6 | N/A | 29.7 |
| | $P_m+P_b$ | 1.3 | (5) | 1.5 | 4.2 | N/A | 44.6 |
| | $P_m+P_b+Q$ | 1.9 | (5) | 2.2 | 6.1 | (4) | 89.1 |
| Support Rod Segments | $P_m$ | 0.4 | 0.1 | 0.5 | 0.2 | N/A | 29.2 |
| | $P_m+P_b$ | 1.9 | 0.8 | 2.2 | 1.8 | N/A | 43.8 |
| | $P_m+P_b+Q$ | 1.9 | 0.8 | 2.2 | 1.8 | 4.8 | 135.9[3] |
| Support Rod Threads | $P_m$ | --- | 0.4 | --- | 0.6 | 11.2 | 45.3[3] |
| Support Rod Sleeves | $P_m$ | 0.2 | 0.0 | 0.2 | 0.0 | N/A | 14.0 |
| | $P_m+P_b$ | 0.2 | 0.0 | 0.2 | 0.1 | N/A | 21.0 |
| | $P_m+P_b+Q$ | 0.2 | 0.0 | 0.2 | 0.1 | 15.2 | 59.1[3] |
| Guide Tube | $P_m$ | 0.1 | 1.1 | 0.1 | 1.8 | N/A | 16.3 |
| | $P_m+P_b$ | 0.1 | 10.3 | 0.1 | 17.0 | N/A | 24.5 |
| | $P_m+P_b+Q$ | 0.1 | 16.8 | 0.1 | 27.8 | 0.0 | 48.9 |

Notes:

(1) Handling stresses include vertical dead weight stresses.

(2) General thermal stress is classified as secondary stress intensity in accordance with NG-3213.12(a). General thermal stress intensity is taken as the linearized membrane plus bending stress intensity.

(3) The controlling secondary stresses due to normal conditions occur in the W21T support rods and sleeves. All other support rod and support sleeve allowable stresses are based on the weaker W21M materials.

(4) Bounded by hottest 2-inch thick stainless steel spacer plate.

(5) Bounded by stainless steel spacer plates in the mid-region of the basket assembly.

## Table 3.5-5 - W21 Canister Shell Assembly Normal Load Combination Results Summary (2 Pages)

| Canister Shell Component | Stress Type | Allowable Stress[1] (ksi) | L.C. A1 ($D_{v1}+P_b$) Maximum Stress[2] (ksi) | L.C. A1 Design Margin | L.C. A2 ($D_v+P+T$) Maximum Stress[2] (ksi) | L.C. A2 Design Margin | L.C. A4 ($D_v+L_{hv}+P+T$) Maximum Stress[2] (ksi) | L.C. A4 Design Margin | L.C. A5 ($D_h+L_{hh1}+P+T$) Maximum Stress[2] (ksi) | L.C. A5 Design Margin |
|---|---|---|---|---|---|---|---|---|---|---|
| Top | $P_m$ | 20.0 | [3] | [3] | 0.1 | +Large | 0.5 | +41.8 | 1.0 | +18.6 |
| Outer Closure | $P_m+P_b$[4] | 30.0 | [3] | [3] | 3.0 | +8.87 | 6.0 | +3.99 | 14.4 | +1.09 |
| Plate | $P_m+P_b+Q$ | 60.0 | [3] | [3] | 9.0 | +5.65 | 11.5 | +4.22 | 20.6 | +1.91 |
| Top | $P_m$ | 16.0[5] | [3] | [3] | 1.0 | +14.8 | 2.7 | +4.84 | 4.5 | +2.57 |
| Outer Closure | Shear[6] | 9.6[5] | [3] | [3] | 0.25 | +37.4 | 1.0 | +8.50 | 0.6 | +14.5 |
| Weld | $P_m+P_b+Q$[4] | 48.0[5] | [3] | [3] | 5.8 | +7.32 | 12.0 | +3.00 | 24.6 | +0.95 |
| Top | $P_m$ | 20.0 | 0.5 | +40.8 | 0.2 | +Large | 0.5 | +38.7 | 2.3 | +7.55 |
| Inner Closure | $P_m+P_b$ | 30.0 | 9.4 | +2.20 | 1.2 | +23.6 | 2.5 | +11.1 | 10.1 | +1.98 |
| Plate | $P_m+P_b+Q$ | 60.0 | 9.4 | +5.38 | 7.9 | +6.60 | 8.5 | +6.07 | 15.4 | +2.91 |
| Top | $P_m$ | 18.0[7] | 0.8 | +21.4 | 1.2 | +14.7 | 3.2 | +4.56 | 13.6 | +0.32 |
| Inner Closure | Shear[6] | 10.8[7] | 0.4 | +25.9 | 0.6 | +17.8 | 1.6 | +5.67 | 6.8 | +0.58 |
| Weld | $P_m+P_b+Q$ | 54.0[7] | 0.8 | +66.5 | 1.0 | +53.7 | 4.3 | +11.5 | 16.1 | +2.35 |
| Top Shield Plug | $P_m$ | 20.0 | 0.1 | +Large | 0.0 | +Large | 0.1 | +Large | [9] | [9] |
| Bottom Support Plate[8] | $P_m+P_b$ | 30.0 | 0.9 | +30.8 | 1.0 | +30.1 | 1.2 | +24.5 | [9] | [9] |
| Cylindrical | $P_m$ | 20.0 | 1.6 | +11.8 | 2.1 | +8.52 | 5.5 | +2.67 | 11.5 | +0.73 |
| Shell | $P_m+P_b$ | 30.0 | 2.1 | +13.3 | 4.7 | +5.35 | 22.0 | +0.37 | 24.9 | +0.20 |
| | $P_m+P_b+Q$ | 60.0 | 2.1 | +27.6 | 5.3 | +10.3 | 22.3 | +1.69 | 25.4 | +1.36 |
| Bottom | $P_m$ | 20.0 | 0.2 | +98.5 | 0.1 | +Large | 3.0 | +5.61 | 14.0 | +0.43 |
| Shell Extension[8] | $P_m+P_b$ | 30.0 | 0.5 | +55.9 | 0.1 | +Large | 3.9 | +6.80 | 19.7 | +0.53 |
| Bottom | $P_m$ | 20.0 | 0.2 | +91.2 | 0.1 | +Large | 0.7 | +27.5 | 2.0 | +9.25 |
| Closure | $P_m+P_b$ | 30.0 | 1.0 | +29.3 | 0.5 | +65.4 | 13.0 | +1.31 | 10.0 | +1.99 |
| Plate | $P_m+P_b+Q$ | 60.0 | 1.0 | +59.0 | 7.9 | +6.57 | 19.6 | +2.07 | 16.4 | +2.66 |
| Bottom End | $P_m$ | 20.0 | 0.1 | +Large | 0.1 | +Large | 0.3 | +61.3 | 2.4 | +7.40 |
| Plate | $P_m+P_b$ | 30.0 | 0.1 | +Large | 0.1 | +Large | 9.7 | +2.10 | 19.1 | +0.57 |
| (Excluding W21T-LL) | $P_m+P_b+Q$ | 60.0 | 0.1 | +Large | 6.5 | +8.29 | 15.4 | +2.90 | 25.4 | +1.36 |

Notes: See next page.

## Table 3.5-5 - W21 Canister Shell Assembly Normal Load Combination Results Summary (2 Pages)

| Canister Shell Component | Stress Type | Allowable Stress(1) (ksi) | L.C. A1 ($D_{v1}+P_b$) | | L.C. A2 ($D_v+P+T$) | | L.C. A4 ($D_v+L_{hv}+P+T$) | | L.C. A5 ($D_h+L_{hh1}+P+T$) | |
|---|---|---|---|---|---|---|---|---|---|---|
| | | | Maximum Stress(2) (ksi) | Design Margin | Maximum Stress(2) (ksi) | Design Margin | Maximum Stress(2) (ksi) | Design Margin | Maximum Stress(2) (ksi) | Design Margin |
| W21T-LL Bottom End Plate | $P_m$ | 31.4 | 0.1 | +Large | 0.1 | +Large | 0.3 | +Large | 2.5 | +11.6 |
| | $P_m+P_b$ | 47.1 | 0.2 | +Large | 0.1 | +Large | 12.2 | +2.87 | 33.7 | +0.40 |
| | $P_m+P_b+Q$ | 94.2 | 0.2 | +Large | 6.6 | +13.26 | 17.8 | +4.29 | 40.1 | +1.35 |
| Top Shield Plug Supt. Ring Weld(8) | Shear | 9.0 | 0.2 | +52.3 | 0.1 | +78.7 | 0.1 | +70.4 | 0.0 | +Large |
| Shell Extension Top Weld(8) | Shear | 9.0 | 0.2 | +42.5 | 0.1 | +Large | 1.1 | +7.34 | 1.7 | +4.42 |
| Shell Extension Bottom Weld(8) | Shear | 9.0 | 0.2 | +36.2 | 0.0 | +Large | 0.6 | +14.8 | 1.2 | +6.40 |

Notes:

(1) The allowable stresses are based on the properties canister shell materials (Type 304 stainless steel) at 300°F, except for the W21T-LL bottom end plate allowable stresses which are based on SA-240 Type XM-19 stainless steel at 300°F.

(2) Bounding stresses from "bounding" canister shell and W21T-LL canister shell structural evaluations.

(3) For this condition, the canister shell top outer closure plate is not installed and the auxiliary shield plug and strongback are installed on top of the transfer cask and canister.

(4) The maximum bending stress in the top outer closure plate is determined using hand calculations assuming simply support edge conditions to demonstrate that the bending stress in the top outer closure weld may be classified as secondary.

(5) The allowable stresses for the top outer closure weld include a 0.8 weld efficiency factor in accordance with ISG-4.

(6) Shear stress in the welds are determined using hand calculations.

(7) The allowable stresses for the top inner closure weld include a 0.9 weld efficiency factor in accordance with Section 3.1.2.2 of this FSAR.

(8) Evaluated in accordance with Subsection NF of the ASME Code. Accordingly, secondary stresses need not be considered.

(9) Stresses due to load combination A5 are not significant.

## Table 3.5-6 - W21 Canister Basket Assembly Normal Load Combination Results

| Basket Assembly Component | Stress Type | Allowable Stress (ksi) | L.C. A4 ($D_v+L_{hv}+P+T$) Maximum Stress (ksi) | L.C. A4 ($D_v+L_{hv}+P+T$) Minimum Design Margin | L.C. A5 ($D_h+L_{hh1}+P+T$) Maximum Stress (ksi) | L.C. A5 ($D_h+L_{hh1}+P+T$) Minimum Design Margin |
|---|---|---|---|---|---|---|
| 2-inch Thick Stainless Steel Spacer Plate | $P_m$ | 28.8 | 0.0 | +Large | 1.6 | +17.0 |
| | $P_m+P_b$ | 43.2 | 0.1 | +Large | 3.9 | +10.2 |
| | $P_m+P_b+Q$ | 86.4 | 70.6 | +0.22 | 75.9 | +0.14 |
| ¾-inch Thick Carbon Steel Spacer Plate | $P_m$ | 35.9 | 0.0 | +Large | 3.6 | +8.97 |
| | $P_m+P_b$ | 53.9 | 0.3 | +Large | 8.7 | +5.19 |
| | $P_m+P_b+Q$ | 107.7 | 58.0 | +0.86 | 70.0 | +0.55 |
| 2-inch Thick Stainless Steel Bottom End Spacer Plate | $P_m$ | 29.7 | 0.0 | +Large | 1.6 | +17.6 |
| | $P_m+P_b$ | 44.6 | 1.5 | +28.5 | 4.2 | +9.62 |
| | $P_m+P_b+Q$ | 89.1 | 72.5 | +0.23 | 76.4 | +0.17 |
| W21M Support Rod Segment | $P_m$ | 29.2 | 0.5 | +57.4 | 0.2 | +Large |
| | $P_m+P_b$ | 43.8 | 2.2 | +18.9 | 1.8 | +23.3 |
| | $P_m+P_b+Q$ | 87.6 | 2.9 | +29.2 | 2.6 | +32.7 |
| W21M Support Rod Threads | $P_m$ | 29.2 | 3.5 | +7.34 | 4.1 | +6.12 |
| W21M Support Sleeve | $P_m$ | 14.0 | 0.2 | +69.0 | (1) | (1) |
| | $P_m+P_b$ | 21.0 | 0.2 | +Large | (1) | (1) |
| | $P_m+P_b+Q$ | 42.0 | 2.5 | +15.8 | (1) | (1) |
| | Buckling | 1.0 | 0.33 | +2.03 | (1) | (1) |
| W21T Support Rod Segment | $P_m$ | 45.3 | 0.5 | +89.6 | 0.2 | +Large |
| | $P_m+P_b$ | 68.0 | 2.2 | +29.9 | 1.8 | +36.8 |
| | $P_m+P_b+Q$ | 135.9 | 7.0 | +18.4 | 6.6 | +19.6 |
| W21T Support Rod Threads | $P_m$ | 45.3 | 13.0 | +2.48 | 13.6 | +2.33 |
| W21T Support Sleeve | $P_m$ | 19.7 | 0.2 | +97.5 | (1) | (1) |
| | $P_m+P_b$ | 29.6 | 0.2 | +Large | (1) | (1) |
| | $P_m+P_b+Q$ | 59.1 | 15.5 | +2.81 | (1) | (1) |
| | Buckling | 1.0 | 0.87 | +0.15 | (1) | (1) |
| Guide Tube | $P_m$ | 16.3 | 0.1 | +Large | 1.8 | +8.06 |
| | $P_m+P_b$ | 24.5 | 0.1 | +Large | 17.0 | +0.44 |
| | $P_m+P_b+Q$ | 48.9 | 0.1 | +Large | 27.8 | +0.76 |

Notes:

(1) Bounded by load combination A4.

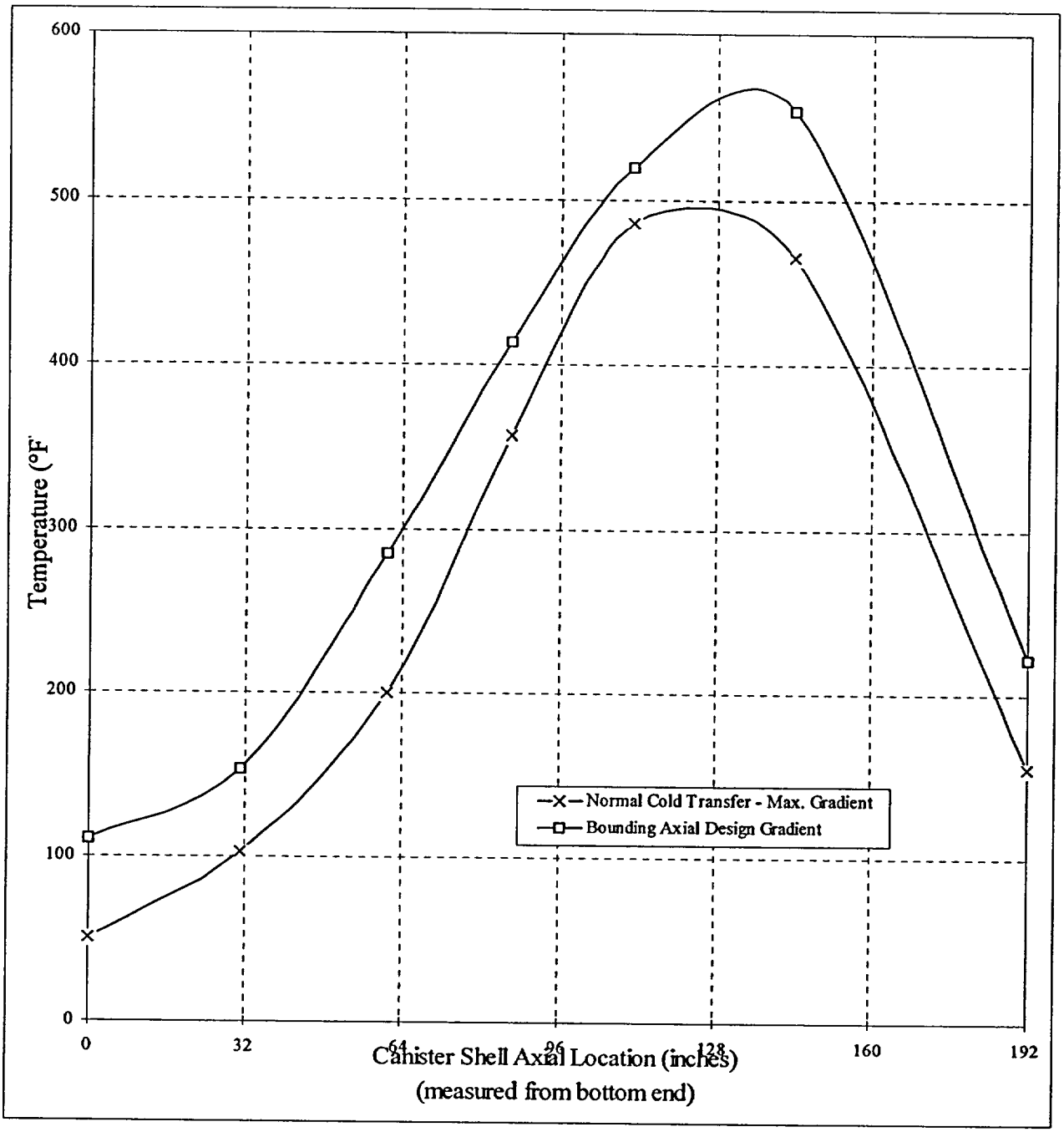


**Figure 3.5-1 - W21 Canister Shell Axial Temperature Distribution for the Bounding Normal Thermal Condition**

## 3.7 Evaluation of Accident Conditions

The FuelSolutions™ W21 canister is evaluated for a range of postulated accidents and natural phenomena, as defined in Sections 2.3.3 and 2.3.4 of this FSAR.

The design basis postulated accident conditions and natural phenomena considered are in accordance with ANSI/ANS-57.9,[25] and include events that are postulated because their consequences may result in maximum potential impact on the immediate environs. In accordance with 10CFR72, evaluations are performed for a range of postulated accidents, including those with the potential to result in an annual dose greater than 25 mrem outside the controlled area. The design basis postulated accident and natural phenomena events evaluated for the W21 canister include the following:

- Fully blocked storage cask inlet and outlet vents
- Loss of transfer cask neutron shield
- Cask drop and tip-over
- Fire
- Flood
- Earthquake
- Accident Internal Pressure

As discussed in Sections 2.3.3 and 2.3.4, the canister is not subjected to loads due to explosive overpressure; tornado; wind; burial under debris; lightning; and snow and ice.

The results of the structural evaluations performed herein demonstrate that the FuelSolutions™ W21 canisters described in Section 1.2.1.3 can withstand the effects of all credible accident conditions and natural phenomena without affecting structural safety function and remain in compliance with the applicable acceptance criteria. The load combinations evaluated for postulated accident conditions are defined in Table 2.3-1. The load combinations include normal loads, which are evaluated in Section 3.5; off-normal loads, which are evaluated in Section 3.6; and accident loads, which are evaluated in this section. The accident load combination evaluations are provided in Section 3.7.10.

The structural evaluations of W21 canister shells is performed for the bounding W21 canister shell designs, determined to be the W21M-LD, W21T-LS, and W21T-LL canister shell assemblies, as discussed in Section 3.1.1.1.

The W21 basket assembly structural evaluations are performed for the bounding W21 basket assembly components as described in Section 3.1.1.2.

---

[25] ANSI/ANS-57.9, *Design Criteria for an Independent Spent Fuel Storage Installation (Dry Storage Type)*, American National Standards Institute, 1984.

The evaluation for the effects of the design basis postulated accident events on the FuelSolutions™ W150 Storage Cask and W100 Transfer Cask is provided in the FuelSolutions™ Storage System FSAR.

### 3.7.1 Fully Blocked Storage Cask Inlet and Outlet Vents

The FuelSolutions™ W21 canister, loaded with design basis fuel assemblies and dry stored vertically in the storage cask, is evaluated for a postulated accident thermal event in which complete blockage of all storage cask inlet and outlet vents occurs. A steady-state ambient temperature of 100°F with insolation, as defined in the FuelSolutions™ Storage System FSAR, are conservatively postulated to occur concurrently.

As shown in Chapter 4 of this FSAR, the maximum temperatures in the W21 canister assembly due to the storage cask blocked vent accident thermal condition are bounded by those resulting from the transfer cask loss of neutron shield accident thermal condition. The peak canister internal pressure for accident thermal conditions is discussed in Section 4.6 of this FSAR, and is 68.7 psig. A bounding design basis accident pressure of 69.0 psig structural evaluation of all W21 canister shell configurations, with the exception of the W21T-LL. The maximum accident pressure for the W21T-LL canister is 45.0 psig. The W21T-LL canister shell stresses are calculated based on a bounding 45.1 psig accident internal pressure. Therefore, the canister shell accident pressure analysis discussed in Section 3.7.9 bounds the pressure due to the blocked vent condition.

In general, thermal stresses within the canister result from internal thermal gradients. These gradients are generally highest for the thermal conditions with the highest internal heat generation rate and the lowest ambient temperature. As shown in Figure 4.6-2, the thermal gradient between the maximum spacer plate temperature and the maximum canister shell temperature is reduced during the blocked vent storage accident. In the same manner, the thermal gradients within the canister shell and basket assemblies are also reduced during the postulated blocked vent accident. For this reason, and since the maximum canister temperatures for the storage cask blocked condition are bounded by those for the transfer cask loss of neutron shield accident, the canister thermal stresses for the storage cask blocked vent condition are bounded by other conditions.

### 3.7.2 Loss of Transfer Cask Neutron Shield

The FuelSolutions™ W21 canister, loaded with design basis fuel assemblies while in the transfer cask, is evaluated for a postulated accident thermal event in which the transfer cask liquid neutron shield is drained. A steady-state ambient temperature of 100°F with insolation, as defined in the FuelSolutions™ Storage System FSAR, are conservatively postulated to occur concurrently.

As discussed in Section 4.6 of this FSAR, the W21 canister internal pressure resulting from the loss of neutron shield accident is less than the design basis accident pressure of 69.0 psig. Therefore, the canister shell accident pressure analysis discussed in Section 3.7.9 bounds the pressure due to the loss of neutron shield condition.

In general, thermal stresses within the canister result from internal thermal gradients. These gradients are generally highest for the thermal conditions with the highest internal heat

generation rate and the lowest ambient temperature. As shown in Section 4.6 of this FSAR, the thermal gradient between the maximum spacer plate temperature and the maximum canister shell temperature is significantly reduced during the loss of neutron shield accident. In the same manner, the thermal gradients within the canister shell and basket assemblies are also reduced during the postulated loss of neutron shield accident. Therefore, the canister thermal stresses for the loss of neutron shield accident are bounded by other conditions, with the exception of the basket assembly support rods.

As discussed in Section 3.5.1.3.3, thermal stresses in the W21 support rods and support sleeves result from differential thermal expansion of dissimilar materials at elevated temperatures. These stresses are highest for the maximum support rod temperatures. As shown in Chapter 4 of this FSAR, the loss of neutron shield accident thermal condition results in the highest overall support rod temperature for all normal, off-normal, and accident conditions of 733°F. Therefore, the bounding support rod accident thermal stresses are evaluated for this condition. Since general thermal stress is classified as secondary in accordance with Subsection NG of the ASME Code, the support rod stresses due to loss of neutron shield accident need not be evaluated using the ASME Service Level D allowable stress design criteria. However, a buckling evaluation of the W21 support sleeves, which are loaded in axial compression as a result of the differential thermal expansion, is performed in accordance with NUREG/CR-6322 to assure that the support sleeves remain stable under these conditions.

The W21 support sleeve stresses are calculated for a bounding temperature of 750°F using the same methodology that is used for the support rod assembly normal thermal stress evaluation. The support sleeve thermal stresses are determined using hand calculations, treating the support rod segments as axial members which act in parallel with the support sleeves and spacer plates. As shown in Section 3.5.1.3.3, the thermal stresses in the W21T support rod assemblies are much higher than those in the W21M support rod assemblies due to the different support rod materials used. Furthermore, the normal thermal stress evaluation shows that the maximum thermal stresses for any W21T basket occur in the W21T-SS support rod assemblies. Therefore, thermal stresses for the loss of neutron shield accident are only calculated for the W21T-SS support sleeves. The maximum axial load in the W21T-SS support rod assembly at the bounding temperature of 750°F is calculated based on the principal of static equilibrium to be 50.1 kips. The resulting axial compressive stress in the support sleeves is 22.5 ksi.

The W21T support sleeve allowable axial compressive stress for accident conditions is calculated in accordance with NUREG/CR-6322 using Equation 33 for carbon steel material. The allowable axial compressive stress for the longest W21T-SS support sleeve, based on SA-106, Grade C carbon steel material properties at 750°F, is 24.5 ksi. Therefore, the maximum axial compressive stress in the W21T-SS support sleeves is lower than the corresponding allowable axial compressive stress for accident conditions and the support sleeves will not buckle under the most severe on-site storage and transfer accident thermal condition.

### 3.7.3 Storage Cask Drop

The storage cask is evaluated for a non-mechanistic drop as discussed in Section 2.3.3.2 and evaluated in the FuelSolutions™ Storage System FSAR. The accidental storage cask drop scenario is a postulated vertical drop onto the bottom end of the storage cask from a height of

36 inches. The storage cask end drop results in a canister assembly rigid-body response, characterized as a half-sine wave pulse with a peak acceleration of 28*g*. The FuelSolutions™ W21 canister is evaluated for the postulated storage cask end drop scenario using equivalent static loads. The equivalent static end drop accelerations are equal to the peak accelerations multiplied by a Dynamic Load Factors (DLFs) to account for possible dynamic amplification within the canister. The maximum DLF for an undamped system subjected to a half-sine wave pulse is 1.75 (Figure 2.15 of NUREG/CR-3966[26]). Therefore, the maximum equivalent static acceleration for the W21 canister shell and basket assemblies due to the postulated storage cask end drop is 49*g*. A bounding storage cask end drop equivalent static acceleration of 50*g* is conservatively used for the evaluation of the W21 canister.

### 3.7.3.1 Canister Shell Assembly

The two bounding W21 canister shell assembly designs discussed in Section 3.1.1.1 (e.g., "bounding" canister and W21T-LL canister) are evaluated for a bounding 50*g* bottom end drop using finite element analysis. The stresses in all of the canister shell components are evaluated using the axisymmetric finite element models discussed in Section 3.9.3.1.

In the event of a storage cask bottom end drop, the canister is supported by the crush pipes located in the bottom end of the storage cask. The storage cask crush pipes provide uniform support over the outer 14-inch radius of the canister bottom plate. As discussed in Section 3.9.3.1, uniform gap element support is assumed over the entire surface of the bottom end plate, rather than just the outer 14.0 inches of the canister radius. However, this difference has no significant impact on the resulting stresses in the bottom region of the canister shell due to the rigidity of the canister shell bottom end plates.

The load from the W21 canister contents (basket assembly and SNF assemblies) is supported on the bottom end of the cavity. The load from the contents is modeled as a uniform pressure on the inner surface of the bottom end closure. For the "bounding" axisymmetric model which applies to all W21 canister types except for the W21T-LL, a bounding payload weight of 57.0 kips is conservatively used. For the W21T-LL canister shell analysis, a bounding contents weight of 51.0 kips is conservatively used. The resulting pressure loads applied to the bottom end closure of the finite element models are 865.5 psi for the "bounding" model and 774.5 psi for the W21T-LL model. A vertical acceleration of 50*g* is applied to the models to account for the self-weight of the shell assemblies. The bounding canister shell stress intensities resulting from the 50*g* bottom end drop load are reported in Table 3.7-4. The results show that all stresses within the canister shell are lower than the Service Level D allowable stresses.

For the postulated storage cask end drop condition, an additional stress evaluation is performed for the canister shell top inner closure plate and weld using hand calculations, conservatively assuming no support from the top shield plug assembly. The maximum bending stress in the top inner closure plate for the 50*g* end drop is calculated assuming the plate behaves as a simply supported circular plate subjected to a uniform pressure load due to its own self weight based on Roark (Table 24, case 10a). The maximum bending stress in the top inner closure plate for this

[26] U.S. Nuclear Regulatory Commission, *Methods for Impact Analysis of Shipping Containers*, NUREG/CR-3966, November 1987.

condition is 18.8 ksi versus an allowable Service Level D primary membrane plus bending stress intensity of 69.3 ksi for SA-240, Type 304 stainless steel at 300°F. The corresponding shear stress in the top inner closure weld 0.8 ksi versus an allowable weld shear stress of 22.1 ksi, based on SA-240, Type 304 stainless steel at 300°F with a 0.9 weld efficiency factor as discussed in Section 3.1.2.2 of this FSAR. Therefore, the top inner closure plate and weld stresses due to the 50*g* bottom end drop load, calculated assuming no support from the top shield plug, are lower than the Service Level D allowable stresses.

The bending stress in the canister shell top carbon steel shield plug assembly due to the 50*g* bottom end drop load is determined using hand calculations. The top shield plug is conservatively assumed to support the entire weight of the top inner and outer closure plates in addition to its own weight. The stresses in the carbon steel top shield plug are calculated using Roark, Table 24, case 10a, treating the shield plug as a simply supported circular plate subjected to a uniform pressure load. The uniform pressure load acting on the 7.25-inch thick carbon steel top shield plug due to a 50*g* end drop load, including the load from the top inner and outer closure plates, is 146.5 psi. The resulting maximum bending stress is 3.6 ksi versus an allowable Service Level D primary membrane plus bending stress intensity of 60.8 ksi for A36 carbon steel at 300°F.

The stability of the W21 canister shell is evaluated for the postulated storage cask end drop to assure that it has adequate design margin against buckling. The end drop condition results in the highest axial compressive stresses in the canister shell. Internal pressure loads that result in tensile stresses in the shell, thereby offsetting the impact loads, are conservatively ignored for the buckling evaluation. The canister shell is loaded by its self-weight and the weight of the top closure components for a bottom end drop. The load from the canister payload does not load the canister shell since it is supported directly by the bottom end closure. The buckling evaluation of the canister shell is performed in accordance with ASME Code Case N-284.

The results of the storage cask bottom end drop show that the maximum axial compressive stress in the shell is 6.8 ksi. The calculated axial compressive stress is adjusted to account for a factor of safety and capacity reduction factors. A factor of safety of 1.34 is used for accident conditions in accordance with ASME Code Case N-284. Therefore the shell axial stress is multiplied by 1.34. In addition, the capacity reduction factor for axial compression, $\alpha_{\phi L} = 0.207$, is based on the canister shell geometry and material properties in accordance with Paragraph -1511 of ASME Code Case N-284, resulting in an adjusted shell compressive stress of 44.0 ksi.

The theoretical buckling stress is calculated in accordance with Paragraph -1712 of ASME Code Case N-284 to be 306.5 ksi, based on nominal shell dimensions and material properties at a bounding temperature of 400°F. The resulting canister shell buckling interaction ratio for the bounding 50*g* bottom end drop is:

$$\frac{44.0}{306.5} = 0.14 \leq 1.0$$

Therefore, the W21 canister shell does not buckle due to the bounding 50*g* end drop load.

### 3.7.3.2 Canister Basket Assembly

#### 3.7.3.2.1 Spacer Plates

For the storage cask bottom end drop load condition, each of the W21 spacer plates support only its own weight, except for the bottom end spacer plate, which supports the guide tube assemblies via the attachment brackets. The fuel assemblies within the basket assembly are supported in the longitudinal direction by the canister bottom end closure. Therefore, the fuel assemblies do not load the spacer plates in the event of a bottom end drop. Each spacer plate in both the W21T and W21M basket assemblies is supported in the longitudinal direction by the eight support rod assemblies. The W21 spacer plates are conservatively designed for a bounding 50*g* bottom end drop acceleration load.

For the storage cask bottom end drop, the W21 spacer plate loading is proportional to the vertical dead weight loading and boundary conditions are identical to those for vertical dead weight. However, the attachment brackets which secure the guide tubes to the bottom end spacer plate are not designed to withstand the bottom end drop load, but will fail at an acceleration load less than the 50*g* bottom end drop load. The lowest design margin in the W21 guide tube attachments for vertical dead weight loading occurs in the welded connection between the bottom space plate and the guide tube. However, weld efficiency factors, excess weld deposition, and higher weld metal material properties, make prediction of the weld failure load difficult. Therefore, the upper bound ultimate load capacity of the guide tube attachment brackets is conservatively based on the ultimate shear capacity of the 5/16-inch wide "necked-down" shear section. The ultimate load capacity of the attachment bracket is determined to be 17.9*g*. An upper bound failure load of 20*g* is conservatively assumed.

The W21 spacer plate bottom end drop stresses are determined by scaling the maximum vertical dead weight stresses. The maximum stresses in the bottom end stainless steel spacer plate for the bottom end drop condition are taken as the larger of 20 times the bottom end spacer plate (i.e., with guide tubes attached) vertical dead weight stresses or 50 times the stainless steel spacer plate (i.e., spacer plate self-weight only) vertical dead weight stresses. The bottom end drop stresses in the other W21 carbon steel and stainless steel spacer plates are equal to 50 times the maximum vertical dead weight stresses. The maximum stresses in the W21 spacer plates due to the storage cask bottom end drop are presented in Table 3.7-5. The results show that the W21 spacer plate stresses due to the storage cask bottom end drop are less than the Service Level D allowable stresses.

#### 3.7.3.2.2 Support Rod Assemblies

For the postulated storage cask end drop condition, the W21 support rod assemblies (e.g. support rod segments and support sleeves) provide longitudinal support for the spacer plates. The stability of the support rod assemblies is of primary importance for the storage cask end drop condition since they preserve basket geometry, thus maintaining criticality safety after the postulated storage cask end drop condition.

The W21 support rod assembly components (i.e., support rod segments and support sleeves) are evaluated for the postulated storage cask end drop condition in this section as a beam-column

system in accordance with NUREG/CR-6322,[27] which uses the criteria of Section III, Appendix F, Article F-1334.5, of the ASME Code for linear type component supports subjected to combined axial compression and bending. As discussed in Section 3.7.3, the storage cask end drop equivalent static acceleration load is 47*g*. The W21 support rod assemblies are conservatively evaluated for a bounding equivalent static end drop load of 50*g*.

In addition to the 50*g* end drop, the W21 support rods are evaluated for a 20*g* end drop, which represents the maximum load that can be supported by the connection of the guide tubes to the bottom spacer plate. Therefore, at 20*g*, reactions from the bottom spacer plate includes the weight of the guide tubes. Because this additional weight is applied to the bottom plate only, the sleeves are not affected. The 50*g* end drop represents the maximum load level expected for this accident condition and does not include the weight of the guide tubes.

Of all eight W21 basket assembly configurations, the W21M-LD basket assembly support rods are controlling for the storage cask end drop since the W21M-LD basket assembly is the heaviest and the longest, and the strength of the W21M support rod assembly materials is lower than that of the W21T support rod assembly. Therefore, the structural evaluation of the W21M-LD support rod assemblies for the storage cask end drop bounds that of all other W21M and W21T support rod assemblies.

*Support Sleeves*

As discussed in Section 3.1.1.2, support sleeves are used to maintain the longitudinal position of the carbon steel spacer plates within each support rod span (i.e., the span between stainless steel spacer plates). In the event of an end drop, the loads from the carbon steel spacer plates and support sleeves within a span are carried through the support sleeves to the lower stainless steel spacer plate, which transfers the loads into the support rod segments. The highest support sleeve stresses due to the postulated storage cask end drop, within each support rod span, occurs in the support sleeve at the bottom end of the span. A free body diagram of the support sleeves within a typical support rod span is shown in Figure 3.7-1.

The support sleeve axial and bending loads from the ¾-inch thick carbon steel spacer plates are obtained from the spacer plate 50*g* end drop finite element analysis reaction loads. The axial and bending loads from each of the carbon steel spacer plates are 1.88 kips and 5.05 in-kips for the case of lower bound rod stiffness For fixed plate boundaries, maximum axial and bending loads are 1.86 kips and 5.14 in-kips, respectively. The total axial load on each of the support sleeves within a support rod span is calculated as follows:

$$P_i = 50g \times W_{si} + R_{pi-1} + P_{si-1}$$

where $W_{si}$ is the weight of support sleeve *i*, $R_{pi-1}$ is the reaction load from the carbon steel spacer plate above support sleeve *i*, and $P_{si-1}$ is the axial load from the support sleeve above sleeve *i*. The bending moment reaction at each spacer plate is distributed to the upper and lower support

[27] NUREG/CR-6322, UCRL-ID-119697, *Buckling Analysis of Spent Fuel Basket*, Lee, A. S., and Bumpas, S. E., U.S. Nuclear Regulatory Commission, May 1995.

sleeves based on their relative bending stiffness. Since each support sleeve has the same section properties, the bending stiffness is inversely proportional to the sleeve length.

The envelope support sleeve loads for the 50*g* end drop load are 16.36 kips (4.25 in. span) and 3.63 in-kips (1.25 in. span). The corresponding axial compressive and bending stresses in the most highly loaded W21 support sleeve are 7.34 ksi and 2.11 ksi, respectively. Since the 4.25-inch support sleeve span is not the longest in the basket, a bounding length of 4.6 inches is conservatively used to develop lower bound allowable stresses for the support sleeve buckling evaluation.

Per NUREG/CR-6322, members subjected to combined compression and bending must satisfy interaction equations (26), (27) and (28) as follows:

$$\frac{f_a}{F_a}+\frac{C_{mx}f_{bx}}{\left(1-\frac{f_a}{F'_{ex}}\right)F_{bx}}+\frac{C_{my}f_{by}}{\left(1-\frac{f_a}{F'_{ey}}\right)F_{by}}\le 1.0 \qquad \text{(Interaction Eq. 26)}$$

$$\frac{f_a}{2\times 0.6S_y}+\frac{f_{bx}}{F_{bx}}+\frac{f_{by}}{F_{by}}\le 1.0 \qquad \text{(Interaction Eq. 27)}$$

$$\text{If}\frac{f_a}{F_a}\le 0.15,\frac{f_a}{F_a}+\frac{f_{bx}}{F_{bx}}+\frac{f_{by}}{F_{by}}\le 1.0 \qquad \text{(Interaction Eq. 28)}$$

A $C_m$ value of 0.85 is applicable for members in frames not braced against sidesway. Per NUREG/CR-6322, the allowable compressive stress is defined as follows:

$$F_a=\frac{P_{EQ40}}{A_g}$$

where:

$A_g$ = 2.228 in$^2$, the gross area of support sleeve.

$P_{EQ40}$ is the allowable compressive load determined in accordance with Equation 40 of NUREG/CR-6322 as follows:

$$P_{EQ40}=\frac{(P_{EQ45})(P_{EQ33})}{P_{EQ43}}=24.1\text{kips}$$

where $P_{EQ45}$, $P_{EQ33}$, and $P_{EQ43}$ are the allowable compressive loads from Equations (45), (33), and (43) of NUREG/CR-6322, which are calculated as follows:

$$\lambda=\left(\frac{KL}{r}\right)\left(\frac{1}{\pi}\right)\sqrt{\frac{S_y}{E}}=0.0374$$

$$P_{EQ45}=\left(0.47-\frac{120\lambda}{444\sqrt{2}}\right)S_yA_g=16.2\text{ kips (for }\lambda\le\sqrt{2})$$

$$P_{EQ33} = \frac{(1-\lambda^2/4)}{1.11+0.5\lambda+0.17\lambda^2-0.28\lambda^3} S_y A_g = 30.6 \text{ kips} \quad (\text{for } 0 \le \lambda \le 1)$$

$$P_{EQ43} = \frac{(1-\lambda^2/4)}{\frac{5}{3}+\frac{3}{8}\left(\frac{\lambda}{\sqrt{2}}\right)-\frac{1}{8}\left(\frac{\lambda}{\sqrt{2}}\right)^3} S_y A_g = 20.6 \text{ kips} \quad (\text{for } \lambda \le \sqrt{2})$$

where:

K = 1.2, Effective length factor for a fixed-slider boundary condition.

L = 4.60 inches, Maximum support sleeve length.

r = 1.164 inches, Support sleeve radius of gyration.

$A_g$ = 2.228 $in^2$, Support sleeve gross area.

$S_y$ = 15.5 ksi, Yield strength of Type 304L stainless steel at 600°F.

E = $25.3 \times 10^3$ ksi, Elastic modulus of Type 304L stainless steel at 600°F.

Therefore, the allowable compressive stress for the most heavily loaded support sleeve is

$$F_a = 24.1 \text{ kips} \div 2.228 \text{ in}^2 = 10.8 \text{ ksi.}$$

The Euler buckling stress, including a 1.46 factor of safety for stainless steel material and hypothetical accident conditions, per Section 6.32 of NUREG/CR-6322, is defined as:

$$F_e' = \frac{\pi^2 E}{1.46(KL/r)^2} = 7{,}605 \text{ ksi}$$

The allowable bending stress for compact sections, $F_b$, is defined in NUREG/CR-6322 as:

$$F_b = fS_y = 21.0 \text{ ksi}$$

where the plastic shape factor, f, is given by Table 1, Case 15, of Roark as:

$$f = 1.698\left(\frac{R_o^4 - R_o R_i^3}{R_o^4 - R_i^4}\right) = 1.353$$

where $R_o$ and $R_i$ are the outer and inner radii of the support sleeve, respectively.

Interaction equations (26) and (27) are satisfied as follows, where a $C_m$ value of 0.85 is applicable in equation (26) for members in frames not braced against sidesway:

$$\frac{7.34}{10.8} + \frac{(0.85)(2.11)}{\left(1-\frac{7.34}{7{,}605}\right)(21.0)} = 0.77 \qquad (26)$$

$$\frac{7.34}{2 \times 0.6(15.5)} + \frac{2.11}{21.0} = 0.50 \qquad (27)$$

Therefore, the most heavily loaded W21M-LD support sleeves meet the stress acceptance criteria for the bounding 50*g* end drop load. The support sleeve end drop interaction ratios for all other W21M and W21T assemblies are bounded by those calculated for the W21M-LD design.

*Support Rod Segments*

In the event of an end drop, each support rod segment is loaded by its self-weight in addition to the upper joint loads. The support rod segment upper joint loads include the reaction loads from the stainless steel spacer plate, the loads from the upper support rod segment, and the support sleeve loads from the upper support rod span. The support sleeve loads from the upper support rod span include the inertial load of the carbon steel spacer plates and support sleeves, which are transferred through the support sleeves down to the supporting stainless steel spacer plate, as shown in Figure 3.7-1. The most heavily loaded support rod segment is closest to the impacting end since it supports the inertial load of the most spacer plates and support sleeves. However, the unsupported length of the support rod end segment is smaller than that of the interior support rod segments resulting in lower allowable stresses. Therefore, each of the support rod segments is evaluated for the end drop to demonstrate structural adequacy.

The support rod segment axial and bending loads from the ¾-inch thick carbon steel spacer plates and the 2-inch thick stainless steel spacer plates are obtained by scaling reactions from the spacer plate vertical deadweight finite element analyses. Two end drop load levels are evaluated: 20*g* and 50*g*. The 20*g* end drop represents the maximum load that can be supported by the connection of the guide tubes to the bottom spacer plate. Therefore, at 20*g*, reactions from the bottom spacer plate include the weight of the guide tubes. The 50*g* end drop represents the maximum load level expected for this accident condition and does not include the weight of the guide tubes. The spacer plate analysis considers a lower bound support rod bending stiffness to model the plate rotational boundary conditions and also considers fixed rotational boundaries. The axial force and bending moment reaction loads at the rod or sleeve connection from each of the spacer plates are summarized in Table 3.7-1 for the 20*g* and 50*g* end drop conditions.

The maximum compressive stress in each of the seven support rod segments due to the 50*g* end drop load is:

$$f_a = \frac{P}{A} = \frac{\sum_{i=1}^{7}(P_{Ri} + P_{ji-1})}{A}$$

where $P_{Ri}$ is the inertial load from support rod segment i, $P_{ji-1}$ is the axial load from joint (i-1), and A is the gross area of the support rod segment. The support rod segment inertial load is equal to the support rod weight multiplied by the 20*g* or 50*g* equivalent static end drop load. The joint axial load includes the 2-inch thick stainless steel spacer plate reaction load and the axial load from the support sleeves and ¾-inch thick carbon steel spacer plates in the span above the joint. The bending moments from the spacer plates are distributed to the adjacent support rod segments based on their relative rigidities. Each support rod segment is conservatively assumed to carry the entire bending moment reaction from the adjacent 2-inch thick stainless steel spacer plates.

The allowable support rod stresses for the end drop are calculated in accordance with NUREG/CR-6322, as described above for the support sleeves, and summarized in Table 3.7-2. As discussed previously in this section, a bounding support rod end drop evaluation is performed based on the W21M support rods since they are the most highly loaded and have lower material strength properties than the W21T support rods. The bounding support rod end drop evaluation utilizes material properties at a temperature of 600°F, which bounds the maximum support rod temperatures for all normal on-site transfer and storage thermal conditions.

The calculated stresses, allowable stresses, and interaction equations for the support rod segments in the W21M-LD basket design are summarized in Table 3.7-3. The results show that the highest interaction ratio of 0.84 occurs in the support rod segment number 6 (i.e., first interior span at the bottom end of the basket) for the 50*g* end drop. Similarly, the highest interaction ratio at 20*g* (i.e., failure load for guide tube attachment brackets) is 0.73. The maximum support rod interaction ratios for both conditions are lower than the limit of 1.0. Therefore, the W21 support rods meet the buckling design criteria of NUREG/CR-6322 for the bounding 50*g* storage cask end drop load.

#### 3.7.3.2.3 Guide Tubes

For the postulated storage cask bottom end drop condition, the W21 guide tube assemblies are loaded only by their own weight. The top and bottom end details of all W21 guide tube assemblies are identical and all W21 guide tubes are fabricated from the same material. Therefore, the most heavily loaded W21 guide tubes are the W21M-LD guide tubes since they are the longest and the heaviest.

*Guide Tube Stresses*

The most heavily loaded W21 guide tubes are evaluated for the postulated storage cask bottom end drop condition using hand calculations. A bounding equivalent static acceleration load of 50*g* is conservatively used for the guide tube bottom end drop evaluation. The limiting guide tube vertical deadweight stress is uniaxial compression at the bottom end which bears on the supporting canister shell bottom end closure. The W21M-LD guide tube assemblies are the heaviest, weighing 210 pounds each. The guide tube area at the bottom end is reduced due to the 6.5-inch wide cutouts on all four faces. The uniform axial compressive stress in the guide tube due to a 50*g* HAC end drop load is calculated as follows:

$$f_a = \frac{WG}{A_b} = 14.0 \text{ ksi}$$

where:

$W$ = 210 lb., weight of heaviest guide tube

$A_b$ = guide tube area, less cutouts

= $4(8.95 + 0.075)(0.075) - 4(6.5)(0.075)$

= $0.75 \text{ in}^2$

The corresponding Service Level D allowable primary membrane stress intensity, conservatively based on Type 316 stainless steel material properties at 700°F, is 39.1 ksi. Therefore, the W21 guide tubes meet the stress acceptance criteria for the postulated storage cask bottom end drop condition.

*Guide Tube Buckling*

The elastic stability of the most heavily loaded W21 guide tube is evaluated for the postulated storage cask end drop condition using hand calculations. The lowest factor of safety against buckling occurs at the bottom end of the guide tube where the axial compressive stresses are highest and the free edges in the region of the cutouts result in the lowest theoretical buckling stress. The critical guide tube buckling stress is calculated treating the bottom end of the guide tube as a rectangular plate, simply supports on three edges and free on the fourth edge, and subjected to uniform axial compressive loading (Roark, Table 35, Case 1d) as follows:

$$\sigma = K\frac{E}{1-\nu^2}\left(\frac{t}{b}\right)^2 = 206 \text{ ksi}$$

where:

E = $24.8 \times 10^6$ psi, elastic modulus of Type 316 stainless steel at 700°F,

t = 0.075 in., guide tube thickness,

b = (9.025 - 6.5)/2 = 1.263 in., width of the corner piece of guide tube panel,

ν = 0.29, Poisson's ratio

K = 2.16 for a / b = 1/1.263 = 0.8

Per NUREG/CR-6322, the design allowable is limited to 2/3 of the theoretical buckling stress, or 137 ksi. Therefore, the minimum design margin for buckling of the most heavily loaded W21 guide tube is +8.79.

## 3.7.4 Storage Cask Tip-Over

The storage cask is evaluated for a postulated accidental tip-over event as discussed in Section 2.3.3.3 and evaluated in Section 3.7.4 of the FuelSolutions™ Storage System FSAR. The storage cask tip-over event results in a peak rigid body acceleration of 21.9g at the top end of the storage cask, with a ramped load having a 15 msec rise time characterized as an isosceles triangular pulse with a duration of 0.010 seconds and a peak acceleration of 41.4g. The structural evaluation of the W21 canister for the postulated tip-over condition is performed using equivalent static loads. The equivalent static acceleration load is equal to the peak rigid-body acceleration multiplied by a DLF to account for possible dynamic amplification within the canister assembly. For transverse natural frequencies of the W21 canister assembly are all greater than 100 Hz. Per Figure 2.1 of NUREG/CR-3966, the maximum DLF for $t_r/T$ greater than or equal to 1.5 (e.g., for natural frequencies of 100 Hz and greater) is approximately 1.2. Therefore,

the maximum equivalent static acceleration at the top end of the canister for the storage cask tip-over is 26.3*g*. A bounding equivalent static acceleration load of 30*g* is conservatively used for the W21 canister tip-over structural evaluation.

### 3.7.4.1 Canister Shell Assembly Tip-over Analysis

For the postulated storage cask tip-over condition, the W21 canister shell assembly is supported by the two storage cask rails which run the full length of the canister shell and are located at 22.5° on both sides of the canister bottom centerline. The canister shell is loaded by its own weight in addition to the weight of the basket assembly and SNF assemblies contained in the canister shell cavity. The structural evaluation of the W21 canister shell assembly for the postulated storage cask tip-over load condition is performed using the three-dimensional ½-symmetry finite element model described in Section 3.9.3.2. This model represents the top end region of the W21M-LS canister shell and basket assembly. Since the tip-over loads at the bottom end of the canister shell assembly are much lower than those at the top end, the stresses in the bottom end of the canister shell are bounded by those in the top end region and, consequently, need not be evaluated.

As discussed in Section 3.9.3.2, the W21M-LS canister is selected as the bounding design since it has the largest overall combined weight for the basket assembly and fuel and the heaviest top shield plug. The W21M-LS top shield plug and basket assembly spacer plates are included in the finite element model and connected to the canister shell with gap elements in order to accurately capture the non-linear interaction between the these components and the canister shell for the tip-over load condition. In addition, radial gap elements are used to model the non-linear support interface between the outside of the canister shell and the storage cask rail supports. A more detailed description of the W21 canister shell three-dimensional ½-symmetry finite element model is provided in Section 3.9.3.2.

For the tip-over condition, the canister shell is loaded by its own weight plus the weight of the basket assembly and fuel. The inertial loads of the canister shell, top outer and inner closure plates, the shield plug, and the self weight of the spacer plates are accounted for by applying an appropriate acceleration in the direction of the loading. The inertial loads of the fuel assembly and the guide tube are applied as uniform pressure loads over the width of the supporting spacer plate ligaments, as shown in Figure 3.9-7. The ligament pressure load are calculated for each spacer plate based upon the guide tube and fuel tributary weights presented in Table 3.9-3.

The stresses in the canister shell due to the tip-over load condition are calculated using a linear-elastic static analysis. The maximum stresses in the canister shell due to the tip-over condition are summarized in Table 3.7-4. The maximum stresses in the W21 canister shell due to the bounding 30*g* tip-over load are shown to be lower than the corresponding Service Level D allowable stresses.

### 3.7.4.2 Basket Assembly Tip-over Analysis

#### 3.7.4.2.1 Spacer Plates

When subjected to tip-over loading, the W21 spacer plates are relied upon to support and maintain the positions of the guide tube assemblies and SNF assemblies for criticality control.

The W21 spacer plates are loaded by their own weight and the weight of the SNF assemblies, guide tube assemblies, and support rod assemblies. The spacer plates are supported by the canister shell in the region of impact and the canister shell is supported by two storage cask rails.

As discussed in Section 3.7.4, the W21 basket assembly is designed for a bounding 30*g* tip-over load. A linear-elastic stress analysis is performed based on a uniform fuel load assumption. In addition, a plastic stress analysis is performed assuming the fuel load is applied to the spacer plates as concentrated loads at the fuel grid spacer locations. The primary purpose of the plastic stress analysis is to determine the maximum spacer plate permanent deformation resulting from the storage cask tip-over for consideration in the criticality evaluation. Lastly, buckling evaluations of the spacer plates are performed for the storage cask tip-over, considering both beam-column buckling in accordance with NUREG/CR-6322 and general instability in accordance with Appendix F of the ASME Code.

*Tip-over Elastic Stress Analysis*

The W21 spacer plate stress evaluation for the bounding 30*g* storage cask tip-over load is performed using an elastic system analysis based on a uniform fuel load assumption (i.e., spacer plate fuel loads proportional to spacer plate longitudinal pitch). For the spacer plate tip-over evaluation, the spacer plate is assumed to be supported only at the locations of the storage cask rails, conservatively neglecting the support provided by the canister shell. This is conservative since the assumed boundary conditions result in more concentrated reaction loads which produce higher stresses in the spacer plates.

Only the most highly loaded W21 carbon steel and stainless steel spacer plates are evaluated for the 30*g* storage cask tip-over load. For the tip-over condition, the acceleration load varies in magnitude, from approximately zero at the bottom end of the canister to the maximum acceleration at the top end of the canister. The impact load for each spacer plate is equal to the product of the transverse acceleration at its longitudinal location and the spacer plate tributary weight. The W21 spacer plates having the highest tributary weights are those near the mid-length of the basket assembly since they have the largest longitudinal pitch. Therefore, in order to provide a bounding analysis for the postulated storage cask tip-over condition, the bounding 30*g* tip-over acceleration, which occurs at the top end of the canister, is applied to the W21 spacer plates in the basket mid-region which support the largest tributary weight.

As discussed in Section 3.9.1, the W21 carbon steel and stainless steel spacer plates with the highest tributary weights are those in mid-region of the W21M-SD or W21T-SL basket assembly. The most highly loaded carbon steel and stainless steel spacer plates have total tributary weights of 1,587 pounds and 2,106 pounds, respectively. Therefore, the most highly loaded W21 carbon steel and stainless steel spacer plates support total loads for the 30*g* storage cask tip-over of 47.6 kips and 63.2 kips, respectively.

The W21 spacer plate tip-over elastic stress analysis is performed using the plane stress finite element model described in Section 3.9.3.3.1. The spacer plate loading from the support rod assemblies, guide tube assemblies, and fuel assemblies are determined for the 30*g* tip-over load as described in Section 3.9.3.3.1. Linear-elastic static analyses are performed and the resulting spacer plate stresses are evaluated using linear stresses as discussed in Section 3.9.2.3.

The results of the W21 spacer plate tip-over elastic system stress analyses show that the total reaction loads from the finite element solutions are equal to the tip-over impact loads calculated above. The maximum primary membrane and primary membrane plus bending stress intensities in the carbon steel spacer plates are 18.4 ksi and 46.0 ksi, respectively. The Service Level D allowable primary membrane and primary membrane plus bending stress intensities for the carbon steel spacer plate material at 700°F are 75.4 ksi and 113.1 ksi, respectively. Therefore, the stresses in the most highly loaded W21 carbon steel spacer plate due to bounding 30*g* storage cask tip-over loading are less than the corresponding Service Level D allowable stress intensities.

The maximum primary membrane and primary membrane plus bending stress intensities in the most highly loaded W21 stainless steel spacer plate for the bounding 30*g* tip-over loading are 9.3 ksi and 23.3 ksi, respectively. The Service Level D allowable primary membrane and primary membrane plus bending stress intensities for SA-240, Type XM-19 stainless steel at 700°F are 60.6 ksi and 90.8 ksi, respectively. Therefore, the maximum primary membrane and membrane plus bending stress intensities in the most highly loaded W21 stainless steel spacer plate due to the bounding 30*g* storage cask tip-over load are less than the corresponding Service Level D allowable stress intensities.

*Tip-over Plastic Stress Analysis*

The W21 spacer plates are evaluated for the bounding 30*g* storage cask tip-over load using plastic system analysis. The purpose of this plastic analysis is to determine the maximum permanent deformation of the W21 spacer plates due to the storage cask tip-over loading. For this analysis, the loads from the SNF assemblies are conservatively applied to the supporting basket assembly structure as concentrated loads at the fuel grid spacer locations. Since the W21 canisters are designed for a range of fuel types, the total SNF assembly weight tributary to each grid spacer and the location of the grid spacers relative to the basket assembly spacer plates can vary. The worst case loading for each W21 spacer plate results from the SNF fuel with the highest grid spacer tributary weight for the fuel assembly grid spacer located directly over that spacer plate. As discussed in Section 3.9.1, the maximum spacer plate stresses under these assumed loading conditions occur in the W21M-SD or W21T-SL basket assemblies loaded with WE 15x15 fuel with control components. The analysis for the postulated storage cask tip-over condition is performed using a bounding 30*g* tip-over acceleration, occurring at the top end of the canister, which is conservatively applied to the W21 spacer plates in the W21M-SD and W21T-SL basket mid-regions which support the largest in-plane tributary weight.

The W21 spacer plates plastic stress analysis for the storage cask tip-over condition is performed using the ½-symmetry multi-span plane-stress finite element model described in Section 3.9.3.3.3. The finite element model includes three spacer plates; the center spacer plate over which the fuel grid spacers are assumed to be positioned, and the adjacent spacer plates on either side. For the evaluation of the W21 carbon steel spacer plates, all spacer plates are assumed to be ¾-inch thick carbon steel plates with at uniform pitch of 5.00 inches. Similarly, for the evaluation of the W21 stainless steel plates, the center spacer plate is modeled as a 2.00-inch thick stainless steel plate and the adjacent plates are modeled as ¾-inch thick carbon steel plates. The pitch between the W21 stainless steel spacer plate and adjacent carbon steel spacer plates is modeled as 5.475 inches. For both models, the W21 guide tubes extend 2.50 inches beyond the centerlines of the outer spacer plates on each side. The finite element

model construction, material properties, boundary conditions, and loading are described in detail in Section 3.9.3.3.3.

For the W21 spacer plate tip-over plastic analysis, the model loads are ramped up to 30*g* and then reduced to 1*g* in order to determine permanent deformations. The results of the W21 carbon steel and stainless steel spacer plate plastic tip-over analyses show that plastic strain in the most highly loaded spacer plates occur only in a few very local regions. The maximum equivalent plastic strain in the most highly loaded W21 carbon steel and stainless steel spacer plates resulting from the bounding 30*g* tip-over load are 1.6% and 0.8%, respectively. Per Section II, Part A of the ASME Code, the minimum elongation of SA-517, Grade P carbon steel and SA-240, Type XM-19 stainless steel are 16% and 35%, respectively. Therefore, the plastic strain in the most highly loaded W21 carbon steel and stainless steel spacer plates is much less than that corresponding to ultimate tensile failure. The maximum permanent deformation in the most highly loaded W21 carbon steel and stainless steel spacer plates resulting from the bounding 30*g* tip-over load are 0.005 inches and 0.002 inches, respectively.

*Tip-over Buckling Analysis*

The buckling evaluation of the spacer plates for the postulated storage cask tip-over condition considers beam-column buckling in accordance with NUREG/CR-6322 and general plastic instability in accordance with Appendix F of the ASME Code.

The W21 spacer plates are evaluated for buckling due to the storage cask tip-over condition as linear type supports subjected to combined axial compression and bending in accordance with NUREG/CR-6322. Buckling evaluations are performed for the most highly loaded ligaments in both the W21 carbon steel and stainless steel spacer plates for the bounding 30*g* tip-over loading both with and without the bounding normal thermal loads superimposed. For this buckling evaluation, the spacer plate stresses are calculated using an elastic system analysis.

The maximum stresses in the W21 spacer plates due to the storage cask tip-over are evaluated using interaction equations (26), (27), and (28) of NUREG/CR-6322, defined as follows:

$$\frac{f_a}{F_a}+\frac{C_{mx}f_{bx}}{\left(1-\frac{f_a}{F'_{ex}}\right)F_{bx}}+\frac{C_{my}f_{by}}{\left(1-\frac{f_a}{F'_{ey}}\right)F_{by}}\le 1.0 \qquad \text{(Eq. 26)}$$

$$\frac{f_a}{2\times 0.6S_y}+\frac{f_{bx}}{F_{bx}}+\frac{f_{by}}{F_{by}}\le 1.0 \qquad \text{(Eq. 27)}$$

If $f_a/F_a \le 0.15$, then equation (28) may be used in lieu of equations (26) and (27):

$$\frac{f_a}{F_a}+\frac{f_{bx}}{F_{bx}}+\frac{f_{by}}{F_{by}}\le 1.0 \qquad \text{if } \frac{f_a}{F_a}\le 0.15 \qquad \text{(Eq. 28)}$$

The allowable axial stress, $F_a$, bending stress, $F_b$, and Euler buckling stress, $F_e'$, are calculated for all ligament sizes for both the W21 carbon steel and stainless steel spacer plate. Per

NUREG/CR-6322, the allowable compressive stress for carbon steel and stainless steel spacer plates are defined as follows:

$$F_a = \frac{P_{33}}{A_g} \text{ (Carbon Steel)}$$

$$F_a = \frac{P_{40}}{A_g} \text{ (Stainless Steel)}$$

where, $A_g$ is the gross area of the spacer plate ligament, and the maximum allowable loads, $P_{33}$ and $P_{40}$, are the allowable compressive load determined in accordance with NUREG/CR-6322 as follows:

$$P_{33} = \frac{(1-\lambda^2/4)}{1.11+0.5\lambda+0.17\lambda^2-0.28\lambda^3} S_y A_g \quad (\text{for } 0 \le \lambda \le 1)$$

$$P_{40} = \frac{(P_{45})(P_{33})}{P_{43}}$$

where:

$$\lambda = \left(\frac{KL}{r_x}\right)\left(\frac{1}{\pi}\right)\sqrt{\frac{S_y}{E}}$$

$$P_{45} = \left(0.47 - \frac{120\lambda}{444\sqrt{2}}\right) S_y A_g \quad (\text{for } \lambda \le \sqrt{2})$$

$$P_{43} = \frac{(1-\lambda^2/4)}{\frac{5}{3}+\frac{3}{8}\left(\frac{\lambda}{\sqrt{2}}\right)-\frac{1}{8}\left(\frac{\lambda}{\sqrt{2}}\right)^3} S_y A_g \quad (\text{for } \lambda \le \sqrt{2})$$

where:

K = 0.65, Effective length factor for fixed-fixed support per Figure 6 of NUREG/CR-6322

L = 9.43 in., Unsupported length of spacer plate ligaments

$r_x$ = $\sqrt{I_x / A_g}$ in., Ligament radius of gyration

$I_x$ = $b^3t/12$, Ligament moment of inertia

$A_g$ = bt, Ligament gross area

b = Ligament width
= 1.945 in., Center ligaments (hereafter referred to as Ligament "A")
= 1.345 in., Outermost ligaments (hereafter referred to as Ligament "B")

t = Spacer plate thickness
= 0.75 in., Carbon steel spacer plate
= 2.00 in., Stainless steel spacer plate

$S_y$ = Spacer plate material yield strength at 700°F
= 83.0 ksi (carbon steel spacer plate)
= 36.3 ksi (stainless steel spacer plate)

E = Spacer plate material elastic modulus at 700°F
= $25.5(10)^3$ ksi (carbon steel spacer plate)
= $24.8(10)^3$ ksi (stainless steel spacer plate)

$C_m$ = 0.85, Coefficient for members in frames where sidesway is permitted per NUREG/CR-6322

The Euler buckling stress, calculated in accordance with Section 6.32 of NUREG/CR-6322, is defined as follows:

$$F_e' = \frac{\pi^2 E}{1.46(KL/r_x)^2} \quad \text{(stainless steel)}$$

$$F_e' = \frac{\pi^2 E}{1.30(KL/r_x)^2} \quad \text{(carbon steel)}$$

The allowable bending stress for compact sections, $F_b$, is defined in NUREG/CR-6322 as:

$$F_b = fS_y$$

where the plastic shape factor is f=1.5 for a solid rectangular section per Roark, Table 1, Case 2.

The allowable stresses are calculated for each of the W21 spacer plate ligament types and summarized in Table 3.7-6.

As discussed previously, the spacer plate stresses used for the buckling evaluation are calculated using an elastic system analysis. The spacer plate stresses are determined for the bounding 30*g* tip-over load, both with and without thermal loading superimposed. The 30*g* tip-over loads for the spacer plates are calculated and applied to the W21 spacer plate plane stress finite element model as described in Section 3.9.3.3.1. The thermal gradient which is applied to the model is based on the temperature distribution in the hottest W21 carbon steel spacer plate for normal cold storage conditions. As discussed in Section 3.5.1.3.2, the normal cold storage thermal condition results in the highest spacer plate thermal stresses, and therefore, the worst case initial condition

for spacer plate buckling. In order to facilitate application of the thermal gradient to the model, the spacer plate gradient is approximated using the following third order polynomial equation, which provides the temperature (T) as a function of the radial distance from the spacer plate centerline:

$$T(r) = 0.0342r^3 - 2.0138r^2 + 25.76r + 475.45$$

Figure 3.7-3 shows the design thermal gradient versus the actual W21 spacer plate temperatures for the normal cold storage thermal condition. A comparison of the thermal stresses calculated using the polynomial function and those from the actual thermal gradient shows that the design thermal gradient produces thermal stresses in the W21 carbon steel spacer plate which bound those calculated for the normal cold storage thermal gradient. Therefore, the design thermal gradient is bounding.

The maximum axial compressive stress and bending stress in the W21 carbon steel and stainless steel spacer plate ligaments for the tip-over loading, both with and without thermal loading superimposed, are summarized in Table 3.7-7 along with the resulting interaction ratios. The results show that the highest interaction ratios resulting from the bounding 30*g* tip-over load are 0.31 in centermost (Ligament A) of the W21 carbon steel spacer plate for combined tip-over plus thermal loading and 0.70 in outermost (Ligament B) of the W21 stainless steel spacer plate for combined tip-over plus thermal loading. Therefore, the most highly loaded W21 spacer plate meet the buckling design criteria of NUREG/CR-6322 for the bounding 30*g* tip-over load.

In addition to the NUREG/CR-6322 elastic beam-column buckling analysis, general plastic instability of the W21 spacer plates is evaluated for the bounding 30*g* storage cask tip-over load, both with and without the bounding normal thermal loading, using plastic large deflection analyses. Since the longitudinal bending stiffness of the W21 carbon steel spacer plates is proportional to the plate thickness squared, the bending stiffness of the 2.00-inch thick W21 stainless steel spacer plates much greater than that of the ¾-inch thick W21 carbon steel spacer plates. In addition, the results of the W21 spacer plate elastic stress analysis for the tip-over load show that the spacer plate stress levels relative to the material yield strengths are comparable. Therefore, general instability will be controlled by the carbon steel spacer plates and the stainless steel spacer plates need not be evaluated.

For this analysis, the loads from the SNF assemblies are conservatively applied to the supporting basket assembly structure as concentrated loads at the fuel grid spacer locations. Since the W21 canisters are designed for a range of fuel types, the total SNF assembly weight tributary to each grid spacer and the location of the grid spacers relative to the basket assembly spacer plates can vary. The worst case loading for each W21 spacer plate results from the SNF fuel with the highest grid spacer tributary weight for the fuel assembly grid spacer located directly over that spacer plate. As discussed in Section 3.9.1, the controlling W21 basket configuration for this loading condition occurs in the W21M-SD or W21T-SL basket assemblies loaded with WE 15x15 fuel with control components. The bounding storage cask tip-over acceleration at the top end of the canister is 30*g*. For the W21 spacer plate plastic instability analysis, the bounding 30*g* tip-over acceleration is conservatively applied to the W21 spacer plates in the W21M-SD and W21T-SL basket mid-regions which support the largest tributary weight.

The W21 carbon steel spacer plate plastic large deflection buckling analysis for the storage cask tip-over condition is performed using the full multi-span shell finite element model described in Section 3.9.3.3.5. The finite element model includes three spacer plates; the center spacer plate over which the fuel grid spacers are assumed to be positioned, and the adjacent spacer plates on either side. For the evaluation of the W21 carbon steel spacer plates, all spacer plates are assumed to be ¾-inch thick carbon steel plates with at uniform pitch of 5.00 inches. The spacer plates are modeled using plastic shell elements which have both membrane and bending stiffness. The spacer plates are supported longitudinally at the locations of the support rods. In addition, the bending support provided by the support rods is modeled using spring elements. A lower bound support rod bending stiffness is conservatively used for this evaluation.

The bi-linear kinematic hardening material model with a 0.1% tangent modulus is conservatively used for the spacer plate and guide tube materials. For the tip-over loads without thermal, the material properties at 700°F are assumed. For the combined tip-over plus thermal loading, the temperature dependent material properties from Section 3.3.1 are used for the spacer plates and guide tubes.

The fuel load is applied to the bottom panel of the guide tubes directly above the center spacer plate. The spacer plate self-weight and the weight of the guide tubes are accounted for by applying an in-plane acceleration load. The support rod loads are applied to the spacer plates at the nodes nearest the support rod centerlines. The support rod forces are calculated based upon the spacer plate tributary lengths. In addition to the in-plane model loading, a constant 10*g* longitudinal acceleration load is applied to the finite element model to introduce an initial eccentricity to the spacer plates.

The thermal gradient which is applied to the model is based on the temperature distribution in the hottest W21 carbon steel spacer plate for normal cold storage conditions. The bounding design thermal gradient discussed previously is conservatively used for this analysis. The finite element model construction, material properties, boundary conditions, and loading are described in detail in Section 3.9.3.3.5.

For the W21 spacer plate tip-over plastic large deflection buckling analysis, the loads are applied such that the variable "time" is equal to the load factor (i.e., time = 3.0 corresponds to 3 times the tip-over load). The 10*g* longitudinal acceleration and thermal gradient are applied as initial conditions (i.e., time = 0.01 seconds). All model in-plane loads are ramped up to three times the tip-over load (i.e., 90*g* at time = 3.00 seconds). Spacer plate plastic instability is indicated by numerical instability in the finite element solution (i.e., unconverged solution). The results show that the most highly loaded W21 carbon steel spacer plate fails due to plastic instability at load factors of 2.2 for the tip-over loading and 2.3 for tip-over plus thermal loading. The buckled shape of the W21 carbon steel spacer plate for the tip-over condition is shown in Figure 3.7-4. The spacer plate deflections are slightly higher for the case which includes thermal loading than for tip-over loading alone. However, the lowest buckling factor of safety occurs without thermal loading. This is due to the fact that the spacer plate is shown to buckle near the rail supports and thermal loading produces tensile stresses at the edge of the spacer plates which oppose the compressive stresses near the rail supports which result from the tip-over loads.

#### 3.7.4.2.2 Support Rod Assemblies and Guide Tubes

The support rod assembly and guide tube loads due to the postulated storage cask tip-over condition are bounded by those due to the transfer cask side drop. Furthermore, the support rod assembly and guide tube boundary conditions for the storage cask tip-over are similar to those for the transfer cask side drop. Therefore, the support rod assembly and guide tube stresses need not be evaluated for the postulated storage cask tip-over condition.

## 3.7.5 Transfer Cask Drop

The transfer cask is evaluated for a postulated accidental side drop event as discussed in Section 2.3.3.2.2 and evaluated in Section 3.7.5 of the FuelSolutions™ Storage System FSAR. The accidental transfer cask drop scenario is a postulated side drop from a height of 72 inches. The transfer cask side drop results in a rigid body response, characterized as a half-sine wave shape with a duration of $t_1$ = 0.0225 msec and a peak acceleration of 46g. The FuelSolutions™ W21 canister is evaluated for the postulated transfer cask side drop scenario using equivalent static loads. The equivalent static side drop acceleration is equal to the peak acceleration multiplied by a DLF to account for possible dynamic amplification within the canister. The maximum DLF for the W21 canister assembly is based on the natural frequencies of the W21 canister structural components. The lowest natural frequency of the W21 canister assembly is 111 Hz for the spacer plates. From Figure 2.15 of NUREG/CR-3966, the maximum DLF for a half-sine pulse load where t1/T - 2.5 (= 0.0225 x 111) or higher is 1.15. Therefore, the maximum equivalent static acceleration for the transfer cask side drop is 53*g*. The FuelSolutions™ W21 canister is evaluated for a bounding 60*g* side drop deceleration resulting from the postulated transfer cask side drop scenario in the following sections.

### 3.7.5.1 Canister Shell Assembly Side Drop Analysis

For the postulated transfer cask side drop condition, the W21 canister shell assembly is supported by the transfer cask inner shell and loaded by its own weight in addition to the weight of the basket assembly and SNF assemblies contained in the canister shell cavity. The W21 canister shell assembly is evaluated for the postulated transfer cask side drop analysis using a bounding equivalent static deceleration load of 60*g*. The side drop load condition is evaluated using the three-dimensional half-symmetry finite element model described in Section 3.9.3.2. This model represents the top end region of the W21M-LS canister shell and basket assembly. As discussed in Section 3.9.3.2, the W21M-LS canister is selected as the bounding design since it has the largest overall combined weight for the basket assembly and fuel and the heaviest top shield plug. The W21M-LS top shield plug and basket assembly spacer plates are included in the finite element model and connected to the canister shell with gap elements in order to accurately capture the non-linear interaction between the these components and the canister shell for the tip-over load condition. In addition, radial gap elements are used to model the non-linear support interface between the outside of the canister shell and inside shell of the transfer cask. A more detailed description of the W21 canister shell three-dimensional ½-symmetry finite element model is provided in Section 3.9.3.2.

For the transfer cask side drop condition, the canister shell is loaded by its own weight plus the weight of the basket assembly and fuel. The inertial loads of the canister shell, top outer and inner closure plates, the shield plug, and the self weight of the spacer plates are accounted for by

applying an appropriate acceleration in the direction of the loading. The inertial loads of the fuel assembly and the guide tube are applied as uniform pressure loads over the width of the supporting spacer plate ligaments, as shown in Figure 3.9-7. The ligament pressure load are calculated for each spacer plate based upon the guide tube and fuel tributary weights presented in Table 3.9-3.

The stresses in the canister shell due to the 60*g* side drop load condition are calculated using a linear-elastic static analysis. The maximum primary membrane and primary membrane plus bending stress intensities in the canister shell due to the 60g side drop are reported in Table 3.7-4. The results of the canister shell side drop analysis show that the maximum stresses are less than the corresponding Service Level D allowable stresses.

### 3.7.5.2 Canister Basket Assembly Side Drop Analysis

#### 3.7.5.2.1 Spacer Plates

When subjected to the postulated transfer cask side drop loading, the W21 basket assembly spacer plates provide structural support for the spent fuel assemblies, guide tube assemblies, support rods, and support sleeves. The structural stability of the spacer plates is of primary importance for the side drop condition since the spacer plates are relied on to maintain the relative spacing of the poisoned guide tube assemblies and fuel assemblies and assure criticality safety. A rigorous structural evaluation of the W21 spacer plates is performed for a postulated transfer cask side drop condition. As discussed in Section 3.7.5, a bounding side drop load of 60*g* is used for the evaluation of the W21 basket assembly components for side drop.

Structural evaluations of the most highly loaded W21 spacer plates are performed for the postulated transfer cask side drop condition using two bounding fuel loading assumptions: (1) Uniform fuel loading assumption (i.e., fuel weight distributed uniformly to basket assembly spacer plates), and (2) Concentrated fuel loading at the fuel assembly grid spacers. The uniform fuel loading assumption is used for elastic system stress analyses in accordance with Appendix F of the ASME Code. The concentrated fuel loading assumption is used for plastic stress analyses to determine the maximum spacer plate permanent deformation in the most highly loaded W21 carbon steel and stainless steel spacer plates resulting from the 60*g* side drop load for consideration in the criticality evaluation. Finally, a buckling evaluation of the W21 spacer plates is performed which considers beam-column buckling in accordance with NUREG/CR-6322 (uniform fuel load), and general instability in accordance with Appendix F of the ASME Code (concentrated fuel load).

*Elastic Stress Analysis - Uniform Fuel Loading*

The W21 spacer plate side drop elastic stress analysis is performed using the plane stress finite element model described in Section 3.9.3. Only the most highly loaded W21 carbon steel and stainless steel spacer plates are evaluated for the 60*g* side drop. Since the side drop acceleration load does not vary in magnitude over the length of the basket assembly, the most heavily loaded W21 spacer plates are those which support the largest tributary weight. The spacer plate in-plane tributary weights are defined as the portion of the SNF assembly (and fuel spacer, if required), guide tube, support rod, and support sleeve weights that are supported by each spacer plate in the transverse direction, combined with the spacer plate self-weight.

The maximum tributary weights of the Type A stainless steel and Type B carbon steel spacer plates are 2,106 pounds and 1,587 pounds, respectively. Therefore, the most highly loaded W21 stainless steel and carbon steel spacer plates support total loads for the 60*g* side drop of 126.4 kips and 95.2 kips, respectively.

A total of four side drop impact orientations are analyzed for both spacer plates, including 0°, 15°, 30°, and 45°, as shown in Figure 3.7-5. Since the spacer plate is symmetric with respect to the horizontal and vertical centerlines, these impact orientations encompass all of the orientations expected to cause the most severe spacer plate stresses. The spacer plate loading from the support rod assemblies, guide tube assemblies, and fuel assemblies are determined for each impact orientation.

For each side drop orientation, a linear-elastic static analysis is performed. The primary stress intensities in the spacer plates are evaluated as discussed in Section 3.9.2.3. The maximum primary membrane ($P_m$) and primary membrane plus bending ($P_m$+$P_b$) stress intensities in the most highly loaded W21 carbon steel stainless steel spacer plates are summarized in Table 3.7-8 for each side drop orientation.

The stress results show that the highest carbon steel spacer plate primary membrane and primary membrane plus bending stress intensities due to the HAC side drop load result from the 0° and 15° impact orientations, respectively. The maximum primary membrane and primary membrane plus bending stress intensities are 23.3 ksi and 75.2 ksi, respectively. The Service Level D allowable primary membrane and primary membrane plus bending stress intensities for the carbon steel spacer plate material at 700°F are 75.4 ksi and 113.1 ksi, respectively. Therefore, the maximum primary membrane and membrane plus bending stress intensities in the most highly loaded W21 carbon steel spacer plate due to bounding 60*g* side drop loading are less than the corresponding Service Level D allowable stress intensities.

The maximum primary membrane ($P_m$) and primary membrane plus bending ($P_m$+$P_b$) stress intensities in the most highly loaded W21 stainless steel spacer plate are summarized in Table 3.7-8. The stress results show that the highest spacer plate primary membrane and primary membrane plus bending stress intensities due to the HAC side drop load result from the 30° impact orientation. The maximum primary membrane and primary membrane plus bending stress intensities are 12.4 ksi and 45.8 ksi, respectively. The Service Level D allowable primary membrane and primary membrane plus bending stress intensities for SA-240, Type XM-19 stainless steel at 700°F are 60.6 ksi and 90.8 ksi, respectively. Therefore, the maximum primary membrane and membrane plus bending stress intensities in the most highly loaded W21 stainless steel spacer plate due to the bounding 60*g* side drop loading are less than the corresponding Service Level D allowable stress intensities.

*Plastic Stress Analysis - Concentrated Fuel Loading at Fuel Grid Spacers*

In addition to the uniform fuel load case, the loads from the SNF assemblies are conservatively applied to the supporting basket assembly structure as concentrated loads at the fuel grid spacer locations. Since the W21 canisters are designed for a range of fuel types, the total SNF assembly weight tributary to each grid spacer and the location of the grid spacers relative to the basket assembly spacer plates can vary. The worst case loading for each W21 spacer plate results from the SNF fuel with the highest grid spacer tributary weight for the fuel assembly grid spacer

located directly over that spacer plate. The maximum spacer plate stresses under these assumed loading conditions occur in the W21M-SD or W21T-SL basket assemblies loaded with WE 15x15 fuel with control components. The highest spacer plate stresses occur in the spacer plates in the basket mid-region since these plates have the largest tributary length and therefore support the largest load. Therefore, bounding side drop plastic stress analyses are performed for the W21 carbon steel and stainless steel spacer plates in the W21M-SD and W21T-SL basket mid-regions.

The W21 spacer plates are evaluated for the bounding 60*g* transfer cask side drop load using plastic system analysis. The purpose of this plastic analysis is determine the maximum permanent deformation of the W21 spacer plates due to the transfer cask side drop loading. For this analysis, as with the uniform loading condition, impact orientations of 0° and 45° are considered.

The W21 spacer plates plastic stress analyses for the transfer cask side drop condition are performed using the full multi-span plane-stress finite element model described in Section 3.9.3.3.4. The finite element model include three spacer plates; the center spacer plate over which the fuel grid spacers are assumed to be positioned, and the adjacent spacer plates on either side. For the evaluation of the W21 carbon steel spacer plates, all spacer plates are assumed to be ¾-inch thick carbon steel plates. For the evaluation of the W21 stainless steel plates, the center spacer plate is modeled as a 2.00-inch thick stainless steel plate and the adjacent plates are modeled as ¾-inch thick carbon steel plates. For both models, the W21 guide tubes extend 2.50 inches beyond the centerlines of the outer spacer plates on each side.

The finite element model loads for the 60*g* side drop conditions are calculated and applied as described in Section 3.9.3.3.4. The model loading includes the self-weight of the W21 spacer plates and guide tubes, the weight of the support rods and support sleeves tributary to each spacer plate, and the fuel assembly weights. The self-weight of the spacer plates and guide tubes are included in the model and accounted for by applying in-plane accelerations to the model in the direction of impact. The support rod and sleeve tributary weights are applied as concentrated loads on each spacer plate. The fuel weight is applied as a concentrated load to the guide tube directly above the center spacer plate in the model, as discussed above. W21 spacer plate 60*g* side drop plastic analysis, the model loads are ramped up to 60*g* and then reduced to 1*g* in order to determine the spacer plate permanent deformations.

The results of the W21 carbon steel and stainless steel spacer plate 60*g* side drop plastic analyses are summarized in Table 3.7-9. The analyses shows that the plastic strain in the most highly loaded W21 carbon steel and stainless steel spacer plate for the bounding 60*g* side drop load is small and occurs only in localized regions.

The maximum equivalent plastic strain in the most highly loaded W21 carbon steel spacer plate is 0.7% and occurs for the 0° impact orientation, The minimum elongation of SA-517, Grade P carbon steel is 16%. Therefore, the plastic strain in the W21 carbon steel spacer plates is much less than that corresponding to ultimate tensile failure. The maximum permanent deformation in the W21 carbon steel spacer plate results from the 45° impact orientation and is calculated to be 0.03 inches.

The maximum equivalent plastic strain in the most highly loaded W21 stainless steel spacer plate from the bounding 60*g* side drop load is 1.0% and occurs for the 45° impact orientation. The

minimum elongation of SA-240, Type XM-19 stainless steel is 35%. Thus, the plastic strain in the W21 stainless steel spacer plates is much less than that corresponding to ultimate tensile failure. The maximum permanent deformation in the W21 stainless steel spacer plate also occurs for the 45° impact orientation and is calculated to be 0.049 inches.

*Spacer Plate Buckling*

The buckling evaluation of the spacer plates for the postulated transfer cask side drop condition considers both beam-column buckling in accordance with NUREG/CR-6322 and general plastic instability in accordance with Appendix F of the ASME Code.

For the beam-buckling condition, the W21 spacer plates are evaluated for buckling due to the postulated transfer cask side drop condition using the criteria of NUREG/CR-6322 for linear type supports subjected to combined axial compression and bending. Buckling evaluations are performed for the most highly loaded ligaments in both the W21 carbon steel and stainless steel spacer plates for the bounding 60*g* side drop loading, both with and without the bounding normal thermal loads superimposed.

The maximum stresses in the W21 spacer plates due to the postulated transfer cask side drop are evaluated using interaction equations (26), (27), and (28) of NUREG/CR-6322, as defined in Section 3.7.4.2.1. The allowable stresses are calculated for each of the W21 spacer plate ligament types and summarized in Table 3.7-6.

As discussed previously, the spacer plate stresses used for the NUREG/CR-6322 buckling evaluation are calculated on an linear-elastic basis using the W21 spacer plate plane stress finite element model described in Section 3.9.3.3.1. The spacer plate stresses are determined for the bounding 60*g* side drop load, both with and without thermal loading superimposed. The 60*g* side drop loads for the spacer plates are calculated and applied to the finite element models as described in Section 3.9.3.3.1. The thermal gradient which is applied to the model is based on the temperature distribution in the hottest W21 carbon steel spacer plate for normal cold storage conditions. The bounding design thermal gradient discussed in Section 3.7.4.2.1 is conservatively used for this analysis.

The maximum axial compressive stress and bending stress in the W21 carbon steel and stainless steel spacer plate ligaments for the 60*g* side drop loading, both with and without the bounding normal thermal loading superimposed, are summarized in Table 3.7-10 along with the resulting interaction ratios. The results of the analysis show that the highest interaction ratios resulting from the bounding 60*g* side drop load are 0.49 for the W21 carbon steel spacer plate and 0.94 for the W21 stainless steel spacer plate. Therefore, the stresses in the most highly loaded W21 spacer plates satisfy the buckling criteria of NUREG/CR-6322 for the bounding 60g side drop load.

In addition to the elastic beam-column buckling analysis, general plastic instability of the W21 spacer plates is evaluated for the bounding 60*g* transfer cask side drop load, both with and without thermal loading, using plastic large deflection analyses. General instability of the W21 spacer plates occurs when the spacer plate experiences a global longitudinal plate buckling mode. Since the longitudinal bending stiffness of the W21 carbon steel spacer plates is proportional to the plate thickness squared, the bending stiffness of the 2.00-inch thick W21 stainless steel spacer plates is much greater than that of the ¾-inch thick W21 carbon steel spacer plates. In addition, the results of the W21 spacer plate elastic stress analysis for the side drop load show

that the spacer plate stress levels relative to the material yield strengths are comparable. Therefore, general instability will be controlled by the carbon steel spacer plates and the stainless steel spacer plates need not be evaluated.

The W21 carbon steel spacer plate plastic large deflection buckling analysis for the transfer cask side drop condition is performed using the full 3-D finite element model described in Section 3.9.3.3.5. The finite element model includes three ¾-inch thick carbon steel spacer plates: the center spacer plate, over which the fuel grid spacers are assumed to be positioned, and the adjacent spacer plates on either side. The spacer plates are modeled using plastic shell elements which have both membrane and bending stiffness. The spacer plates are supported longitudinally at the locations of the support rods. In addition, the bending support provided by the support rods is modeled using spring elements. A lower bound support rod bending stiffness is conservatively used for this evaluation.

For this analysis, the loads from the SNF assemblies are conservatively applied to the supporting basket assembly structure as concentrated loads at the fuel grid spacer locations. As discussed in Section 3.9.1, the controlling W21 basket configuration for the concentrated fuel loading assumption is the W21M-SD or W21T-SL basket assemblies loaded with WE 15x15 fuel with control components. In addition to the fuel weight, the spacer plates are loaded by their self-weight plus the weight of the support rod assemblies and guide tube assemblies. The W21 spacer plate loads are calculated and applied to the finite element model as described in Section 3.9.3.3.5. In addition to the 60*g* side drop in-plane loading, a constant 10*g* longitudinal acceleration load is applied to the finite element model to introduce an initial eccentricity to the spacer plates.

The bi-linear kinematic hardening material model with a 0.1% tangent modulus is conservatively used for the spacer plate and guide tube materials. For the side drop loads without thermal, the material properties at 700°F are assumed. For the combined side drop plus thermal loading, temperature dependent material properties are used for the spacer plates and guide tubes. The thermal gradient which is applied to the model is based on the temperature distribution in the hottest W21 carbon steel spacer plate for normal cold storage conditions

For the W21 spacer plate side drop plastic large deflection buckling analysis, all in-plane loads are ramped up to two times the side drop load (i.e., 120*g*). Spacer plate plastic instability is indicated by numerical instability in the finite element solution (i.e., unconverged solution). The results show that the most highly loaded W21 carbon steel spacer plate fails due to plastic instability at a load factor of greater than 1.5 (90*g*) for the side drop loading, both with and without thermal loading superimposed. The spacer plate deflections are slightly higher for the case which includes thermal loading than for side drop loading alone.

#### 3.7.5.2.2 Support Rods and Support Sleeves

The support rod is evaluated using simple beam theory. Two sections of the rod are considered: the cantilever section at the top and bottom end and the longest span between any two adjacent 2-inch thick stainless steel spacer plates. Conservatively, no credit is taken for the support provided to the support rods by the carbon steel spacers because of the small gap that exists between the rods and the spacer holes. The longest center-to-center span between the stainless spacers is 48.7 inches (W21M-LD) and the cantilever is conservatively taken as 9 inches. Since

the spacer rod segments are tightened to 150 ft-lbs and also due to a symmetry condition existing during a side drop, both ends of the support rod span are considered as fixed. The bounding side drop acceleration of 60g is considered for the evaluation of support rods for the side drop condition.

The shear force and bending moment at the ends of the cantilever and the fixed end span are calculated using classical beam formulas. The bounding lengths are taken for both reactions. The maximum shear and bending stresses occur at the ends of each support rod segment in the male and female sections of the connections, since the section properties at these locations are much lower than those of the solid rod. The male section consists of the solid threaded rod (minor diameter of the 2-12 UN external thread) while the female section consists of the hollow circle (major diameter of 2-12 UN internal thread). The maximum shear force and bending moment in the longest support rod span for the 60*g* side drop loading are 3.92 kips and 31.78 in-kips, respectively. The resulting maximum shear and bending stresses at the ends of the support rod are 1.38 ksi and 47.36 ksi, respectively.

The shear and bending stresses are used to determine the primary membrane and primary membrane plus bending stress intensities in the support rod sections, as follows:

$$P_m = 2\tau \qquad P_m + P_b = 2\sqrt{\left(\frac{\sigma_b}{2}\right)^2 + \tau^2}$$

The maximum primary membrane and primary membrane plus bending stress intensities, occurring in the longest span of the support rod at the male end connector, are 2.8 ksi and 47.4 ksi, respectively. The results show that the maximum stresses in the W21 support rods due to the 60*g* side drop load are less than the corresponding Service Level D allowable stresses.

The bending moment at the support rod end connections is reacted by shear on the support rod threads. The thread shear is assumed to vary linearly across the diameter of the support rod. The maximum thread shear load per unit length of circumference is calculated as follows:

$$V_{max} = \frac{M}{\left(\pi d^2/4\right)} = 11.23 \text{kips/in}$$

where:

M = 31.78 in-kips, moment resisted at the connection

d = 1.898 inch, minor diameter of 2-12 UN-2A thread

The thread shear stress is calculated as follows:

$$\tau = \frac{V_{max}(\pi d)}{A_e L} = 11.07 \text{ksi}$$

where:

$A_e$ = 3.456 $in^2$, the external thread shear area per unit length per Boucher[28]

L = 1.75 inches, minimum length of thread engagement

The maximum primary membrane stress intensity in the support rod threads is equal to twice the shear stress, or 22.14 ksi. The Service Level D allowable primary membrane stress intensity, conservatively based on the weaker SA-479, Type XM-19 stainless steel support rod material at 600°F, is 61.5 ksi. Therefore, the W21 support rod threads are structurally adequate for the bounding 60*g* side drop load.

Lateral loads do not produce any stresses in the support sleeves because the sleeves are supported along the entire length by the support rods. The support rod analysis above includes loads due to the weight of the support sleeves.

#### 3.7.5.2.3 Guide Tubes

When subjected to the transfer cask side drop loading, each guide tube assembly is supported by the basket spacer plates and loaded by its own weight in addition to the weight of a single SNF assembly. Each SNF assembly loads the supporting guide tube panel which, in turn, carries to load to the supporting spacer plate ligaments. The side drop structural evaluation of the W21 guide tubes considers two bounding conditions for the fuel loading on the guide tube: (1) Linear elastic and plastic analyses are performed using a uniform fuel load assumption, and (2) A plastic analysis is performed assuming the fuel loads on the guide tube are concentrated at the SNF assembly grid spacers. The W21 guide tubes are conservatively evaluated for a bounding 60*g* side drop acceleration load. The results of the side drop analysis for the guide tubes are summarized in Table 3.7-5.

*Uniform Fuel Loading - Elastic Stress Analysis*

Since the guide tube side drop loading for the uniform fuel load assumption is uniform over its entire length, the largest unsupported guide tube spans in each W21 canister basket are the most highly loaded. Calculations are performed for the largest guide tube free spans of each W21 canister using the maximum SNF assembly line loads from Section 3.9.1 for each design. The results of the hand calculations show that the maximum bending stress occurs in the W21M-SD/W21T-SL guide tubes for the WE 15x15 fuel with control components. Therefore, a detailed finite element analysis of this guide tube assembly is performed for the 60*g* side drop.

The stresses in the governing span of the most highly loaded W21 guide tube due to the 60*g* side drop load are evaluated using finite element methods. The guide tube 60*g* side drop elastic stress analysis is performed using the half-symmetry periodic finite element model described in Section 3.9.3.4.1. The W21 guide tube neutron absorber sheets and stainless steel wrapper are not included in the finite element model, conservatively neglecting the support they provide to the guide tube. However, their mass is included in the model. The load from the heaviest SNF assembly (WE 15x15 with control components) is applied as a uniform pressure load on the supporting guide tube panel. The uniform pressure load due the fuel weight, calculated as

[28] Boucher, R. C., *Strength of Threads*, Product Engineering, November 27, 1961.

described in Section 3.9.3.4.1, is 65.2 psi. The guide tube stresses are determined using a linear elastic static analysis. The maximum membrane and membrane plus bending stress intensities in the W21 guide tube due to the 60*g* side drop load are 13.6 ksi and 54.0 ksi, respectively. These stress intensities are conservatively classified as primary. The Service Level D allowable primary membrane and primary membrane plus bending stress intensities for SA-240, Type 316 stainless steel at an upper bound design temperature of 700°F are 39.1 ksi and 58.7 ksi, respectively. Therefore, the guide tube bending stresses are within the Service level D allowable limits.

The stresses in the W21 guide tube longitudinal seam weld at ¼ panel width due to the bounding 60*g* side drop load are also evaluated using the maximum nodal moment reactions from the finite element solution. The results show that the maximum primary membrane and primary membrane plus bending stress intensities in the W21 guide tube longitudinal seam weld due to the 60*g* side drop loading are 4.1 ksi and 23.6 ksi, respectively. In accordance with Table NG-3352-1 of the ASME Code, the efficiency factor for a full-penetration weld with surface PT examination is 0.65. However, a conservative 60% weld efficiency factor is applied to the allowable stresses for a full penetration weld with surface PT examination. Therefore, the W21 guide tube seam weld Service Level D allowable primary membrane and primary membrane plus bending stress intensities are 23.5 ksi (39.1 x 0.6) and 35.2 ksi (58.7 x 0.6), respectively. Therefore, the W21 guide tube stresses resulting from the bounding 60*g* side drop load are lower than the corresponding Service Level D allowable stresses.

*Uniform Fuel Loading - Plastic Stress Analysis*

In addition to the linear-elastic stress analysis discussed above, the W21 guide tubes are evaluated for the bounding 60*g* side drop load on a plastic basis assuming a uniform fuel load distribution to determine the maximum guide tube permanent deformation. The finite element model used for the guide tube plastic analysis has the same geometry, loading, and boundary conditions as that used for the linear-elastic stress analysis. The plastic material properties of Type 316 stainless steel at a bounding temperature of 700°F from Table 3.3-4 are used for the guide tube plastic analysis. The guide tube permanent deformation is determined by applying the loads corresponding to the 60*g* transverse load and subsequently removing the loads. The maximum permanent deformation at the center of the guide tube panel that supports the load from the SNF assembly is 0.079 inch. The maximum equivalent plastic strain in the guide tube is 0.8%, which is less than the 40% minimum elongation of SA-240, Type 316 stainless steel.

*Guide Tube Buckling*

Buckling of the W21 guide tube is evaluated for the transfer cask side drop using the criteria of NUREG/CR-6322 for linear-type members subjected to combined axial compressive and bending loads. The axial compressive stress and bending stress in the side panels of the W21 guide tube are determined using classical solutions. The side panel is evaluated as a fixed-fixed span, assuming half of the panel weight is applied at the end (top panel contribution) and the self-weight of the side panel is distributed along its length. As a result, the axial compression is not constant but varies along the side panel length. Since the theoretical buckling stress for linearly varying axial compressive stress in a column is higher than that of a column subjected to a uniform axial compressive stress on which the NUREG/CR-6322 acceptance criteria are based, an equivalent value of axial stress is calculated for use in the interaction equations.

The maximum bending stress in the guide tube side panel due to moment reactions from the top and bottom panels is calculated based on the maximum guide tube bending stress in the top and bottom panel due to the 60g side drop load. Since buckling is a global effect, the bending stress is averaged over the span between the spacer plates.

The allowable axial and bending stresses for the guide tube are calculated in accordance with NUREG/CR-6322 for linear members subjected to combined axial compressive and bending loads. Since the ratio of $f_a / F_a$ is less than 0.15, equation (28) of NUREG/CR-6322 may be used. The allowable bending stress per NUREG/CR-6322 is $F_b = fS_y$ or 27.2 ksi, where f =1.5 is the plastic shape factor for rectangular cross-section. Therefore, the interaction ratio for equation (28) of NUREG/CR-6322 is calculated as follows:

$$\frac{f_a}{F_a}+\frac{f_b}{F_b}=\frac{0.242}{1.76}+\frac{9.2}{27.2}=0.48<1$$

No thermal stresses exist in the W21 guide tube because sufficient clearances are provided. Therefore, the W21 guide tube is adequate to withstand the 60*g* side drop without buckling.

*Neutron Absorber Panel Stresses*

The maximum bearing stress in the neutron absorber panel occurs at the carbon steel spacer plate because its tributary load is close to that of the stainless spacer, albeit the thickness is much lower. The bearing stress is calculated to be 549 psi. Although evaluation of bearing stress is not required per the ASME Code for accident conditions, the bearing stress in the neutron absorber panel is considered to assure that no local damage results from the side drop. The ultimate strength of the neutron absorber panel material at room temperature is 10 ksi. Therefore, recognizing that the ultimate strength of the neutron absorber material will be somewhat lower at the guide tube design temperature, the bearing stress level in the neutron absorber sheets due to the 60*g* side drop load is not sufficient to cause any damage to the neutron absorber panels.

*Concentrated Loading at Fuel Grid Spacers*

The W21 guide tubes are evaluated for the 60*g* side drop load assuming the fuel assembly loads are applied to the guide tube as concentrated loads at the fuel grid spacer locations. The purpose of this evaluation is to determine the maximum guide tube permanent displacements which could result from the postulated side drop condition.

The 60*g* side drop evaluation of the W21 guide tube with a concentrated load at the fuel grid spacer is performed using the ½-symmetry multi-span finite element model described in Section 3.9.3. As discussed in Section 3.1.1.2, the highest grid spacer tributary weight of 256.9 pounds, which occurs on the W21M-SD/W21T-SL guide tubes loaded by WE 15x15 fuel with control components. These basket assemblies have a maximum spacer plate center-to-center spacing of 5.00 inches. The only other W21 basket assemblies which have larger spacer plate center-to-center spacing (5.35 inches) are the W21M-LD and W21T-LL. Since the maximum SNF assembly grid spacer tributary load for these designs is considerably lower than that of the W21M-SD or W21T-SL basket assemblies (56%), the stresses in the W21M-SD or W21T-SL basket assembly guide tubes will bound all others. Therefore, a bounding side drop analysis is performed based on the W21M-SD/W21T-SL guide tubes loaded by WE 15x15 fuel with control components.

The fuel load is applied to the model at the mid-span of the largest guide tube span (i.e., midway between spacer plate supports) since this will result in the largest guide tube deformations for a given load. The applied loads are illustrated in Figure 3.7-6 and include: (1) a *60g* side drop acceleration applied to account for the guide tube self-weight, (2) a displacement imposed on the guide tube bottom panel nodes in the region of the grid spacer, and (3) a uniform pressure load applied to those spans which do not have the imposed displacement loading to account for the balance of the fuel weight not accounted for by the imposed displacement.

The magnitude of the imposed displacement is chosen based upon the maximum protrusion of the grid spacer beyond the fuel rod envelope (i.e., distance from edge of grid spacer to outermost fuel rod), recognizing that the displacement of the guide tube is limited by this fuel parameter. The maximum grid spacer protrusion has been calculated for each PWR fuel class. The results show that the maximum grid spacer protrusion is 0.081 inches for Haddam Neck fuel (which is not being qualified for storage, but nonetheless provides the maximum grid strap protrusion). For conservatism, a bounding 0.10-inch displacement is imposed onto the guide tube bottom panel in the area of the grid spacer support.

The analysis results show that the maximum stress intensity and maximum equivalent plastic strain at the middle fiber of the guide tube shell elements are 15.7 ksi and 4.4%, respectively. The maximum stress intensity and equivalent plastic strain at the extreme fibers (i.e., top and bottom) of the guide tube shell elements are 39.0 ksi and 13.9%, respectively. The Service Level D plastic analysis allowable primary membrane and primary membrane plus bending stress intensities for SA-240, Type 316 stainless steel at 700°F are 50.3 ksi and 64.6 ksi, respectively. Therefore, for the 60*g* side drop evaluation of the W21 guide tubes, the Service Level D allowable limits are satisfied for the concentrated load condition. As shown in Figure 3.7-7, the plastic strain in the guide tube occurs only in the span which supports the fuel grid spacer and is limited to a small region near the edge of the grid spacer footprint. The minimum elongation of Type 316 stainless steel is 40%. The permanent deformation in the guide tube resulting from the 60*g* side drop with the concentrated fuel load at the grid spacers is shown in Figure 3.7-8. The maximum permanent deformation of the guide tube, occurring at the location of the concentrated grid spacer loading, is 0.09 inches. The permanent deformation of the guide tube is considered in the W21 canister criticality evaluation.

### 3.7.6 Fire

The FuelSolutions™ W21 canister in the storage cask is evaluated for a postulated accidental fire event defined in Section 2.3.3.4 of the FuelSolutions™ Storage System FSAR. The storage cask evaluation for this postulated fire accident is discussed in Section 11.2.5 of the FuelSolutions™ Storage System FSAR.

As documented in Section 4.6, the maximum canister pressure as a result of the postulated fire accident is bounded by the design basis accident pressure of 69.0 psig. Further, the external heating acts to reduce the thermal gradients on the canister, resulting in lower thermal gradients and therefore lower stresses than for the normal ambient conditions. Therefore, the structural effects of this postulated accident on the canister are bounded by the accident pressure condition evaluated in Section 3.7.9 and the bounding thermal gradients evaluated in Section 3.5.1.3.

## 3.7.7 Flood

The FuelSolutions™ W21 canister is evaluated for the effects of an enveloping design basis flood, postulated to result from natural phenomena such as a tsunami and seiches, as specified by 10 CFR 72.122(b). For the purpose of this evaluation, a 50-foot flood height is used as defined in Section 2.3.4.1. The W21 canister is protected from the lateral forces due to the flood current by the storage cask. The only flood load affecting the canister is the 21.7 psi hydrostatic pressure due to the 50-foot flood head.

The effects of the flood hydrostatic pressure on the W21 canister are much less severe than those of the design basis 69 psig accident internal pressure load evaluated in Section 3.7.9. This is due to the relative magnitude of the flood pressure load compared with that of the design basis accident internal pressure and the nature of the pressure loads. Internal pressure loading produces higher stresses in the end regions of the shell assembly than does external pressure loading, since the canister closure plates are supported by the shield plugs under external pressure loading only. Therefore, the canister shell stresses due to flood loading are bounded by those due to accident internal pressure.

Shell buckling due to an external pressure of 21.7 psi is governed by hoop compression. The hoop stress due to an external pressure of 21.7 psi is 1.14 ksi. Using Paragraph -1712 of ASME Code Case N-284, the theoretical hoop buckling stress is 10.64 ksi, based on nominal shell dimensions and material properties at a bounding temperature of 600°F. Applying a factor of safety of 2.0 and a capacity reduction factor of 0.8 in accordance with Paragraphs -1400 and -1511 of ASME Code Case N-284, respectively, the allowable hoop buckling stress is 4.26 ksi. Using the interaction equations of Paragraph -1713.1.1 of ASME Code Case N-284, the maximum interaction equation due to an external pressure of 21.7 psi is:

$$1.14/4.26 = 0.27 < 1.0$$

Therefore, the canister shell does not buckle due to the 50-foot head external flood pressure.

## 3.7.8 Earthquake

As discussed in the FuelSolutions™ Storage System FSAR, the design basis seismic accelerations for the FuelSolutions™ storage system are 0.25*g* horizontally (in each of two orthogonal directions, or a 0.35*g* resultant horizontal acceleration) and 0.25*g* vertically. Since the lowest fundamental frequency of the W21 canister is much greater than 33 Hz, no amplification of the seismic loading occurs within the W21 canister assembly. Bounding seismic accelerations of 1.1*g* along the canister longitudinal axis and 1.3*g* transverse to the canister longitudinal axis are conservatively used for the structural evaluation of the W21 canister basket assembly.

### 3.7.8.1 Canister Shell Assembly

The canister shell assembly stresses due to the design basis seismic loads are considered to be bounded by those due to the postulated cask drop conditions. This is due to the relative magnitudes of the seismic and drop loads (i.e., 0.25*g* versus a 50*g* end drop and 0.35*g* 60*g* side drop). Therefore, the canister shell stresses are not calculated for the seismic load condition.

#### 3.7.8.2 Canister Basket Assembly

A bounding seismic evaluation of the basket assembly components is performed using a 1.3*g* transverse acceleration combined with a 1.1*g* longitudinal acceleration. The W21 basket assembly component stresses due to the transverse seismic acceleration are calculated by scaling the maximum stresses due to the horizontal dead weight load by 1.3. Similarly, the stresses due to the longitudinal seismic acceleration are determined by scaling the maximum stresses due to the vertical dead weight load by 1.1. The resulting stresses due to transverse and longitudinal seismic loads are added together, irrespective of location, to arrive at the total seismic stresses shown in Table 3.7-5. The results show that the maximum W21 basket assembly component stresses due to the bounding seismic load are much lower than the stresses due to the accident drop conditions. The W21 basket assembly stresses due to seismic loading are combined with other normal, off-normal, and accident condition stresses in the load combination evaluation presented in Section 3.7.10.2.

### 3.7.9 Accident Internal Pressure

As discussed in Section 4.6.1.4, the maximum internal pressure in the FuelSolutions™ W21 canister for all accident thermal conditions is 68.7 psig, based on the required backfill quantity of helium in accordance with the *technical specification* contained in Section 12.3 of this FSAR, and a concurrent non-mechanistic failure of 100% of the fuel rods with complete release of their fill gas and 30% of their fission gasses into the canister cavity. All gas is assumed to be at the extreme off-normal condition canister cavity gas temperature. For all W21 canisters with the exception of the W21T-LL, a bounding accident internal pressure of 69.0 psig is conservatively used for the structural evaluation. The maximum accident pressure for the W21T-LL canister is 45.0 psig. The W21T-LL canister shell stresses are calculated based on a bounding 45.1 psig accident internal pressure.

The structural evaluation of these two W21 canister shell assemblies for the accident internal pressure condition is performed using the axisymmetric finite element models described in Section 3.9.3.1 of this FSAR. The analysis methodology, including the methodology for application of the pressure loads and calculation of stresses, is described in Section 3.5.2.2 of this FSAR. The resulting bounding W21 canister shell stresses due to these accident internal pressures applied to the canister pressure boundary, including the top inner and outer closure plates, are provided in Table 3.7-4. All canister shell stresses due to accident internal pressure are within the allowable values.

### 3.7.10 Accident Condition Load Combinations

Load combinations are performed for the FuelSolutions™ W21 canister in accordance with Section 2.3 for accident conditions. The load combinations include normal loads evaluated in Section 3.5, off-normal loads evaluated in Section 3.6, and accident loads evaluated in this FSAR section. Load combinations are summarized in Table 2.3-1. The structural evaluation of the W21 canister shell assembly and basket assembly for accident load combinations are presented in the following sections.

### 3.7.10.1 Canister Shell Assembly

The W21 canister accident load combinations defined in Table 2.3-1 are simplified by identifying the bounding load combinations. Since load combination D8 is bounded by load combinations D1 and D2, load combination D8 need not be evaluated. For Service Level D conditions, general thermal stresses are classified as secondary and consequently need not be considered. Therefore, load combination D7 reduces to vertical dead weight plus off-normal internal pressure, which is identical to load combination C1 evaluated in Section 3.6.6.1. Since the allowable stresses for Service Level D conditions are greater than those for Service Level C conditions, load combination D7 need not be evaluated. In addition, load combination D6 includes seismic loads, which are insignificant when compared to the postulated cask drop and tip-over loads. Therefore, load combination D6 is also insignificant in comparison to those load combinations which include the postulated cask drop and tip-over loads. Consequently load combination D6 is not evaluated for the W21 canister shell assembly. The W21 canister shell load combination evaluations for the remaining accident load combinations (i.e., D1 through D5) are performed as described below.

The canister shell assembly stressed due to load combinations D1 through D5 are evaluated using the axisymmetric and three-dimensional finite element models described in Sections 3.9.3.1 and 3.9.3.2, respectively. Load combination evaluations are performed for both the "bounding" canister shell model, which bounds all W21 canister shell assemblies with the exception of the W21T-LL, and the W21T-LL canister shell assembly. Separate evaluations are performed for internal pressure acting on both the top inner and outer closures. Thermal loads are not considered since thermal stresses are classified as secondary, and as such need not be evaluated for Service Level D conditions.

For load combination D1, vertical dead weight, vertical transfer, and accident internal pressure loads are applied simultaneously to the canister shell axisymmetric finite element models. For this condition, the canister shell is supported vertically at the location of the vertical transfer pintle plate bolt circle on top outer closure plate. The evaluation for load combination D3 is performed in a similar manner to load combination D1, but includes the storage cask end drop and off-normal internal pressure loads. For load combination D3, the canister shell is supported at the bottom end. For load combination D2, both the axisymmetric and three-dimensional finite element models are used. The axisymmetric model is used to determine the canister shell stresses due to normal horizontal canister transfer and accident internal pressure loads. The canister shell stresses due to horizontal dead weight, which are calculated using the three-dimensional half-symmetry finite element model described in Section 3.9.3.2, are conservatively added absolutely to the maximum stresses calculated with the axisymmetric model. Load combinations D4 and D5 are evaluated using only the three-dimensional finite element model. The load combination D4 (side drop plus off-normal internal pressure) evaluation is performed in the same manner as the side drop stress evaluation described in Section 3.7.5.1, but includes the off-normal internal pressure load on the inside of the canister shell. Similarly, the load combination D5 (tip-over plus off-normal internal pressure) evaluation is performed in the same manner as the tip-over stress evaluation described in Section 3.7.4.1, but includes the off-normal internal pressure load on the inside of the canister shell.

The maximum stresses in the W21 canister shell due to load combinations D1 through D5 are summarized in Table 3.7-11 through Table 3.7-15, respectively. The results show that the

maximum stresses in the W21 canister shell for all accident load combinations are lower than the corresponding Service Level D allowable stresses.

### 3.7.10.2 Canister Basket Assembly

The accident load combinations for the W21 canister include dead weight; normal handling; off-normal and accident internal pressure; normal and accident thermal loads; seismic; and postulated cask drop loads. In addition to the normal, off-normal, and accident load conditions evaluated in the previous sections, the effects of the support rod torque which is applied during fabrication of the basket assembly is also included in the load combinations. As shown in Section 3.9.4, the maximum shear stress in the support rod segment threads due to the torque preload is 1.8 ksi. Since the basket assembly is not a pressure retaining component, it is not subjected to internal pressure loading. In addition, stresses due to thermal loading are classified as secondary stresses, which need not be evaluated for Service Level D conditions. However, thermal loads are considered in combination with drop loads for the basket assembly buckling analyses where the combined loads result in lower factors of safety against buckling.

With the elimination of internal pressure and thermal loads, the accident load combinations for the basket assembly are reduced as follows. Load combinations D1 and D2 reduce to dead weight plus normal handling, and are bounded by load combination A4 evaluated in Section 3.5.5.2. Load combinations D3 and D5 consist of postulated cask drop and tip-over loads only, which are evaluated in the previous sections of this Chapter. Load combination D6 reduces to dead weight plus seismic. For load combination D6, the basket assembly stresses are conservatively determined by adding the bounding dead weight stresses to the maximum seismic stresses, irrespective of sign and location. Load combination D7 reduces to horizontal dead weight only and is bounded by load combination A3. The W21 canister basket assembly stresses for accident load combinations D3 through D6 are reported in Table 3.7-16. The results show that all stresses are lower than the corresponding Service Level D allowable stresses.

## Table 3.7-1 - W21 Spacer Plate End Drop Reaction Loads for Support Rod Assembly Evaluation

| Load Conditions and Spacer Plate Reactions[1] | | Spacer Plate Reaction Loads | | | |
|---|---|---|---|---|---|
| | | On Rod Segment | | On Support Sleeve | |
| | | Lower Bound[2] | Fixed[2] | Lower Bound[2] | Fixed[2] |
| 20*g* End Drop | CS Spacer Pl. Axial Load (lbs) | N/A | N/A | 750 | 750 |
| | CS Spacer Pl. Moment (in-lbs) | N/A | N/A | 2,020 | 2,060 |
| | SS Spacer Pl. Axial Load (lbs) | 2,240 | 2,040 | N/A | N/A |
| | SS Spacer Pl. Moment (in- lbs) | 4,140 | 5,620 | N/A | N/A |
| | Bottom SS Spacer Pl. Axial Load (lbs) | 17,220 | 14,830 | N/A | N/A |
| | Bottom SS Spacer Pl. Moment (in-lbs) | 55,320 | 78,730 | N/A | N/A |
| 50*g* End Drop | CS Spacer Pl. Axial Load (lbs) | N/A | N/A | 1,880 | 1,860 |
| | CS Spacer Pl. Moment (in- lbs) | N/A | N/A | 5,050 | 5,140 |
| | SS Spacer Pl. Axial Load (lbs) | 5,590 | 5,090 | N/A | N/A |
| | SS Spacer Pl. Moment (in- lbs) | 10,330 | 14,050 | N/A | N/A |

Notes:

(1) Spacer plate end drop reactions are scaled from the vertical deadweight reactions.

(2) Two sets of spacer plate reactions are summarized: the first value shown is based on a lower bound support rod/sleeve bending stiffness; the second value is based on fixed conditions at the support rod/sleeve locations.

## Table 3.7-2 - W21M-LD Support Rod Allowable Loads and Stresses

| Support Rod Segment Number | Unsupported Span Length (in.) | Effective Length Factor, K | KL/r | λ | Allowable Loads and Stresses | | | | | | |
|---|---|---|---|---|---|---|---|---|---|---|---|
| | | | | | P (Eq. 33) (lbs) | P (Eq. 43) (lbs) | P' (Eq. 45) (lbs) | P (lbs) | $F_a$ (psi) | $F'_e$ (psi) | $F_b$ (psi) |
| 1 (top) | 9.00 | 2.0 | 24.0 | 0.29 | 204,067 | 147,985 | 109,139 | 150,500 | 21,291 | 296,924 | |
| 2 | 29.00 | 1.2 | 46.4 | 0.57 | 173,538 | 134,031 | 95,344 | 123,448 | 17,464 | 79,439 | |
| 3 | 32.40 | 1.2 | 51.8 | 0.63 | 166,592 | 130,083 | 91,994 | 117,813 | 16,667 | 63,641 | |
| 4 | 48.70 | 1.2 | 77.9 | 0.95 | 136,053 | 108,386 | 75,933 | 95,316 | 13,484 | 28,169 | 63,335 |
| 5 | 31.40 | 1.2 | 50.2 | 0.61 | 168,614 | 131,266 | 92,979 | 119,434 | 16,896 | 67,759 | |
| 6 | 27.00 | 1.2 | 43.2 | 0.53 | 177,719 | 136,256 | 97,315 | 126,928 | 17,957 | 91,643 | |
| 7 (bot) | 2.00 | 2.0 | 5.3 | 0.07 | 230,379 | 156,406 | 120,635 | 177,690 | 25,138 | 6,012,706 | |

## Table 3.7-3 - W21 Support Rod Segment End Drop Results

| End Drop Case | Rod Segment Number | Axial Load (lbs.) | Bending Moment (in-lb.) | $f_a$ (psi) | $f_b$ (psi) | $f_a/F_a$ | Interaction Ratios (Eq. Number) (26) | (27) | (28) |
|---|---|---|---|---|---|---|---|---|---|
| **20*g* Bottom End Drop** | | | | | | | | | |
| Lower Bound Support Rod Bending Stiffness[1] | 1 (top) | 502 | 0 | 71 | 0 | 0.00 | --- | --- | 0.00 |
| | 2 | 5,431 | 4,140 | 768 | 1,562 | 0.04 | --- | --- | 0.07 |
| | 3 | 13,790 | 4,140 | 1,951 | 1,562 | 0.12 | --- | --- | 0.14 |
| | 4 | 22,121 | 4,140 | 3,130 | 1,562 | 0.23 | 0.26 | 0.09 | --- |
| | 5 | 32,175 | 4,140 | 4,552 | 1,562 | 0.27 | 0.29 | 0.13 | --- |
| | 6 | 39,603 | 55,320 | 5,603 | 20,870 | 0.31 | 0.61 | 0.45 | --- |
| | 7 (bot) | 61,670 | 55,320 | 8,725 | 20,870 | 0.35 | 0.63 | 0.52 | --- |
| Fixed Condition at Support Rods [2] | 1 (top) | 502 | 0 | 71 | 0 | 0.00 | --- | --- | 0.00 |
| | 2 | 5,231 | 5,620 | 740 | 2,120 | 0.04 | --- | --- | 0.08 |
| | 3 | 13,390 | 5,620 | 1,894 | 2,120 | 0.11 | --- | --- | 0.15 |
| | 4 | 21,521 | 5,620 | 3,045 | 2,120 | 0.23 | 0.26 | 0.10 | --- |
| | 5 | 31,375 | 5,620 | 4,439 | 2,120 | 0.26 | 0.29 | 0.13 | --- |
| | 6 | 38,603 | 78,730 | 5,461 | 29,701 | 0.30 | 0.73 | 0.59 | --- |
| | 7 (bot) | 58,280 | 78,730 | 8,245 | 29,701 | 0.33 | 0.73 | 0.65 | --- |
| **50*g* Bottom End Drop** | | | | | | | | | |
| Lower Bound Support Rod Bending Stiffness[1] | 1 (top) | 1,256 | 0 | 178 | 0 | 0.01 | --- | --- | 0.01 |
| | 2 | 13,578 | 10,330 | 1,921 | 3,897 | 0.11 | --- | --- | 0.17 |
| | 3 | 34,496 | 10,330 | 4,880 | 3,897 | 0.29 | 0.35 | 0.17 | --- |
| | 4 | 55,338 | 10,330 | 7,829 | 3,897 | 0.58 | 0.65 | 0.24 | --- |
| | 5 | 80,502 | 10,330 | 11,389 | 3,897 | 0.67 | 0.74 | 0.32 | --- |
| | 6 | 99,088 | 10,330 | 14,018 | 3,897 | 0.78 | 0.84 | 0.37 | --- |
| | 7 (bot) | 116,825 | 10,330 | 16,527 | 3,897 | 0.66 | 0.71 | 0.43 | --- |
| Fixed Condition at Support Rods [2] | 1 (top) | 1,256 | 0 | 178 | 0 | 0.01 | --- | --- | 0.01 |
| | 2 | 13,038 | 14,050 | 1,844 | 5,300 | 0.11 | --- | --- | 0.19 |
| | 3 | 33,336 | 14,050 | 4,716 | 5,300 | 0.28 | 0.36 | 0.19 | --- |
| | 4 | 53,578 | 14,050 | 7,580 | 5,300 | 0.56 | 0.66 | 0.25 | --- |
| | 5 | 78,082 | 14,050 | 11,046 | 5,300 | 0.65 | 0.74 | 0.33 | --- |
| | 6 | 96,068 | 14,050 | 13,591 | 5,300 | 0.76 | 0.84 | 0.39 | --- |
| | 7 (bot) | 113,185 | 14,050 | 16,012 | 5,300 | 0.64 | 0.71 | 0.44 | --- |

Notes:

(1) Results are calculated using spacer plate reactions based on a lower bound support rod/sleeve bending stiffness.

(2) Results are calculated using spacer plate reactions based on fixed conditions at the support rod/sleeve locations.

## Table 3.7-4 - W21 Canister Shell Assembly Accident Condition Stress Summary

| Shell Component | Stress Type | Maximum Stresses (ksi) | | | | Allowable Stress[1] (ksi) |
|---|---|---|---|---|---|---|
| | | Accident Internal Pressure | Storage Cask End Drop | Storage Cask Tip-over | Transfer Cask Side Drop | |
| Top Outer Closure Plate | $P_m$ | 1.1 | 0.9 | 5.4 | 14.7 | 46.2 |
| | $P_m+P_b$[2] | 22.3 | 9.4 | 9.1 | 24.3 | 69.3 |
| Top Outer Closure Weld | $P_m$ | 7.4 | 4.4 | 7.6 | 11.4 | 37.0[3] |
| | Shear[4] | 1.8 | 0.8 | [5] | [5] | 22.1[3] |
| Top Inner Closure Plate | $P_m$ | 1.3 | 1.6 | 12.4 | 21.4 | 46.2 |
| | $P_m+P_b$ | 9.2 | 16.5 | 26.6 | 42.9 | 69.3 |
| Top Inner Closure Weld | $P_m$ | 8.7 | 10.0 | 34.6 | 32.4 | 41.6[5] |
| | Shear[4] | 4.3 | 5.0 | 17.3 | 16.2 | 24.9[5] |
| Top Shield Plug Btm. Support Pl. (DU/Pb) | $P_m$ | 0.0 | 1.9 | [6] | [6] | 46.2 |
| | $P_m+P_b$ | 0.3 | 48.4 | [6] | [6] | 69.3 |
| Cylindrical Shell | $P_m$ | 15.8 | 11.8 | 12.4 | 23.3 | 46.2 |
| | $P_m+P_b$ | 49.9 | 25.7 | 31.0 | 31.0 | 69.3 |
| Bottom Shell Extension | $P_m$ | 6.4 | 8.0 | [7] | [7] | 46.2 |
| | $P_m+P_b$ | 7.9 | 29.8 | [7] | [7] | 69.3 |
| Bottom Closure Plate | $P_m$ | 1.7 | 2.0 | [8] | [8] | 46.2 |
| | $P_m+P_b$ | 29.7 | 8.8 | [8] | [8] | 69.3 |
| Bottom End Plate (Except W21T-LL) | $P_m$ | 2.3 | 3.1 | [8] | [8] | 46.2 |
| | $P_m+P_b$ | 23.1 | 5.1 | [8] | [8] | 69.3 |
| W21T-LL Bottom End Plate | $P_m$ | 4.8 | 2.2 | [8] | [8] | 66.1 |
| | $P_m+P_b$ | 34.5 | 11.7 | [8] | [8] | 99.1 |
| Top Shield Plug Supt. Ring Weld | Shear | 0.1 | 5.3 | [6] | [6] | 16.2 |
| Shell Extension Top Weld | Shear | 2.3 | 12.4 | [7] | [7] | 16.2 |
| Shell Extension Bottom Weld | Shear | 1.1 | 13.7 | [7] | [7] | 16.2 |

Notes:

(1) Allowable stress intensities are based on the weaker of the W21M and W21T canister shell materials (SA-240, Type 304 stainless steel) properties at 300°F, except for the W21T-LL bottom end plate allowable stresses which are based on SA-240, Type XM-19 stainless steel at 300°F.

(2) The maximum bending stress in the top outer closure plate is determined using hand calculations assuming simply support edge conditions to demonstrate that the bending stress in the top outer closure weld may be classified as secondary.

(3) The allowable stresses for the top outer closure weld include a 0.8 weld efficiency factor in accordance with ISG-4.

(4) Shear stress in the welds are determined using hand calculations.

(5) The allowable stresses for the top inner closure weld include a 0.9 weld efficiency factor in accordance with Section 3.1.2.2 of this FSAR.

(6) Bounded by stresses due to storage cask end drop.

(7) Bounded by stresses in canister shell top end region.

(8) Bounded by stresses in the top inner closure plate.

# Table 3.7-5 - W21 Canister Basket Assembly Accident Condition Stress Summary

| Basket Component | Stress Type | Maximum Stresses (ksi) | | | | Allowable Stress[1] (ksi) |
|---|---|---|---|---|---|---|
| | | Earth-quake | Storage Cask End Drop | Storage Cask Tip-over | Transfer Cask Side Drop | |
| 2-inch Thick Stainless Steel Spacer Plate | $P_m$ | 1.0 | 0.0 | 9.3 | 12.4 | 60.6 |
| | $P_m+P_b$ | 2.6 | 6.1 | 23.3 | 45.8 | 90.8 |
| | Buckling I.R.[3] | N/A | N/A | 0.70 | 0.94 | 1.0 |
| ¾-inch Thick Carbon Steel Spacer Plate | $P_m$ | 2.4 | 0.0 | 18.4 | 23.3 | 75.4 |
| | $P_m+P_b$ | 5.9 | 14.6 | 46.0 | 75.2 | 113.1 |
| | Buckling I.R.[3] | N/A | N/A | 0.31 | 0.49 | 1.0 |
| 2-inch Thick Stainless Steel Bottom End Spacer Plate | $P_m$ | 1.0 | 0.0 | [6] | [6] | 61.5 |
| | $P_m+P_b$ | 3.9 | 26.3 | [6] | [6] | 92.2 |
| | Buckling I.R.[3] | N/A | N/A | [6] | [6] | 1.0 |
| Support Rod | $P_m$ | 0.5 | 16.5 | [7] | 2.8 | 62.4[2] |
| | $P_m+P_b$ | 3.1 | 37.9 | [7] | 47.4 | 93.6[2] |
| | Buckling I.R.[3] | N/A | 0.84 | [7] | N/A | 1.0[2,3] |
| W21M Supt. Rod Threads | $P_m$ | .0.5 | --- | [7] | 22.1 | 61.5 |
| W21T Supt. Rod Threads | $P_m$ | 0.5 | --- | [7] | 22.1 | 95.3 |
| Support Sleeve | $P_m$ | [4] | 7.3 | [4] | [4] | 33.6[2] |
| | $P_m+P_b$ | [4] | 9.5 | [4] | [4] | 50.4[2] |
| | Buckling I.R.[3] | N/A | 0.77 | N/A | N/A | 1.0[2,3] |
| Guide Tube | $P_m$ | 1.5 | 14.0 | [7] | 13.6 | 39.1 |
| | $P_m+P_b$ | 13.5 | 14.0 | [7] | 54.0 | 58.7 |
| | Buckling | N/A[4] | 14.0[5] | [7] | 0.48[3] | 137[5]/1.0[3] |
| Guide Tube Longitudinal Seam Weld | $P_m$ | [7] | [7] | [7] | 4.1 | 23.5[8] |
| | $P_m+P_b$ | [7] | [7] | [7] | 23.6 | 35.2[8] |

Notes:

(1) Allowable stresses are based on design temperatures presented in Table 3.5-1, unless otherwise noted.

(2) The allowable stresses reported for the W21 support rods and sleeves are based on the smaller of the W21M and W21T allowable stresses.

(3) Buckling interaction ratio (I.R.) in accordance with NUREG/CR-6322.

(4) Bounded by storage cask end drop condition.

(5) The allowable guide tube axial compressive stress for the storage cask end drop condition is 137 ksi, as discussed in Section 3.7.3.2.3.

(6) Bounded by other 2-inch stainless steel spacer plates.

(7) Bounded by transfer cask side drop condition.

(8) Allowable stresses include a 60% weld efficiency factor. This is applicable only to a full penetration weld with surface PT examination only and restricted in location to the ¼ span of panel width.

## Table 3.7-6 - W21 Spacer Plate Allowable Buckling Stresses

| Spacer Plate Type | Carbon Steel | | Stainless Steel | |
|---|---|---|---|---|
| Ligament Type | A | B | A | B |
| Width, b (in.) | 1.90 | 1.30 | 1.90 | 1.30 |
| Thickness, t (in.) | 0.75 | 0.75 | 2.00 | 2.00 |
| Height, L (in.) | 9.43 | 9.43 | 9.43 | 9.43 |
| Gross Area, $A_g$ ($in^2$) | 1.43 | 0.98 | 3.80 | 2.60 |
| Ixx ($in^4$) | 0.429 | 0.137 | 1.143 | 0.366 |
| $r_x$ (in.) | 0.548 | 0.375 | 0.548 | 0.375 |
| Effective Length Factor, K | 0.65 | 0.65 | 0.65 | 0.65 |
| $KL/r_x$ | 11.18 | 16.33 | 11.18 | 16.33 |
| $S_y$ @ 700°F (ksi) | 83.0 | 83.0 | 36.3 | 36.3 |
| E @ 700°F (ksi) | $25.5x10^3$ | $25.5x10^3$ | $24.8x10^3$ | $24.8x10^3$ |
| Lambda | 0.203 | 0.297 | 0.136 | 0.199 |
| $P_{33}$ (kips) | 96.3 | 62.5 | 116.3 | 77.0 |
| $P_{43}$ (kips) | N/A | N/A | 80.6 | 54.4 |
| $P_{45}$ (kips) | N/A | N/A | 61.2 | 40.8 |
| $P_{40}$ (kips) | N/A | N/A | 88.3 | 57.7 |
| $F_a$ (ksi) | 67.5 | 64.1 | 23.2 | 22.2 |
| $F_b$ (ksi) | 124.5 | 124.5 | 54.5 | 54.5 |
| $F_e'$ (ksi) | 1550.1 | 725.7 | 1342.4 | 628.4 |

## Table 3.7-7 - Tip-over Buckling Stresses and Interaction Ratios

| Load Condition | Stress or Interaction Ratio | Carbon Steel[1] | | Stainless Steel[1] | |
|---|---|---|---|---|---|
| | | Ligament A | Ligament B | Ligament A | Ligament B |
| Tip-over | Axial Compressive Stress (ksi) | 6.84 | 4.62 | 3.41 | 2.32 |
| | Bending Stress (ksi) | 10.08 | 2.74 | 5.01 | 1.48 |
| | Interaction Equation 26 | 0.17 | 0.09 | 0.23 | 0.13 |
| | Interaction Equation 27 | 0.15 | 0.07 | 0.17 | 0.08 |
| Tip-over + Thermal | Axial Compressive Stress (ksi) | 12.61 | 12.46 | 9.93 | 11.31 |
| | Bending Stress (ksi) | 17.75 | 9.46 | 13.80 | 12.23 |
| | Interaction Equation 26 | 0.31 | 0.26 | 0.64 | 0.70 |
| | Interaction Equation 27 | 0.27 | 0.20 | 0.48 | 0.48 |

Note:

(1) Ligament A is located closest to the spacer plate centerline. Ligament B is the outermost ligament. Maximum ligament A and B axial compressive stress and bending stress occur in the bottom ligaments for the tip-over load condition.

## Table 3.7-8 - Summary of W21 Spacer Plate 60*g* Side Drop Elastic Stress Analysis Results

| Impact Angle | Carbon Steel Spacer Plate Maximum Stress Intensities (ksi) | | Stainless Steel Spacer Plate Maximum Stress Intensities (ksi) | |
|---|---|---|---|---|
| | $P_m$ | $P_m+P_b$ | $P_m$ | $P_m+P_b$ |
| 0° | 23.3 | 58.8 | 11.2 | 39.6 |
| 15° | 18.5 | 75.2 | 11.9 | 40.6 |
| 30° | 16.4 | 59.6 | 12.4 | 45.8 |
| 45° | 14.8 | 60.4 | 11.7 | 43.6 |

## Table 3.7-9 - Summary of W21 Spacer Plate 60*g* Side Drop Plastic Analysis Results

| Impact Orientation(1) | Carbon Steel Spacer Plate | | Stainless Steel Spacer Plate | |
|---|---|---|---|---|
| | Equivalent Plastic Strain | Permanent Deformation | Equivalent Plastic Strain | Permanent Deformation |
| 0° | 0.7% | 0.007 in. | 0.8% | 0.003 in. |
| 45° | 0.6% | 0.028 in. | 1.0% | 0.049 in. |

Note:
(1) See Figure 3.7-5 for illustration of impact orientations.

## Table 3.7-10 - W21 Spacer Plate Side Drop Stresses and Buckling Interaction Ratios

| Drop Condition | Impact Angle | Stress Type | Carbon Steel[1] | | Stainless Steel[1] | |
|---|---|---|---|---|---|---|
| | | | Ligament A | Ligament B | Ligament A | Ligament B |
| 60g Side Drop | 0° | Axial Stress (ksi) | 16.46 | 5.70 | 9.53 | 1.17 |
| | | Bending Stress (ksi) | 7.23 | 5.40 | 6.87 | 3.93 |
| | | Interaction Ratio (Eq. 26) | 0.29 | 0.13 | 0.52 | 0.11 |
| | | Interaction Ratio (Eq. 27) | 0.22 | 0.10 | 0.34 | 0.10 |
| | 15° | Axial Stress (ksi) | 17.85 | 15.97 | 11.14 | 9.31 |
| | | Bending Stress (ksi) | 21.38 | 33.77 | 20.02 | 14.67 |
| | | Interaction Ratio (Eq. 26)[2] | **0.41** | **0.48** | **0.79** | 0.65 |
| | | Interaction Ratio (Eq. 27) | 0.35 | 0.43 | 0.62 | 0.48 |
| | 30° | Axial Stress (ksi) | 16.22 | 13.21 | 9.33 | 10.11 |
| | | Bending Stress (ksi) | 25.14 | 39.57 | 24.16 | 30.72 |
| | | Interaction Ratio (Eq. 26)[2] | 0.41 | 0.48 | 0.78 | **0.94** |
| | | Interaction Ratio (Eq. 27) | 0.36 | 0.45 | 0.66 | 0.80 |
| | 45° | Axial Stress (ksi) | 13.54 | 10.78 | 6.68 | 8.31 |
| | | Bending Stress (ksi) | 28.35 | 38.75 | 23.79 | 32.33 |
| | | Interaction Ratio (Eq. 26) | 0.40 | 0.44 | 0.66 | 0.89 |
| | | Interaction Ratio (Eq. 27) | 0.36 | 0.42 | 0.59 | 0.78 |
| 60g Side Drop + Normal Thermal | 0° | Axial Stress (ksi) | 22.73 | 13.22 | 15.92 | 10.43 |
| | | Bending Stress (ksi) | 1.38 | 4.94 | 1.60 | 8.26 |
| | | Interaction Ratio (Eq. 26) | 0.35 | 0.24 | 0.71 | 0.60 |
| | | Interaction Ratio (Eq. 27) | 0.24 | 0.17 | 0.39 | 0.39 |
| | 15° | Axial Stress (ksi) | 22.59 | 17.89 | 15.89 | 13.18 |
| | | Bending Stress (ksi) | 14.77 | 30.63 | 11.97 | 19.35 |
| | | Interaction Ratio (Eq. 26)[2] | 0.44 | **0.49** | **0.87** | **0.90** |
| | | Interaction Ratio (Eq. 27) | 0.35 | 0.43 | 0.58 | 0.66 |
| | 30° | Axial Stress (ksi) | 14.89 | 16.02 | 14.92 | 12.29 |
| | | Bending Stress (ksi) | 38.47 | 30.13 | 14.43 | 18.93 |
| | | Interaction Ratio (Eq. 26)[2] | **0.49** | 0.46 | 0.87 | 0.85 |
| | | Interaction Ratio (Eq. 27) | 0.46 | 0.40 | 0.61 | 0.63 |
| | 45° | Axial Stress (ksi) | 12.78 | 14.30 | 13.44 | 11.52 |
| | | Bending Stress (ksi) | 39.37 | 28.12 | 16.89 | 17.34 |
| | | Interaction Ratio (Eq. 26) | 0.46 | 0.42 | 0.84 | 0.79 |
| | | Interaction Ratio (Eq. 27) | 0.44 | 0.37 | 0.62 | 0.58 |

Notes:

(1) Ligament A is located closest to the spacer plate centerline. Ligament B is the outermost ligament. Maximum ligament A and B axial compressive stress and bending stress occur in the bottom ligaments for the tip-over load condition.

(2) The impact angle for each drop condition with the highest interaction ratio for each of the four ligaments analyzed is shown in **bold**.

## Table 3.7-11 - W21 Canister Shell Assembly Accident Load Combination D1 Results

| Shell Component | Stress Type | Allowable Stress[1] (ksi) | Maximum Stress (ksi) | Minimum Design Margin |
|---|---|---|---|---|
| Top Outer | $P_m$ | 46.2 | 1.2 | +36.4 |
| Closure Plate | $P_m+P_b$[2] | 69.3 | 25.1 | +1.76 |
| Top Outer | $P_m$ | 37.0[3] | 8.9 | +3.13 |
| Closure Weld | Shear[4] | 22.1[3] | 2.5 | +7.70 |
| Top Inner | $P_m$ | 46.2 | 1.6 | +27.5 |
| Closure Plate | $P_m+P_b$ | 69.3 | 10.4 | +5.66 |
| Top Inner | $P_m$ | 41.6[5] | 10.7 | +2.89 |
| Closure Weld | Shear[4] | 24.9[5] | 5.3 | +3.66 |
| Top Shield Plug Btm. | $P_m$ | 46.2 | 0.1 | +Large |
| Support Pl. (DU/Pb) | $P_m+P_b$ | 69.3 | 1.4 | +47.3 |
| Cylindrical | $P_m$ | 46.2 | 18.3 | +1.52 |
| Shell | $P_m+P_b$ | 69.3 | 47.3 | +0.47 |
| Bottom Shell | $P_m$ | 46.2 | 8.5 | +4.42 |
| Extension | $P_m+P_b$ | 69.3 | 10.4 | +5.64 |
| Bottom | $P_m$ | 46.2 | 2.1 | +20.8 |
| Closure Plate | $P_m+P_b$ | 69.3 | 38.4 | +0.80 |
| Bottom End Plate | $P_m$ | 46.2 | 0.9 | +51.3 |
| (Except W21T-LL) | $P_m+P_b$ | 69.3 | 26.2 | +1.65 |
| W21T-LL | $P_m$ | 66.1 | 0.8 | +82.9 |
| Bottom End Plate | $P_m+P_b$ | 99.1 | 35.1 | +1.83 |
| Top Shield Plug Supt. Ring Weld | Shear | 16.2 | 0.2 | +79.2 |
| Shell Extension Top Weld | Shear | 16.2 | 3.0 | +4.39 |
| Shell Extension Bottom Weld | Shear | 16.2 | 1.5 | +10.1 |

Notes:

(1) Allowable stress intensities are based on the weaker of the W21M and W21T canister shell materials (SA-240, Type 304 stainless steel) properties at 300°F, except for the W21T-LL bottom end plate allowable stresses which are based on SA-240, Type XM-19 stainless steel at 300°F.

(2) The maximum bending stress in the top outer closure plate is determined using hand calculations assuming simply support edge conditions to demonstrate that the bending stress in the top outer closure weld may be classified as secondary.

(3) The allowable stresses for the top outer closure weld include a 0.8 weld efficiency factor in accordance with ISG-4.

(4) Shear stress in the welds are determined using hand calculations.

(5) The allowable stresses for the top inner closure weld include a 0.9 weld efficiency factor in accordance with Section 3.1.2.2 of this FSAR.

## Table 3.7-12 - W21 Canister Shell Assembly Accident Load Combination D2 Results

| Shell Component | Stress Type | Allowable Stress[1] (ksi) | Maximum Stress (ksi) | Minimum Design Margin |
|---|---|---|---|---|
| Top Outer Closure Plate | $P_m$<br>$P_m+P_b$[2] | 46.2<br>69.3 | 1.8<br>33.4 | +24.1<br>+1.07 |
| Top Outer Closure Weld | $P_m$<br>Shear[4] | 37.0[3]<br>22.1[3] | 10.8<br>2.2 | +2.42<br>+9.28 |
| Top Inner Closure Plate | $P_m$<br>$P_m+P_b$ | 46.2<br>69.3 | 3.5<br>17.8 | +12.3<br>+2.90 |
| Top Inner Closure Weld | $P_m$<br>Shear[4] | 41.6[5]<br>24.9[5] | 21.0<br>10.5 | +0.98<br>+1.37 |
| Top Shield Plug Btm. Support Pl. (DU/Pb) | $P_m$<br>$P_m+P_b$ | 46.2<br>69.3 | 0.9<br>2.6 | +48.2<br>+25.9 |
| Cylindrical Shell | $P_m$<br>$P_m+P_b$ | 46.2<br>69.3 | 25.1<br>55.6 | +0.84<br>+0.25 |
| Bottom Shell Extension | $P_m$<br>$P_m+P_b$ | 46.2<br>69.3 | 13.4<br>19.2 | +2.45<br>+2.61 |
| Bottom Closure Plate | $P_m$<br>$P_m+P_b$ | 46.2<br>69.3 | 3.8<br>47.7 | +11.2<br>+0.45 |
| Bottom End Plate (Except W21T-LL) | $P_m$<br>$P_m+P_b$ | 46.2<br>69.3 | 2.7<br>34.0 | +16.4<br>+1.04 |
| W21T-LL Bottom End Plate | $P_m$<br>$P_m+P_b$ | 66.1<br>99.1 | 2.5<br>34.6 | +25.2<br>+1.87 |
| Top Shield Plug Supt. Ring Weld | Shear | 16.2 | 0.1 | +Large |
| Shell Extension Top Weld | Shear | 16.2 | 3.1 | +4.22 |
| Shell Extension Bottom Weld | Shear | 16.2 | 1.6 | +9.23 |

Notes:

(1) Allowable stress intensities are based on the weaker of the W21M and W21T canister shell materials (SA-240, Type 304 stainless steel) properties at 300°F, except for the W21T-LL bottom end plate allowable stresses which are based on SA-240, Type XM-19 stainless steel at 300°F.

(2) The maximum bending stress in the top outer closure plate is determined using hand calculations assuming simply support edge conditions to demonstrate that the bending stress in the top outer closure weld may be classified as secondary.

(3) The allowable stresses for the top outer closure weld include a 0.8 weld efficiency factor in accordance with ISG-4.

(4) Shear stress in the welds are determined using hand calculations.

(5) The allowable stresses for the top inner closure weld include a 0.9 weld efficiency factor in accordance with Section 3.1.2.2 of this FSAR.

## Table 3.7-13 - W21 Canister Shell Assembly Accident Load Combination D3 Results

| Shell Component | Stress Type | Allowable Stress[1] (ksi) | Maximum Stress (ksi) | Minimum Design Margin |
|---|---|---|---|---|
| Top Outer | $P_m$ | 46.2 | 0.7 | +63.1 |
| Closure Plate | $P_m+P_b$[2] | 69.3 | 6.9 | +9.01 |
| Top Outer | $P_m$ | 37.0[3] | 2.8 | +12.3 |
| Closure Weld | Shear[4] | 22.1[3] | 0.5 | +44.1 |
| Top Inner | $P_m$ | 46.2 | 1.5 | +30.3 |
| Closure Plate | $P_m+P_b$ | 69.3 | 16.6 | +3.18 |
| Top Inner | $P_m$ | 41.6[5] | 9.4 | +3.44 |
| Closure Weld | Shear[4] | 24.9[5] | 4.7 | +4.32 |
| Top Shield Plug Btm. | $P_m$ | 46.2 | 1.9 | +22.9 |
| Support Pl. (DU/Pb) | $P_m+P_b$ | 69.3 | 48.4 | +0.43 |
| Cylindrical | $P_m$ | 46.2 | 8.7 | +4.34 |
| Shell | $P_m+P_b$ | 69.3 | 26.2 | +1.64 |
| Bottom Shell | $P_m$ | 46.2 | 7.7 | +5.01 |
| Extension | $P_m+P_b$ | 69.3 | 28.8 | +1.40 |
| Bottom | $P_m$ | 46.2 | 2.1 | +20.7 |
| Closure Plate | $P_m+P_b$ | 69.3 | 9.0 | +6.69 |
| Bottom End Plate | $P_m$ | 46.2 | 3.0 | +14.7 |
| (Except W21T-LL) | $P_m+P_b$ | 69.3 | 5.0 | +13.0 |
| W21T-LL | $P_m$ | 66.1 | 2.1 | +30.1 |
| Bottom End Plate | $P_m+P_b$ | 99.1 | 11.3 | +7.80 |
| Top Shield Plug Supt. Ring Weld | Shear | 16.2 | 5.3 | +2.04 |
| Shell Extension Top Weld | Shear | 16.2 | 11.9 | +0.36 |
| Shell Extension Bottom Weld | Shear | 16.2 | 13.3 | +0.22 |

Notes:

(1) Allowable stress intensities are based on the weaker of the W21M and W21T canister shell materials (SA-240, Type 304 stainless steel) properties at 300°F, except for the W21T-LL bottom end plate allowable stresses which are based on SA-240, Type XM-19 stainless steel at 300°F.

(2) The maximum bending stress in the top outer closure plate is determined using hand calculations assuming simply support edge conditions to demonstrate that the bending stress in the top outer closure weld may be classified as secondary.

(3) The allowable stresses for the top outer closure weld include a 0.8 weld efficiency factor in accordance with ISG-4.

(4) Shear stress in the welds are determined using hand calculations.

(5) The allowable stresses for the top inner closure weld include a 0.9 weld efficiency factor in accordance with Section 3.1.2.2 of this FSAR.

## Table 3.7-14 - W21 Canister Shell Assembly Accident Load Combination D4 Results

| Shell Component | Stress Type | Allowable Stress[1] (ksi) | Maximum Stress (ksi) | Minimum Design Margin |
|---|---|---|---|---|
| Top Outer Closure Plate | $P_m$<br>$P_m+P_b$[2] | 46.2<br>69.3 | 14.8<br>25.0 | +2.12<br>+1.77 |
| Top Outer Closure Weld | $P_m$<br>Shear[4] | 37.0[3]<br>22.1[3] | 13.7<br>0.3 | +1.70<br>+84.0 |
| Top Inner Closure Plate | $P_m$<br>$P_m+P_b$ | 46.2<br>69.3 | 20.6<br>44.6 | +1.24<br>+0.55 |
| Top Inner Closure Weld | $P_m$<br>Shear[4] | 41.6[5]<br>24.9[5] | 31.8<br>15.9 | +0.31<br>+0.57 |
| Top Shield Plug Btm. Support Pl. (DU/Pb) | $P_m$<br>$P_m+P_b$ | 46.2<br>69.3 | (6)<br>(6) | (6)<br>(6) |
| Cylindrical Shell | $P_m$<br>$P_m+P_b$ | 46.2<br>69.3 | 24.5<br>36.6 | +0.89<br>+0.89 |
| Bottom Shell Extension | $P_m$<br>$P_m+P_b$ | 46.2<br>69.3 | 24.5<br>36.6 | +0.89<br>+0.89 |
| Bottom Closure Plate | $P_m$<br>$P_m+P_b$ | 46.2<br>69.3 | 20.6<br>44.6 | +1.24<br>+0.55 |
| Bottom End Plate (Except W21T-LL) | $P_m$<br>$P_m+P_b$ | 46.2<br>69.3 | 20.6<br>44.6 | +1.24<br>+0.55 |
| W21T-LL Bottom End Plate | $P_m$<br>$P_m+P_b$ | 66.1<br>99.1 | 20.6<br>44.6 | +2.21<br>+1.22 |
| Top Shield Plug Supt. Ring Weld | Shear | 16.2 | (6) | (6) |
| Shell Extension Top Weld | Shear | 16.2 | (6) | (6) |
| Shell Extension Bottom Weld | Shear | 16.2 | (6) | (6) |

Notes:

(1) Allowable stress intensities are based on the weaker of the W21M and W21T canister shell materials (SA-240, Type 304 stainless steel) properties at 300°F, except for the W21T-LL bottom end plate allowable stresses which are based on SA-240, Type XM-19 stainless steel at 300°F.

(2) The maximum bending stress in the top outer closure plate is determined using hand calculations assuming simply support edge conditions to demonstrate that the bending stress in the top outer closure weld may be classified as secondary.

(3) The allowable stresses for the top outer closure weld include a 0.8 weld efficiency factor in accordance with ISG-4.

(4) Shear stress in the welds are determined using hand calculations.

(5) The allowable stresses for the top inner closure weld include a 0.9 weld efficiency factor in accordance with Section 3.1.2.2 of this FSAR.

(6) Stresses are insignificant.

## Table 3.7-15 - W21 Canister Shell Assembly Accident Load Combination D5 Results

| Shell Component | Stress Type | Allowable Stress[1] (ksi) | Maximum Stress (ksi) | Minimum Design Margin |
|---|---|---|---|---|
| Top Outer | $P_m$ | 46.2 | 5.6 | +7.25 |
| Closure Plate | $P_m+P_b$[2] | 69.3 | 10.9 | +5.36 |
| Top Outer | $P_m$ | 37.0[3] | 8.0 | +3.62 |
| Closure Weld | Shear[4] | 22.1[3] | 0.3 | +84.0 |
| Top Inner | $P_m$ | 46.2 | 12.1 | +2.82 |
| Closure Plate | $P_m+P_b$ | 69.3 | 26.6 | +1.61 |
| Top Inner | $P_m$ | 41.6[5] | 32.8 | +0.27 |
| Closure Weld | Shear[4] | 24.9[5] | 16.4 | +0.52 |
| Top Shield Plug Btm. | $P_m$ | 46.2 | [6] | [6] |
| Support Pl. (DU/Pb) | $P_m+P_b$ | 69.3 | [6] | [6] |
| Cylindrical | $P_m$ | 46.2 | 18.6 | +1.48 |
| Shell | $P_m+P_b$ | 69.3 | 32.2 | +1.15 |
| Bottom Shell | $P_m$ | 46.2 | 18.6 | +1.48 |
| Extension | $P_m+P_b$ | 69.3 | 32.2 | +1.15 |
| Bottom | $P_m$ | 46.2 | 12.1 | +2.82 |
| Closure Plate | $P_m+P_b$ | 69.3 | 26.6 | +1.61 |
| Bottom End Plate | $P_m$ | 46.2 | 12.1 | +2.81 |
| (Except W21T-LL) | $P_m+P_b$ | 69.3 | 26.6 | +1.61 |
| W21T-LL | $P_m$ | 66.1 | 12.1 | +4.46 |
| Bottom End Plate | $P_m+P_b$ | 99.1 | 26.6 | +2.73 |
| Top Shield Plug Supt. Ring Weld | Shear | 16.2 | [6] | [6] |
| Shell Extension Top Weld | Shear | 16.2 | 9.8 | +0.65 |
| Shell Extension Bottom Weld | Shear | 16.2 | 9.8 | +0.65 |

Notes:

(1) Allowable stress intensities are based on the weaker of the W21M and W21T canister shell materials (SA-240, Type 304 stainless steel) properties at 300°F, except for the W21T-LL bottom end plate allowable stresses which are based on SA-240, Type XM-19 stainless steel at 300°F.

(2) The maximum bending stress in the top outer closure plate is determined using hand calculations assuming simply support edge conditions to demonstrate that the bending stress in the top outer closure weld may be classified as secondary.

(3) The allowable stresses for the top outer closure weld include a 0.8 weld efficiency factor in accordance with ISG-4.

(4) Shear stress in the welds are determined using hand calculations.

(5) The allowable stresses for the top inner closure weld include a 0.9 weld efficiency factor in accordance with Section 3.1.2.2 of this FSAR.

(6) Stresses are insignificant.

## Table 3.7-16 - W21 Canister Basket Assembly Accident Load Combination Results

| Basket Component | Stress Type | Allowable Stress (ksi) | L.C. D3 ($T+A_s$) | | L.C. D4 ($T+A_t$) | | L.C. D5 ($T+A_{s1}$) | | L.C. D6 ($D^{(1)}+T+E$) | |
|---|---|---|---|---|---|---|---|---|---|---|
| | | | Maximum Stress (ksi) | Minimum Design Margin | Maximum Stress (ksi) | Minimum Design Margin | Maximum Stress (ksi) | Minimum Design Margin | Maximum Stress (ksi) | Minimum Design Margin |
| 2-inch Thick Stainless Steel Spacer Plate | $P_m$ | 60.6 | 0.0 | +Large | 12.4 | +3.89 | 9.3 | +5.52 | 1.8 | +32.7 |
| | $P_m+P_b$ | 90.8 | 6.1 | +13.9 | 45.8 | +0.98 | 23.3 | +2.90 | 4.5 | +19.2 |
| | Buckling I.R.(2) | 1.0 | (7) | (7) | 0.94 | +0.06 | 0.70 | +0.43 | (7) | (7) |
| ¾-inch Thick Carbon Steel Spacer Plate | $P_m$ | 75.4 | 0.0 | +Large | 23.3 | +2.24 | 18.4 | +3.10 | 4.2 | +17.0 |
| | $P_m+P_b$ | 113.1 | 14.6 | +6.75 | 75.2 | +0.50 | 46.0 | +1.46 | 10.2 | +10.1 |
| | Buckling I.R.(2) | 1.0 | (7) | (7) | 0.49 | +1.04 | 0.31 | +2.23 | (7) | (7) |
| 2-inch Thick Stainless Steel Bottom End Spacer Plate | $P_m$ | 62.4 | 0.0 | +Large | (6) | (6) | (6) | (6) | 1.8 | +33.7 |
| | $P_m+P_b$ | 93.6 | 26.3 | +2.56 | (6) | (6) | (6) | (6) | 5.8 | +15.1 |
| | Buckling I.R.(2) | 1.0 | (6) | (6) | (6) | (6) | (6) | (6) | (6) | (6) |
| Support Rod Segments | $P_m$ | 61.5 | 16.5 | +2.73 | 2.8 | +21.0 | (7) | (7) | 0.9 | +67.3 |
| | $P_m+P_b$ | 92.2 | 37.9 | +1.43 | 47.4 | +0.95 | (7) | (7) | 5.0 | +17.4 |
| | Buckling I.R.(2) | 1.0 | 0.84 | +0.19 | (4) | (4) | (4) | (4) | (4) | (4) |
| W21M Supt. Rod Threads | $P_m$ | 61.5 | (7) | (7) | 25.6 | +1.40 | (7) | (7) | 4.4 | +13.0 |
| W21T Supt. Rod Threads | $P_m$ | 95.3 | (7) | (7) | 35.1 | +1.72 | (7) | (7) | 13.9 | +5.86 |
| Support Sleeve | $P_m$ | 33.6 | 7.3 | +3.58 | (4) | (4) | (4) | (4) | (4) | (4) |
| | $P_m+P_b$ | 50.4 | 9.5 | +4.33 | (4) | (4) | (4) | (4) | (4) | (4) |
| | Buckling I.R.(2) | 1.0 | 0.63 | +0.59 | (4) | (4) | (4) | (4) | (4) | (4) |
| Guide Tube | $P_m$ | 39.1 | 14.0 | +1.79 | 13.6 | +1.88 | (7) | (7) | 2.6 | +14.0 |
| | $P_m+P_b$ | 58.7 | 14.0 | +3.19 | 54.0 | +0.09 | (7) | (7) | 23.8 | +1.47 |
| | Buckling | 1.0(2)/137(5) | 14.0(5) | +8.79 | 0.48(2) | +1.08 | (7) | (7) | (7) | (7) |
| Guide Tube Longitudinal Seam Weld | $P_m$ | 23.5(8) | (7) | (7) | 4.1 | +4.73 | (7) | (7) | (7) | (7) |
| | $P_m+P_b$ | 35.2(8) | (7) | (7) | 23.6 | +0.49 | (7) | (7) | (7) | (7) |

Notes on following page:

Notes for Table 3.7-16:

(1) Either vertical or horizontal dead weight.

(2) Buckling interaction ratio (I.R.) calculated in accordance with NUREG/CR-6322.

(3) Bounded by buckling evaluation of most highly loaded 2-inch stainless steel spacer plate.

(4) Bounded by storage cask end drop condition.

(5) The allowable guide tube axial compressive stress for the storage cask end drop condition is 137 ksi, as discussed in Section 3.7.3.2.3.

(6) Bounded by other 2-inch stainless steel spacer plates.

(7) Bounded by transfer cask side drop condition.

(8) Allowable stresses include a 60% weld efficiency factor. This is applicable only to a full penetration weld with surface PT examination only and restricted in location to the ¼ span of panel width.

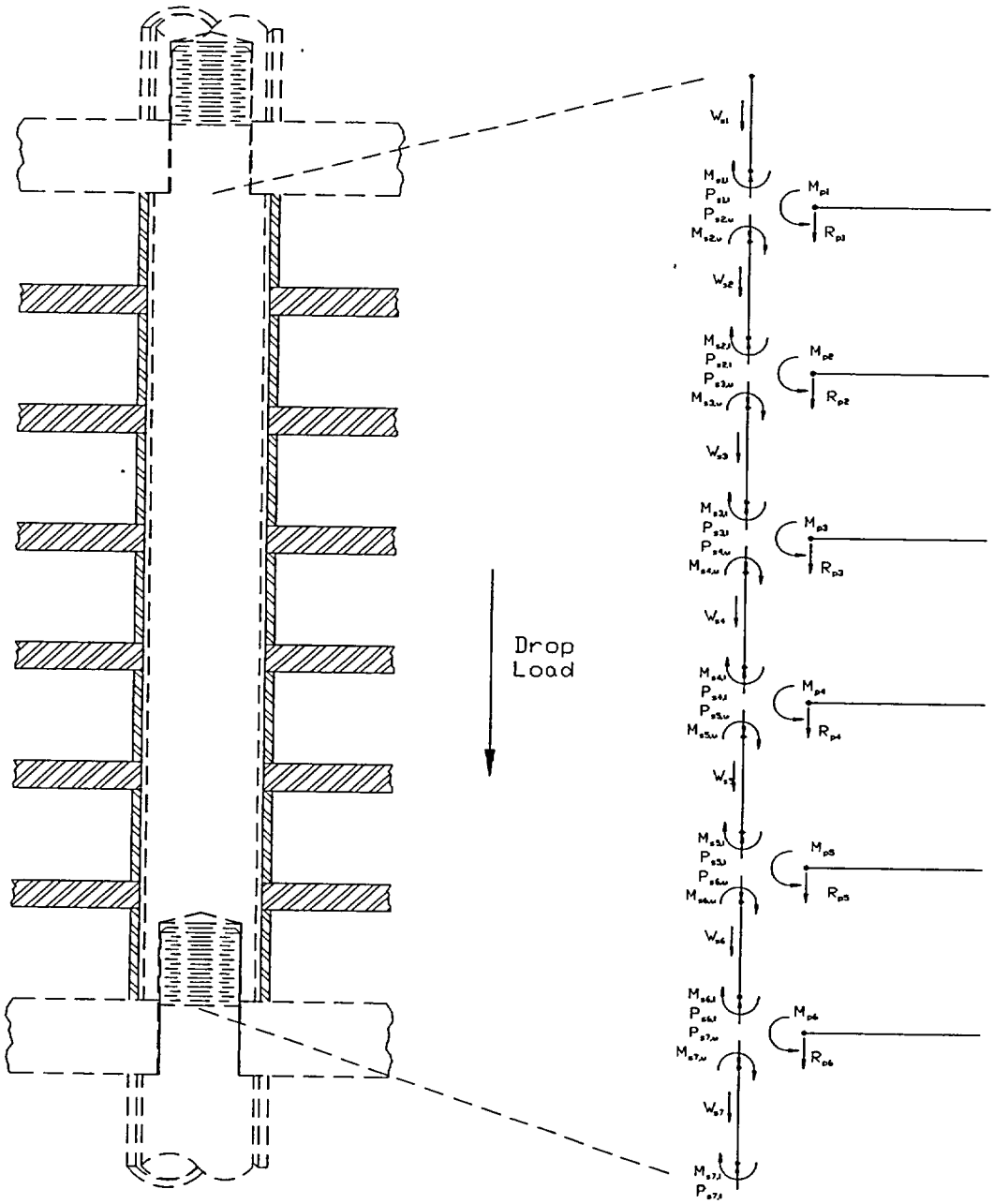


**Figure 3.7-1 - W21 Support Sleeve End Drop Free Body Diagram**

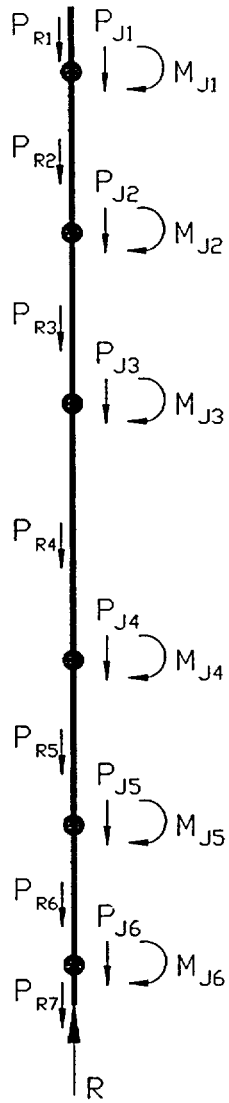


**Figure 3.7-2 - W21 Support Rod End Drop Free Body Diagram**

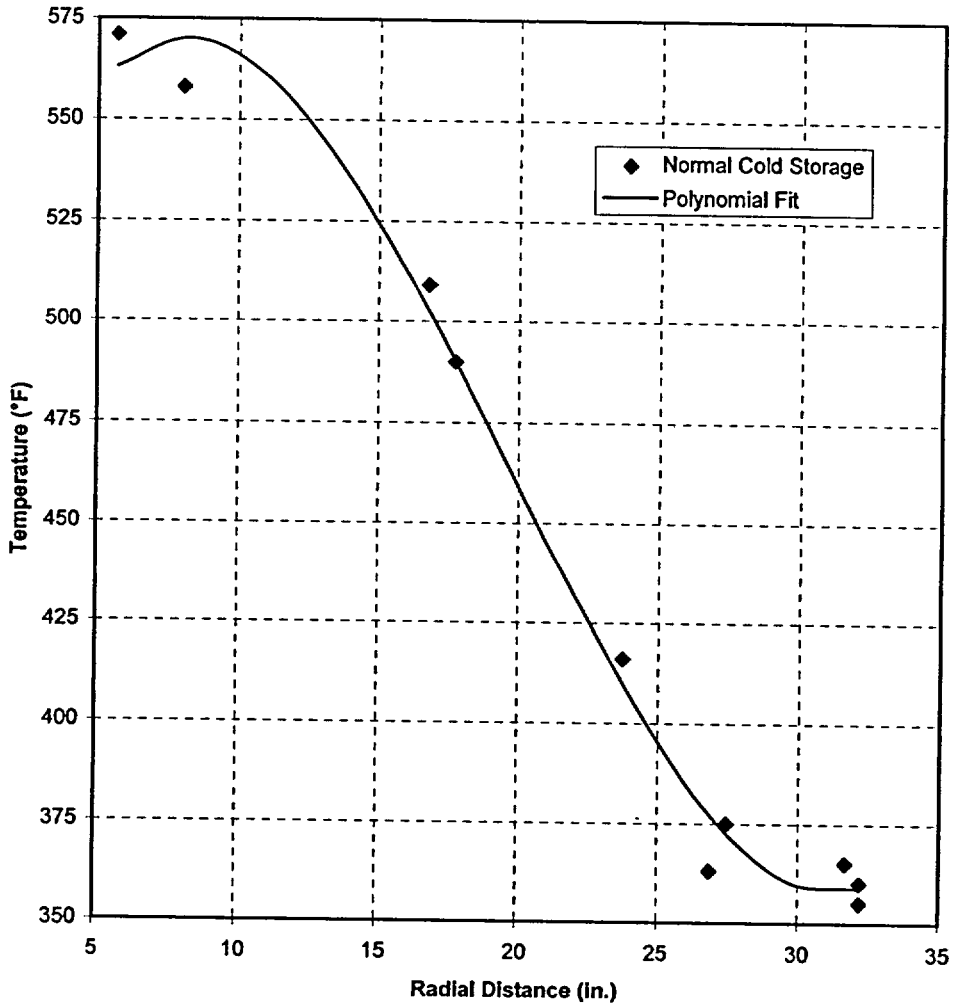


**Figure 3.7-3 - W21 Carbon Steel Spacer Plate Design Thermal Gradient**

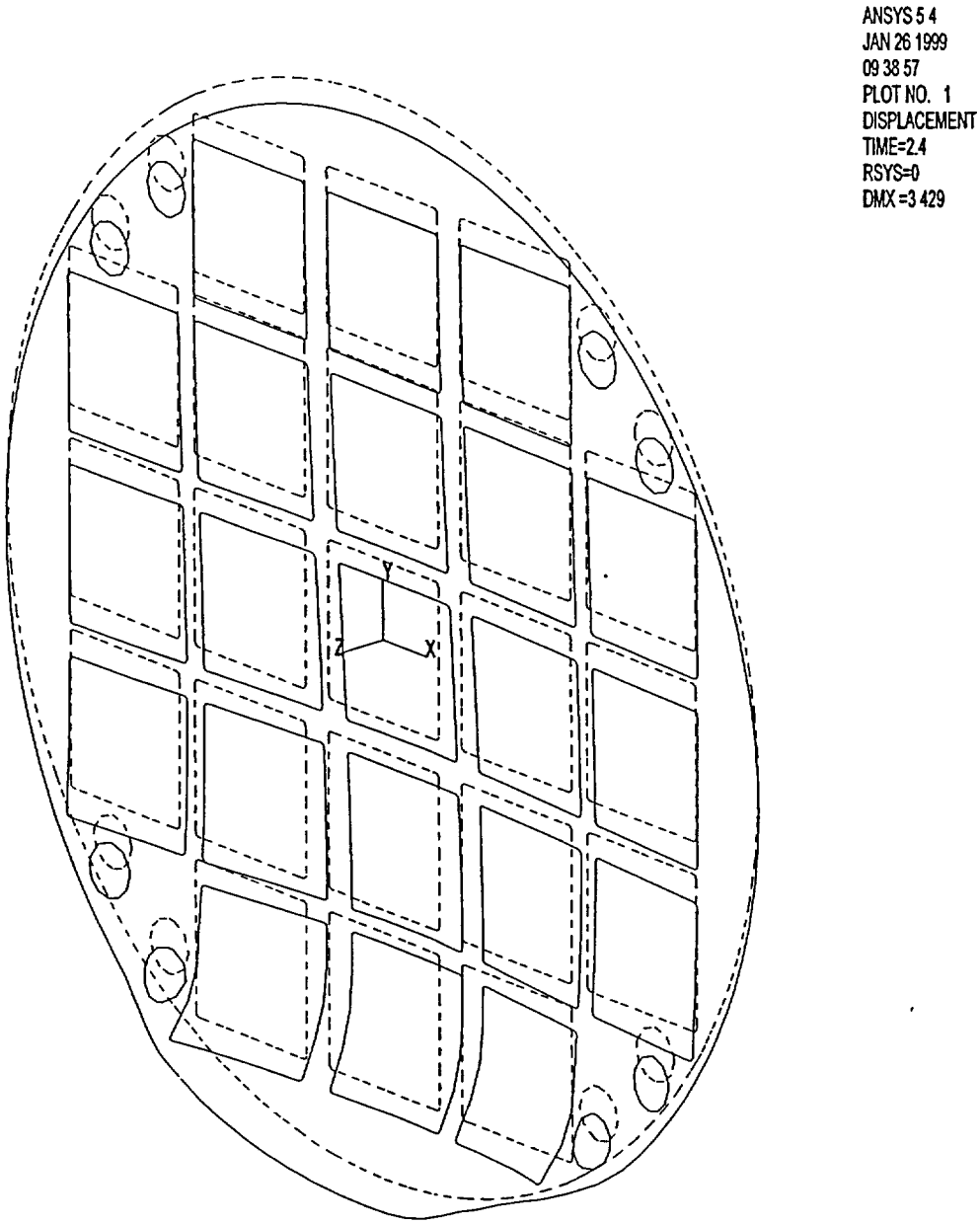


**Figure 3.7-4 - W21 Spacer Plate Deformed Shape for Combined Tip-over and Thermal Loading (Time=2.4)**

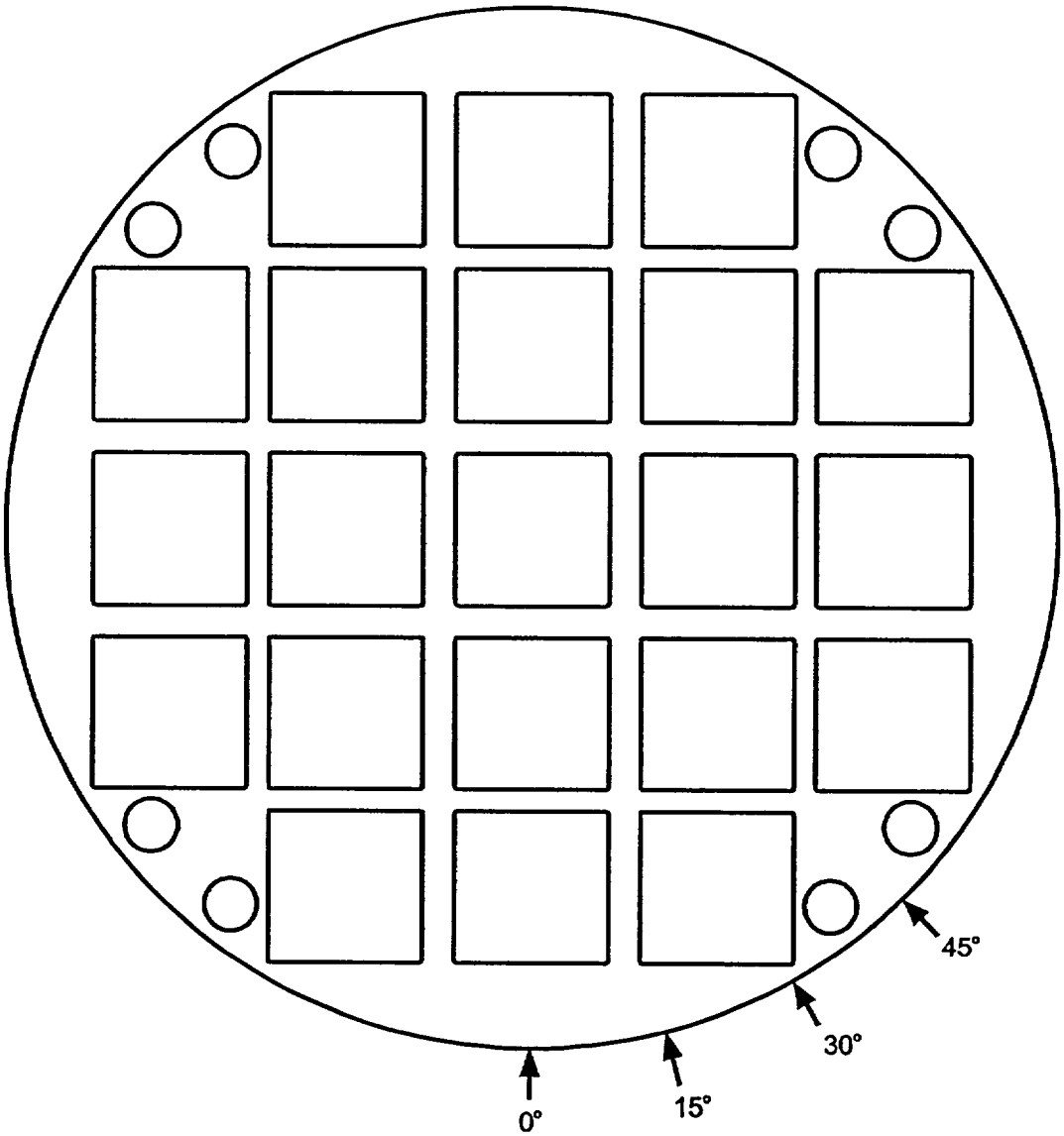


**Figure 3.7-5 - W21 Spacer Plate Side Drop Impact Orientations Evaluated**

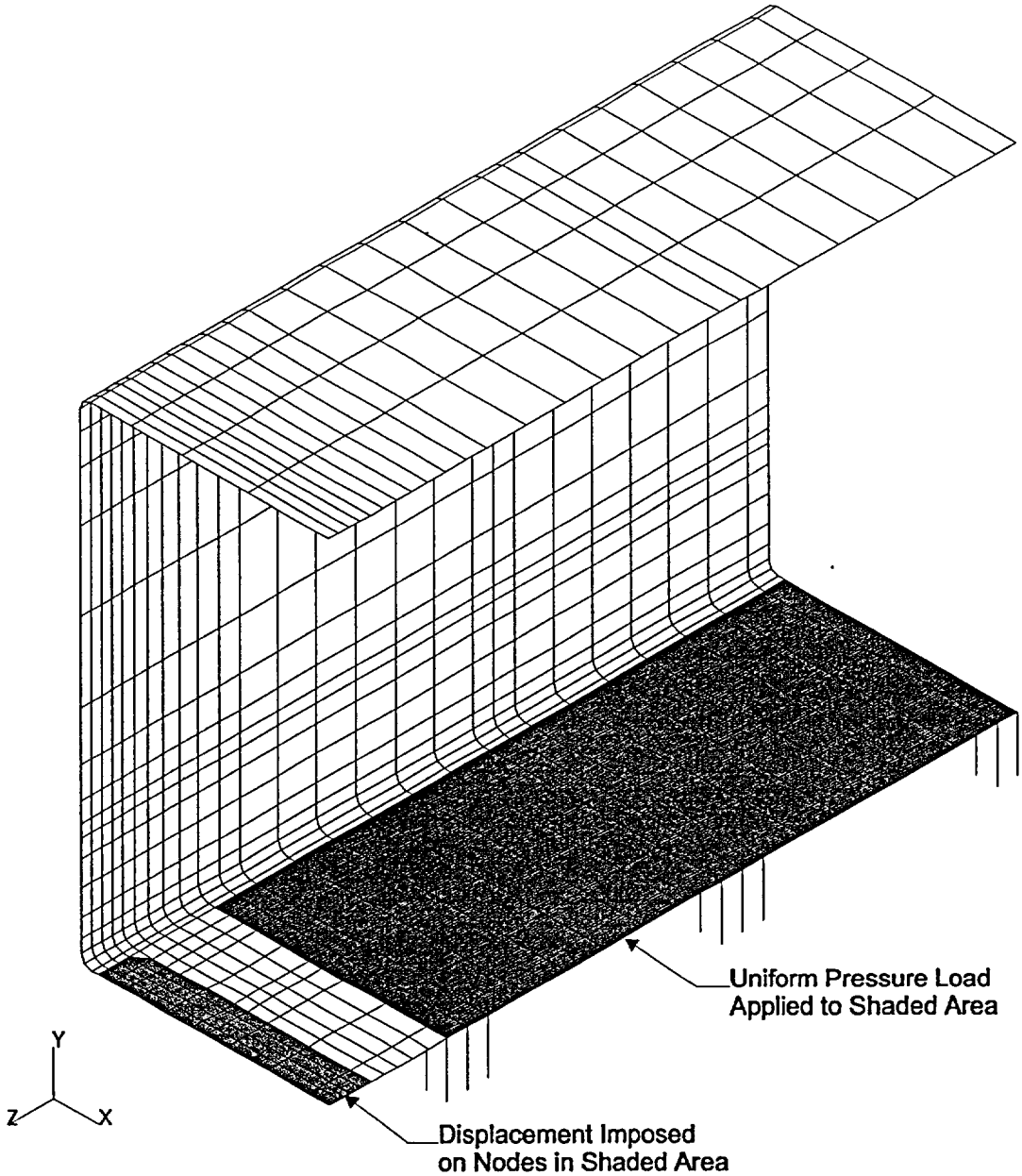


**Figure 3.7-6 - W21 Guide Tube 60*g* Side Drop Loads for Concentrated Fuel Grid Spacer Loading Evaluation**

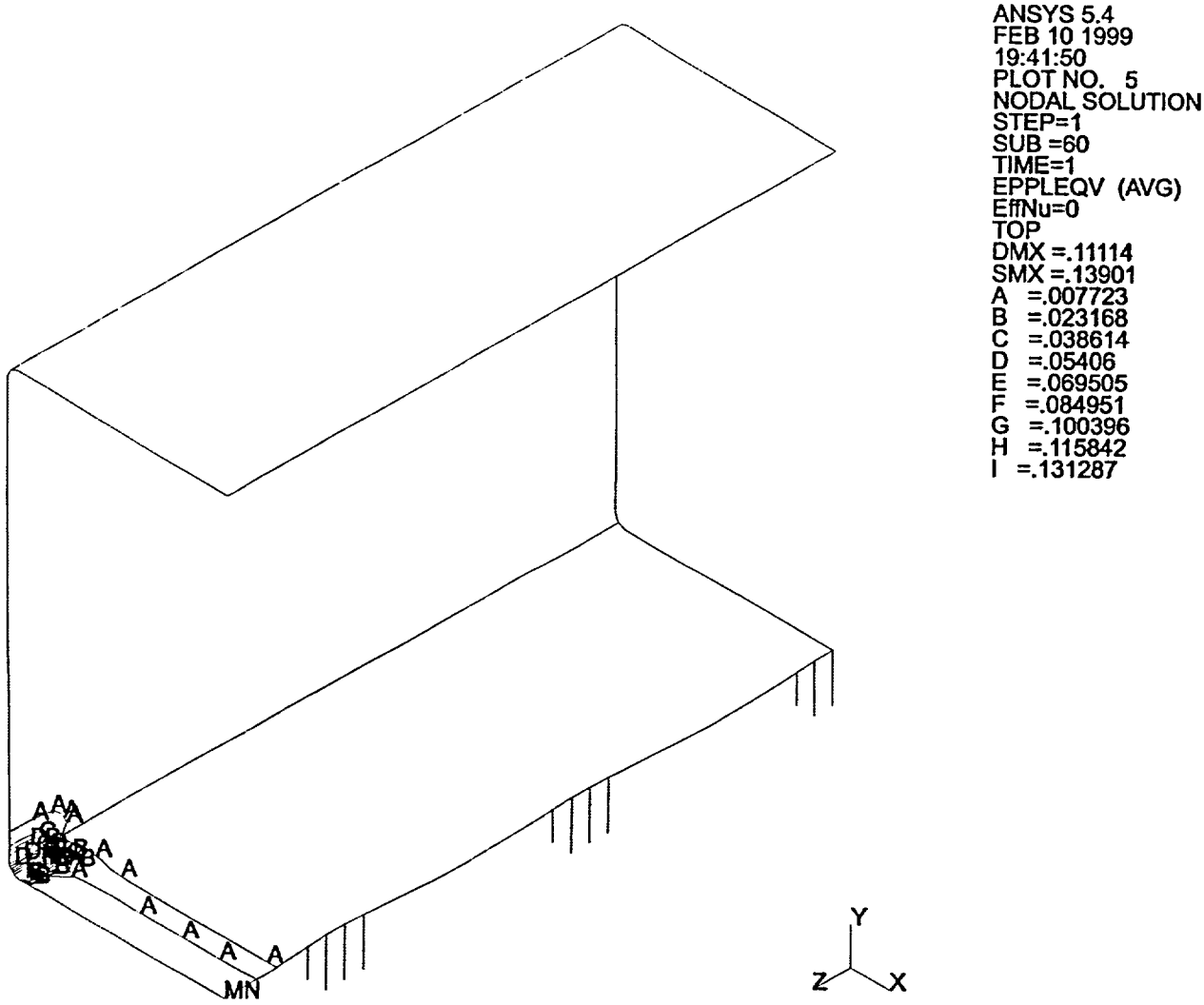


**Figure 3.7-7 - W21 Guide Tube 60*g* Side Drop Plastic Strain for Concentrated Fuel Load At Grid Spacers**

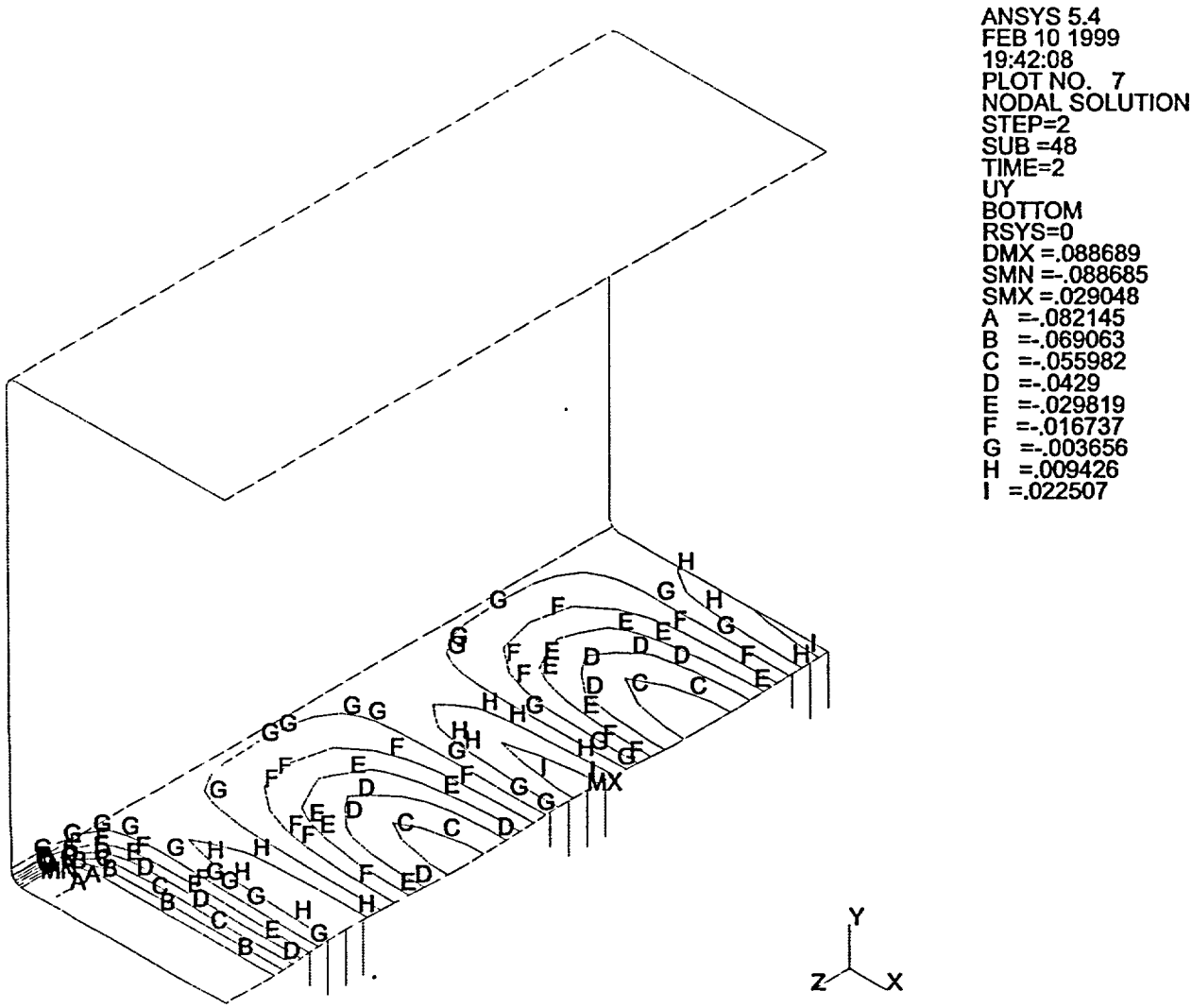


**Figure 3.7-8 - W21 Guide Tube 60*g* Side Drop Permanent Deformation for Concentrated Fuel Load At Grid Spacers**

This page intentionally left blank.

## Table 4.5-1 - Maximum W21 Canister System Temperature at $Q_{max}$ for Storage[1]

| Component | Case 8<br>Off-Normal Cold Storage | Case 9<br>Off-Normal Hot Storage | Case 13b [4]<br>Horizontal Unloading, Initial/Peak | Allowable Temperature[5] |
|---|---|---|---|---|
| Peak Fuel Rod Cladding | 314.5°C | 389.8°C | 368.8°C / 395.5°C | 400°C |
| Guide Tube | 550°F | 696°F | 655°F / 710°F | 800°F / 1000°F |
| Spacer Plates: | | | | |
| Stainless Steel | 539°F | 687°F | 646°F / 702°F | 800°F / 1000°F |
| Carbon Steel | 534°F | 683°F | 642°F / 700°F | 700°F / 1000°F |
| Support Rod | 325°F | 497°F | 449°F / 622°F | 650°F / 1000°F |
| Helium Bulk | 357°F | 515°F | 472°F / 594°F | N/A |
| Canister Shell | 261°F | 440°F | 391°F / 558°F | 800°F / 1000°F |
| Max. Concrete | 6°F | 211°F | 158°F / 216°F | 350°F |
| Cask Liner Thermocouple[2] | -9°F | 190°F | 133°F / 203°F | N/A |
| *Reference Results from Tables 4.4-7 and 4.5-2 of the FuelSolutions™ Storage System FSAR* | | | | |
| *Canister Shell[3]* | *290°F* | *473°F* | *423°F / 662°F* | -- |
| *Max. Concrete[3]* | *12°F* | *228°F* | *169°F / 348°F* | -- |
| *Cask Liner Thermocouple[2,3]* | *0°F* | *210°F* | *150°F / 312°F* | -- |

Notes:

(1) Except as noted, temperatures in this table are based on a heat load of 25.1 kW.

(2) Estimated thermocouple reading for analyzed condition.

(3) Temperatures based on heat load of 28 kW.

(4) Peak temperatures taken from 14 hour point in the transient analysis.

(5) Short-term allowable steel temperatures from Table 4.3-1 apply for cases 8 and 9. Mitigating actions are required prior to exceeding long-term allowable temperatures for case 13b (see Section 12.3 of this FSAR). Canister allowable temperatures are from Table 4.3-1. Storage cask allowable temperatures are from Table 4.3-1 of the FuelSolutions™ Storage System FSAR.

## Table 4.5-2 - W21 Canister Off-Normal Pressures[1]

| Parameter | Case 8<br>Off-Normal Cold Storage | Case 9<br>Off-Normal Hot Storage | Case 13b<br>Horizontal Unloading, Initial/Peak[3] |
|---|---|---|---|
| Helium Bulk | 357°F | 515°F | 472°F / 684°F |
| Helium Pressure[2] | 20.6 psia | 24.6 psia | 23.5 psia / 28.8 psia |

Notes:

(1) Temperatures/pressures in this table are based on a heat load of 25.1 kW.

(2) Estimated canister pressure based on a design pressure of 24 psia at "normal hot storage" condition and ideal gas law. Pressurization due to fuel rod failure is not included.

(3) Peak temperature and pressure taken from 60-hour point in transient.

backfill gas presented in Table 4.4-5 and Table 4.4-6 for the limiting PWR fuel assembly class. Assuming 100% rod failures, the maximum total moles of rod gas (fill gas + 60 GWd/MTU fission gas + control component gas) shown in Table 4.4-5 for the limiting PWR fuel (WE 17x17 with control components [CC]) are 523.1 moles (228.6 + 230.5 + 64.0). The total moles of canister fill gas shown in Table 4.4-6 for the limiting PWR fuel (WE 17x17, 60 GWd/MTU w/ CC) are 220 moles, for a total canister content of 743.1 moles. Assuming 10% rod failures, the maximum total moles of gas in the canister would be 272.3 moles (52.3 + 220). The reduction in the number of moles would result in a proportional 37% reduction in canister pressure (272.3 moles / 743.1 moles), while the increased absolute accident temperature would result in only a 21.5% proportional pressure increase (1158°R / 953°R). The net effect is a pressure which is 45% of the accident pressure with 100% rod failures under off-normal hot storage conditions.

#### 4.6.1.5 Maximum Thermal Stresses

W21 canister thermal stresses resulting from accident conditions are addressed in Sections 3.7.1 and 3.7.6 of this FSAR.

#### 4.6.1.6 Evaluation of Canister Performance for Accident Conditions

##### 4.6.1.6.1 All Vents Blocked

A transient analysis of the all vents blocked case demonstrates that the short-term allowable material temperatures for the W21 canister and the storage cask are not exceeded for the enveloping canister thermal rating for any site within the contiguous United States, provided the all vents blocked conditions do not exist for longer than a 41-hour period. Therefore, the W21 canister in the FuelSolutions™ W150 Storage Cask provides adequate protection of the fuel cladding and canister components during a credible blocked vent event for the storage cask. The operational *technical specification* contained in Section 12.3 of the FuelSolutions™ Storage System FSAR provides for daily monitoring and corrective actions to mitigate any vent blockage conditions.

##### 4.6.1.6.2 Fire Accident

A transient analysis of the fire accident for the W21 canister in the storage cask demonstrates that the W21 canister short-term allowable material temperatures are not exceeded for a fire accident, consistent with the requirements of 10CFR71.73(c)(4). Therefore, the W21 canister and storage cask are suitable for the dry storage of fuel with thermal ratings that are bounded by the W21 canister thermal rating summarized in Table 4.1-4.

## Table 4.6-1 - W21 Canister System Temperature for All Vents Blocked[1]

| Component | Case 11 All Vents Blocked, Initial/Peak[2] | Material Allowable[5] |
|---|---|---|
| Peak Fuel Rod Cladding | 368.8°C / 485.8°C | 570°C |
| Guide Tube | 655°F / 878°F | 1000°F |
| Spacer Plates: | | |
| Stainless Steel | 646°F / 870°F | 1000°F |
| Carbon Steel | 642°F / 868°F | 1000°F |
| Support Rod | 449°F / 701°F | 1000°F |
| Helium Bulk | 472°F / 698°F | N/A |
| Canister Shell | 391°F / 655°F | 1000°F |
| Max. Concrete | 158°F / 350°F | 350°F |
| Cask Liner Thermocouple[3] | 133°F / 339°F | N/A |
| *Reference Results from Tables 4.4-7 and 4.6-2 of the FuelSolutions™ Storage System FSAR* | | |
| *Canister Shell[4]* | *423°F / 644°F* | -- |
| *Max. Concrete[4]* | *169°F / 349°F* | - |
| *Cask Liner Thermocouple[3,4]* | *150°F / 334°F* | -- |

Notes:

(1) Except as noted, temperatures in this table are based on a heat load of 25.1 kW.

(2) Peak temperature taken from the 60-hour point in the transient analysis.

(3) Estimated thermocouple reading for analyzed condition.

(4) Temperatures based on heat load of 28 kW.

(5) Canister allowable temperatures are from Table 4.3-1. Storage cask material allowable temperatures are from Table 4.3-1 of the FuelSolutions™ Storage System FSAR.

## 6.1 Discussion and Results

The FuelSolutions™ W21 canister design is established on the basis of both favorable geometry and permanent fixed neutron absorber materials (poison). The criticality evaluation credits only 75% of the minimum assured boron content and the continued efficacy of fixed neutron absorber materials is demonstrated. The criticality acceptance criteria are demonstrated to be satisfied for the range of fuel assembly classes defined in Section 2.2 of this FSAR without reliance on credit for fuel burnup or fuel-related burnable neutron absorbers.

The criticality evaluation includes analyses for fuel assembly types grouped into fuel assembly classes according to physical characteristics important to criticality. For assembly types within a given assembly class, most physical parameters are the same. Some parameters, however, vary over a limited range for assemblies within a given class. A bounding assembly configuration is defined for each assembly class which has the most limiting values for each variable assembly parameter. Maximum allowable enrichments for each assembly class are calculated based upon this bounding assembly configuration. Additional analyses which verify that specific assembly types within a given class are less reactive than the bounding assembly configuration defined for that class are also performed.

Each of the assembly physical parameters that are important to criticality are specified for each assembly class in the fuel specifications given in Table 6.1-1, based upon the bounding assembly configuration defined for that class. For parameters that vary for assemblies within the class, the bounding case values are specified as maximum or minimum allowable values in the fuel specification, depending on whether decreasing or increasing the parameter value increases reactivity. Any fuel assembly that meets the fuel parameter specifications for a given assembly class may be loaded into the FuelSolutions™ W21 canister, as long as its enrichment is below the maximum allowable value specified for that assembly class. This includes, but is not limited to, all the specific assembly types that are explicitly shown by analysis to be less reactive than the defined bounding assembly configuration for their assembly class. A list of specific assembly types that fall into each defined criticality class shown in Table 6.1-1 is provided in the fuel specifications given in Section 2.2 of this FSAR.

The maximum allowable enrichment levels shown for each assembly class in Table 6.1-1 are derived from calculations that demonstrate the highest calculated $k_{eff}$ that might occur under any loading condition involving loading, closure, transfer, or on-site dry storage; and that satisfies the $k_{eff} \leq 0.95$ acceptance criteria for criticality. Maximum allowable enrichment levels are calculated for the two FuelSolutions™ W21 canister loading specifications defined in the *technical specification* contained in Section 12.3 of this FSAR: W21-1, loading of up to 21 intact assemblies; and W21-2 partial loading of up to 20 intact assemblies with an empty guide tube in the central location (shown in Figure 6.3-4). The W21-2 canister configuration employs a mechanical block-out over the opening of the central guide tube in order to prevent inadvertent loading of assemblies into that location.

## Table 6.1-1 - W21 Canister Fuel Specification by PWR Assembly Class (2 Pages)

| Fuel Assembly Class | B&W 15x15 | B&W 17x17 | CE 14x14 | CE 14x14 A | CE 15x15 P | 15x16 | 15x16 A |
|---|---|---|---|---|---|---|---|
| Clad Material | Zr | Zr | Zr | Zr | Zr | Zr | Zr |
| W21-1 Initial Enrichment (w/o $^{235}U$)(1,2) | ≤ 4.70 | ≤ 4.60 | ≤ 5.00 | ≤ 5.00 | ≤ 5.00 | ≤ 5.00 | ≤ 5.00 |
| W21-2 Initial Enrichment (w/o $^{235}U$)(1,3) | ≤ 5.00 | ≤ 4.90 | ≤ 5.00 | ≤ 5.00 | ≤ 5.00 | ≤ 5.00 | ≤ 5.00 |
| Pellet Stack $UO_2$ Density(4) | ≤ 96.5 % | ≤ 96.5 % | ≤ 96.5 % | ≤ 96.5 % | ≤ 97.5 % | ≤ 96.5 % | ≤ 96.5 % |
| Number of Fuel Rods | 208 | 264 | 176 | 176 | 208 - 216 | 231 | 237 |
| Clad O.D. (in) | ≥ 0.430 | ≥ 0.377 | ≥ 0.440 | ≥ 0.440 | ≥ 0.4135 | ≥ 0.365 | ≥ 0.365 |
| Clad Thickness (in) | ≥ 0.0265 | ≥ 0.022 | ≥ 0.026 | ≥ 0.026 | ≥ 0.024 | ≥ 0.024 | ≥ 0.024 |
| Pellet Diameter (in) | ≥ 0.3675 | ≥ 0.3232 | ≥ 0.370 | ≥ 0.3795 | ≥ 0.350 | ≥ 0.3105 | ≥ 0.3105 |
| Fuel Rod Pitch (in) | 0.568 | 0.502 | 0.58 | 0.568 | 0.55 | 0.472 | 0.468 |
| Active Fuel Length (in)(4) | ≤ 150 | ≤ 150 | ≤ 150 | ≤ 150 | ≤ 150 | ≤ 150 | ≤ 150 |
| Number of Guide / Instrument Tube Locations(5) | 17 | 25 | 5(6) | 5(6) | 1 - 9 | 1 | 1 |
| Bottom Nozzle Height (in)(4) | ≥ 1.97 | ≥ 1.97 | ≥ 1.97 | ≥ 1.97 | ≥ 1.97 | ≥ 1.97 | ≥ 1.97 |

## Table 6.1-1 - W21 Canister Fuel Specification by PWR Assembly Class (2 Pages)

| Fuel Assembly Class | CE 16x16 | W 14x14 | W 15x15 | W 15x15 A | W 17x17 | W 17x17 A | W 17x17 B |
|---|---|---|---|---|---|---|---|
| Clad Material | Zr | Zr | Zr | Zr | Zr | Zr | Zr |
| W21-1 Initial Enrichment (w/o $^{235}U$)(1,2) | ≤ 5.00 | ≤ 5.00 | ≤ 4.70 | ≤ 4.90 | ≤ 4.70 | ≤ 4.60 | ≤ 4.60 |
| W21-2 Initial Enrichment (w/o $^{235}U$)(1,3) | ≤ 5.00 | ≤ 5.00 | ≤ 5.00 | ≤ 5.00 | ≤ 5.00 | ≤ 4.90 | ≤ 4.90 |
| Pellet Stack $UO_2$ Density(4) | ≤ 96.5 % | ≤ 96.5 % | ≤ 96.5 % | ≤ 96.5 % | ≤ 96.5 % | ≤ 96.5 % | ≤ 96.5 % |
| Number of Fuel Rods | 236 | 179 | 204 | 204 | 264 | 264 | 264 |
| Clad O.D. (in) | ≥ 0.382 | ≥ 0.400 | ≥ 0.420 | ≥ 0.424 | ≥ 0.374 | ≥ 0.360 | ≥ 0.360 |
| Clad Thickness (in) | ≥ 0.025 | ≥ 0.0243 | ≥ 0.024 | ≥ 0.030 | ≥ 0.0225 | ≥ 0.0225 | ≥ 0.025 |
| Pellet Diameter (in) | ≥ 0.325 | ≥ 0.3444 | ≥ 0.3659 | ≥ 0.3565 | ≥ 0.3195 | ≥ 0.3088 | ≥ 0.303 |
| Fuel Rod Pitch (in) | 0.506 | 0.556 | 0.563 | 0.563 | 0.496 | 0.496 | 0.496 |
| Active Fuel Length (in)(4) | ≤ 150 | ≤ 150 | ≤ 150 | ≤ 150 | ≤ 150 | ≤ 150 | ≤ 150 |
| Number of Guide / Instrument Tube Locations(5) | 5(6) | 17 | 21 | 21 | 25 | 25 | 25 |
| Bottom Nozzle Height (in)(4) | ≥ 1.97 | ≥ 1.97 | ≥ 1.97 | ≥ 1.97 | ≥ 1.97 | ≥ 1.97 | ≥ 1.97 |

Table 6.1-1 Notes:

(1) The maximum allowable enrichments apply for all assemblies that meet the specified physical parameter requirements for the defined assembly class. The maximum allowable enrichments are defined as the maximum planar average enrichment at any axial assembly location. An exception is the CE 15x15 P assembly class, for which the maximum allowable enrichment applies to each individual fuel pin within the assembly.

(2) Loading Specification W-21-1 is up to 21 SNF assemblies.

(3) Loading Specification W-21-2 is up to 20 SNF assemblies with the center location empty.

(4) For these parameters, bounding values (for all PWR fuel) are conservatively assumed for all assembly types in the criticality analyses.

(5) The guide (and instrument) tubes displace water and reduce assembly reactivity. The criticality analyses conservatively neglect the presence of the guide tubes, and model water filled spaces in the guide tube locations. Therefore, whereas the number of guide tube locations is a specified parameter, the materials and dimensions of the guide tubes are not specified, since any quantity of steel or zircaloy in the guide tube locations will reduce assembly reactivity.

(6) The CE 14x14 and CE 16x16 assembly guide tubes occupy four fuel rod locations within the assembly array.

This page intentionally left blank.

FuelSolutions™ W21 hypothetical accident conditions model that has been sliced with vertical planes to expose the lower and upper portions of the canister.

As shown in Figure 6.3-5, the lower portion of the model begins at the top of the bottom end inner closure plate. Next, the water gap between the bottom closure plate and the bottom spacer plate is modeled. The bottom of the fuel appears near the top of the bottom spacer plate at an elevation of 1.97 inches above the bottom closure plate. The bottoms of the guide tubes are modeled in the region between the bottom and first spacer plates at an elevation of 3.75 inches above the bottom closure plate. The bottom of the BORAL® panel is modeled just below the first spacer plate at an elevation of 5.25 inches above the bottom closure plate. This modeled panel elevation conservatively covers any potential accident configuration, as discussed below. The modeled position of the bottom of the BORAL® neutron absorber panel relative to the bottom of the fuel leaves about 3.28 inches of active fuel in an unpoisoned region in the basket. The basket guide tubes are modeled axially to the top of the BORAL® neutron absorber panels as shown in Figure 6.3-6. The axial placement of the guide tubes within the basket is consistent with the damage expected to occur from a nine meter drop in a representative transportation cask (as specified for the hypothetical accident in 10CFR71).

Under normal conditions, the bottoms of the guide tubes are 0.1 inches off the bottom of the canister cavity. The bottoms of the BORAL® panel are 2.0 inches from the canister bottom ( i.e., 1.9 inches from the guide tube bottom). As a result of a nine-meter drop, however, the guide tubes separate axially from the basket structure and are free to move in the axial direction within the boundaries of the spacer plate openings. To maximize the effect of the guide tube relocation on system reactivity, the tops of the guide tubes are modeled resting against the top shield plug. This results in a vertical guide tube shift of approximately 2.0 inches. The tabs at the top of the guide tubes are also assumed to flatten out during the cask drop accident resulting in an additional upward shift of 0.75 inch. Finally, the BORAL® panel is free to shift upwards (inside the guide tube wrapper) by 0.5 inch, due to the presence of a half-inch thermal expansion gap that lies above the panel in the wrapper cavity. Due to these factors, the bottom ends of the guide tubes and BORAL® panels may shift upward from their original positions by up to 2.75 inches and 3.25 inches, respectively. Thus, the final position of the bottom of the BORAL® panel following the hypothetical cask end drop is conservatively assumed to be 5.25 inches above the inner closure plate. Due to the presence of the 1.0-inch-high flow channels at the bottom of each guide tube wall, the bottom 1.0 inch of the guide tube structure is not modeled (i.e., is conservatively modeled as water). Due to this, and the upward shift of 2.75 inches, the bottom of the guide tubes is modeled at 3.75 inches above the canister bottom. Figure 6.3-6 shows the position of the top of one BORAL® panel when the top end of the guide tubes rest against the top shield plug.

The active fuel stack is conservatively modeled beginning at a height of 1.97 inches and ending at a height of 151.97 inches. This position represents an active fuel length of 150 inches, which is an upper bound value for all fuel assembly types considered for storage in the FuelSolutions™ W21 canister (Table 6.2-1). The placement of the active fuel stack beginning at a height of 1.97 inches above the bottom closure plate is consistent with the height of the shortest bottom nozzle listed in Table 6.2-1.

The fabrication tolerances for the guide tubes, neutron absorber panels, spacer plates, spacer plate openings, support rods, and support sleeves are summarized in Table 6.3-1. The factors that primarily affect the reactivity of the FuelSolutions™ canister system are radiative neutron absorption and fuel assembly separation. The parameters that affect radiative neutron absorption are the neutron absorber panel thickness and the spacer plate thickness. The parameters that affect fuel assembly separation include fuel assembly position; spacer plate opening size and location; guide tube wall thickness; guide tube inside width; and neutron absorber panel thickness. Tolerances are applied to the FuelSolutions™ W21 canister in such a manner to maximize system reactivity as follows:

- The radiative neutron absorption within the FuelSolutions™ canister is influenced by the thickness of the neutron absorber panel, the spacer plates, and the guide tube wall. The application of the material and fabrication tolerances that increase the neutron absorber, spacer plate, and guide tube wall thickness result in a decrease in the parasitic neutron absorption of the system. Increasing the thickness of the spacer plates and guide tube walls displaces water within the flux traps between guide tubes, and reduces their efficiency at thermalizing and then absorbing neutrons. For a given specified minimum neutron absorber panel boron areal density, increasing the thickness of the panel reduces its neutron absorption. If the areal density is constant, increasing the thickness reduces the boron density within the panel, which reduces the macroscopic neutron absorption cross section of the poison material. The decrease in the parasitic neutron absorption within the system results in an increase in the neutrons available for fission, which correspondingly increases system reactivity.
- As fuel assemblies are brought closer together in the FuelSolutions™ W21 canister, the neutron interaction between assemblies increases, resulting in a higher system reactivity. The fuel assembly separation in the FuelSolutions™ W21 models is decreased by shifting the fuel/guide tube assemblies within the spacer plate openings and by applying component material and fabrication tolerances. The directions of the fuel/guide tube assembly shift for the FuelSolutions™ W21 model is shown in Figure 6.3-7. As shown in Figure 6.3-7, the fuel assemblies are moved into the appropriate corner of each guide tube which is subsequently relocated within the spacer plate opening toward the center of the basket. The tolerances that further minimize separation of the fuel assemblies are then applied as follows: a) the spacer plate opening size is increased; b) the spacer plate opening locations are moved toward the center of the basket; and c) the inside width of the guide tube is increased.
- Another adjustment is made to the guide tube walls to incorporate the bounding 0.08-inch permanent deformation that occurs for the basket *g*-loads expected under a hypothetical nine-meter transportation cask drop. These assumed *g*-loads are bounding for all storage conditions and drop events. The lower face on each guide tube wall is deflected downward along the full length of the guide tube. This is a conservative representation of the permanent guide tube deformation, since the actual deformation does not occur over the full length of the guide tube (i.e., the deformation is limited to regions between basket spacer plates). The effect of the guide tube deflection in the hypothetical accident conditions model is to further decrease the center-to-center spacing of the fuel assemblies in the FuelSolutions™ W21 canister model.

The neutron shield assembly for the transportation cask (i.e., solid neutron shielding material, support ribs, and outer jacket), shown in Figure 6.3-3, is expected to experience damage during a hypothetical nine meter cask drop. For this reason, it is completely removed in the hypothetical accident conditions model.

### 6.3.1.2 Normal Operating Condition

The normal operating conditions model for the FuelSolutions™ W21 canister includes the following: complete flooding with water at a density sufficient for optimum moderation, worst case asymmetric assembly placement within the guide tubes, and application of worst case material and fabrication tolerances.

The normal operating conditions model includes an accurate representation of the FuelSolutions™ W21 basket assembly in the radial and axial directions. The canister is modeled axially from the top of the bottom end inner closure plate to a point just below the top shield plug. Reflected planes are inserted at these locations preventing axial leakage of neutrons from the canister. Figure 6.3-8 and Figure 6.3-9 show side views of the FuelSolutions™ W21 normal operating conditions model that has been sliced with vertical planes to expose the lower and upper portions of the canister.

As shown in Figure 6.3-8, the lower portion of the model begins at the top of the bottom closure plate. Next, the water gap between the bottom closure plate and the bottom spacer plate is modeled. As discussed in Section 6.3.1.1, the nominal axial locations of the guide tube bottoms and BORAL® panel bottoms are 0.1 inch and 2.0 inches above the canister cavity bottom, respectively. Due to the presence of the flow channels in the guide tube walls, the guide tube bottom is modeled at an elevation of 1.0 inch (between the bottom closure plate and the bottom spacer plate). Due to the half-inch thermal expansion gap above the top of the BORAL® panel (discussed in Section 6.3.1.1), the bottom of the BORAL® panel is conservatively modeled at an elevation of 2.5 inches above the canister bottom (in the middle of the bottom spacer plate), to account for any potential upward shift of the panel. The bottom of the active fuel is located near the top of the bottom spacer plate at an elevation of 1.97 inches above the bottom closure plate. The position of the bottom of BORAL® neutron absorber panel relative to the bottom of the fuel results in a small amount of active fuel (0.53 in.) in an unpoisoned region of the basket. The basket guide tubes are modeled axially to the top of the BORAL® neutron absorber panel as shown in Figure 6.3-9.

The active fuel stack is conservatively modeled beginning at a height of 1.97 inches and ending at a height of 151.97 inches. This represents an active fuel length of 150 inches, which is bounding for all PWR assembly types considered for storage in the FuelSolutions™ W21 canister (see Table 6.2-1). The placement of the active fuel stack beginning at a height of 1.97 inches above the bottom closure plate is consistent with the height of the shortest bottom nozzle listed in Table 6.2-1.

The nominal dimensions for the guide tubes, neutron absorber panels, spacer plates, spacer plate openings, support rods, and support sleeves can be found in Figure 6.3-1 and Figure 6.3-2 as well as in drawings provided in Section 1.5.1 of this FSAR. Material and fabrication tolerances are specifically evaluated for effects on system reactivity in case studies presented in

Section 6.4.2.1.1. Worst case material and fabrication tolerances are summarized in Table 6.3-1. The factors that primarily affect the reactivity of the FuelSolutions™ canister system are radiative neutron absorption and fuel assembly separation. The parameters that affect radiative neutron absorption are the neutron absorber panel thickness, the guide tube wall thickness, and the spacer plate thickness. The parameters that affect fuel assembly separation include: fuel assembly location; spacer plate opening size and location; and guide tube inside width. With the exception of the accident induced guide tube deformation and axial detachment, tolerances are applied in the normal conditions model consistent with the description provided in Section 6.3.1.1 for accident conditions.

## 6.3.2 Material Properties

The number densities used to model moderator materials and the FuelSolutions™ W21 canister basket, shell and reflector materials are presented in Table 6.3-2 through Table 6.3-11. These material properties are used in all FuelSolutions™ W21 canister single package and multiple package array models.

The FuelSolutions™ W21 canister basket incorporates panels of BORAL® neutron-absorbing material. BORAL® is a thermal neutron absorber (poison) material composed of boron carbide and 1100 alloy aluminum. The boron carbide, in the form of fine particles, is homogeneously dispersed throughout the central layer of the BORAL® panels. The outer layers of the panel are composed of 1100 alloy aluminum. The two materials, boron carbide and aluminum, are ideally suited for long-term use in dry storage cask radiation and thermal environments. Aluminum contact with borated pool water during short-term wet loading operations in PWR spent fuel pools is prevented by sealing the panels in stainless steel guide tube wrappers. BORAL® is manufactured by AAR Advanced Structures under the control and surveillance of a Quality Assured/Quality Control Program that conforms to the requirements of 10CFR50 Appendix B, "Quality Assurance Criteria for Nuclear Power Plants." Additional product literature for this material is provided in Section 1.5.2 of this FSAR.

The continued efficacy of BORAL® is demonstrated by the process controls under which the material is manufactured and verified. These controls assure a homogeneous dispersion of boron throughout the material. In addition, the effects of long-term exposure to neutron flux from irradiated fuel is negligible because the thermal neutron flux during dry storage is low. This fact, coupled with the use of the minimum specified boron concentration further reduced by 25%, more than accounts for any boron depletion which may occur over the 100-year design life of the FuelSolutions™ W21 canister.

The neutron shield region of the modeled transportation cask geometry contains NS-4-FR neutron shielding material, at a volume fraction of 94.2%, stainless steel 304 backing bars at a volume fraction of 2.6%, and pure copper fins at a volume fraction of 3.2%. These components are mixed into a homogenous material that fills the neutron shield region in the criticality analyses. Table 6.3-11 gives the material description for pure NS-4-FR neutron shield material. The densities shown in the table are multiplied by 0.942 to yield the densities present in the homogenous mixture. The stainless steel 304 atom densities shown in Table 6.3-5 are multiplied

by 0.026 and added to the mixture. Finally, the atom density of pure copper (0.08493 atoms/barn-cm) is multiplied by 0.032 and added to the mixture.

## Table 6.3-1 - Worst Case Material and Fabrication Tolerances for the FuelSolutions™ W21 Canister

| Parameter | Tolerance (cm) |
|---|---|
| BORAL® Thickness | + 0.0127 |
| BORAL® Width | - 0.127 |
| Type A Spacer Plate Thickness | + 0.3175 (W21M Design),<br>+ 0.0762 (W21T Design) |
| Type B Spacer Plate Thickness | + 0.0762 |
| Spacer Plate Opening Width | + 0.0381 |
| Spacer Plate Opening Location(1) | - 0.0381 |
| Guide Tube Thickness | + 0.01778 |
| Guide Tube Inner Dimension | + 0.127 |
| Guide Tube Outer Wrapper Dimension | + 0.0051 |

Note:

(1) See Figure 6.3-7 for a diagram showing orientation for location tolerances.

## Table 6.3-2 - $UO_2$ Number Densities as a Function of Enrichment

| Enrichment (w/o) | Number Density (atoms/b-cm) | | | | $UO_2$ Material Density (atoms/b-cm) |
|---|---|---|---|---|---|
| | $UO_2$ | $^{235}U$ | $^{238}U$ | O | |
| 4.0 | 0.0235956 | 0.0009554 | 0.0226402 | 0.0471912 | 0.0707867 |
| 4.1 | 0.0235958 | 0.0009793 | 0.0226166 | 0.0471917 | 0.0707875 |
| 4.2 | 0.0235961 | 0.0010032 | 0.0225929 | 0.0471922 | 0.0707883 |
| 4.3 | 0.0235964 | 0.0010271 | 0.0225693 | 0.0471928 | 0.0707891 |
| 4.4 | 0.0235966 | 0.0010509 | 0.0225457 | 0.0471933 | 0.0707899 |
| 4.5 | 0.0235969 | 0.0010748 | 0.0225221 | 0.0471938 | 0.0707907 |
| 4.6 | 0.0235972 | 0.0010987 | 0.0224985 | 0.0471943 | 0.0707915 |
| 4.7 | 0.0235974 | 0.0011226 | 0.0224748 | 0.0471949 | 0.0707923 |
| 4.8 | 0.0235977 | 0.0011465 | 0.0224512 | 0.0471954 | 0.0707931 |
| 4.9 | 0.023598 | 0.0011704 | 0.0224276 | 0.0471959 | 0.0707939 |
| 5.0 | 0.0235982 | 0.0011942 | 0.022404 | 0.0471965 | 0.0707947 |

## Table 6.3-3 - Water Number Densities as a Function of Density

| $H_2O$ Density ($g/cm^3$) | $H_2O$ Molecular Weight (g/mole) | H Number Density (atoms/b-cm) | O Number Density (atoms/b-cm) | $H_2O$ Material Density (atoms/b-cm) |
|---|---|---|---|---|
| 1.0 | 18.01528 | 0.066863 | 0.033432 | 0.1002949 |
| 0.9 | 18.01528 | 0.060177 | 0.030088 | 0.0902654 |
| 0.8 | 18.01528 | 0.053491 | 0.026745 | 0.0802359 |
| 0.7 | 18.01528 | 0.046804 | 0.023402 | 0.0702064 |
| 0.6 | 18.01528 | 0.040118 | 0.020059 | 0.0601769 |
| 0.5 | 18.01528 | 0.033432 | 0.016716 | 0.0501474 |
| 0.4 | 18.01528 | 0.026745 | 0.013373 | 0.0401179 |
| 0.3 | 18.01528 | 0.020059 | 0.010029 | 0.0300885 |
| 0.2 | 18.01528 | 0.013373 | 0.006686 | 0.020059 |
| 0.1 | 18.01528 | 0.006686 | 0.003343 | 0.0100295 |
| 0.08 | 18.01528 | 0.005349 | 0.002675 | 0.0080236 |
| 0.06 | 18.01528 | 0.004012 | 0.002006 | 0.0060177 |
| 0.04 | 18.01528 | 0.002675 | 0.001337 | 0.0040118 |
| 0.02 | 18.01528 | 0.001337 | 0.000669 | 0.0020059 |

## Table 6.3-4 - Zircaloy-4 Number Densities

| Element | Zirc-4 Density ($g/cm^3$) | Element Molecular Weight (g/mole) | Weight Percent (w/o) | Number Density (atoms/b-cm) |
|---|---|---|---|---|
| Sn | 6.56 | 118.71 | 1.45 | 0.000483 |
| Fe | 6.56 | 55.847 | 0.21 | 0.000149 |
| Cr | 6.56 | 51.9961 | 0.10 | $7.6 \times 10^{-05}$ |
| Zr | 6.56 | 91.224 | 98.0975 | 0.042487 |
| 0 | 6.56 | 15.9994 | 0.12 | 0.000296 |
| C | 6.56 | 12.011 | 0.014 | $4.61 \times 10^{-05}$ |
| Si | 6.56 | 28.0855 | 0.0085 | $1.2 \times 10^{-05}$ |
| Zirc-4 Material Density (atoms/b-cm) | | | | 0.043548 |

## Table 6.3-5 - 304 Stainless Steel Number Densities

| Element | SS-304 Density ($g/cm^3$) | Element Molecular Weight (g/mole) | Weight Percent (w/o) | Number Density (atoms/b-cm) |
|---|---|---|---|---|
| Fe | 8.027 | 55.847 | 69.75 | 0.06038 |
| Mn | 8.027 | 54.93805 | 2.0 | 0.00176 |
| Cr | 8.027 | 51.9961 | 19.0 | 0.017666 |
| Ni | 8.027 | 58.69 | 9.25 | 0.00762 |
| SS-304 Material Density (atoms/b-cm) | | | | 0.087426 |

## Table 6.3-6 - BORAL® Number Densities

| $^{10}B$ Loading (g/cm2) | Thickness (cm) | | Number Density (atoms/b-cm) | | | | |
|---|---|---|---|---|---|---|---|
| | BORAL® Core | BORAL® Total | $^{10}B$ Actual/ 75% Credit | $^{11}B$ Actual/ 75% Credit | C | Al | BORAL® |
| 0.02 | 0.127 | 0.1905 | 0.0094724<br>**0.0071043** | 0.0381276<br>**0.0285957** | 0.0119000 | 0.0568629 | 0.1044630 |
| 0.025 | 0.1524 | 0.2159 | 0.0098671<br>**0.0074003** | 0.0397163<br>**0.0297872** | 0.0123958 | 0.0592322 | 0.1088156 |
| 0.03 | 0.19304 | 0.25654 | 0.0093478<br>**0.0070108** | 0.037626<br>**0.0282195** | 0.0117434 | 0.0561147 | 0.1030884 |

## Table 6.3-7 - 316 Stainless Steel Number Densities

| Element | SS-316 Density ($g/cm^3$) | Element Molecular Weight (g/mole) | Weight Percent (w/o) | Number Density (atoms/b-cm) |
|---|---|---|---|---|
| Fe | 8.027 | 55.847 | 65.75 | 0.056918 |
| Mn | 8.027 | 54.93805 | 2.0 | 0.00176 |
| Si | 8.027 | 28.0855 | 0.75 | 0.001291 |
| Cr | 8.027 | 51.9961 | 17.0 | 0.015806 |
| Ni | 8.027 | 58.69 | 12.0 | 0.009885 |
| Mo | 8.027 | 95.94 | 2.5 | 0.00126 |
| SS-316 Material Density (atoms/b-cm) | | | | 0.086920 |

## Table 6.3-8 - 517 Gr. P Carbon Steel Number Densities

| Element | Carbon Steel Density ($g/cm^3$) | Element Weight Percent (w/o) | Element Molecular Weight (g/mole) | Element Number Density (atoms/b-cm) |
|---|---|---|---|---|
| Fe | 7.86 | 96.51 | 55.847 | 0.0818076 |
| Mn | 7.86 | 0.59 | 54.93805 | 0.0005084 |
| Cr | 7.86 | 1.025 | 51.9961 | 0.0009332 |
| Mo | 7.86 | 0.525 | 95.94 | 0.0002590 |
| Ni | 7.86 | 1.35 | 58.69 | 0.0010889 |
| A-517 Material Density (atoms/b-cm) | | | | 0.0845971 |

## Table 6.3-9 - XM-19 Stainless Steel Number Densities

| Element | XM-19 Density ($g/cm^3$) | Element Weight Percent (w/o) | Element Molecular Weight (g/mole) | Element Number Density (atoms/b-cm) |
|---|---|---|---|---|
| Fe | 8.027 | 57.5 | 55.847 | 0.049776 |
| Mn | 8.027 | 5.0 | 54.93805 | 0.004400 |
| Si | 8.027 | 0.75 | 28.0855 | 0.001291 |
| Cr | 8.027 | 22.0 | 51.9961 | 0.020455 |
| Ni | 8.027 | 12.5 | 58.69 | 0.010297 |
| Mo | 8.027 | 2.25 | 95.94 | 0.001134 |
| XM-19 Material Density (atoms/b-cm) | | | | 0.087353 |

## Table 6.3-10 - Depleted Uranium Number Densities

| Isotope | Depleted Uranium Density ($g/cm^3$) | Isotope Weight Percent (w/o) | Isotope Molecular Weight (g/mole) | Isotope Number Density (atoms/b-cm) |
|---|---|---|---|---|
| $^{235}U$ | 18.9 | 0.22 | 235.043924 | 0.000106545 |
| $^{238}U$ | 18.9 | 99.78 | 238.050785 | 0.047712715 |
| Depleted Uranium Material Density (atoms/b-cm) | | | | 0.04781926 |

## Table 6.3-11 - Solid Neutron Shielding Number Densities

| Element or Isotope | Density ($g/cm^3$) | Element or Isotope Weight Percent (w/o) | Element or Isotope Molecular Weight (g/mole) | Element or Isotope Number Densities (atoms/b-cm) |
|---|---|---|---|---|
| Al | 1.62 | 21.07 | 26.982 | 0.007619 |
| C | 1.62 | 27.58 | 12.011 | 0.022407 |
| H | 1.62 | 5.88 | 1.008 | 0.056919 |
| O | 1.62 | 41.94 | 15.999 | 0.025576 |
| N | 1.62 | 1.96 | 14.007 | 0.001365 |
| $^{10}B$ | 1.62 | 0.29 | 10.013 | 0.000211(1) |
| $^{11}B$ | 1.62 | 1.28 | 11.009 | 0.000849(1) |
| NS-4 Material Density (atoms/b-cm) | | | | 0.114947 |

Note:

(1) Boron atom densities are reduced by 25%.

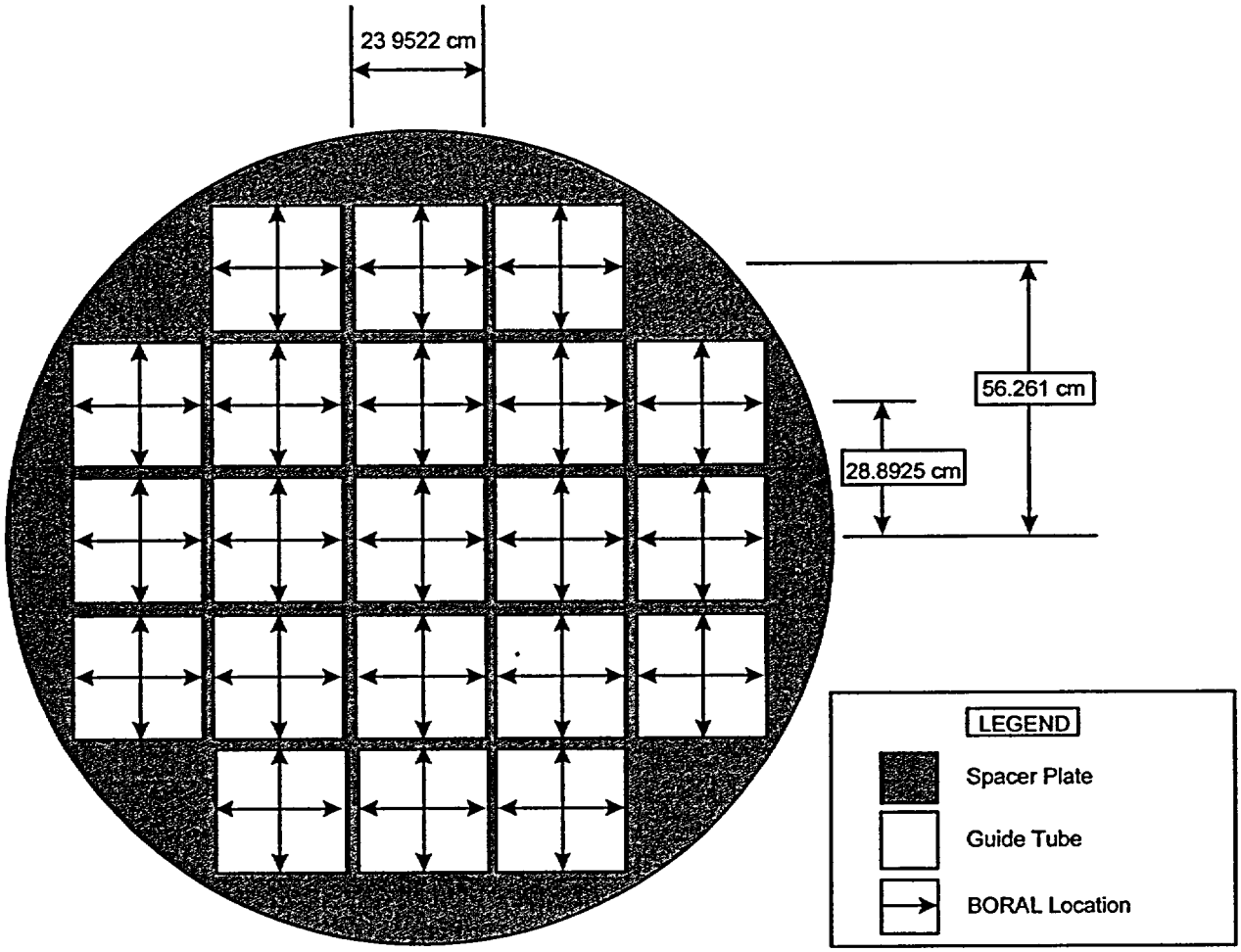


**Figure 6.3-1 - FuelSolutions™ W21 Basket (Nominal Dimensions)**

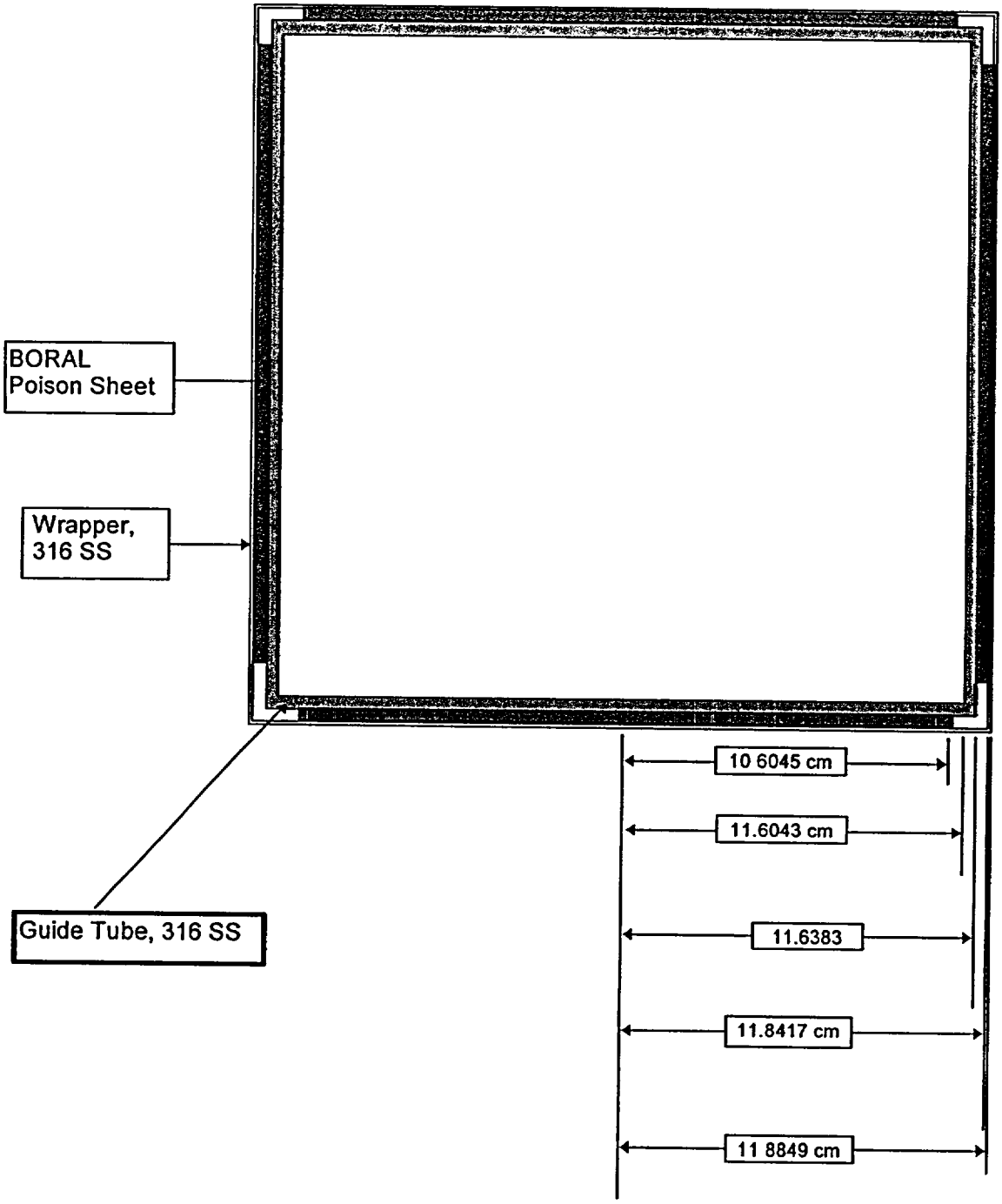


**Figure 6.3-2 - FuelSolutions™ W21 Guide Tube Assembly (Nominal Dimensions)**

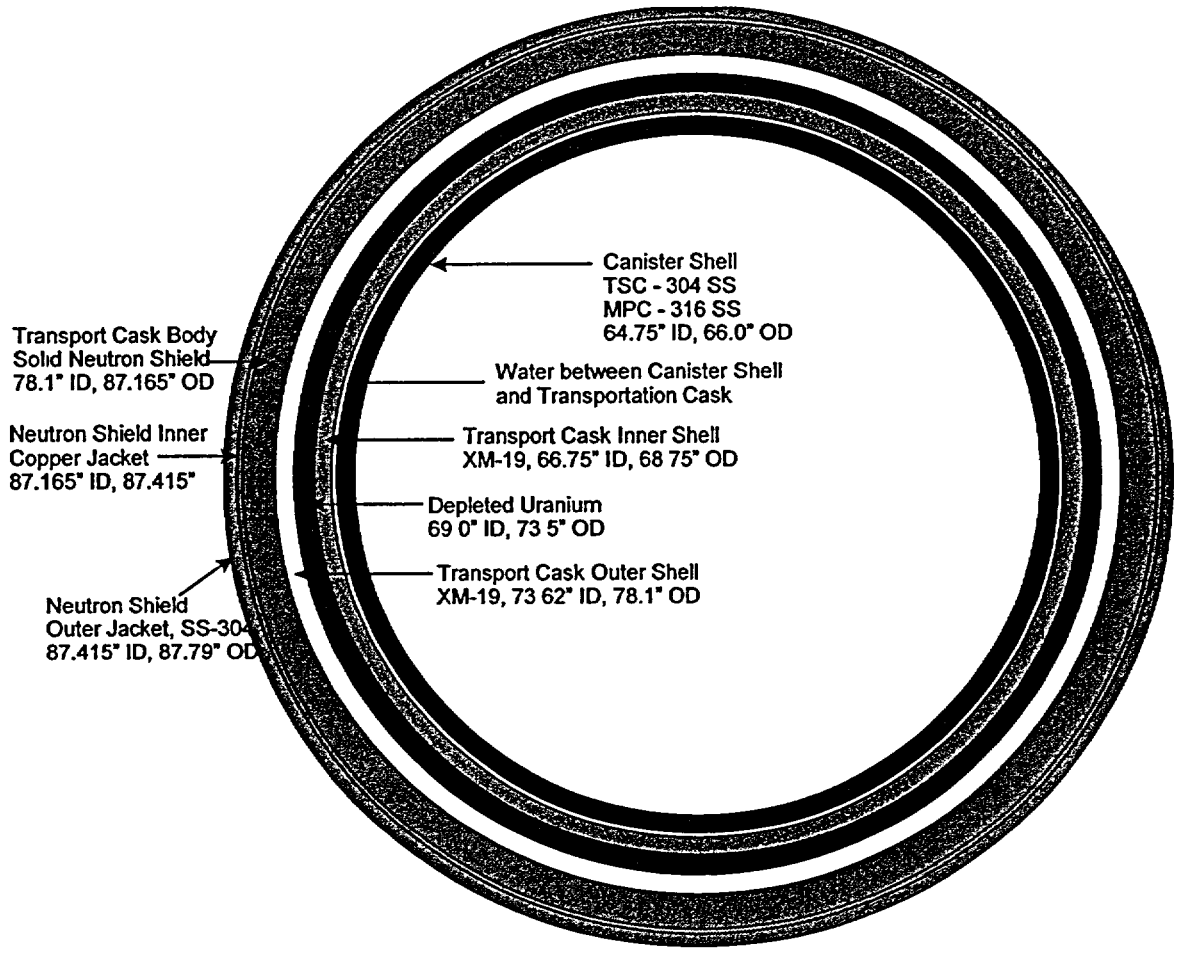


(Not To Scale)

**Figure 6.3-3 - FuelSolutions™ W21 Shell Assembly and Transport Cask**

(For Clarity, Basket Not Shown)

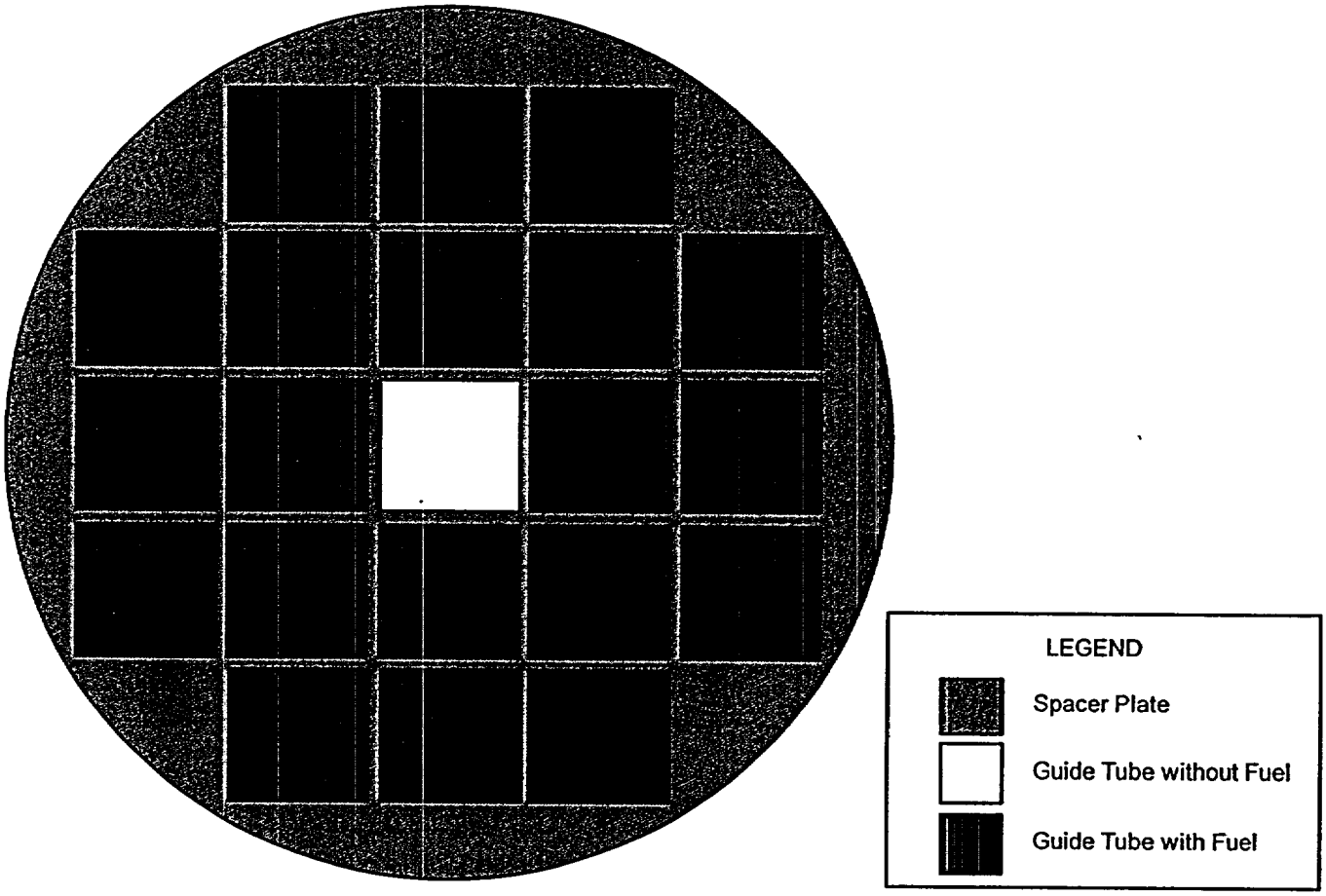


**Figure 6.3-4 - Configuration for Canister Loading Specification W21-2**

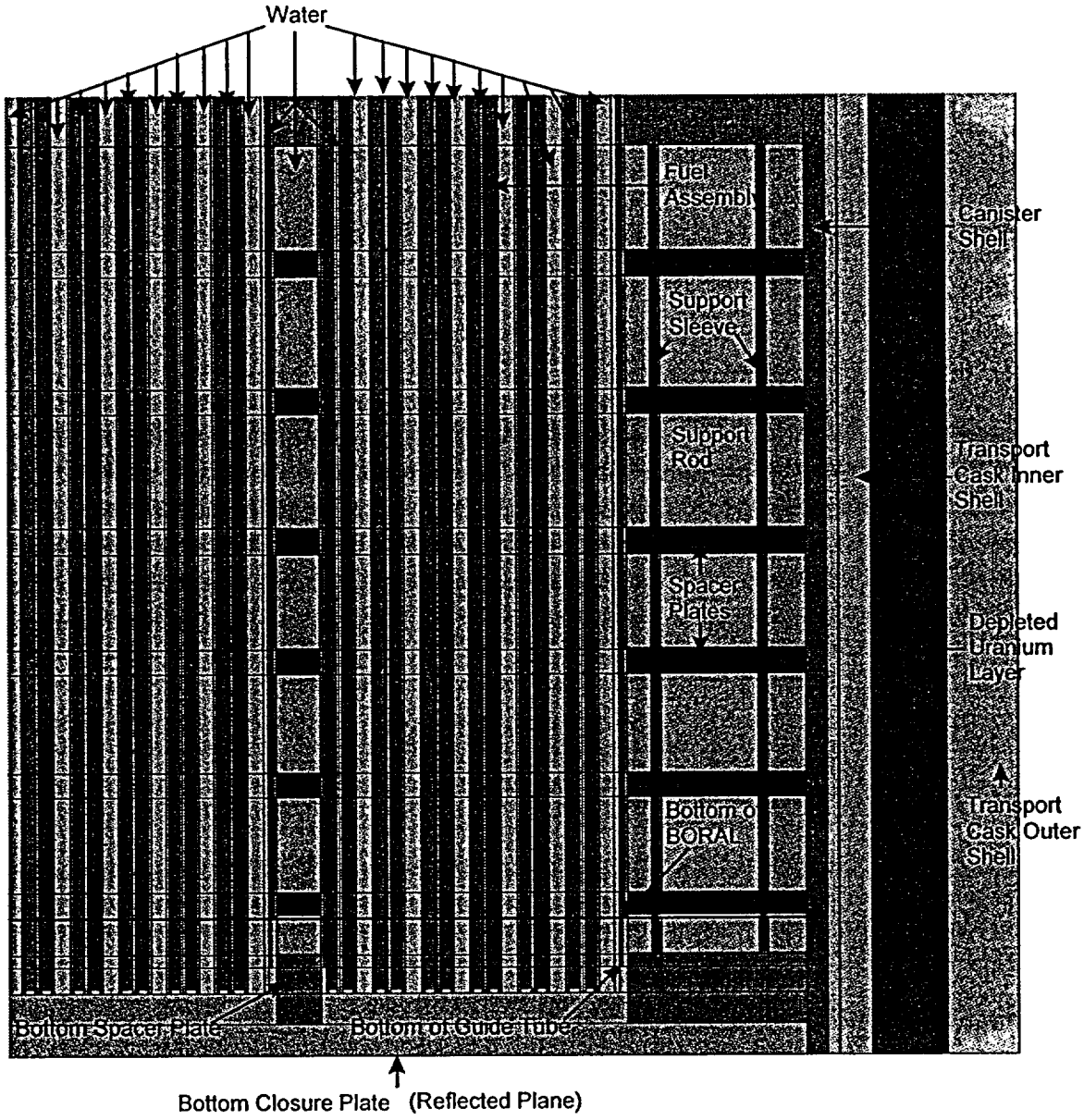


**Figure 6.3-5 - Side View of Lower Portion of the W21 Canister Hypothetical Accident Conditions Model (cut-away)**

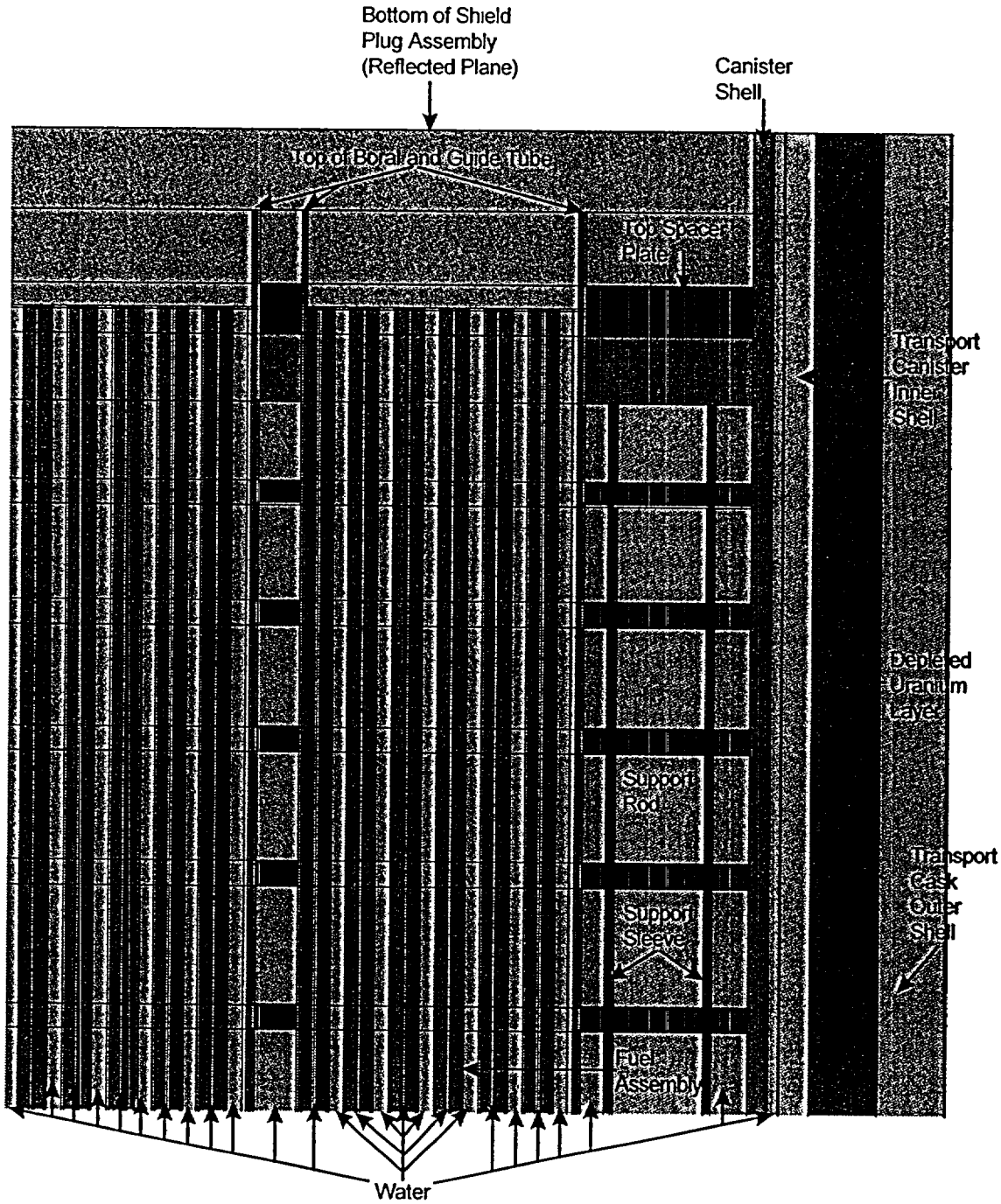


**Figure 6.3-6 - Side View of Upper Portion of the W21 Canister Hypothetical Accident Conditions Model (cut-away)**

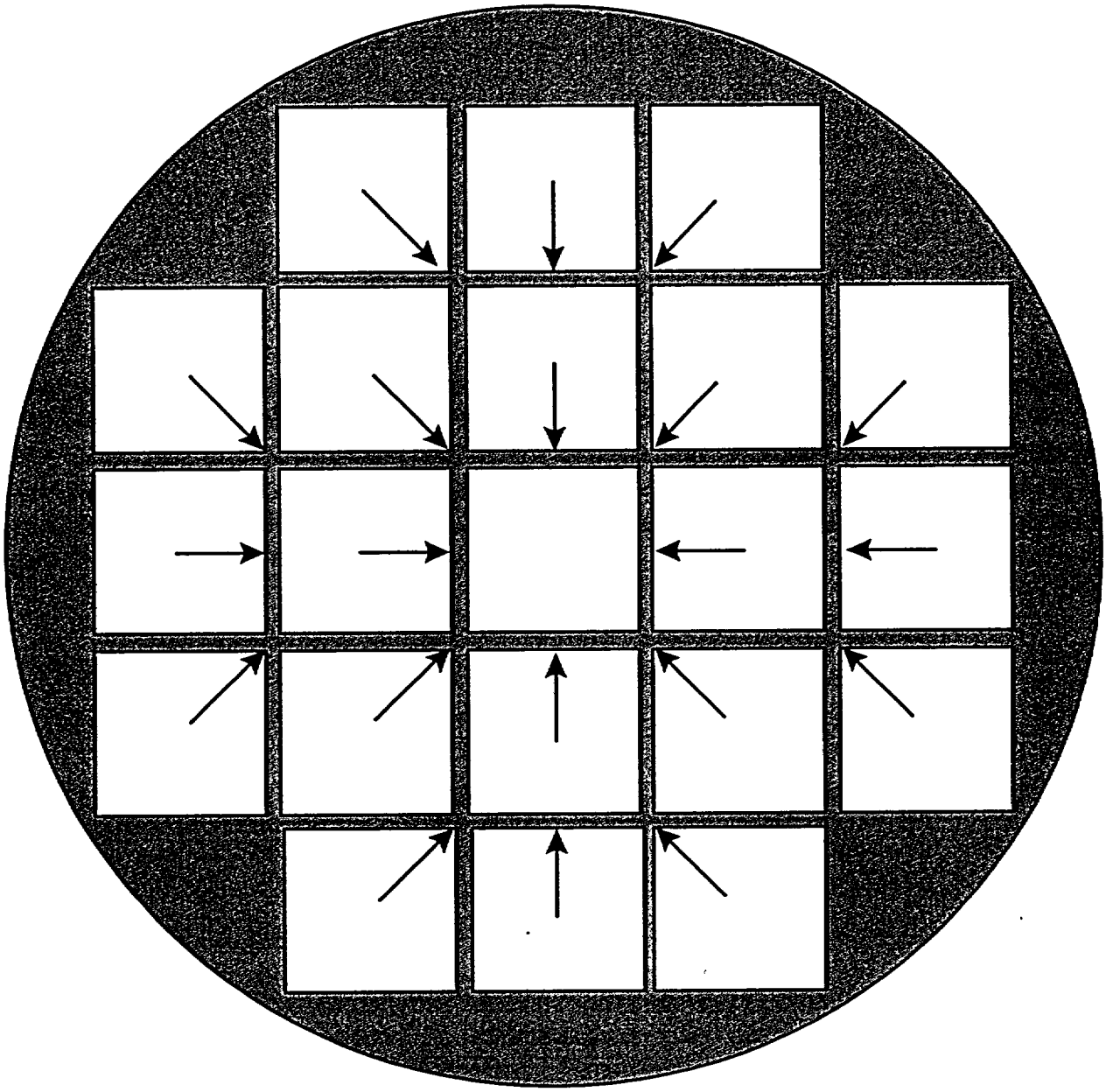

**Figure 6.3-7 - Asymmetric Fuel Assembly Shift for the W21 Canister**

Note: The arrows indicate the direction of application for the spacer plate opening location tolerance.

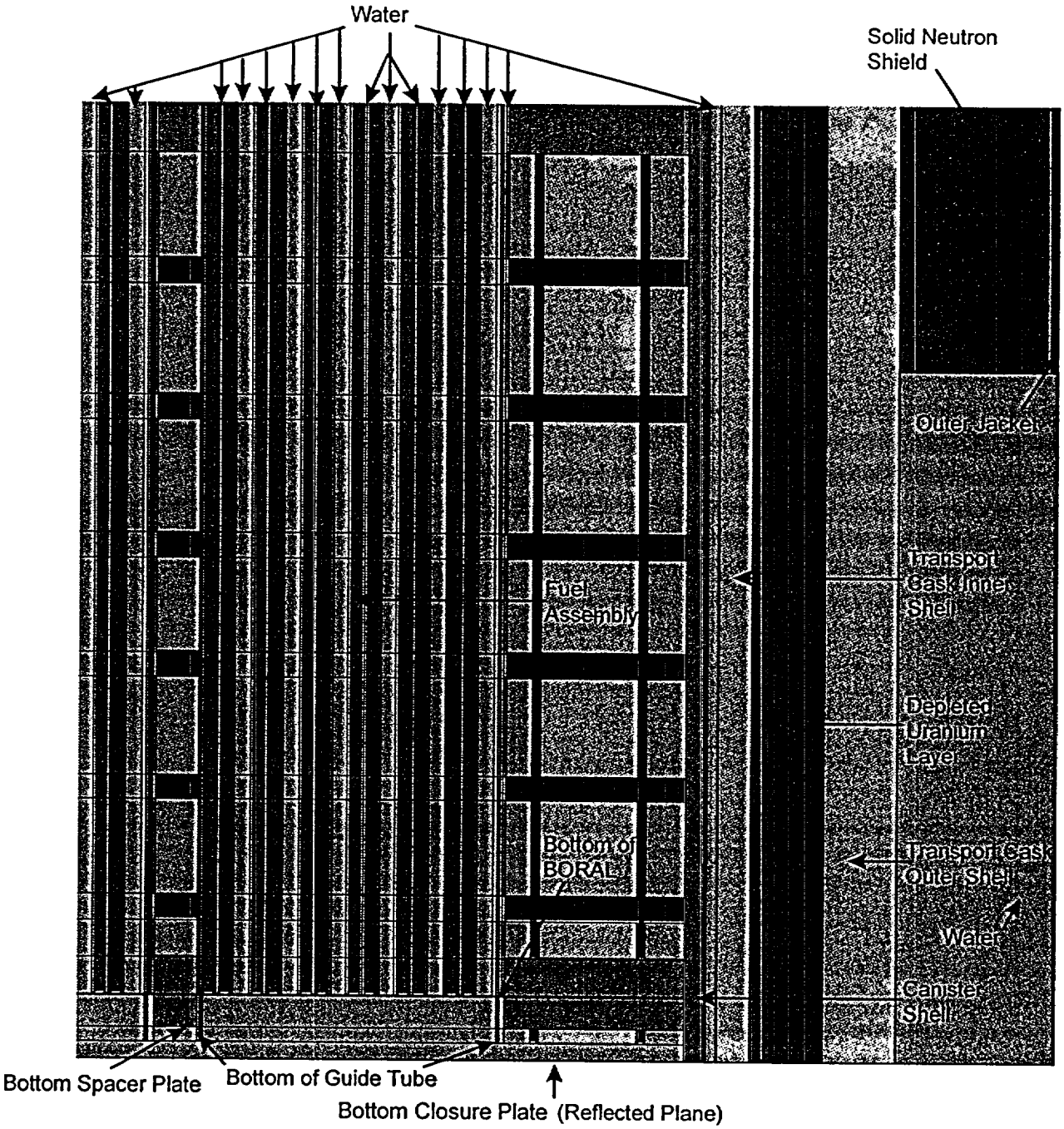


**Figure 6.3-8 - Side View of Lower Portion of the W21 Normal Conditions Model (cut-away)**

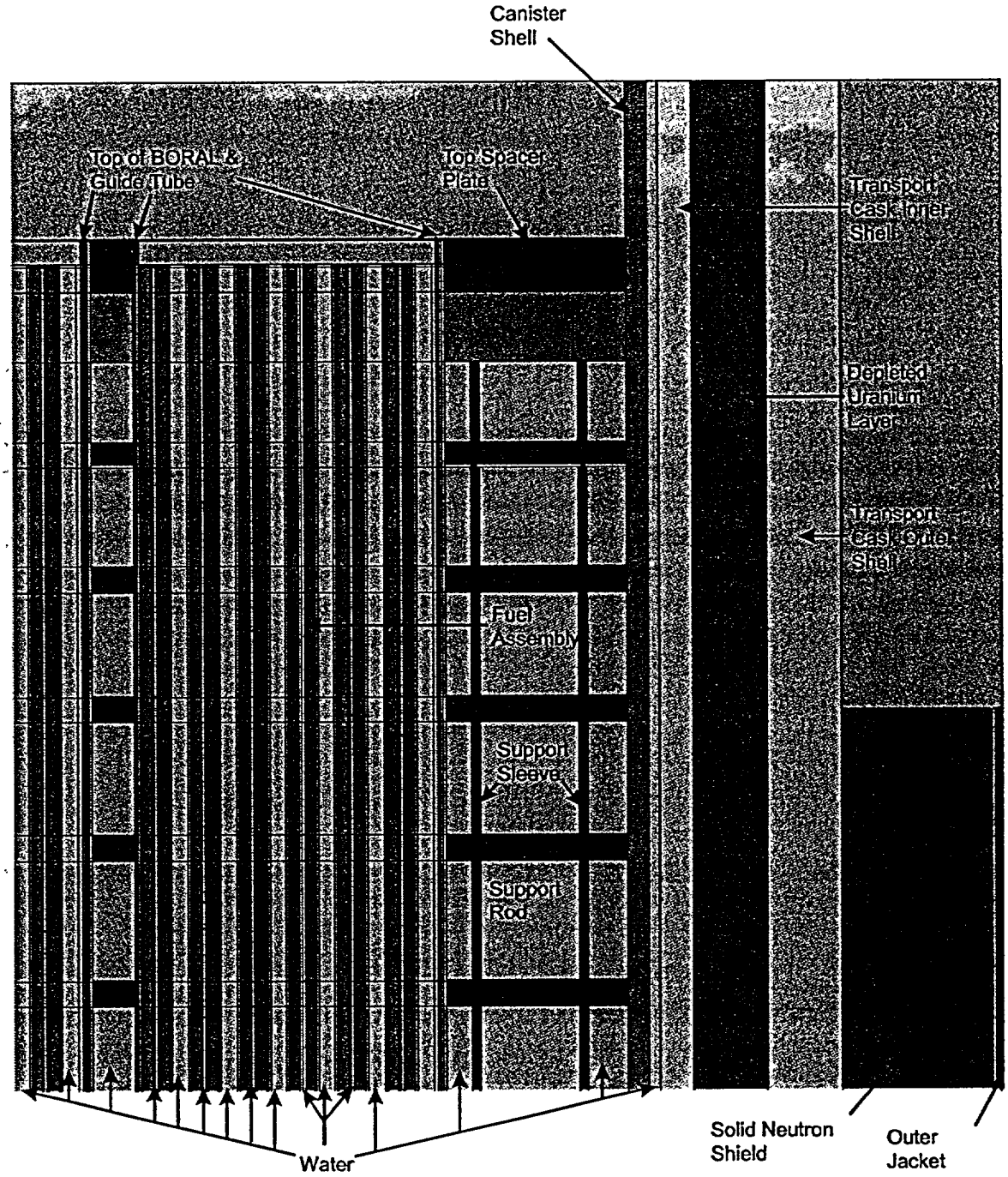


**Figure 6.3-9 - Side View of Upper Portion of the W21 Normal Conditions Model (cut-away)**

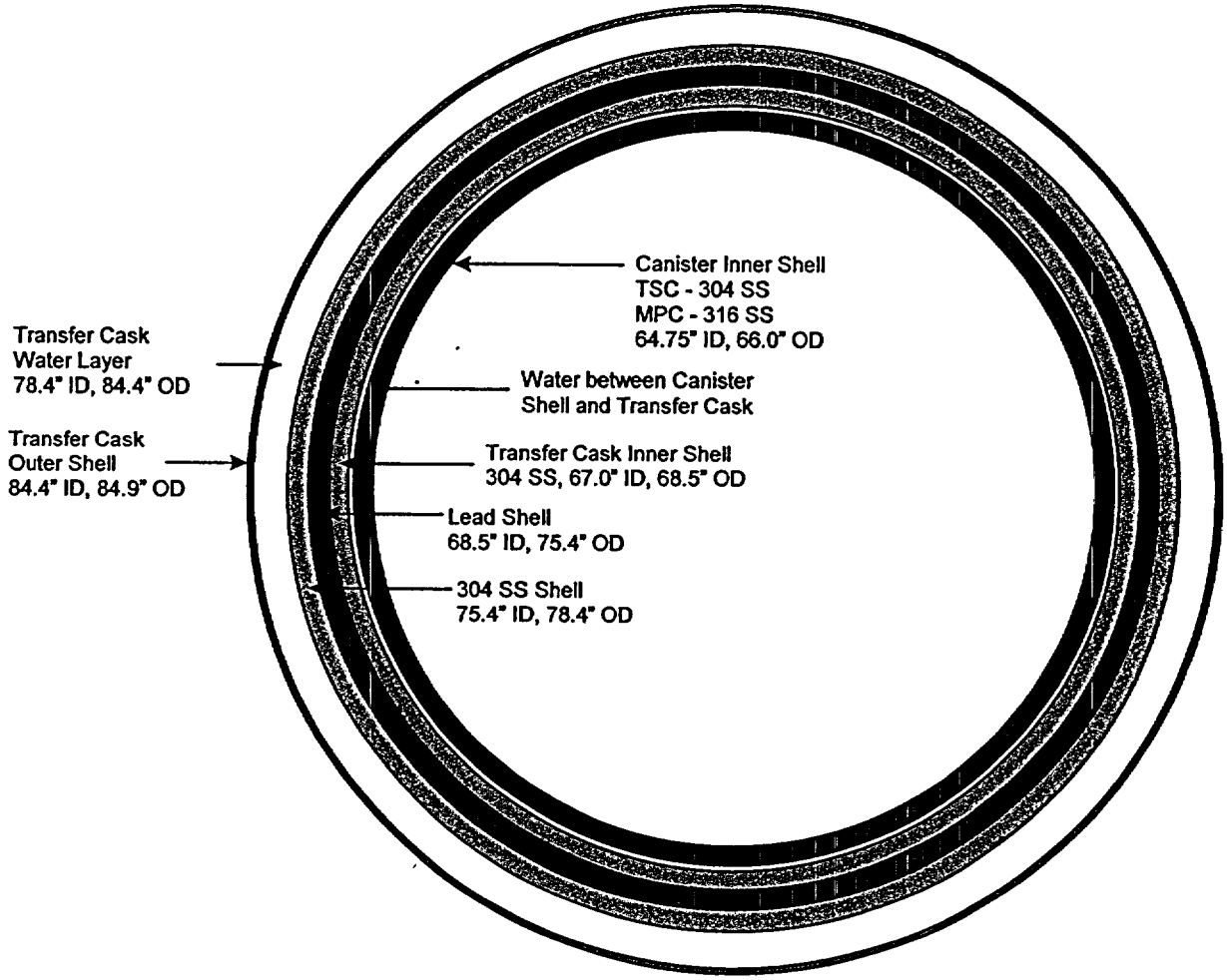


(Not To Scale)

**Figure 6.3-10 - FuelSolutions™W21 Shell Assembly and Transfer Cask**

(For Clarity, Basket Not Shown)

#### 11.1.1.4 Corrective Actions

The FuelSolutions™ W21 canister is conservatively designed to safely accommodate steady-state extreme off-normal ambient conditions. Therefore, no corrective actions are required.

### 11.1.2 Off-Normal Internal Pressure

As discussed in Section 2.3.2.2 and summarized in Table 2.0-1 of this FSAR, the design basis off-normal condition internal pressure for the FuelSolutions™ W21 canister is 16 psig. The maximum internal pressure for this condition, as calculated in Section 4.5 of this FSAR, is based on the required helium backfill in accordance with the *technical specification* provided in Section 12.3, elevated to the extreme off-normal condition canister cavity gas temperature. In addition, a concurrent non-mechanistic failure of 10% of the fuel rods with complete release of their fill gas and 30% of their fission gasses into the canister cavity elevated to the extreme off-normal condition canister cavity gas temperature is assumed. The resulting calculated internal pressure is bounded by the design basis internal pressure, as shown in Table 4.1-5.

#### 11.1.2.1 Postulated Cause of the Event

After fuel assembly loading, the canister is drained, dried, and backfilled with an inert cover gas (helium) to assure long-term cladding integrity during dry storage. Therefore, the probability of failure of intact rods in dry storage is low. Nonetheless, such an event is postulated and evaluated.

#### 11.1.2.2 Detection of the Event

No monitoring of the canister internal pressure is required since the canister design is adequate to withstand the design basis off-normal internal pressure

#### 11.1.2.3 Summary of Event Consequences and Regulatory Compliance

*Structural*

The structural evaluation of the canister for off-normal internal pressure conditions is described in Section 3.6 of this FSAR. The resulting stresses for this loading condition are provided in Table 3.6-1. As discussed in Section 3.6.2, all stresses are within the allowable values.

*Thermal*

The canister internal pressure for off-normal conditions is performed using the methodology, material properties, thermal models, and design basis heat loads described in Section 4.5 of this FSAR. The temperatures resulting from the off-normal thermal analysis are used to determine the corresponding internal pressure provided in Tables 4.5-2, 4.5-3, and 4.5-5. As can be seen from these tables, the 16 psig design basis internal pressure used in the structural evaluation described above bounds these calculated values.

*Shielding*

There is no effect on the shielding performance of the canister as a result of this off-normal event.

*Criticality*

There is no effect on the criticality control features of the canister as a result of this off-normal event.

*Confinement*

As discussed in the structural evaluation above, all stresses remain within allowable values, assuring canister integrity. The effects of this event on the release for the design basis canister leak rate is evaluated in Section 7.2 of this FSAR.

*Radiation Protection*

The postulated release will result in an increase in dose to the public. The analysis of this event is provided in Section 7.2 of this FSAR, and the resulting occupational exposures and off-site doses are addressed in Sections 10.3 and 10.4 of this FSAR, respectively.

#### 11.1.2.4 Corrective Actions

The FuelSolutions™ W21 canister is conservatively designed to safely accommodate the internal pressure resulting from this off-normal condition. Therefore, no corrective actions are required.

### 11.1.3 Cask Misalignment During Horizontal Canister Transfer

The FuelSolutions™ storage system is evaluated for a maximum hydraulic ram load of 70 kips pushing or 50 kips pulling resulting from cask misalignment or interference during horizontal canister transfer, as defined in Section 2.3.2.3 of this FSAR. The ram load is applied on the top or bottom end of the canister shell assembly. However, the limiting case is the pulling condition because the outer closure plate is required to carry the entire transfer load. For the pushing case, the shield plug and inner closure plate also assist in carrying the load, resulting in significantly less strain in the outer closure plate and therefore lower stresses. The structural consequences of this event are evaluated for all horizontal canister transfer scenarios.

#### 11.1.3.1 Postulated Cause of the Event

As described in Section 1.2.2.3 of the FuelSolutions™ Storage System FSAR, a hydraulic ram is used during horizontal transfer of the canister to the casks. The ram slides the canister from cask to cask by pushing or pulling it between the storage cask and the transfer cask; the transfer cask and the transportation cask; or the storage cask and the transportation cask. Under normal conditions, the hydraulic ram loads are equal to the force required to overcome friction forces between the canister shell and the cask guide rails. Prior to performing horizontal canister transfer operations, the casks are docked, closely aligned, and secured together to prevent shifting or separation. In addition, beveled lead-ins are provided on the ends of the canister shell, cask openings, and the cask guide rails to minimize the possibility of interference during horizontal transfer. However, it is postulated that in the unlikely event that the storage cask and the transfer cask; the transfer cask and the transportation cask; or the storage cask and the transportation cask are not properly aligned during transfer, the hydraulic ram load could exceed the normal design loads.

### 11.1.3.2 Detection of the Event

During horizontal transfer operations, the hydraulic ram pressure (load) is monitored. In addition, the hydraulic ram loads are limited by the hydraulic system using automatic shut-off switches so that normal condition ram loads are not exceeded. If the hydraulic system shuts down, indicating the possibility of a misalignment or interference, the operator may use override controls to increase the hydraulic ram loads up to the maximum design load of 70 kips pushing or 50 kips pulling after rechecking the cask for proper alignment. The override controls do not allow hydraulic ram loads to be increased above the maximum design load.

### 11.1.3.3 Summary of Event Consequences and Regulatory Compliance

*Structural*

The stress evaluation for increased ram force postulated to occur due to misalignment of the canister is discussed in Section 3.6.3 of this FSAR. The resulting stresses for this condition are provided in Table 3.6-1. All stresses are within the allowable values.

*Thermal*

There is no effect on the thermal performance of the canister as a result of this off-normal event.

*Shielding*

There is no effect on the shielding performance of the canister as a result of this off-normal event.

*Criticality*

There is no effect on the criticality performance of the canister as a result of this off-normal event.

*Confinement*

There is no effect on the confinement performance of the canister as a result of this off-normal event.

*Radiation Protection*

As there is no degradation in shielding or confinement capabilities, there is no effect on public exposures as a result of this off-normal event.

Recovery from this event, as discussed in Section 11.1.3.4, results in slight increases in occupational exposure due to the additional recovery operations. The estimated occupational exposure for recovery operations is discussed in Section 11.1.2.3.1 of the FuelSolutions™ Storage System FSAR.

### 11.1.3.4 Corrective Actions

The corrective action for a canister misalignment or interference is discussed in Section 11.1.2.4 of the FuelSolutions™ Storage System FSAR.

## 11.1.4 Hydraulic Ram Failure During Horizontal Canister Transfer

The FuelSolutions™ storage system is evaluated for the effects of failure of the hydraulic ram during horizontal canister transfer operations, as defined in Section 2.3.2.5 of this FSAR.

### 11.1.4.1 Postulated Cause of the Event

The postulated cause of this event is discussed in Section 11.1.3.1 of the FuelSolutions™ Storage System FSAR.

### 11.1.4.2 Detection of the Event

The detection of this event is discussed in Section 11.1.3.2 of the FuelSolutions™ Storage System FSAR.

### 11.1.4.3 Summary of Event Consequences and Regulatory Compliance

*Structural*

There are no structural consequences as a result of this postulated event.

*Thermal*

In Section 4.5.2 of this FSAR, a thermal analysis of the canisters is performed for the transfer cask in the horizontal position for off-normal conditions. This analysis, as described in Section 4.5.2, shows that under steady-state conditions, no canister components exceed the allowable temperatures in the transfer cask.

For the storage cask, the cask liner thermocouple temperature is monitored in accordance with the *technical specification* in Section 12.3 of this FSAR, and corrective actions completed as necessary. The canister temperatures while in the horizontal storage cask is discussed in Section 4.5.1 and reported in Table 4.5-1 of this FSAR.

*Shielding*

There are no effects on the shielding performance of the canisters as a result of this off-normal event.

*Criticality*

The are no effects on the criticality performance of the canisters as a result of this off-normal event.

*Confinement*

There are no effects on the confinement function of the canisters as a result of this off-normal event.

*Radiation Protection*

As there is no degradation in shielding or confinement, there is no effect on public exposures as a result of this off-normal event. Effects of recovery from this event are discussed in Section 11.1.3.3 of the FuelSolutions™ Storage System FSAR.

#### 11.1.4.4 Corrective Action

The corrective action for this event is discussed in Section 11.1.3.4 of the FuelSolutions™ Storage System FSAR.

### 11.1.5 Canister Reopening/Reflood

The FuelSolutions™ W21 canister is evaluated for the effects of reflooding the canister after the canister cavity is drained and dried. This could occur prior to or after dry storage. The limiting internal pressure for this condition is 100 psig as defined in Section 2.3.2.4 of this FSAR. The evaluation provided in this section demonstrates that the FuelSolutions™ W21 canister can accommodate the reflood condition without compromising the integrity of the canister.

#### 11.1.5.1 Postulated Cause of the Event

Under normal conditions, reopening and/or reflooding of the FuelSolutions™ W21 canister is not anticipated to occur. However, it may be required to reflood the canister to remove the fuel for an undetermined reason, possibly for transfer of title of the SNF to DOE. Therefore, the event is postulated and evaluated.

#### 11.1.5.2 Detection of the Event

Reflooding of the canister is a planned activity.

#### 11.1.5.3 Analysis of Effects and Consequences

*Structural*

The stress evaluation of the canister for internal pressure resulting from the reflood is provided in Section 3.6.4 of this FSAR. All stresses are within the allowable values. The resulting canister pressure stresses are summarized in Table 3.6-1 of this FSAR. The fuel cladding thermal stress effects due to reflood are discussed in Section 4.4.2.3 of this FSAR and shown to remain within allowable values.

*Thermal*

The thermal evaluation of the canister during reflood conditions is provided in Section 4.4.2.3 of this FSAR. All material temperatures remain within the off-normal allowable temperatures for this condition, as defined in Table 4.3-1.

*Shielding*

There is no effect on the shielding performance of the canister as a result of this activity.

*Criticality*

There is no effect on the criticality performance of the canister as a result of this activity. As described in Chapter 6 of this FSAR, the canister is evaluated for a full range of pure water moderator densities, and for the most reactive moderator density. No soluble boron credit is taken in the criticality analysis. Therefore, the criticality evaluation bounds the conditions expected during reflood.

*Confinement*

Since this operation is predicated upon opening the canister, there is no confinement function provided by the canister during this activity.

*Radiation Protection*

As there is no degradation in shielding or confinement capabilities, there is no effect on public exposures as a result of this off-normal operation. Performing this operation results in occupational exposure which is estimated to be equivalent to the occupational exposure incurred for canister draining, drying, and closure operations. Sampling of the canister internal atmosphere prior to reflood is performed, as discussed in Section 8.2.3.2 of the FuelSolutions™ Storage System FSAR, to preclude unanticipated release of radionuclides. The occupational exposures for these operations is discussed in Section 10.3 of the FuelSolutions™ Storage System FSAR.

#### 11.1.5.4 Corrective Action

There is no corrective action for this off-normal operation.

### 11.1.6 Off-Normal Load Combinations

Load combinations for off-normal conditions are performed for the FuelSolutions™ W21 canister in accordance with Section 2.3.5 of this FSAR. The load combinations include normal loads, which are evaluated in Section 3.5, and off-normal loads, which are evaluated in Section 3.6. The load combination results for the canister are reported in Table 3.6-2. As shown in the table, all stresses are within allowable values.

in Section 3.7.7, the effects of this loading are bounded by the accident internal pressure effects evaluated in Section 11.2.8.

*Thermal*

Under postulated flood conditions, the storage cask vents and annular space are filled with water. While this precludes the natural convective air flow relied upon for heat removal during normal storage conditions, the water provides superior heat transfer, and the large thermal mass of the flood water results in lower temperatures than those associated with normal storage conditions as discussed in Section 4.6.1 of the FuelSolutions™ Storage System FSAR. For the case of only the inlet vents blocked, either by flood waters or by debris left as a result of flooding, this condition is bounded by the blocked vent case discussed in Section 11.2.1.

*Shielding*

There is no reduction in shielding performance as a result of this postulated accident.

*Criticality*

There is no reduction in criticality control performance of the canister as a result of this postulated accident. Since the canister shell assembly remains intact, there is no water inside the canister as a result of this event. The presence of water outside the canister and cask is bounded by the reflector conditions assumed in the criticality analysis as discussed in Chapter 6.

*Confinement*

There is no reduction in confinement capability of the canister as a result of this postulated accident.

*Radiation Protection*

Since there is no effect on shielding and confinement performance of the canister, there is no effect on radiation protection.

#### 11.2.6.4 Corrective Action

The corrective action for this event is discussed in Section 11.2.7.4 of the FuelSolutions™ Storage System FSAR.

### 11.2.7 Earthquake

The FuelSolutions™ W21 canister is evaluated for the effects of seismic loads during dry storage in the storage cask and during on-site transport in the transfer cask.

#### 11.2.7.1 Postulated Cause of the Event

The postulated cause of this event is discussed in Section 11.2.9.1 of the FuelSolutions™ Storage System FSAR.

#### 11.2.7.2 Detection of the Event

The detection of this event is discussed in Section 11.2.9.2 of the FuelSolutions™ Storage System FSAR.

#### 11.2.7.3 Summary of Event Consequences and Regulatory Compliance

*Structural*

Design basis seismic accelerations for the canister are evaluated in Section 3.7.8 of this FSAR. The resulting basket stresses are summarized in Table 3.7-5. All stresses are within the allowable stress values.

As discussed in Section 3.7.8, the canister shell stresses for this event are bounded by those for the postulated cask drop and tip-over conditions.

*Thermal*

There is no effect on the thermal performance of the canister as a result of this postulated accident.

*Shielding*

There is no effect on the shielding performance of the canister as a result of this postulated accident.

*Criticality*

There is no effect on the criticality control performance of the canister as a result of this postulated accident.

*Confinement*

There is no effect on the confinement performance of the canister as a result of this postulated accident.

*Radiation Protection*

Since there is no effect on shielding and confinement, there is no effect on radiation protection.

#### 11.2.7.4 Corrective Action

Since the canister is not compromised by this postulated accident, and since the storage cask and transfer cask are not compromised as documented in the FuelSolutions™ Storage System FSAR, no corrective actions are required.

### 11.2.8 Accident Internal Pressure

As discussed in Section 4.6 and summarized in Table 4.6-2, the accident condition internal pressure for the FuelSolutions™ W21 canister is 68.7 psig, which is less than the design basis pressure of 69 psig. The accident pressure is based on the required helium backfill in accordance with the *technical specification* provided in Section 12.3, elevated to the extreme off-normal condition canister cavity gas temperature. In addition, a concurrent non-mechanistic failure of 100% of the fuel rods with complete release of their fill gas and 30% of their fission gasses into the canister cavity elevated to the extreme off-normal condition canister cavity gas temperature is assumed, as defined in Section 2.3.3.4.